

Aus dem Pathologischen Institut der
Ludwig-Maximilians-Universität München

Direktor: Prof. Dr. med. Thomas Kirchner

**The role of the stem cell marker
OLFACTOMEDIN-4 and the microRNA
generator DICER1 in colorectal
carcinogenesis**

Dissertation

zum Erwerb des Doktorgrades der Naturwissenschaften
an der Medizinischen Fakultät der Ludwig-Maximilians-Universität München

vorgelegt von

Stefanie Anna Jaitner

aus Würzburg

2015

Gedruckt mit Genehmigung der Medizinischen Fakultät der Ludwig-Maximilians-Universität München

Dissertation eingereicht am: 20. Januar 2015

Betreuer: Prof. Dr. rer. nat. Andreas Jung

Zweitgutachter: Prof. Dr. rer. nat. Wolfgang Zimmermann

Dekan: Prof. Dr. med. dent. Reinhard Hickel

Tag der mündlichen Prüfung: 27. Januar 2016

Eidesstattliche Versicherung

Ich erkläre hiermit an Eides statt, dass ich die vorliegende Dissertation mit dem Thema “The role of the stem cell marker Olfactomedin-4 and the microRNA generator DICER1 in colorectal carcinogenesis“ selbstständig verfasst, mich außer der angegebenen keiner weiteren Hilfsmittel bedient und alle Erkenntnisse, die aus dem Schrifttum ganz oder annähernd übernommen sind, als solche kenntlich gemacht und nach ihrer Herkunft unter Bezeichnung der Fundstelle einzeln nachgewiesen habe.

Ich erkläre des Weiteren, dass die hier vorgelegte Dissertation nicht in gleicher oder ähnlicher Form bei einer anderen Stelle zur Erlangung eines akademischen Grades eingereicht wurde.

München, den 08. Februar 2016

(Stefanie Jaitner)

Meinen Eltern

Table of Content

Summary	1
Zusammenfassung	3
1 Introduction	5
1.1 The intestine is a pivotal organ	5
1.1.1 Structure of the intestine	5
1.1.2 Intestinal cell types.....	6
1.1.3 Regulation of the crypt homeostasis by different pathways	7
1.1.4 The Wnt signaling pathway in the intestine	10
1.2 Alterations of the intestinal homeostasis result in colorectal cancer.....	12
1.2.1 Epidemiology and risks of cancer	12
1.2.2 Forms of hereditary CRC	13
1.2.3 Initiation of CRC by an activated Wnt signaling pathway.....	15
1.2.3.1 Mutations of the Wnt signaling pathway	15
1.2.3.2 β -catenin target genes.....	16
1.2.3.3 Other mutations in CRC.....	17
1.2.3.4 Wnt signaling pathway activity in human tumors - the β -catenin paradox.....	18
1.2.3.5 Cancer stem cells.....	19
1.2.3.6 Epithelial mesenchymal transition (EMT)	21
1.2.3.7 Metastasis	22
1.2.3.8 Chemoresistance.....	23
1.2.4 Treatment of CRC	24
1.2.4.1 Classical chemotherapy.....	24
1.2.4.2 CSC targeted therapy	25
1.3 Olfactomedin-4 (OLFM4) and its role in cancer	26
1.3.1 Characterization of OLFM4.....	26
1.3.2 OLFM4 in association with cancer	28
1.3.2.1 The role and expression/protein levels of OLFM4 are dependent on the cancer type	28
1.3.2.2 The role of OLFM4 in CRC.....	28
1.4 Non-coding RNAs in colorectal cancer.....	29
1.4.1 The microRNAome	29
1.4.2 miRNA biogenesis	30
1.4.3 DICER1	31
1.4.4 DICER1 and miRNAs in cancer	33
1.5 Aims of the study	34
2 Materials and Methods	36
2.1 Materials	36
2.1.1 Chemicals	36
2.1.2 Reagents and Kits.....	37
2.1.3 Consumables	38
2.1.4 Devices	39
2.1.5 Cell culture	39
2.1.6 DNA and protein size standards.....	40
2.1.7 Oligonucleotides.....	40
2.1.7.1 Cloning primers.....	40
2.1.7.2 Sequencing primers	40

2.1.7.3	qPCR primers	40
2.1.7.3.1	qPCR primers for miRNA.....	40
2.1.7.3.2	qPCR primers for mRNA.....	41
2.1.7.4	Genotyping primers.....	41
2.1.7.5	Mouse recombination primers.....	42
2.1.7.6	siRNA Sequences	42
2.1.8	Antibodies	42
2.1.8.1	Primary antibodies.....	42
2.1.8.2	Secondary antibodies.....	43
2.1.9	Plasmids	43
2.1.10	Bacteria.....	44
2.1.11	Cell lines.....	44
2.1.12	Mouse strains.....	44
2.1.13	Software	46
2.1.14	Buffer	46
2.2	Methods.....	49
2.2.1	Methods used for working with DNA.....	49
2.2.1.1	Cloning techniques.....	49
2.2.1.1.1	Amplification of PCR products.....	49
2.2.1.1.2	Digest and ligation.....	49
2.2.1.1.3	Transformation.....	50
2.2.1.1.4	DNA preparation.....	51
2.2.1.2	Genomic DNA isolation and genotyping of cell lines	51
2.2.1.3	Genomic DNA isolation and genotyping of mouse tail biopsies.....	52
2.2.1.4	Verification of the recombination after tamoxifen induction.....	53
2.2.1.5	Agarose gel electrophoresis	54
2.2.1.6	Sanger sequencing.....	54
2.2.2	Methods used for working with RNA.....	55
2.2.2.1	Quantitative reverse transcriptase PCR (RT-qPCR)	55
2.2.2.1.1	RT-qPCR of miRNAs.....	55
2.2.2.1.2	RT-qPCR of mRNAs.....	56
2.2.2.2	Expression analysis	58
2.2.3	Methods used for working with proteins.....	58
2.2.3.1	Immunofluorescence analysis	58
2.2.3.2	Western Blot.....	59
2.2.4	Methods used for working with cells	60
2.2.4.1	Cell culture	60
2.2.4.2	Virus production, conditional expression.....	60
2.2.4.3	Wnt3a production.....	60
2.2.4.4	Knockdown of CTNNB1 using siRNAs	61
2.2.4.5	Luciferase reporter assay.....	61
2.2.4.6	Chemoresistance assay	61
2.2.4.7	MTT assay.....	62
2.2.4.8	Wound healing assay.....	62
2.2.4.9	Methyl cellulose assay	63
2.2.4.10	Flow cytometric analysis of cells (FACS)	63
2.2.4.10.1	Aldefluor assay.....	63
2.2.4.10.2	Antibody staining.....	64
2.2.4.10.3	Cell cycle analysis with propidium iodide (PI).....	64
2.2.4.11	Sphere formation assay	64

2.2.5	Methods used for working with mice.....	65
2.2.5.1	Experimental procedure	65
2.2.5.2	LacZ and eosin staining.....	65
2.2.5.3	Counting of adenomas by stereomicroscopy	66
2.2.6	Methods used for working with tissue	66
2.2.6.1	Staining of mouse tissue.....	66
2.2.6.1.1	Immunohistochemistry.....	66
2.2.6.1.2	H&E staining.....	67
2.2.6.1.3	PAS staining.....	68
2.2.6.2	Human tissue collection	68
2.2.6.2.1	Characteristics of the tissue collection.....	68
2.2.6.2.2	Immunohistochemistry.....	70
2.2.7	Statistical analysis	71
3	Results	72
3.1	The role of OLFM4 in colorectal cancer cell lines	72
3.1.1	Expression of OLFM4 in CRC cell lines and in CSCs	73
3.1.2	OLFM4 was ectopically overexpressed in CRC cell lines and had no influence on marker expression	75
3.1.3	OLFM4 had no influence on proliferation	78
3.1.4	Wnt signaling pathway was not affected by OLFM4	78
3.1.5	OLFM4 did not influence stem cell characteristics	81
3.1.6	Metastatic characteristics were not affected by OLFM4	83
3.2	The role of DICER1 and thus, the miRNAome in intestinal cancer	85
3.2.1	Design and system check of the Apc/Dicer1 mouse model.....	86
3.2.2	An additional deletion of Dicer1 in an Apc knockout mouse model led to a higher adenoma number and a smaller adenoma size in the small intestine.....	89
3.2.3	Loss of DICER1 led to a reduced level of the proliferation marker KI-67 in adenomas.....	92
3.2.4	Validation of CRC cell lines with a disruption of DICER1	95
3.2.5	Disruption of DICER1 led to enhanced expression/protein levels of CSC, metastatic and EMT markers.....	96
3.2.6	A loss of DICER1 resulted in a slower proliferation and enhanced G0/G1 arrest	97
3.2.7	Loss of DICER1 increased chemoresistance	100
3.2.8	Migration capacity was higher without DICER1	101
3.2.9	Wnt signaling pathway increased after loss of DICER1	102
3.2.10	DICER1 levels were higher in adenomas compared to normal colonic mucosa but decreased during progression from adenoma to carcinoma in human CRC	104
3.2.11	Expression of DICER1 was influenced by the Wnt signaling pathway.....	105
4	Discussion.....	108
4.1	The role of OLFM4 in colorectal cancer	108
4.1.1	OLFM4 was not a marker of cells with CSC properties	108
4.1.2	OLFM4 possessed no functional role in CRC cells	109
4.2	The role of DICER1 in intestinal cancer	112
4.2.1	Loss of DICER1 led to increased adenoma formation but reduced adenoma size in a murine intestinal cancer model.....	112

4.2.2	Loss of DICER1 resulted in slower proliferation but increased stemness and metastatic capacities in CRC cell lines	116
4.2.3	Loss of DICER1 led to tumor formation and provides cancer properties in combination with an active oncogenic pathway	119
4.2.4	DICER1 mRNA expression and protein levels increased in adenomas mediated by Wnt signaling pathway but decreased during progression from adenoma to carcinoma in human CRC	120
4.2.5	Future investigations	124
References.....		127
List of Figures		145
List of Tables.....		147
Abbreviations.....		148
Acknowledgements		154
Curriculum vitae		156

Summary

The intestine is a pivotal organ which is divided into two anatomical parts: the small intestine and the large intestine (colon and rectum). Both parts are made up of single-layered epithelium. This epithelium is composed of villi (protrusions) – found only in the small intestine - and crypts (invaginations) leading to an increase of the surface of the intestinal lumen whereby the uptake of nutrients and water is improved. Every five days, the intestinal epithelium is renewed whereby both, crypts and eventually villi, are filled up with new cells. The homeostasis of the crypts/villi relies on adult stem cells (SCs), especially crypt base columnar (CBC) cells, which are located at the base of the crypts. These are regulated by an active Wnt signaling pathway. A deregulation of the Wnt signaling pathway leads to cancer formation found in humans almost exclusively in the colon and rectum. Colorectal cancer (CRC) is worldwide the third most common cause for cancer related deaths. In the majority of CRC, origin and progress are caused by mutations in the adenomatous polyposis coli (*APC*) gene which encodes an essential component of the β -catenin destruction complex that is the central element of the Wnt signaling pathway. As a consequence of these mutations, the executor of the Wnt signaling pathway, β -catenin, which is in this context a transcription factor, cannot be downregulated any more. As a consequence target genes of β -catenin are expressed in an unregulated manner. These target genes regulate features of stem cell biology which confer cancer stemness, metastasis, EMT (epithelial-mesenchymal transition), chemoresistance and other characteristics to colorectal tumor cells. Interestingly, *APC* mutations have only an effect when they occur in the adult stem cells. Thus, the descendend tumor cells show characteristics of these cells and have been termed cancer stem cells (CSCs). Like adult stem cells in the normal crypt CSCs are the origin of cancer and are characterized by an activated - here deregulated - Wnt signaling pathway and thus, by the aforementioned features. Clinically, cancer death is caused in most cases by metastasis which is treated by chemotherapy from which most if not all CRCs escape by the development of chemoresistance which is an intrinsic feature of the CSCs. Therefore, CSC specific targeted therapies might be a promising therapeutic tool for a successful treatment of CRCs. One possibility is the interference of CSC sustaining molecules as these molecules are involved in the induction and maintenance of CSCs.

Here, a promising molecule is olfactomedin-4 (*OLFM4*) which was discussed to be a CSC marker. But the role of *OLFM4* as a CSC marker and important factor for tumorigenesis has been controversially described. Therefore, I investigated in the first part of my thesis the role of *OLFM4* in CRC cells. I demonstrate that *OLFM4* was expressed only in two out of 14 CRC cell lines. The assumption that *OLFM4* was only expressed in cells with characteristics of CSCs and thus, was not detected in the cell lines as they possess only a small proportion of CSCs, was not confirmed. I found that CSCs showed a reduced *OLFM4* expression and thus, *OLFM4* was not coexpressed with other SC markers.

These results indicate that OLFM4 is not a marker of CSCs in CRC. In order to analyze the functional role of OLFM4 in CRC cells, I overexpressed *OLFM4* lentivirally. However, the overexpression of *OLFM4* and thus, high OLFM4 protein levels did not influence the expression of CSC, EMT or differentiation marker. Likewise, OLFM4 did not play a functional role for proliferation, stemness and metastatic features. Therefore, this study demonstrates that OLFM4 is not a CSC marker and has no functional role for the driving activity in the process of colorectal carcinogenesis.

Additionally, I evaluated in the second part of my thesis the role of the microRNAome (miRNAome) in colorectal carcinogenesis, the influence on CSC features and whether the miRNAome might be a tool for specific CSC targeted therapies. microRNAs (miRNAs) are generally downregulated in tumors whereby the miRNA loss promotes tumorigenesis. As the majority of the CRC cases are driven by an *APC* mutation in the SC compartment, I used for my investigations a mouse model with a conditional *Apc* knockout in CBC cells which develops efficiently intestinal adenomas. This mouse model was crossed with another mouse model harboring a conditional knockout of the essential miRNA generator *Dicer1* to investigate the role of a loss of the miRNAome in murine Wnt driven intestinal tumors. In this part of my study I demonstrated that hetero- and homozygous deletion of *Dicer1* in CBC cells, in combination with an *Apc* knockout, enhances significantly the number of adenomas. Moreover, deletion of *Dicer1* resulted in smaller adenomas caused by reduced proliferation. Further analysis of *DICER1* deletion in human CRC cell lines revealed that loss of *DICER1* and thus, miRNAs led likewise to a decreased proliferation. Additionally, I showed that loss of miRNAs increased the expression/protein levels of CSC markers and CSC features indicating that loss of *DICER1* promotes tumorigenesis. Moreover, I translated these mouse model/cell culture results into human colonic normal and tumor tissue as well as CRC. In a collection of different tissues (normal tissue, adenomas and cancers of stages I to IV), increased *DICER1* levels were seen from normal tissue to adenomas followed by decreased levels during carcinoma progression. Increased levels of *DICER1* were also found in the murine Wnt driven adenomas. In support with this I provided finally evidence that *DICER1* expression is regulated by the Wnt signaling pathway thus already early in the beginning of the colorectal tumorigenesis. Thus, this data showed that *DICER1* is a tumor suppressor in intestinal cancer and the loss of *DICER1* and hence, of the miRNAome, influences CSC marker expression and marker protein levels as well as proliferation and CSC features. Therefore, the miRNAome might possibly become a therapeutic target for CSC targeted therapy.

Zusammenfassung

Der Darm ist ein lebenswichtiges Organ, das in zwei anatomische Teile geteilt ist: den Dünndarm und den Dickdarm (Kolon und Rektum), die beide aus einem einschichtigen Epithel bestehen. Dieses Epithel besteht aus Villi (Ausstülpungen) - nur im Dünndarm vorhanden - und Krypten (Einstülpungen) und führt zu einer Vergrößerung der Oberfläche des intestinalen Lumens, wodurch die Aufnahme von Nährstoffen und Wasser verbessert wird. Alle fünf Tage wird das intestinale Epithel erneuert, wodurch Krypten und schließlich auch Villi mit neuen Zellen aufgefüllt werden. Die Homöostase der Krypten/Villi beruht auf adulten Stammzellen (SZ), insbesondere „crypt base columnar“ (CBC)-Zellen, die an der Kryptenbasis angesiedelt sind und durch einen aktiven Wnt Signalweg reguliert werden. Eine Deregulierung des Wnt-Signalweges führt zur Bildung von Krebs, welcher bei Menschen hauptsächlich im Kolon und Rektum auftritt. Unter den Krebsarten stellt das kolorektale Karzinom (KRK) weltweit die dritthäufigste Ursache für Krebs dar. Meist sind sowohl das Auftreten als auch die Progression des KRK durch Mutationen im Adenomatous polyposis coli (*APC*)-Gen verursacht, das eine essentielle Komponente des β -catenin-Abbaukomplexes und daher eine zentrale Komponente des Wnt-Signalweges ist. Als Konsequenz kann der Transkriptionsfaktor des Wnt-Signalweges, β -catenin, nicht mehr herunterreguliert werden, wodurch β -catenin-Zielgene unreguliert exprimiert werden. Diese Zielgene regulieren wichtige Eigenschaften von Krebszellen wie Krebs-Stammzelligkeit, Metastasierung, EMT (Epitheliale-mesenchymale Transition), Chemoresistenz sowie weitere Eigenschaften. Interessanter Weise haben *APC*-Mutationen nur einen Einfluss, wenn sie in adulten SZ auftreten. Die von diesen SZ abstammenden Tumorzellen weisen Charakteristika dieser Zellen auf und werden Krebsstammzellen (KSZ) genannt. KSZ sind verantwortlich für die Krebsbildung, charakterisiert durch einen aktivierten Wnt-Signalweg und daher durch die zuvor genannten Eigenschaften. Die häufigste Ursache für den Krebs sind Metastasen. Metastasen werden mit Chemotherapie behandelt, wobei sich in den meisten Fällen KSZ dieser Behandlung durch die Entwicklung von Chemoresistenz entziehen können. Chemoresistenz ist eine intrinsische Eigenschaft von KSZ. Daher könnten Therapien, welche spezifisch KSZ angreifen, einen vielversprechenden Therapieansatzpunkt darstellen. Eine Möglichkeit dafür ist die Beeinträchtigung stammzellunterstützender Moleküle, da diese in die Induktion und Aufrechterhaltung von KSZ involviert sind.

Ein vielversprechendes Molekül ist olfactomedin-4 (*OLFM4*), das bereits als SZ-Marker diskutiert wurde. Aber die Rolle von *OLFM4* als SZ-Marker und als wichtiger Faktor für die Tumorigenese wurde bisher kontrovers beschrieben. Daher habe ich im ersten Teil meiner Doktorarbeit die Rolle von *OLFM4* in KRK-Zellen untersucht. Ich zeigte, dass *OLFM4* nur in zwei von 14 Zelllinien exprimiert wurde. Die Annahme, dass *OLFM4* nur in Zellen mit KSZ-Eigenschaften exprimiert wird und daher in Zelllinien nicht detektiert wird, da diese nur einen kleinen Anteil an KSZ besitzen, wurde nicht bestätigt.

Des Weiteren habe ich herausgefunden, dass KSZ eine reduzierte *OLFM4*-Expression zeigen, wodurch *OLFM4* nicht zusammen mit anderen SZ-Markern exprimiert wurde. Diese Ergebnisse deuten darauf hin, dass *OLFM4* kein Marker von KSZ im KRK ist. Um die funktionelle Rolle von *OLFM4* in KRK-Zellen zu untersuchen, habe ich *OLFM4* lentiviral überexprimiert. Jedoch beeinflusste eine Überexpression von *OLFM4* und somit hohe *OLFM4*-Proteinlevel nicht die Expression von KSZ-, EMT- und Differenzierungsmarkern. Ebenso spielte *OLFM4* keine funktionelle Rolle in der Proliferation, KSZ- sowie Metastasierungs-Eigenschaften. Daher zeigt diese Studie, dass *OLFM4* kein KSZ-Marker ist und keine funktionelle Rolle als treibende Kraft im kolorektalen Karzinogeneseprozess hat.

Im zweiten Teil meiner Doktorarbeit habe ich die Rolle des miRNAoms in der kolorektalen Karzinogenese und seinen Einfluss auf KSZ-Eigenschaften untersucht mit dem Ziel, ob das miRNAom einen Ansatzpunkt für eine spezifische KSZ-Therapie darstellen könnte. miRNAs sind in Tumoren generell herunterreguliert, was darauf schließen lässt, dass ein miRNA-Verlust die Tumorigenese begünstigt. Da die Mehrheit der KRK-Fälle durch eine *APC*-Mutation im SZ-Kompartiment angetrieben wird, habe ich für meine Untersuchungen ein Mausmodell mit einem konditionalen *Apc*-Knockout in den CBC-Zellen verwendet, welches effizient intestinale Adenome entwickelt. Dieses Mausmodell wurde mit einem anderen Mausmodell mit einem konditionalen Knockout des miRNA-Generators *Dicer1* gekreuzt. Damit konnte die Rolle eines miRNAom-Verlustes in murinen intestinalen Tumoren, welche vom Wnt-Signalweg angetrieben werden, untersucht werden. In diesem Teil meiner Studie zeige ich, dass eine hetero- und homozygote Deletion von *Dicer1* in CBC-Zellen, in Kombination mit einem *Apc*-Knockout, signifikant die Adenomzahl erhöhte. Außerdem resultierte eine *Dicer1*-Deletion in einer kleineren Adenomgröße, was durch eine verringerte Proliferation verursacht wurde. Eine weiterführende Analyse der *DICER1*-Deletion in humanen KRK-Zelllinien zeigte, dass ein Verlust von *DICER1* und folglich miRNAs ebenso zu einer verringerten Proliferation führte. Außerdem erhöhte ein miRNA-Verlust die Expression/Proteinlevel von KSZ-Markern und KSZ-Eigenschaften. Diese Ergebnisse zeigen, dass ein Verlust von *DICER1* die Tumorigenese fördert. Um diese Zellkultur/Mausmodell-Ergebnisse auf den Menschen zu übertragen, habe ich humanes Normal-, Adenom- und Krebsgewebe (Stadium I bis IV) von KRK-Patienten analysiert. Dabei nahm das *DICER1*-Proteinlevel vom Normalgewebe zu den Adenomen zu. Während der Karzinomprogression nahm das *DICER1*-Proteinlevel jedoch von den Adenomen bis hin zum Karzinom ab. Einen Anstieg des *DICER1*-Proteinlevels habe ich auch in murinen Wnt-getriebenen Adenomen gefunden. Daher erbringe ich schlussendlich einen Nachweis, dass die *DICER1*-Expression vom Wnt-Signalweg und daher früh in der Tumorigenese reguliert wird. Folglich zeigen diese Daten, dass *DICER1* im Darmkrebs ein Tumorsuppressor ist und ein Verlust von *DICER1* und somit des miRNAoms KSZ-Markerepression und Markerproteinlevel sowie Proliferation und KSZ-Eigenschaften beeinflusst. Daher könnte das miRNAom möglicherweise einen Ansatzpunkt für Therapien, welche spezifisch KSZ angreifen, darstellen.

1 Introduction

1.1 The intestine is a pivotal organ

An intact intestine is essential for all metazoa as it mainly performs the digestion and resorption of water whereby food and drinks are broken down into the basic nutrients. Subsequently, these are absorbed into the blood stream, transported to cells all over the body and used for the generation of energy, growth and cell repair (<http://www.niddk.nih.gov/Pages/default.aspx>). For the efficient uptake of nutrients, the intestine has developed a specific structure which is subsequently explained.

1.1.1 Structure of the intestine

The intestinal tract is divided into two anatomical parts: the small intestine and the large intestine (colon and rectum). Furthermore, the small intestine is sectioned from proximal to distal in the duodenum, jejunum and ileum (Barker et al., 2008). In the small intestine, the food is mixed with digestive juices coming from the pancreas and bile by peristaltic action of the intestinal musculature. Nutrients are absorbed and the remainings are transported into the large intestine. Here, water is mainly absorbed and additionally, the remaining nutrients are metabolized and absorbed by enterocytes. Thereby stool is generated which is pushed out by peristaltic bowel movement (<http://www.niddk.nih.gov/Pages/default.aspx>).

The epithelium of the intestine possesses a characteristic and functional structure. In the small intestine, the epithelium shows protrusions which are known as villi and invaginations named crypts (Fevr et al., 2007). Each crypt is surrounded by villi like a crown which leads to an increase of the epithelial surface resulting in an enhanced contact between epithelium and the intestinal lumen and thus, improving the uptake of nutrients. In contrast, the epithelium of the colon contains only crypts which are larger as in the small intestine (Pinto and Clevers, 2005) (Fig. 1A).

In both, the small and the large intestine, the epithelium consists of a single layer of epithelial cells (Pinto and Clevers, 2005). This epithelium is renewed roughly every five days as epithelial cells migrate from the bottom towards the top of the crypts in the small intestine or the surface epithelium of the colon respectively, where they become apoptotic and are finally shed into the lumen of the intestine (Pinto and Clevers, 2005). The life cycle of intestinal cells spans from their generation at the crypt base via proliferation,

differentiation, apoptosis and shedding into the lumen. During these five days, crypts or crypt/villi units are renewed completely. Thus, new cells have to substitute the upwards migrated and thus, vanishing cells to make sure that the barrier, defending and absorptive functions of the intestinal mucosa is continued (Pinto and Clevers, 2005). The cellular characteristics, functions, their migration and the homeostasis of the intestinal epithelium are subsequently described in more detail.

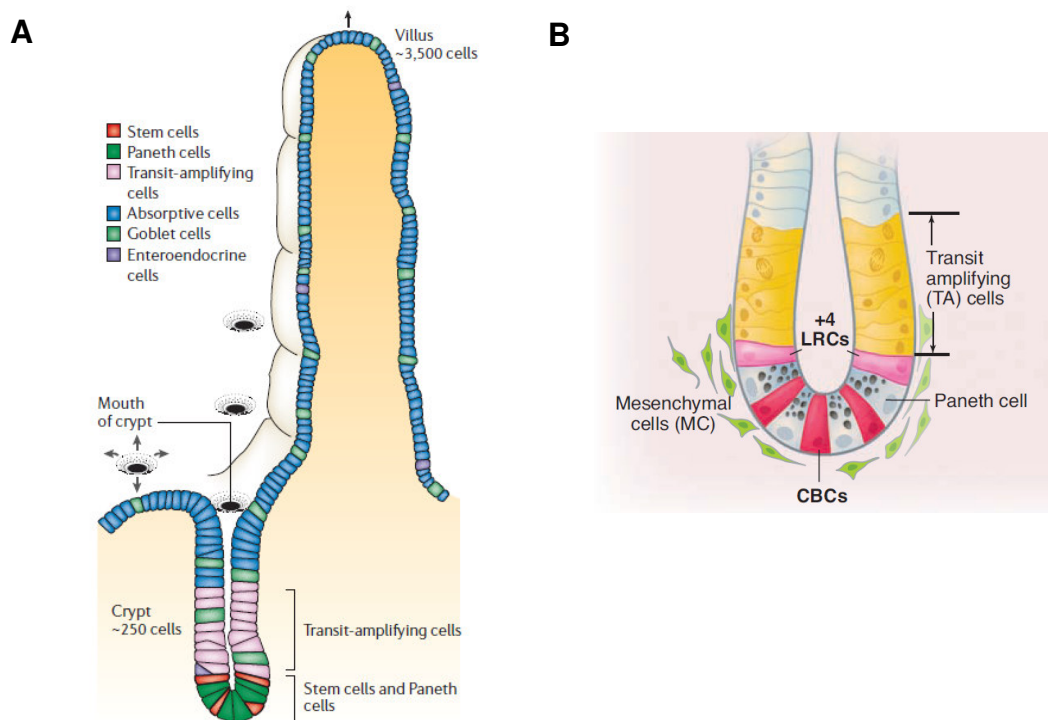


Fig. 1. The structure of the intestinal epithelium and an intestinal crypt.

(A) The epithelium of the small intestine is built of villi and crypts. The large intestine possesses only crypts. This structure is organized by adult stem cells which are located at the base of the crypt. The transit-amplifying (TA) cells stem from the stem cells and differentiate into Paneth, absorptive, goblet and enteroendocrine cells. The arrow indicates the upwards migration of cells out of the crypt (Crosnier et al., 2006). (B) Intestinal crypt structure with cycling, LGR5 positive stem cells (crypt base columnar (CBC) cells) and quiescent, BMI1 positive stem cells at the +4 position. Additionally depicted are TA cells and mesenchymal cells (Li and Clevers, 2010).

1.1.2 Intestinal cell types

Multipotent stem cells (SCs) are responsible for the renewal and fill-up resulting in the crypt homeostasis. SCs are located at the base of the crypts in the SC niche (Pinto and Clevers, 2005). In the small intestine two potential pools of SCs were found: 1) at the base of intestinal crypts, SCs are located which show high proliferative activity and are named

due to their morphological appearance crypt base columnar (CBC) cells (Clevers, 2013). They are characterized by high amounts of the SC marker leucine-rich-repeat-containing G-protein coupled receptor 5 (LGR5) (Barker et al., 2007) (Fig. 1B). 2) Besides these actively proliferating CBC cells, another pool of SCs was found at the +4 position of the crypt. These SCs are characterized by low proliferation (Yan et al., 2012) and by high amounts of the SC marker B lymphoma Mo-MLV insertion region 1 (BMI1) (Fig. 1B) (Li and Clevers, 2010). BMI1 positive SCs do not contribute to the homeostatic regeneration of the small intestine but seem to represent a back-up reservoir which becomes activated by the small intestine after gross cell damage like radiation injury. Thus, these SCs can reconstitute the pool of the radiation-sensitive CBC cells (Potten et al., 2009; Yan et al., 2012).

During the crypt homeostasis, CBC cells divide about every 24 h asymmetrically to give rise to CBC and transit amplifying (TA) cells (Pinto and Clevers, 2005). TA cells proliferate quickly and divide every 12 h for four to five times before they start to differentiate (Marshman et al., 2002; Pinto and Clevers, 2005). By this fast proliferation the amount of crypt cells is massively increased. The subsequent derivatives of TA cells are non-proliferative, accumulate in the crypts and differentiate into the four different cell types: enterocytes, enteroendocrine cells, goblet cells, and small intestinal Paneth cells (Gregorieff and Clevers, 2005) (Fig. 1A). Among these cell types, the enterocytes which are specialized for absorption of nutrients are the most abundant cell type (Crosnier et al., 2006). Enterocytes, hormone-secreting enteroendocrine and mucus-secreting goblet cells migrate upwards to the top of the villi or the surface epithelium of the colon (Gregorieff and Clevers, 2005; Pinto and Clevers, 2005). Paneth cells stay in the base of the crypt (Fig. 1B) and reside there for about 20 days (Pinto and Clevers, 2005). They protect the host from intestinal pathogens by the secretion of antimicrobial peptides and enzymes (Clevers and Bevins, 2013) and provide the niche for the SCs (Sato et al., 2011).

1.1.3 Regulation of the crypt homeostasis by different pathways

The intestinal crypt/villus homeostasis is regulated by different pathways (Fig. 2A). Most important is the canonical Wnt signaling pathway, subsequently termed Wnt signaling pathway, which controls SCs, proliferation and differentiation (Brabletz et al., 2009; van de Wetering et al., 2002).

An active Wnt signaling pathway sustains a proliferative and dedifferentiated phenotype (van de Wetering et al., 2002; van den Brink and Hardwick, 2006). The activity of the Wnt signaling pathway is strongest at the base of the crypt and declines in a gradient towards the tip of the crypt (van de Wetering et al., 2002). Wnt is provided by extraepithelial Wnt sources (Schuijers and Clevers, 2012) such as mesenchymal cells (intestinal subepithelial myofibroblasts (ISEMFs)) which are located around the SC niche and by Paneth cells which are located in the SC niche (Sato et al., 2011). The Paneth cells in turn are matured by the Wnt signaling pathway (van Es et al., 2005a) (Fig. 2A). A disruption of the Wnt signaling pathway activity disturbs the development of the intestinal SC compartment (Korinek et al., 1998) or stops crypt proliferation (Fevr et al., 2007; Kuhnert et al., 2004; van Es et al., 2012). Furthermore, the Wnt signaling pathway is involved in the migration of the intestinal epithelial cells by regulating the expression of *EFNB1* (ephrin-B1) and its receptors *EPHB2* and *EPHB3* (ephrin type-B receptor 2/3). Active Wnt signaling pathway represses *EFNB1* and induces *EPHB2* and *EPHB3* resulting in the expression of *EFNB1* at the top of the crypt and *EPHB2* and *EPHB3* at the crypt base. This leads to the repulsion of cells and therefore, to migration and proper cell positioning (Batlle et al., 2002; Crosnier et al., 2006).

However, other pathways are also important for the modulation of the homeostasis (Brabletz et al., 2009). Another pathway involved in the homeostasis is the Hedgehog signaling (HH) pathway which induces differentiation (van den Brink and Hardwick, 2006). As the expression of its morphogen indian hedgehog (*IHH*) is negatively regulated by the Wnt signaling pathway, the HH signaling pathway activity declines from the top of the crypt to the base of the crypt. Thus, the centers of Wnt and HH signaling are opposed resulting in two counteracting gradients. Moreover, the HH signaling pathway in turn restricts Wnt to the crypt base (van den Brink and Hardwick, 2006) (Fig. 2A, B). *IHH* is expressed and the morphogen is synthesized from non-proliferative epithelial cells in the intestine (Gregorieff and Clevers, 2005).

Furthermore, the BMP (bone morphogenetic protein) pathway plays also a role in crypt/villus homeostasis as it is required for differentiation and maturation of intestinal cells (Vanuytsel et al., 2013). Its morphogen *BMP* is expressed and BMP is synthesized by mature epithelial cells (Gregorieff and Clevers, 2005). The inhibitors of the BMP pathway, noggin (*NOG*) and gremlin, are expressed and synthesized in ISEMFs. As they bind BMP this results in an inhibition of the BMP pathway in this area of the crypt. Thus, BMP signaling declines - like HH signaling - in a gradient from the top to the base of the crypt.

Another parallel is that the BMP signaling pathway can inhibit the Wnt signaling pathway via activation of PTEN (phosphatase and tensin homolog; member of the PI3K (phosphatidylinositol-4,5-bisphosphate 3-kinase) pathway) and thus, inhibition of the serine/threonine kinase AKT (v-akt murine thymoma viral oncogene homolog) which consequently cannot induce the Wnt signaling pathway (Brabletz et al., 2009).

Moreover, the Notch pathway is active in the SC and TA compartment (Brabletz et al., 2009). It is important to maintain, together with Wnt signaling, undifferentiated, proliferative cells (van Es et al., 2005b) and is also involved in the differentiation of absorptive enterocytes. However, for the differentiation of the secretory lineage, an inhibition of the Notch pathway is required (Vanuytsel et al., 2013). The Notch pathway is inhibited by the Hippo pathway which is active in post-mitotic differentiated cells and inhibits proliferation. In the TA and SC compartment, the Hippo pathway is inactive and thus, its transcription factors yes-associated protein (YAP)/transcriptional coactivator with PDZ-binding motif (TAZ) can translocate to the nucleus and be transcriptionally active. Furthermore, YAP can activate the Notch and Wnt signaling pathway (Fig. 2A, B) (Vanuytsel et al., 2013).

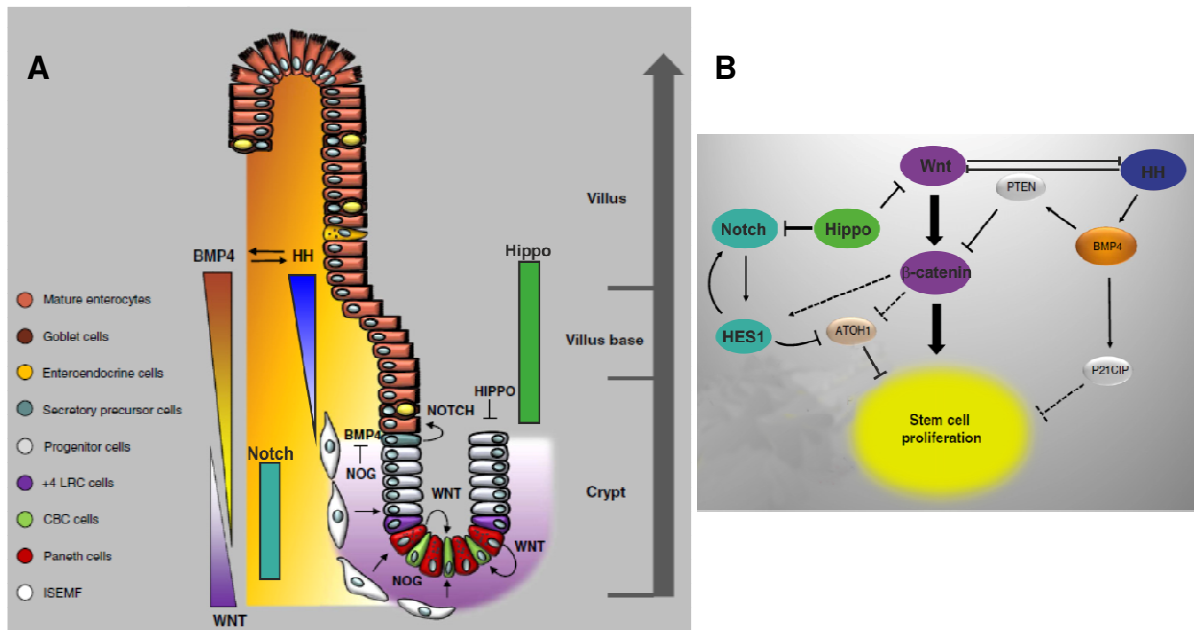


Fig. 2. Schematic representation of the major signaling pathways of the crypt/villus homeostasis and its interaction.

(A) The homeostasis of the intestinal crypts and villi requires several pathways. The dominant force among these pathways is the Wnt signaling pathway which sustains proliferation and dedifferentiation. It declines from the base to the top of the crypt. The Hedgehog pathway (HH) induces differentiation and declines from the top of the crypt to the base of the crypt. Furthermore, the BMP pathway is required for differentiation and maturation of intestinal cells and declines also from the top to the base of the crypt. The Notch pathway is active in the SC and TA compartment, maintains undifferentiated, proliferative cells and is also involved in the differentiation of absorptive enterocytes. The Hippo pathway is active in post-mitotic differentiated cells and inhibits proliferation. (B) The pathways which are active in the crypt/villus compartment interact with each other and can activate or repress other pathways. In this picture, the interaction leading to a SC phenotype is shown. Dotted lines show interactions which were observed in colon cancer cell lines and are possibly also involved in normal SC signaling. Solid lines show interactions known to occur in normal intestinal SCs. Modified from (Brabletz et al., 2009; Vanuytsel et al., 2013).

1.1.4 The Wnt signaling pathway in the intestine

Since the Wnt signaling pathway is the most important pathway in the crypt/villus homeostasis, I focus subsequently on this pathway. The central effector molecule of the Wnt signaling pathway is the transcription factor β -catenin which has two different roles in epithelial cells. In the inactive state of the Wnt signaling pathway (in non-proliferative, differentiated intestinal cells that are located apically of TA cells (Schuijers and Clevers, 2012; van de Wetering et al., 2002)), β -catenin molecules are withdrawn from the Wnt signaling pathway as they interact with cadherin 1 (E-cadherin) at the plasma membrane (Thiery, 2002) and associate via α -catenin with the actin cytoskeleton to form adherens junctions (Conacci-Sorrell et al., 2002). Functionally, this recruitment to the adherens

junctions stabilizes cell-cell adhesions (Conacci-Sorrell et al., 2002) resulting in an epithelial phenotype (Thiery, 2002). In this complex, β -catenin is protected from degradation (Fig. 3A) (Moon et al., 2004). The remaining β -catenin molecules which are not associated with adherens junctions are sequestered by a destruction complex which consists of adenomatous polyposis coli (APC), glycogen synthase kinase 3 (GSK3), casein kinase 1 (CK1) and AXIN. This sequestration by the destruction complex leads to a phosphorylation of β -catenin by CK1 and GSK3 (Moon et al., 2004) near the N-terminus at various highly conserved serine/threonine residues of β -catenin (Clevers, 2006; Gregorieff and Clevers, 2005). Phosphorylated β -catenin is subsequently recognized by the E3 ubiquitin ligase complex, polyubiquitinated and degraded finally in the 28S-proteasome (Conacci-Sorrell et al., 2002). Therefore, only low cytoplasmic and especially nuclear levels of β -catenin exist in such cells and thus, the target genes of β -catenin are not expressed under basal conditions (Fig. 3A) (Clevers, 2006; Moon et al., 2004).

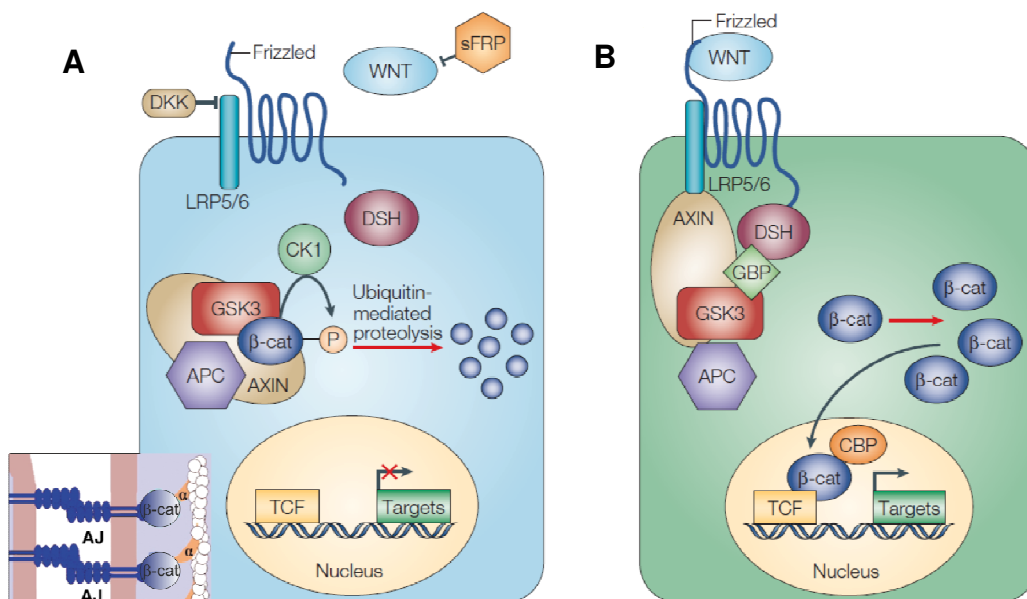


Fig. 3. The canonical Wnt signaling pathway.

(A) In the inactive state of the Wnt signaling pathway, Wnt ligands are absent and some β -catenin molecules are recruited to adherens junctions (AJ) to stabilize cell-cell adhesions and thus, the epithelial phenotype. β -catenin molecules which are not associated with AJ are recruited by a destruction complex (AXIN, GSK3, CK1 and APC), phosphorylated by CK1 and GSK3 at the N-terminus and subsequently proteasomally degraded. Modified from (Conacci-Sorrell et al., 2002; Moon et al., 2004). (B) In the active state, Wnt ligands bind to frizzled receptors whereby the destruction complex is bound to the membrane, AXIN is degraded, GSK3 is inhibited by DSH and GBP and subsequently, β -catenin is stabilized. Here, it works in cooperation with DNA-binding factors of the TCF/LEF-1 family of the HMG (high mobility group factor) family and other coactivators like CBP or p300 as a multi-enhancosome complex as a strong cis-acting transcription factor. (Moon et al., 2004)

In the active state of the Wnt signaling pathway (found in cells at the crypt base and TA cells) (Fig. 3B), an excess of Wnt ligands compared to the inhibitors is present whereby Wnts bind to their receptors, members of the frizzled family, and to the co-receptors LDL receptor-related proteins 5 and 6 (LRP5 and LRP6). By this interaction, the phosphoprotein dishevelled (DSH) is activated and recruited to the membrane and thus, AXIN and the destruction complex are bound to the membrane. By subsequent degradation of AXIN, inhibition of GSK3 by DSH and recruiting of the GSK3 inhibitor GSK3 binding protein (GBP) to the complex, the phosphorylation and degradation of β -catenin are decreased. Thus, levels of β -catenin molecules increase (Moon et al., 2004) and eventually β -catenin is transported by a yet not completely understood mechanism from the cytoplasm into the nucleus most likely either by interaction with lymphoid enhancer-binding factor 1 (LEF1) (Henderson and Fagotto, 2002) or by binding directly to components of the nuclear pore complex (Fagotto et al., 1998). This results in the nuclear accumulation of β -catenin in the nucleus. Here, β -catenin can cooperate with the DNA binding T-cell specific transcription factors (TCF) and LEF transcription factors which are then no longer associated with co-repressors of the groucho (GRO) family (Clevers and Nusse, 2012). This cooperation, together with the binding of the coactivator CREB binding protein (CREBBP; CBP) or E1A binding protein p300 (EP300; p300) (Hecht et al., 2000) and a variety of other factors like legless or pygopus (Townsend et al., 2004) results in a multi-protein activator complex that upregulates the expression of β -catenin target genes (Fig. 3B) (Moon et al., 2004).

1.2 Alterations of the intestinal homeostasis result in colorectal cancer

1.2.1 Epidemiology and risks of cancer

The homeostasis of the intestine is tightly regulated and disturbances in this regulation result in uncontrolled cell growth causing cancer. Cancer is one of the leading causes of disease and death worldwide. In 2012, approximately 14.1 million new cancer cases occurred worldwide, 8.2 million people died in consequence of cancer (World_Cancer_Factsheet, 2008, 2012). The incidences of cancer are higher in Western countries than in developing countries (World_Cancer_Factsheet, 2008, 2012) which is mainly caused by: 1) variations in the age structure of the populations, 2) the life style such as nutrition, alcohol or tobacco (Global_Cancer_Facts_and_Figures, 2nd edition).

Colorectal cancer (CRC) is in regard to the incidence of cancer cases as well as in the mortality among the three most common cancers worldwide (Fig. 4) (World_Cancer_Factsheet, 2012). Similar to the general risk of cancer, the risk of CRC rises with age. The lifestyle that means smoking, alcohol consumption, obesity paired with few physical exercise as well as high amounts of red and especially processed meat increase the risk for CRC.

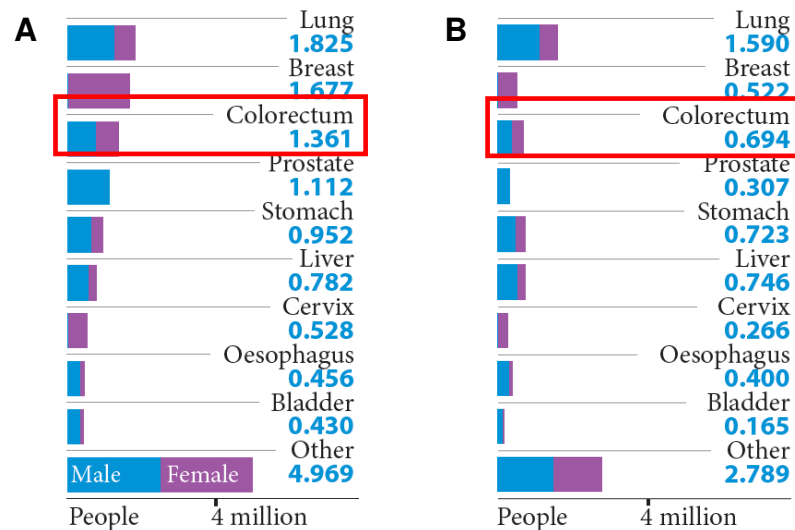


Fig. 4 World cancer burden.

(A) Incidence and (B) mortality rates are shown for both genders worldwide in 2012. Colorectal cancer is one of the leading causes for cancer cases and deaths (World_Cancer_Factsheet, 2012).

Because of the high risk and mortality rate of CRC, it is important to understand how this disease works on the molecular level. Therefore, it is a good basis to understand the regulation of intestinal cells and to compare what is deregulated in CRC. One reasonable approach is to focus on genetic syndromes (Global_Cancer_Facts_and_Figures, 2nd edition) as these usually harbor mutations in relevant genes which are important for the disease. For CRC, mainly two syndromes are known.

1.2.2 *Forms of hereditary CRC*

One hereditary cancer syndrome is the Lynch syndrome which is known as hereditary nonpolyposis colorectal cancer (HNPCC) when it becomes manifest in the gut. Around 3–4% of all cases of CRC are caused by this syndrome. Patients inheriting this syndrome have a lifetime risk of 80% to develop CRC. HNPCC is characterized by heterozygous

germline mutations in one of the four DNA mismatch repair (MMR) genes mutS homolog 2 (*MSH2*), mutS homolog 6 (*MSH6*), human mutL homolog 1 (*MLH1*) and postmeiotic segregation increased 2 (*S. cerevisiae*) (*PMS2*) (Rustgi, 2007). According to the two hit model, the remaining wildtype MMR allele is lost or functionally inactivated by somatic genetic alterations during lifetime CRCs of HNPCC patients (loss of function mutation). This results in a defective MMR system producing errors that arise during replication or maintenance DNA repair which can no longer be repaired. Thus, plenty mutations accumulate especially in mononucleotide microsatellite sequences which are the substrate for the MMR system. Therefore, this type of defect in caretaker genes results in microsatellite instability (MSI). When repetitive microsatellites are located in coding sequences of genes, defects usually lead to frameshift mutations, e.g. in receptors responsible for growth suppression such as the transforming growth factor β (TGF β)-receptor II resulting in growth of tumors (de la Chapelle, 2004; Kinzler and Vogelstein, 1996).

Another hereditary form of CRC is familial adenomatous polyposis (FAP) which causes about 0.2–1% of all cases of CRC (de la Chapelle, 2004; Rustgi, 2007). FAP is genetically associated with mutations on chromosome 5q21. Here, the gene encoding the tumor suppressor *APC*, a component of the β -catenin destruction complex of the Wnt signaling pathway, is located which was identified to be the driver of CRC (Kinzler et al., 1991; Rustgi, 2007). As a tumor suppressor, the second *APC* allele is inactivated (loss of function) by point mutation or loss of heterozygosity (Crabtree et al., 2003) so that the patients develop already in early adolescence hundreds to thousands of small adenomatous polyps in the colon and rectum (Fig. 5). Therefore, the penetrance to develop CRC is practically 100% for these patients already at a young age (de la Chapelle, 2004). Although genetically recessive, FAP is considered phenotypically as a dominant disease due to the high penetrance (Rustgi, 2007).

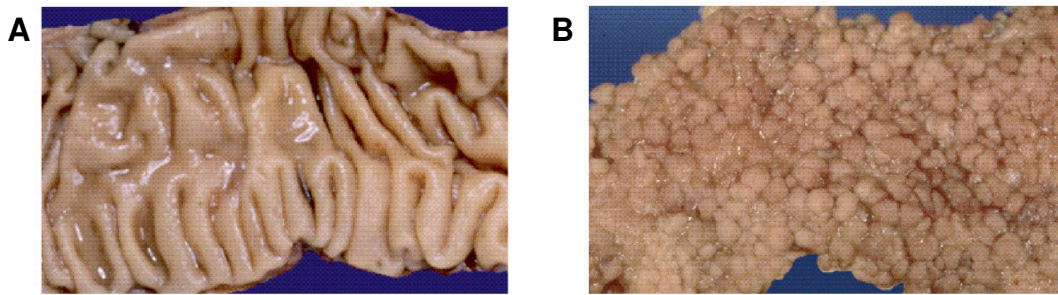


Fig. 5. Familial adenomatous polyposis (FAP).

(A) Normal mucosa of the colon. (B) Multiple polyps (adenomas) in the colon of a FAP patient (Weinberg, 2007).

Besides the hereditary forms, also sporadic abnormalities lead to CRC which resemble phenotypically the hereditary forms HNPCC and FAP. Among the sporadic cases, about 13% are caused by a mutation in an oncogene like *BRAF* (serine/threonine-protein kinase B-Raf) (<http://www.nature.com/tcga/>) which induces upregulation of DNA methyl transferases (DNMT) (Carragher et al., 2010). This results in hypermethylation of CpG islands (CIMP) which can result in MSI caused by hypermethylation of *MLH1* (Pino and Chung, 2010; Weisenberger et al., 2006). These cases resemble phenotypically HNPCC patients. About 80% of sporadic CRC cases are caused by mutations in the *APC* gene (Kinzler and Vogelstein, 1996) and resemble phenotypically FAP patients. As the CRC cases with *APC* mutations are associated with a worse outcome due to the development of metastases than the MSI phenotype (Pino and Chung, 2010), I focus in the following on the former cases.

1.2.3 *Initiation of CRC by an activated Wnt signaling pathway*

1.2.3.1 *Mutations of the Wnt signaling pathway*

When both alleles of the *APC* gene harbor mutations, APC may become functionally inactive whereby the β -catenin destruction complex does not work anymore properly. The importance of the Wnt signaling pathway for the development of CRC is underlined by the fact that β -catenin, the functional driver of the Wnt signaling pathway, is found to be mutated in about 50% of the cases of CRC without *APC* mutations. For the β -catenin gene (*CTNNB1*), which is an oncogene, a single point mutation is sufficient for its activation (gain of function) (Pino and Chung, 2010). Mutations affect the serine/threonine residues in the N-terminus of the protein which are essential targets for the degradation via the APC

destruction complex (Clevers, 2006). Thus, by these mutations β -catenin is protected from a regulatable and thus proper destruction. Both, mutations in the *APC* or *CTNNB1* gene, disturb the regulation of the Wnt signaling pathway (see 1.1.4) and lead to an activation of the Wnt signaling pathway. Thus, β -catenin becomes permanently stabilized, independent of the binding of Wnt ligands, accumulates in the cytoplasm and can eventually translocate into the nucleus and drive transcription of various target genes (Clevers, 2006; Pino and Chung, 2010).

1.2.3.2 β -catenin target genes

β -catenin target genes are involved in or directly confer most of the hallmarks of cancer (Fig. 6). The hallmarks of cancer resemble essential properties of cells that have to be gained for the transformation of normal into cancer cells to survive, become tumorigenic and finally malignant (Hanahan and Weinberg, 2011). Among the hallmarks of cancer are **proliferation** which is controlled by the β -catenin target genes v-myc avian myelocytomatosis viral oncogene homolog (*MYC*) (He et al., 1998), cyclin D1 (*CCND1*) (Shtutman et al., 1999) but also cyclin-dependent kinase inhibitor 2A (*CDKN2A*) (Wassermann et al., 2009) and induction of **angiogenesis** which is induced by the expression and synthesis of vascular endothelial growth factor (*VEGF*) (Zhang et al., 2001b). Furthermore, resistance to **apoptosis** is mediated by baculoviral inhibitor of apoptosis repeat-containing 5 (*BIRC5*) (Zhang et al., 2001a), **invasion and metastasis** by matrix metalloproteinase 7 (*MMP7*) (Brabletz et al., 1999), urokinase-type plasminogen activator (*PLAU*) (Hiendlmeyer et al., 2004) and tenascin C (*TNC*) (Beiter et al., 2005) and **stemness** by cluster of differentiation 44 molecule (*CD44*) (Wielenga et al., 1999) and *LGR5* (Barker et al., 2007). **Epithelial-mesenchymal transition (EMT)** is induced by zinc finger E-box binding homeobox 1 (*ZEB1*) (Sanchez-Tillo et al., 2011) and **chemoresistance** by ATP-binding cassette, sub-family B (MDR/TAP) 1 (*ABCB1*) (Yamada et al., 2000). Moreover, **replicative immortality** is mediated by telomerase reverse transcriptase (*TERT*) (Hoffmeyer et al., 2012; Jaitner et al., 2012). This list may not be complete as more and more β -catenin target genes involved in the regulation of the *hallmarks of cancer* are found every day. For a more complete list see (http://web.stanford.edu/group/nusselab/cgi-bin/wnt/target_genes). The influence of β -catenin on various hallmarks of cancer points out the importance of the Wnt signaling pathway in the process of colorectal carcinogenesis.

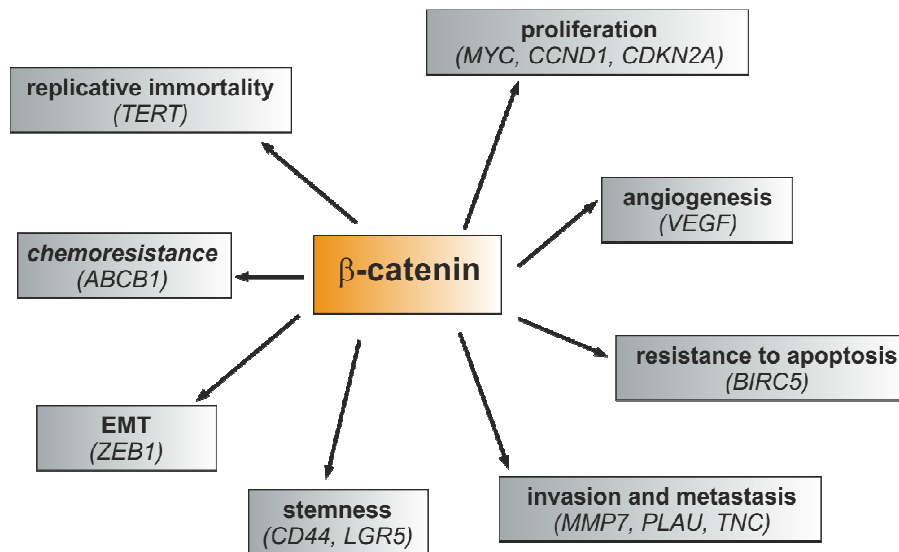


Fig. 6. The influence of β -catenin on hallmarks of cancer and its target genes.

An active Wnt signaling pathway and thus, nuclear β -catenin influences most of the hallmarks of cancer by the expression of its target genes. These hallmarks with some corresponding target genes are listed.

1.2.3.3 Other mutations in CRC

The Wnt signaling pathway and its target genes are very important for CRC, however, for colorectal carcinogenesis the accumulation of further genetic changes is required (Kinzler and Vogelstein, 1996). Thereby the inactivation of the *APC* gene is frequently the initial hit in the majority of cases of colorectal carcinogenesis (Fig. 7). Therefore, APC has been named the gatekeeper of colorectal carcinogenesis (Fearon and Vogelstein, 1990; Kinzler and Vogelstein, 1996). The activation of the Wnt signaling pathway leads to hyperproliferation of affected epithelial cells what results in the development of early adenomas. In the further process of carcinogenesis the *APC* mutated tumor cells acquire additional mutations in other oncogenes and tumor suppressor genes what is known as the multistep carcinogenesis model (Kinzler and Vogelstein, 1996). Originally, due to the combination of different caretaker systems of DNA repair the general mutation rate of the human genome is quite low (1 nucleotide per 10^9 bp and thus about 2 to 3 mutations per round of replication) (Weinberg, 2007). Therefore, tumor cells have to gain intrinsic chromosomal instability (CIN) to be able to acquire additional mutations resulting in the multiple mutations observed in CRCs (Pino and Chung, 2010). Interestingly, mutations of the *APC* gene also contribute in this manner as loss of APC function is also related to chromosomal instability since APC also plays a role in the attachment of microtubules to

the kinetichor region of chromosomes during their segregation in mitosis (Kaplan et al., 2001). Furthermore, the shortening of telomeres by hyperproliferation of the tumor cells leads also to CIN (Hanahan and Weinberg, 2011; Romanov et al., 2001). However, the upregulation of TERT by β -catenin (Hoffmeyer et al., 2012; Jaitner et al., 2012) later in the process of carcinogenesis leads to an elongation of the telomeres and thus, to a stabilization of the chromosome.

Frequently, mutations in the oncogene Kirsten rat sarcoma viral oncogene homolog (*KRAS*) are seen quite early at the stage of intermediate adenomas. Additionally, parts of the chromosome 18q, that include e.g. the tumor suppressor mothers against decapentaplegic homolog 4 (*SMAD4*), are lost and mutations of the tumor suppressor tumor protein p53 (*TP53*; the guardian of the genome) as well as other mutations are frequently observed in CRCs and conduce to the multistep process of carcinogenesis up to the formation of metastases (Fig. 7) (Fearon and Vogelstein, 1990; Kinzler and Vogelstein, 1996). As the genetic alterations may somehow be also associated with the loss of the *APC* gene function, this is another reason besides the early timepoint in the carcinogenesis of CRCs why *APC* is considered to be the gatekeeper in this process (Kinzler and Vogelstein, 1996).

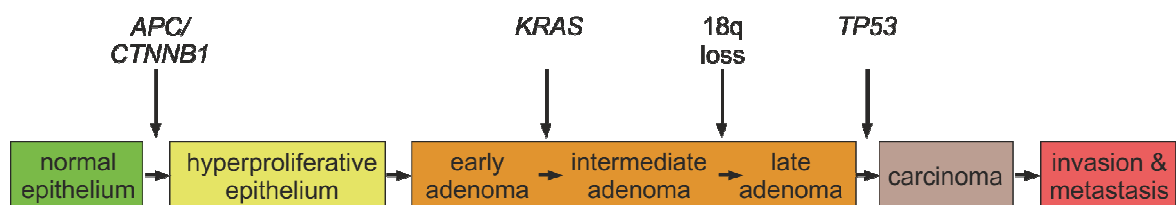


Fig. 7. The multistep carcinogenesis model of colorectal cancer.

A mutation in *APC/CTNNB1* and thus, activation in the Wnt signaling pathway is the initial hit in most CRCs. By this mutation, the affected epithelial cells become hyperproliferative and adenomas are formed. Additionally, loss of *APC* leads to increased CIN (chromosomal instability). Cells acquire additional mutations such as *KRAS*, *TP53* and loss of parts of 18q. These additional mutations conduce to the multistep process of carcinogenesis up to the formation of metastases. Adapted from (Kinzler and Vogelstein, 1996; Weinberg, 2007).

1.2.3.4 *Wnt signaling pathway activity in human tumors - the β -catenin paradox*

Translating these findings into human tumors it turns out that the situation is more complex. Although the activating mutation of the Wnt signaling pathway is an early event in the tumorigenesis and therefore, all tumor cells possess this mutation, only a subset of the tumor cells shows a nuclear localization of β -catenin and thus, expression of β -catenin

target genes indicating an additional regulating force. This phenomenon is called β -catenin paradox (Fodde and Brabletz, 2007). The tumor cells with nuclear β -catenin reside near the stroma (stromal myofibroblasts) of the invasive front of CRCs which provides Wnt and other cytokines and growth factors such as hepatocyte growth factor (HGF) (Vermeulen et al., 2010) and seem to be responsible for the tumor progression and metastases formation (Fodde and Brabletz, 2007). In central areas of the tumor, however, tumor cells show cytoplasmatic β -catenin, are differentiated (Brabletz et al., 2005) and have lost the tumorigenic potential (Vermeulen et al., 2010). Therefore, there are two different populations of cancer cells in a tumor: the cells without nuclear β -catenin which are located in the central parts of the tumor and the cells with nuclear β -catenin and thus, expression of β -catenin target genes which reside at the interface between normal and neoplastic tissue and represent the minority of cancer cells.

1.2.3.5 *Cancer stem cells*

For the sake of simplification, all cells with properties of cancer stem cells (CSCs) are termed subsequently CSCs.

Nuclear β -catenin, reflecting an active Wnt signaling pathway, defines cancer cells as CSCs (Vermeulen et al., 2010). CSCs are regarded as the origin of cancer (Barker et al., 2007). The existence of CSCs was first discovered in the acute myeloid leukemia (Bonnet and Dick, 1997) but later found also in solid tumors (Al-Hajj et al., 2003; Singh et al., 2004) such as CRC (Ricci-Vitiani et al., 2007). CSCs are characterized by several fundamental properties. 1) Only a few cells down to a single cell (Vermeulen et al., 2010) can initiate a tumor when implanted into immunodeficient recipient mice (O'Brien et al., 2007; Ricci-Vitiani et al., 2007). 2) Furthermore, CSCs are characterized by asymmetric division. By this they self-renew and generate differentiated cells at the same time (Marjanovic et al., 2013). 3) CSCs can proliferate and grow unlimited (Frank et al., 2010). 4) In CRC, CSCs can be defined and isolated due to their different marker profile characterized by high amounts of SC markers such as prominin 1 (PROM1, CD133) (O'Brien et al., 2007; Ricci-Vitiani et al., 2007), aldehyde dehydrogenase 1 (ALDH1A1; subsequently termed as ALDH1) (Huang et al., 2009) or CD44 (Du et al., 2008). Most importantly they initiate tumor growth with high incidences compared to tumor cells without high levels of these markers. All these features such as activity of the Wnt

signaling pathway activity, self-renewal, unlimited growth, initiation of new tumors and high amounts of SC markers are defined as cancer stemness features.

The CSC model implies that only CSCs which are a small fraction of tumor cells can drive the growth and progression of the tumor. Therefore, a cellular hierarchy with the CSCs at the top exists in tumors. The CSCs yield by asymmetric cell division both CSCs and differentiated cells by which the tumor mass grows (Fig. 8) (Marjanovic et al., 2013). CSCs originate from adult stem cells by oncogenic transformation (Barker et al., 2009). Alternatively, CSCs can also develop in an inflammatory context as inflammatory regulators can induce EMT by which tumor cells can be shifted into a state of cancer stemness (Marjanovic et al., 2013). This was shown for the inflammatory factor NF- κ B (nuclear factor 'kappa-light-chain-enhancer' of activated B-cells) which enhanced Wnt signaling pathway and thus, induced EMT or dedifferentiation and acquisition of tumor-initiating capacities (Schwitalla et al., 2013). Alternatively, signals from the environment (stromal myofibroblast derived factors) like HGF can also induce EMT and thereby the transdifferentiation of more differentiated tumor cells in CSCs which can initiate tumor growth (Vermeulen et al., 2010). Taken together, differentiated cells (non-CSCs) can transdifferentiate to create CSCs by a dedifferentiation process caused by intrinsic (e.g. mutation) or extrinsic features (e.g. environmental stimuli) throughout tumorigenesis. This is known as the plastic CSC model (Fig.8) (Marjanovic et al., 2013).

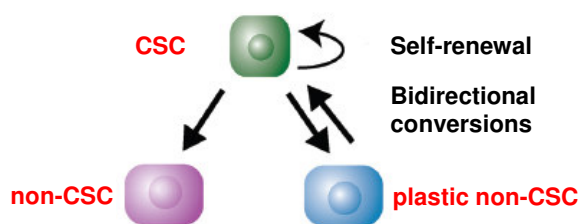


Fig. 8. The plastic CSC model.

This model describes that not only differentiated cells (non-CSCs) arise from the CSCs but rather bidirectional conversions exist. Thereby, also non-CSCs can shift to CSCs throughout tumorigenesis. Adapted from (Marjanovic et al., 2013).

Interestingly, the features of stemness which include proliferation are regulated by β -catenin target genes (Du et al., 2008; He et al., 1998; Shtutman et al., 1999). These genes are activated early and can be expressed throughout all progression steps. Additional mutations like *KRAS* (Horst et al., 2012) or environmental signals can further boost the Wnt signaling pathway (Brabletz et al., 2009; Vermeulen et al., 2010). Histologically, tumor cells with nuclear localization of β -catenin are found focally all over the tumor in small nests and predominantly as a small rim at the invasive front of CRCs (Brabletz et al., 2001; Brabletz et al., 2005) (Fig. 9). Only the cells at the invasive front seem to have a

functional role as their amounts correlate very well with poor prognosis (Ueno et al., 2002). Thus, two types of CSCs were defined, namely the stationary CSCs (SCS cells) found in the central areas of CRCs and the migratory CSCs (MCS cells) found frequently at the invasive front of CRCs (Fig. 9). Due to their exposed location these cells are attributed to be malignant as they can obviously migrate and invade the normal stroma containing blood and lymph vessels.

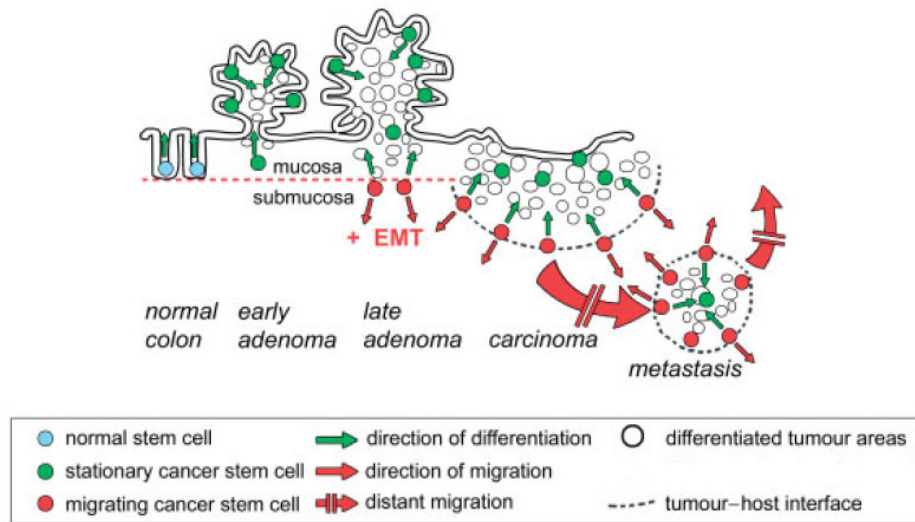


Fig. 9. Concept of stationary and migrating cancer stem cells (SCS and MCS cells).

Cells with nuclear localization of β -catenin are characterized by stemness and proliferation and are named CSCs. At the invasion front, CSCs show a boost of Wnt signaling pathway activity. Here, CSCs are characterized by growth arrest (CDKN2A), EMT (ZEB1) and prerequisites for metastasis (migration and invasion). These CSCs are named MCS cells and require properties which enable them to the process of metastasis (Brabletz et al., 2009).

1.2.3.6 Epithelial mesenchymal transition (EMT)

Interestingly, induction of EMT in tumor cells is related to the induction of properties of cancer stemness (Mani et al., 2008). Originally, EMT and the reverse process, mesenchymal-epithelial transition (MET), are known to be important processes in the embryogenesis during gastrulation but also wound healing (Thiery, 2003; Thiery et al., 2009). Different transcription factors such as snail family zinc finger 1 (SNAI1; SNAIL), snail family zinc finger 2 (SNAI2; SLUG), twist family bHLH transcription factor 1 (TWIST1; TWIST), and ZEB1/2 (Hanahan and Weinberg, 2011) are known to be responsible for the induction of the EMT process and these are considered to be master switches of EMT. Thus, simply by the presence of high amounts of these transcription factors, tumor cells undergo EMT and acquire malignant properties such as invasiveness,

motility, resistance to apoptosis and expression of genes encoding for matrix-degrading enzymes (Cheng et al., 2007; Hanahan and Weinberg, 2011; Huber et al., 2005). Again β -catenin is also involved in the regulation of EMT either by translocation of β -catenin from adherens junctions to the nucleus or by induction of the expression of factors like *SLUG* (Conacci-Sorrell et al., 2003) and *ZEB1* (Spaderna et al., 2008). This leads passively (loss of β -catenin from the zonula adherens) or actively (influencing the expression of EMT master switches) to EMT. *SLUG* and *ZEB1* in turn repress the expression of E-cadherin (*CDH1*) and consequently, E-cadherin becomes absent thus, resulting in the loss of adherens junctions (Brabletz et al., 2005). As adherens junctions are an important component of the polarity mediating apical junctional complex, loss of adherens junctions disturbs cell polarity (Royer and Lu, 2011). Furthermore, the protein complexes par-3 family cell polarity regulator (*PARD3*), crumbs (*CRB*) and scribbled planar cell polarity protein (*SCRIB*) which participate in the apicobasal polarity are repressed by EMT transcription factors such as *SNAIL* and *ZEB1* (Thiery et al., 2009). These changes lead to the loss of cell polarity. Additionally, nuclear β -catenin induces the expression of the mesenchymal markers vimentin (*VIM*) (Gilles et al., 2003) and fibronectin (*FNI*) (Gradl et al., 1999). These changes taking place during EMT lead to a cell morphology change from a polygonal epithelial phenotype to a more spindly mesenchymal phenotype (Hanahan and Weinberg, 2011). Thus, the cells detach from each other and cell sheets disassemble (Hanahan and Weinberg, 2011; Spaderna et al., 2008). As the expression of e.g. N-cadherin (*CDH2*), normally expressed during organogenesis in mesenchymal cells and in migrating neurons, is moreover acquired during the process of EMT, the cells gain invasion and migration capacities (Hanahan and Weinberg, 2011) which are important for metastasis.

1.2.3.7 *Metastasis*

Tumor budding that means tumor cells at the invasion front (MCS cells) are correlated with metastases and poor survival (Brabletz et al., 2005; Christofori, 2006; Ueno et al., 2002). For metastases formation, different gene programs are required. Besides the previously described EMT program which supports the tumor cells at the invasion front to disseminate from the primary tumor to metastatic sites and also to form micrometastases (Hanahan and Weinberg, 2011), stemness associated genes enable tumor cells to colonize foreign tissues and to form metastases (Brabletz et al., 2005). Metastases formation and

invasion can be grouped in different succeeding steps. The cancer cells at the invasion front migrate and invade due to EMT into the host stroma and intravasate finally into lymphatic and blood vessels. There, the cells circulate until they extravasate from the lumina of the vessels into organ parenchyma. In distant tissues CSCs can form micrometastases (Hanahan and Weinberg, 2011; Talmadge and Fidler, 2010). For the outgrowth of the metastases, the tumor cells regain differentiation. Whereas CSCs at the invasion front (MCS cells) are dedifferentiated due to EMT and show growth arrest due to expression of the β -catenin target gene *CDKN2A* (Jung et al., 2001; Wassermann et al., 2009), cells require cellular differentiation and proliferation for the outgrowth of metastases. Thus, they undergo MET at metastatic sites which becomes apparent by the reexpression of *CDHI* (Brabletz et al., 2005).

1.2.3.8 Chemoresistance

Metastases of CRCs are usually targeted by chemotherapy. Unfortunately, metastasis related deaths are caused due to the resistance of the tumor cells to chemotherapeutics (Marjanovic et al., 2013). Interestingly, CSCs are characterized by intrinsic chemoresistance (Brabletz et al., 2005). Therefore, whereas the majority of tumor cells is killed by chemotherapy, CSCs resist the chemotherapy and stay alive (Dean et al., 2005). β -catenin target genes are involved in chemoresistance. For example the increased expression of ATP binding cassette (ABC) transporters such as *ABCB1* (Yamada et al., 2000) leads to improved efflux of drugs (Dean et al., 2005; Frank et al., 2010) as ABC transporter can actively transport drugs and cytotoxic agents out of the cells to protect these (Dean et al., 2005). Furthermore, tumor cells that withstand chemotherapy show a higher expression of genes associated with stemness (Hanahan and Weinberg, 2011) such as *CD44* (Wielenga et al., 1999) and EMT (Creighton et al., 2009; Singh and Settleman, 2010) such as *ZEB1* (Sanchez-Tillo et al., 2011). Since CSCs survive chemotherapy, this results in an accumulation of CSCs in colon tumors (Dylla et al., 2008). Due to its drug resistance, CSCs can enable a relapse of the tumor (Singh and Settleman, 2010).

Taken together, CSCs are the kingpin in the process of colorectal carcinogenesis. Cancer stemness is equivalent to metastases formation, EMT and chemoresistance (Mani et al., 2008; Singh and Settleman, 2010). In the colorectum, tumor cells with characteristics of CSCs are characterized by the nuclear localization of β -catenin and can therefore be

identified also histologically. Mostly, a direct connection between chemoresistance and metastasis and the question whether chemoresistance induces metastasis have not been clarified so far but it might be speculated that they are also related to each other as two other facets of cancer stemness (Fig. 10).

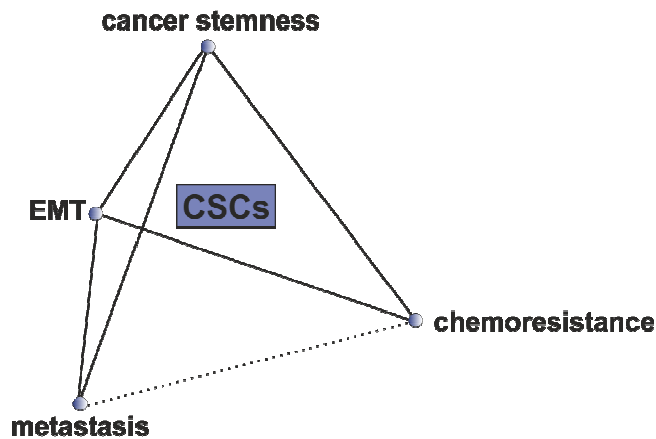


Fig. 10. Model of the CSC features.

CSCs are characterized by the features cancer stemness, metastasis, EMT and chemoresistance. Most of these features are associated with each other and are all influenced by the other features (solid lines). Only the direct connection between chemoresistance and metastasis is not yet clarified (dotted line).

1.2.4 Treatment of CRC

1.2.4.1 Classical chemotherapy

Classical chemotherapy affects rapidly dividing cells what tumor cells are believed to be. It can be used for the treatment of cancer before (neo-adjuvant setting) and/or after surgery (adjuvant therapy), after recurrence or after metastasis (adjuvant second and following lines of therapy). For the treatment of CRC, the antimetabolite drug 5-fluoruracil (5-FU) is widely used which is a fluoropyrimidine where the 5'-hydrogen is replaced by a fluorine. In living cells, 5-FU is converted into active metabolites which can disrupt DNA replication and DNA repair as well as inhibit thymidylate synthetase (Longley et al., 2003). However, as cancers often become resistant to therapies the reason for this might be the CSCs which are known to be resistant to classical chemotherapeutics (Marjanovic et al., 2013). Thus, most anticancer drugs destroy only the bulk of the tumor cells whereas CSCs survive. Therefore, the tumor can start growth again out of the CSC compartment, increase its size and finally form metastases (Fig. 11). In the cases of resistance to classical chemotherapy few or no therapeutic alternatives exist (Fanali et al., 2014; Marjanovic et al., 2013).

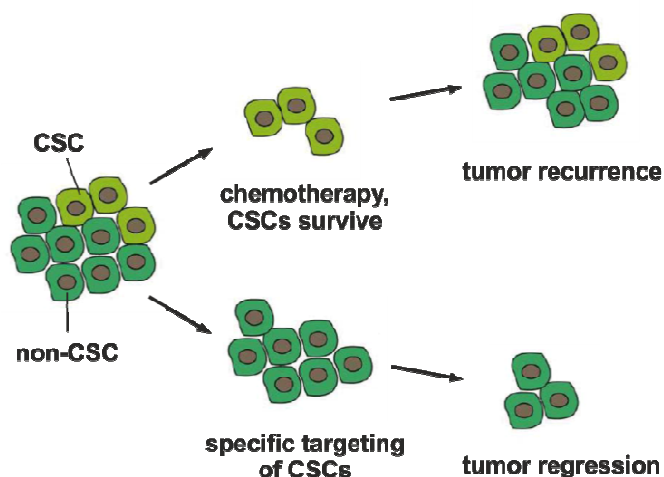


Fig. 11. CSC-specific therapy as a new therapeutic approach.

Most anticancer drugs kill only the bulk population but the resistant CSC pool survives and can repopulate the tumor. In contrast, therapies that target specifically CSCs can kill CSCs whereby the tumor regresses. Modified from (Fanali et al., 2014).

1.2.4.2 CSC targeted therapy

An alternative and a promising therapeutic concept might become CSC targeted therapies that kill the driving force of tumors and thus, leading to their regression (Fig. 11) (Fanali et al., 2014; Frank et al., 2010). As CSCs are characterized by the features cancer stemness, EMT, metastasis and chemoresistance and most if not all of these features are connected with each other, these features are suitable as a target for the CSC targeted therapy. There are several different possible approaches for CSC targeted therapies: 1) One therapeutic approach is to reverse resistance mechanisms that are active in CSCs such as the blockade of multidrug resistance ABC transporters which results in decreased resistance (Frank et al., 2005). 2) Another approach to target CSCs is the differentiation of CSCs whereby the cells undergo a MET and lose, therefore, cancer stemness features and chemoresistance (Singh and Settleman, 2010). For example, the compound salinomycin (Gupta et al., 2009) and microRNAs (miRNAs) such as *let-7* (Yu et al., 2007) led to differentiation of CSCs whereby the expression of CSC markers and the tumor growth decreased. Moreover, BMP4 activated differentiation and stimulated apoptosis in CSCs led in combination with chemotherapeutics to complete, long-term regression of tumors (Todaro et al., 2010). 3) A third approach for the targeting of CSCs is the interference of CSC sustaining molecules. The blockade of the SC marker CD44 inhibited tumor formation (Yang et al., 2008). CSC sustaining molecules are suitable as a therapeutic target since their expression is often restricted to SCs such as CSCs. Because various CSC sustaining molecules are known as SC factors, the investigation of these factors concerning their role in CRC and thus, therapeutic relevance might be a promising tool. And as stemness is associated with the

other CSC features metastasis, EMT and chemoresistance, the interference with stemness should also influence the other features.

1.3 Olfactomedin-4 (OLFM4) and its role in cancer

One molecule that is discussed as a CSC marker is olfactomedin-4 (OLFM4). OLFM4 was originally described as a SC marker in the human intestine. *OLFM4* is expressed in CBC cells which are also characterized by the expression of the SC marker *LGR5*. Therefore, a comparable role of OLFM4 was discussed (van der Flier et al., 2009). Since CSCs can originate by oncogenic transformation from normal tissue SCs such as the CBC cells (Barker et al., 2009), the investigation of SC markers whether they are CSC sustaining and therefore, suitable for CSC targeted therapy is a promising approach.

1.3.1 Characterization of *OLFM4*

OLFM4 (also GW112, hGC-1 or OlfD) belongs to the olfactomedin (OLFM) family which is connected with various functions such as cell adhesion, cytoskeleton organization, cell proliferation, dorsal-ventral patterning and apoptosis. The *OLFM4* gene is located on the chromosome 13q14.3, is 23 kb long and composed of five exons. The translated protein consists of 510 amino acids, has a signal peptide and a molecular mass of about 54 kDa. After translation, the protein undergoes post-translational modifications which come along with the loss of the signal peptide and with the N-linked glycosylation at six glycosylation motifs. At the C-terminus, the protein contains the olfactomedin domain that is involved in the interaction of OLFM4 with cadherins (Fig. 12) (Grover et al., 2010; Zhang et al., 2002).

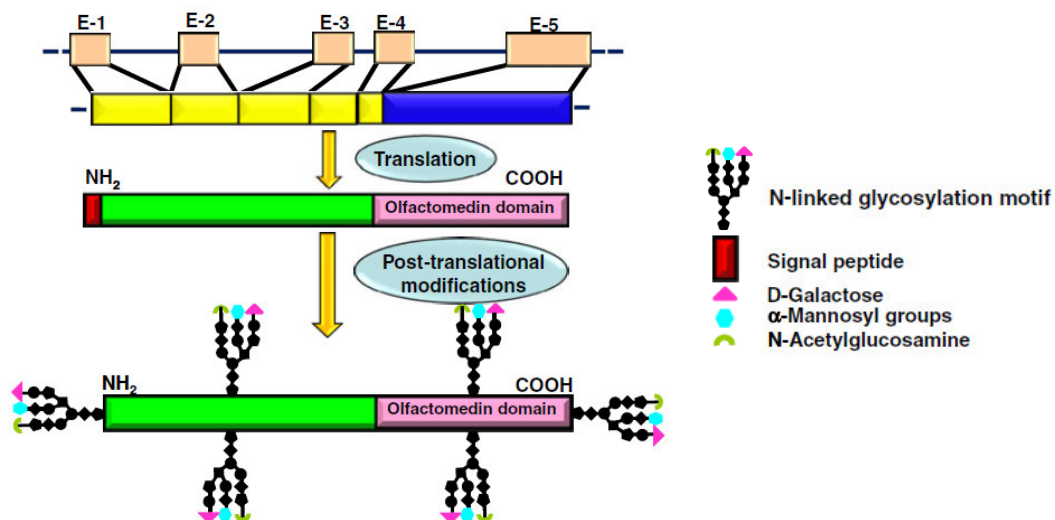


Fig. 12. Gene and protein structure of OLFM4.

The gene is composed of five exons and is translated in a protein with 510 amino acids. This protein undergoes post-translational modifications such as glycosylations. At the C-terminus of the protein, the olfactomedin domain is located. Modified from (Grover et al., 2010).

The intracellular localization of the OLFM4 protein is unclear since different studies reported different results. In one study, the protein was found to be localized in the mitochondria and in the nuclei (Zhang et al., 2004), in another study a localization of OLFM4 in the peri-nuclear cytoplasm and at the cell membrane was observed. It functions as an extracellular matrix glycoprotein (Grover et al., 2010; Zeng et al., 2005), interacts with lectins and cadherins and facilitates thereby cell adhesion (Liu et al., 2006). *OLFM4* expression is regulated by the transcription factor NF- κ B that is involved in the regulation of immune and inflammatory signals (Kim et al., 2010). High amounts of OLFM4 protein were found in the prostate, the small intestine and the colon (Grover et al., 2010; Tomarev and Nakaya, 2009). In the normal intestinal mucosa, *OLFM4* is preferentially expressed at the crypt base in the stem cell niche in CBC cells of the small intestine and colon whereby a comparable role of OLFM4 with LGR5 was discussed (van der Flier et al., 2009). However, another investigation proposed that OLFM4 is not associated with LGR5 positive CBC cells and consequently, no analogous role of OLFM4 and LGR5 can be declared (Ziskin et al., 2013). A knockout of *Olfm4* in mice did not show any detectable phenotype (Schuijers et al., 2014). In contrast, the knockout of *Lgr5* was neonatally lethal (Morita et al., 2004) which is indicative of different roles of OLFM4 and LGR5.

1.3.2 *OLFM4 in association with cancer*

1.3.2.1 *The role and expression/protein levels of OLFM4 are dependent on the cancer type*

The mRNA expression and protein levels of OLFM4 in tumors depend on the tissue. A higher expression of *OLFM4* compared to normal tissue was reported in several cancer tissues such as breast, lung, pancreatic and stomach cancer tissue (Koshida et al., 2007; Zhang et al., 2004). In contrast, *OLFM4* expression was reduced or undetectable in prostate cancer and correlated with advanced tumor stages (Chen et al., 2011; Li et al., 2013). This reduced expression together with another study in which OLFM4 protein levels were described as a prognostic biomarker for differentiation in gastric cancer (Liu et al., 2007) are unexpected results for a SC marker. Moreover, OLFM4 negative tumors were associated with a worse survival rate of patients than OLFM4 positive gastric tumors (Luo et al., 2011; Oue et al., 2009) which was unexpected for a possible marker of cancer stemness. Thus, in most of these studies, OLFM4 did not act like a CSC marker since the expression of CSC markers is usually connected with advanced tumor stages and poor survival.

An inconsistent role of OLFM4 in cancer cell lines was also described. OLFM4 acted as an anti-apoptotic protein in different cancer types such as cervix or gastric cancer (Kim et al., 2010; Liu et al., 2012; Zhang et al., 2004), however this was not observed in pancreatic cancer cells (Kobayashi et al., 2007). On the one hand, OLFM4 was described as a tumor promoter because OLFM4 was necessary for proliferation, anchorage-independent growth and growth as xenografts in gastric cancer cell lines (Kobayashi et al., 2007; Liu et al., 2012). On the other hand, OLFM4 was described as a tumor suppressor because it suppressed proliferation, tumor growth, invasiveness and metastases formation in prostate cancer and melanomas (Chen et al., 2011; Park et al., 2012). Thus, the role and function of OLFM4 is also unclear in different cancer cell lines.

1.3.2.2 *The role of OLFM4 in CRC*

In CRC, a higher expression of *OLFM4* compared to normal tissue was reported (Koshida et al., 2007). In contrast, well-differentiated colorectal tumors exhibited an increased *OLFM4* expression and OLFM4 protein levels, whereas poorly differentiated tumors and metastases showed a reduced *OLFM4* expression/OLFM4 protein levels (Besson et al.,

2011; Liu et al., 2008; Wentzensen et al., 2004). At the invasion front, both, reduction of OLFM4 (Liu et al., 2008) and no loss or reduction of OLFM4 (Seko et al., 2010) were observed. Moreover, OLFM4 protein amounts were described in CRC as nonmetastatic marker (Besson et al., 2011) and OLFM4 negative tumors had a worse survival rate than OLFM4 positive tumors (Seko et al., 2010) which is again not indicative for a possible marker of cancer stemness. Furthermore, it was reported that high amounts of OLFM4 protein caused an alteration in the actin cytoskeleton and the cell morphology and a suppression of cell adhesion and migration (Liu et al., 2008). Hence, based on these studies, the role of OLFM4 in CRC is not yet completely understood. Further investigations have to show whether OLFM4 is a CSC marker (van der Flier et al., 2009) and thus, has a prognostic impact in CRC or whether OLFM4 is not a CSC marker (Ziskin et al., 2013). Moreover, its functional role has to be further examined to clarify whether OLFM4 is a driver or only a passenger in CRC. The investigation of OLFM4 as a CSC marker and its influence in CRC on CSC features would help to clarify its utility as a therapeutic target for CSC therapy.

1.4 Non-coding RNAs in colorectal cancer

Besides the previously described role of β -catenin in the transcription of mRNAs which plays a crucial role in CSC biology, a role of β -catenin in the transcription of non-coding RNAs (ncRNAs) is also conceivable. However, until now, the involvement of the transcription factor β -catenin in the expression of ncRNAs has only been minorly investigated. ncRNAs control gene expression (Mattick and Makunin, 2006) and comprise e.g. miRNAs, small nucleolar RNAs (snoRNAs), PIWI-interacting RNAs (piRNAs) and large intergenic non-coding RNAs (lincRNAs) (Esteller, 2011).

1.4.1 *The microRNAome*

Among these ncRNAs, the miRNAs are mostly investigated (Esteller, 2011). Mammalian miRNAs can modulate more than 60% of genes that are coding for proteins (Melo and Kalluri, 2012) and mediate mostly gene silencing by controlling the translation of mRNAs into proteins (Esteller, 2011; Vasudevan et al., 2007). Thereby, a large number of target

mRNAs can be downregulated by the same miRNA. Over 1000 miRNAs exist in the cells of higher plants and animals (Filipowicz et al., 2008) and are involved in most cellular processes (Esteller, 2011). In cancer cells a global downregulation of miRNAs takes place (Lu et al., 2005). A transcriptional regulation leading to loss of the miRNAome (miRNAome) is possible. In this context, a transcriptional role of β -catenin in miRNA repression was reported in a study in which β -catenin repressed the tumor suppressor miRNA *let-7* (Cai et al., 2013). Further miRNA targets of β -catenin are possible which repression might e.g. lead to an upregulation of oncogenes, stemness sustaining molecules or EMT transcription factors and thus, to tumor promotion. As miRNAs repress e.g. EMT and metastatic features (Korpál et al., 2008; Siemens et al., 2011), a transcriptional repression of the miRNAome by β -catenin would support CSC features. Thus, downregulation of the miRNAome might be an additional feature that characterizes CSCs.

Besides a possible transcriptional repression of miRNAs, a downregulation of DROSHA (drosha, ribonuclease type III) or DICER1 (dicer 1, ribonuclease type III) or mutations in *XPO5* (exportin 5) or *TRBP* (TAR RNA-binding protein), that are components of the miRNA biogenesis, were reported (Lujambio and Lowe, 2012). Because the miRNA biogenesis is essential for a functioning miRNAome, disruption of the miRNA biogenesis leads to a loss of the miRNAome which might again result in increased CSC features such as EMT and metastatic features (Korpál et al., 2008; Siemens et al., 2011). Thus, investigations of the loss of the miRNAome might clarify whether the miRNAome might be a promising target for CSC targeted therapy.

1.4.2 *miRNA biogenesis*

The working miRNA biogenesis is an essential prerequisite for the maturation and thus, function of the miRNAome. During the canonical biogenesis, miRNAs pass through different steps (Fig. 13). In the beginning, primary miRNAs (pri-miRNAs) are transcribed by the RNA polymerase II from miRNA genes (Esquela-Kerscher and Slack, 2006). One pri-miRNA can comprise sequences for different miRNAs. Afterwards, the pri-miRNAs are folded into hairpin structures that consist of base-paired stems that do not match perfectly. Next, the RNase III enzyme DROSHA processes together with its partner DiGeorge syndrome critical region gene 8 (DGCR8) the pri-miRNAs to about 70 nucleotide hairpins, the pre-miRNAs (Filipowicz et al., 2008). Subsequently, exportin 5 transports the pre-miRNAs from the nucleus to the cytoplasm where they are further

processed. DICER1 interacts with TRBP and cleaves off the loop of the hairpin of the pre-miRNAs whereby 20-25 nucleotides long miRNA-miRNA*-duplexes are produced (Barca-Mayo and Lu, 2012; Esquela-Kerscher and Slack, 2006). Subsequently, the passenger strand (miRNA*) is degraded and the other strands are loaded onto the argonaute (AGO) proteins containing miRNA-associated multiprotein RNA-induced silencing complex (miRISC) and functions as mature miRNA (Dueck and Meister, 2010). The mature miRNA binds to complementary sites in the mRNA target. If the miRNAs can bind with imperfect complementarity, the protein translation of the target gene is repressed. The binding sites for this mechanism are commonly found in the 3' untranslated regions (3'UTR). In the case of perfect complementarity, the cleavage of the mRNA is induced. These binding sites are commonly found in the open reading frame (ORF) of the targeted mRNA. The interaction between miRNA and mRNA target takes place by the pairing of the nucleotides 2–8 of the miRNAs, the 'seed' region, with the mRNA target site (Esquela-Kerscher and Slack, 2006).

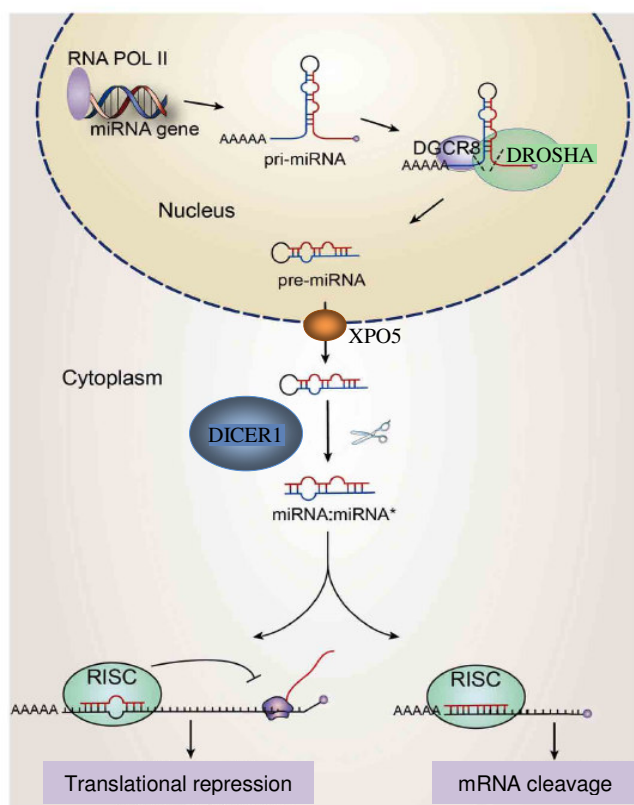


Fig. 13. The canonical biogenesis of miRNAs.

Pri-miRNAs are transcribed from the miRNA gene by the RNA Polymerase II. Subsequently, the pri-miRNAs are processed by DROSHA together with DGCR8. The resultant pre-miRNAs are transported by XPO5 from the nucleus to the cytoplasm. There, the hairpin of the pre-miRNAs is cleaved by DICER1 together with TRBP into a miRNA-miRNA* duplex without hairpin. The mature strand is incorporated into the miRISC, the passenger strand (miRNA*) is degraded. An imperfect complementary binding between miRNA and mRNA results in translational repression (binding in the 3'UTR), a perfect complementary binding results in mRNA cleavage (binding in the ORF). Modified from (Barca-Mayo and Lu, 2012))

1.4.3 *DICER1*

During miRNA biogenesis, DICER1 possesses different functions and thus, a central role. DICER1 cleaves during miRNA biogenesis precursor miRNA (pre-miRNA) hairpins into

mature miRNAs, is responsible for loading of small RNAs onto AGO proteins in the RNA-induced silencing complex (RISC) and additionally, DICER1 is involved in the protein-protein interactions between the RISC-loading complex and other complexes (Foulkes et al., 2014). Thus, DICER1 has an essential role in the biogenesis of miRNAs and is therefore a good target to investigate the influence of a disruption of the miRNA biogenesis and thus, the loss of the miRNAome in cancer.

The *DICER1* gene is located on chromosome 14q32.13 and consists of 27 exons (Fig. 14A). The multi-domain enzyme of 219 kDa assembles in a L-like structure. At the upper half of the L, the Platform and PAZ (piwi, argonaute, zwiille) domains are located and form binding pockets for the 5'-phosphate and 3'-overhang parts of a dsRNA substrate, respectively. At the lower half of the L, both RNase III domains, RNase IIIa and RNase IIIb, are located which build a dimer and form the catalytic core. Each strand of the dsRNA substrate is cleaved by one RNase III domain. The helicase domain is placed at the bottom of the L, folds a clamp-like structure and is probably designated to reorganize and wind around the dsRNA (Fig. 14B) (Foulkes et al., 2014).

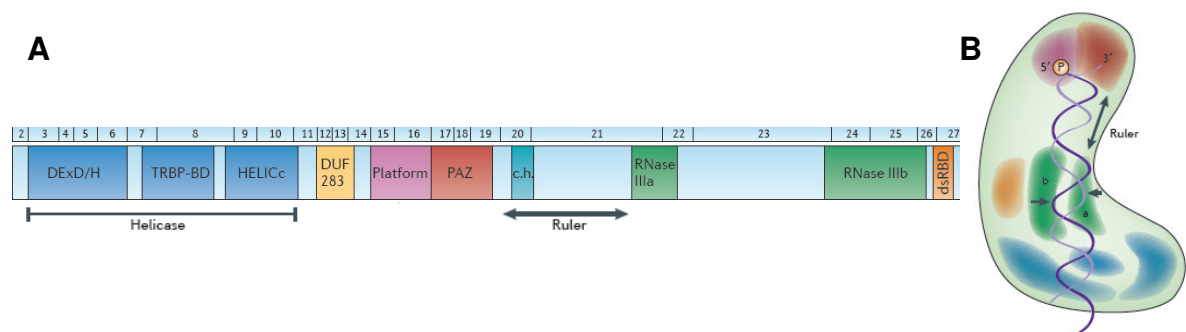


Fig. 14. Structure and domains of DICER1.

(A) Schema of the unfolded protein structure. *DICER1* is constituted of 27 exons and is encoding several domains. (B) Domain organization of the folded, L-shaped DICER1 protein. Colors of the domains correspond with those of the linear form in (A). Platform and PAZ domains build binding pockets for the 5'-phosphate and 3'-overhang parts of a dsRNA substrate, respectively. RNase IIIa and IIIb domains build a dimer and the catalytic core for the cleavage of the dsRNA substrate. The clamp-like helicase domain reorganizes and winds around the dsRNA. Modified from (Foulkes et al., 2014).

For the investigation of the consequences of a *DICER1* disruption and thus, miRNAome loss several models exist. One example is a cell culture model in which the helicase domain (exon 5) of *DICER1* is disrupted and thus, the DICER1 function is impaired. Hence, these cells show an impaired miRNA biogenesis. Furthermore, a conditional, Cre

inducible knockout mouse model was generated as the complete loss of DICER1 in the embryogenesis resulted in early lethality at embryonic day 7.5 (Bernstein et al., 2003). For that reason, loxP (flox, fl) sites are inserted around the second RNaseIII domain of *Dicer1*. The floxed *Dicer1* alleles can be removed in any tissue in which the Cre recombinase (*Cre*) is expressed. By the recombination, mediated by the Cre recombinase, a gene region encoding 90 aa is removed and thus, the enzymatic activity of DICER1 is destroyed. Hence, the miRNA biogenesis is disturbed and almost no mature miRNA levels are still detectable (Harfe et al., 2005). Thus, these models are suitable tools for the investigation of the role of DICER1 and thus, the miRNAome in the biology of colorectal tumorigenesis.

1.4.4 *DICER1 and miRNAs in cancer*

The function of DICER1 in cancer development and progression depends on the tissue type. In human lung, ovarian and colorectal cancer, a deletion or decreased expression of *DICER1* took place and was associated with poorly differentiated tumors, advanced tumor stages and reduced survival (Faggad et al., 2010; Faggad et al., 2012; Karube et al., 2005; Kumar et al., 2009; Merritt et al., 2008). Hence, DICER1 and thus, the miRNAome had a tumor suppressive influence in these contexts. This is in agreement with cell culture studies. For example in breast cancer, sarcoma, lung cancer and CRC cell lines, knockdown of *DICER1* led to inhibition of cell growth, increased apoptosis (Bu et al., 2009; Ravi et al., 2012) and enhanced sensitivity to the chemotherapeutic cisplatin (Bu et al., 2009). Additionally, the downregulation of *DICER1* in lung cancer cell lines was associated with EMT (Hinkal et al., 2011; Iliou et al., 2014; Martello et al., 2010), cell migration and invasion (Martello et al., 2010) and the downregulation of specific miRNAs in colorectal CSCs led to increased stemness (Bitarte et al., 2011). These results suggest that DICER1 and thus, the miRNAome act as tumor suppressors.

In support with this, most of the studies of *Dicer1* knockout in mouse models showed similar results. In these studies, loss of DICER1 and thus, loss of the miRNAome led to cellular transformation, a higher tumor formation, more invasiveness of the tumors and a reduced survival (Kumar et al., 2007; Kumar et al., 2009). Moreover, deletion of *Dicer1* accelerated *in vivo* intestinal inflammation-associated tumorigenesis in a CRC mouse model (Yoshikawa et al., 2013). These tumor promoting features have been reported both after hetero- and homozygous deletion of *Dicer1* (Kumar et al., 2007), but also after only heterozygous deletion (Kumar et al., 2009; Lambertz et al., 2010). In

contrast, in a B-cell lymphoma mouse model, a loss of DICER1 inhibited lymphoma development (Arrate et al., 2010). In most of the mouse models, however, DICER1 and thus, the miRNAome was recognized as an important tumor suppressor.

Human CRCs are mostly driven by the Wnt signaling pathway (Pino and Chung, 2010). However, loss of DICER1 and thus, the miRNAome has not yet been investigated in this context. A mouse model with an activated Wnt signaling pathway combined with a disruption of *Dicer1* and thus, loss of the miRNAome would reflect the human situation best. To follow this idea, two independent recombinational steps would have to be integrated. Therefore, a good approach is to activate the Wnt signaling pathway by the knockout of the tumor suppressor *Apc* and additionally, to delete the whole miRNAome of the cell by the knockout of *Dicer1*. This might especially be a good approach as it was shown that changes in the miRNAome as a whole are transferable to the biology of the tumor entity as mentioned before. Thus, this approach might help to clarify the question whether the miRNAome might be a target for CSC therapy.

1.5 Aims of the study

CSCs are the driver of intestinal cancer and are responsible for metastases formation and chemoresistance. Furthermore, these cells are characterized by the features cancer stemness and EMT. Because CSCs can escape classical chemotherapy, targeted therapy for CSCs could be an alternative to chemotherapy. For the specific targeting of CSCs, the four aforementioned CSC features are suitable for treatment. As most of these features are connected with each other, the interference of one feature might influence also most of the other features.

Due to the importance of functional SC markers (CSC sustaining molecules) as potential additional targets for therapeutic intervention I investigated in this study

- 1) whether OLFM4 is, as discussed, a SC marker.
- 2) Subsequently, I analyzed the expression of *OLFM4* in cells with CSC features and in CRC cell lines.
- 3) Additionally, I examined the effects of high amounts of OLFM4 protein on CSC features such as proliferation, stemness, EMT and metastasis. For that purpose, I

investigated the influence of high amounts of OLFM4 protein concerning SC, EMT and differentiation marker expression/protein levels and on the functional level that means proliferation, activity of the Wnt signaling pathway, ALDH1 activity, tumor initiation and metastasis features.

In a second experimental approach I focused on the role of the miRNAome in colorectal carcinogenesis and the influence on CSC features.

- 1) Therefore, I established a mouse model which allowed the combined knockout of *Apc* and thus, Wnt signaling pathway activation in CBC cells together with knockout of *Dicer1* and thus, loss of the miRNAome. This mouse model should help to understand the role of the influence of the miRNAome in Wnt driven adenomas in a complex *in vivo* situation including microenvironmental factors.
- 2) To shed more light on the underlying mechanism I employed CRC cell lines with a homozygous disruption of *DICER1* to study CSC, EMT and metastases marker expression/protein levels and also on a functional level proliferation and CSC features such as stemness, chemoresistance and metastatic properties.
- 3) Furthermore, I translated these results into human CRC disease.

2 Materials and Methods

2.1 Materials

2.1.1 Chemicals

<i>Chemical</i>	<i>Company</i>
5-fluorouracil (5-FU)	Sigma-Aldrich; medac GmbH
acrylamide rotiphorese gel30	Carl Roth GmbH
agar	Carl Roth GmbH
agarose	Biozym
ammoniumpersulfate (APS)	Sigma-Aldrich
dimethylformamide	Carl Roth GmbH
ampicillin	Sigma-Aldrich
dimethyl sulfoxide (DMSO)	Sigma-Aldrich
eosin Y	Sigma-Aldrich
ethylenediaminetetraacetic acid solution (EDTA)	Sigma-Aldrich
ethanol	Carl Roth GmbH
ethidium bromide	Sigma-Aldrich
formaldehyde	Carl Roth GmbH
glutaraldehyde 50 %	Carl Roth GmbH
glycine	Carl Roth GmbH
hydrochloric acid solution (HCl) 1N	Sigma-Aldrich
isopropanol	Carl Roth GmbH
kanamycin	Sigma-Aldrich
lysogeny broth (LB) medium	Carl Roth GmbH
magnesium chloride (MgCl ₂)	Carl Roth GmbH
methanol	Carl Roth GmbH
methyl cellulose	Sigma-Aldrich
non-fat dry milk	Bio-Rad
NP40	Sigma-Aldrich
paraformaldehyde	Sigma-Aldrich
polybrene	Sigma-Aldrich
potassium chloride (KCl)	Carl Roth GmbH
potassium dihydrogen phosphate (KH ₂ PO ₄)	Sigma-Aldrich
potassium hexacyanoferrate(III) (K ₃ Fe(CN) ₆)	Sigma-Aldrich
potassium hexacyanoferrate(III) trihydrate (K ₃ Fe(CN) ₆ x 3H ₂ O)	Sigma-Aldrich
hydrochloric acid	Merck
sodium chloride (NaCl)	Carl Roth GmbH
sodium deoxycholate	Sigma-Aldrich
sodium dodecyl sulfate (SDS)	Sigma-Aldrich

sodium hydroxide (NaOH)	Merck
sodium phosphate dibasic heptahydrate (Na ₂ HPO ₄ ·7H ₂ O)	Sigma-Aldrich
tamoxifen	Sigma-Aldrich
TBE (tris/borate/EDTA)	Thermo Scientific
tetramethylethylenediamin (TEMED)	Carl Roth GmbH
tris base	Carl Roth GmbH
tris hydrochloride (Tris-HCl)	Carl Roth GmbH
Triton-X100	Sigma-Aldrich
trypan blue	Sigma-Aldrich
Tween-20	AppliChem GmbH
sunflower seed oil from <i>Helianthus annuus</i>	Sigma-Aldrich
X-Gal (5-bromo-4-chloro-3-indoxyl-β-D-galactopyranoside)	Carl Roth GmbH
xylene	Carl Roth GmbH

2.1.2 Reagents and Kits

Reagent or Kit	Company
AEC (3-Amino-9-ethylcarbazole) solution	Invitrogen
ALDEFLUOR™ Kit	Stemcell Technologies
CellTiter 96® Non-Radioactive Cell Proliferation Assay	Promega
Complete® protease inhibitor	Roche
DAB+ (3,3'-diaminobenzidine) Chromogen	Dako
DC™ Protein Assay	Bio-Rad
DCS Crystal MausBlock	DCS
dNTP Mix, 10 mM each	Thermo Scientific
dual luciferase reporter assay	Promega
DyeEx 2.0 Spin Kit	Qiagen
Epitope Retrieval Solution (ERS6)	Novocastra
ExiLENT SYBR Green Master Mix	Exiqon
FastDigest <i>Bam</i> HI	Thermo Scientific
FastDigest <i>Not</i> I	Thermo Scientific
FirePol DNA polymerase	Solis BioDyne
Fugene 6	Promega
Gateway LR Clonase Enzyme Mix	Life Technologies
Hematoxyline Gill's Formula	Vector
HiDi (highly deionized) formamide	Life Technologies
Hot Start Taq DNA polymerase	Fermentas
Immobilon™ Western Chemiluminescent HRP (<i>Horseradish peroxidase</i>) substrate (ECL (Enhanced chemi-luminescence))	Millipore

ImmPRESS Reagent Kit anti-rabbit Ig	Vector
ImmPRESS Reagent Kit anti-mouse Ig	Vector
Kaiser's glycerol gelatine	Merck
KOD DNA polymerase	Novagen
Lipofectamine RNAi Max	Invitrogen
MinElute PCR Purification Kit	Qiagen
mitomycin C	Sigma-Aldrich
miRNeasy Mini Kit	Qiagen
ProLong Gold antifade reagent with DAPI (4',6'-diamidino-2-phenylindole)	Life Technologies
propidium iodide (PI) solution	Sigma-Aldrich
ProTaqS IV Antigen Enhancer	Quartett
Proteinase Type XXIV	Sigma-Aldrich
protein block	Dako
PureYield™ Plasmid Midiprep System	Promega
QIAamp® DNA FFPE Tissue Kit	Qiagen
QIAprep Spin Miniprep Kit	Qiagen
QIAquick Gel Extraction Kit	Qiagen
QIAquick PCR Purification Kit	Qiagen
RevertAid Reverse Transcriptase	Thermo Scientific
RiboLock RNase Inhibitor	Thermo Scientific
RNase A	Sigma-Aldrich
RNeasy Mini Kit	Qiagen
rotiload loading buffer	Carl Roth GmbH
shrimps alkaline phosphatase (SAP)	Thermo Scientific
streptavidin HRP	Novocastra
Target Retrieval Solution	Dako
Universal cDNA Synthesis Kit II	Exiqon
Universal Probe Library	Roche
VectaMount Mounting Medium	Vector
XT ultraView DAB Kit	Ventana Medical Systems

2.1.3 Consumables

Consumables	Company
cell culture flasks, plates, dishes	Corning Incorporated
cover slips	Carl Roth GmbH
filter	Sartorius AG
ibidi chamber	ibidi
needles	B. Braun Melsungen AG
pipette tips	Biozym Scientific GmbH
plates for luciferase reporter assay	Thermo Scientific

PVDF (polyvinylidene difluoride)-membrane 0.2 µm	Bio-Rad
scalpel	Bayha GmbH
superfrost microscope slides	Thermo Scientific
syringes	B. Braun Melsungen AG

2.1.4 *Devices*

<i>Device</i>	<i>Company</i>
ABI 3130	Life Technologies
Axiovert 200M microscope	Zeiss
balance	Sartorius
BD Accuri C6 flow cytometer	Becton & Dickinson
centrifuges	Eppendorf, Thermo Scientific
CF440 Imager	Kodak
DMD108	Leica
FACS Aria® Cell Sorter	Becton & Dickinson
incubator	Thermo Scientific
laminar flow hood	Thermo Scientific
LightCycler® 480	Roche
microscope cell culture	Zeiss
Mini Trans-Blot® Cell system	Bio-Rad
Nanodrop	Thermo Scientific
PCR devices	Eppendorf
pipettes	Eppendorf
Stemi SV6	Zeiss
Tissue Tek TEC	Sakura
Tissue Tek Prisma	Sakura
Varioskan	Thermo Scientific
Ventana Benchmark XT autostainer	Ventana Medical Systems, Roche

2.1.5 *Cell culture*

<i>Medium</i>	<i>Company</i>
DMEM (Dulbecco's Modified Eagle's medium)	Biochrom AG
FCS (fetal calf serum)	Biochrom AG
FGFb (fibroblast growth factor basic)	Life Technologies
penicillin/streptomycin	Biochrom AG
PBS (phosphate buffered saline)	Biochrom AG
RPMI (Roswell Park Memorial Institute medium)	Biochrom AG
StemProR hESC SFM medium	Life Technologies
trypsin	Biochrom AG

2.1.6 DNA and protein size standards

<i>Size standard</i>	<i>Company</i>
GeneRuler 100 bp DNA Ladder	Thermo Scientific
GeneRuler 1 kb DNA Ladder	Thermo Scientific
GeneRuler Low Range DNA Ladder	Thermo Scientific
PageRuler Plus Prestained Protein Ladder	Thermo Scientific

2.1.7 Oligonucleotides

2.1.7.1 Cloning primers

<i>Name</i>	<i>Sequence</i>
<i>Bam</i> HI-Kozak-CAT-FW	5' CATGGATCCGCCGCCACCATGGAGAAAAAATCAC TGG 3'
<i>CAT</i> <i>Not</i> I- REV	5' GTAGCGGCCGCAGCGCCCCGCCCTGCCACTCATC 3'
<i>Bam</i> HI-Kozak- <i>OLFM4</i> - FW	5' CATGGATCCGCCGCCACCATGAGGCCCGGCCTCTCA TTTC 3'
<i>OLFM4</i> - <i>Not</i> I-REV	5' TAGCGGCCGCAGCTGGGGCTTCTGCAAGACAG 3'

2.1.7.2 Sequencing primers

<i>Name</i>	<i>Sequence</i>
<i>OLFM4</i> Seq 1 FW	5' CAGCTCCAGCCGCAGCTTAG 3'
<i>OLFM4</i> Seq 2 REV	5' GTGGTGTCTGGCAGGGAAAC 3'
<i>OLFM4</i> Seq 3 FW	5' GGTAGAAGTGAAGGAGATGG 3'
<i>OLFM4</i> Seq 4 FW	5' GTTCAGCTCAACTGGAGAGG 3'
<i>OLFM4</i> Seq 5 FW	5' CTTTGCTGTGGATGAGAATGG 3'
<i>OLFM4</i> Seq 6 FW	5' CTCATTTCTCCTAGCCCTTC 3'

2.1.7.3 qPCR primers

2.1.7.3.1 qPCR primers for miRNA

hsa-miR-21-5p LNA™ PCR primer set (Exiqon)
hsa-miR-200a-3p LNA™ PCR primer set (Exiqon)
SNORD48 (hsa) (Exiqon)

2.1.7.3.2 qPCR primers for mRNA

<i>Name</i>	<i>Sequence</i>	<i>UPL</i>	<i>Final conc.</i>
<i>ALDH1</i> FW	5' CCAAAGACATTGATAAAGCCATAA 3'	#82	300 nM
<i>ALDH1</i> REV	5' CACGCCATAGCAATTCACC 3'	#82	50 nM
<i>ACTB</i> FW	5' CCAACCGCGAGAAGATGA 3'	#64	900 nM
<i>ACTB</i> REV	5' CCAGAGGCGTACAGGGATAG 3'	#64	300 nM
<i>AXIN2</i> FW	5' CCACACCCTTCTCCAATCC 3'	#36	900 nM
<i>AXIN2</i> REV	5' TGCCAGTTTCTTTGGCTCTT 3'	#36	900 nM
<i>CD44</i> FW	5' GGTCCCATAACCACTCATGGA 3'	#39	300 nM
<i>CD44</i> REV	5' TCCTTATAGGACCAGAGGTTGTG 3'	#39	900 nM
<i>CDH1</i> FW	5' CCCGGGACAACGTTTATTAC 3'	#35	300 nM
<i>CDH1</i> REV	5' GCTGGCTCAAGTCAAAGTCC 3'	#35	600 nM
<i>CTNNB1</i> FW	5' AGCTGACCAGCTCTCTCTTCA 3'	#21	900 nM
<i>CTNNB1</i> REV	5' CCAATATCAAGTCCAAGATCAGC 3'	#21	900 nM
<i>DICER1</i> FW	5' TGTTCCAGGAAGACCAGGTT 3'	#8	900 nM
<i>DICER1</i> REV	5' ACTATCCCTCAAACACTCTGGAA 3'	#8	300 nM
<i>HPRT1</i> FW	5' TGACCTTGATTTATTTTGCATACC 3'	#73	900 nM
<i>HPRT1</i> REV	5' CGAGCAAGACGTTTCAGTCCT 3'	#73	900 nM
<i>KRT20</i> FW	5' TGTCCTGCAAATTGATAATGCT 3'	#66	300 nM
<i>KRT20</i> REV	5' AGACGTATTCCTCTCTCAGTCTCATA 3'	#66	300 nM
<i>LGR5</i> FW	5' AATCCCCTGCCAGTCTC 3'	#25	300 nM
<i>LGR5</i> REV	5' CCCTTGGAATGTATGTCAGA 3'	#25	300 nM
<i>MUC2</i> FW	5' CATCTGTTCCATTACGACACG 3'	#77	300 nM
<i>MUC2</i> REV	5' GGTGGTAGTGGTGAAGGAGGT 3'	#77	300 nM
<i>OLFM4</i> FW	5' ATCAAAACACCCCTGTCGTC 3'	#24	900 nM
<i>OLFM4</i> REV	5' GCTGATGTTACCACACCAC 3'	#24	900 nM
<i>PROM1</i> FW	5' TCCACAGAAATTTACCTACATTGG 3'	#83	300 nM
<i>PROM1</i> REV	5' CAGCAGAGAGCAGATGACCA 3'	#83	300 nM
<i>SNAI1</i> FW	5' GCTGCAGGACTCTAATCCAGA 3'	#11	300 nM
<i>SNAI1</i> REV	5' ATCTCCGGAGGTGGGATG 3'	#11	300 nM
<i>SNAI2</i> FW	5' TGGTTGCTTCAAGGACACAT 3'	#7	900 nM
<i>SNAI2</i> REV	5' GTTGCAGTGAGGGCAAGAA 3'	#7	900 nM
<i>VIM</i> FW	5' TACAGGAAGCTGCTGGAAGG 3'	#13	900 nM
<i>VIM</i> REV	5' ACCAGAGGGAGTGAATCCAG 3'	#13	600 nM
<i>ZEB1</i> FW	5' GGGAGGAGCAGTGAAAGAGA 3'	#3	300 nM
<i>ZEB1</i> REV	5' TTTCTTGCCCTTCCTTTCTG 3'	#3	300 nM

2.1.7.4 Genotyping primers

<i>Name</i>	<i>Sequence</i>	<i>System</i>
<i>Apc</i> FW	5' GTTCTGTATCATGGAAAGATAGGTGGTC 3'	mouse
<i>Apc</i> REV	5' CACTCAAACGCTTTTGAGGGTTGATTC 3'	mouse

<i>Dicer1</i> FW	5' CCTGACAGTGACGGTCCAAAG 3'	mouse
<i>Dicer1</i> REV	5' CATGACTCTTCAACTCAAAC 3'	mouse
<i>DICER1 ex5</i> FW	5' TCCCATGCTTTCCTGATTTC 3'	cell line
<i>DICER1 ex5</i> REV	5' CTGCAGCCAAACTCCCAATA 3'	cell line
<i>Lgr5-CreER^{T2}</i> FW	5' CTGCTCTCTGCTCCCAGTCT 3'	mouse
<i>Lgr5-CreER^{T2}</i> WT REV	5' ATACCCCATCCCTTTTGAGC 3'	mouse
<i>Lgr5-CreER^{T2}</i> MUT REV	5' GAACTTCAGGGTCAGCTTGC 3'	mouse
<i>ROSA26 LacZ</i> FW	5' AAAGTCGCTCTGAGTTGTTAT 3'	mouse
<i>ROSA26 LacZ</i> REV 1	5' GCGAAGAGTTTGTCTCAACC 3'	mouse
<i>ROSA26 LacZ</i> REV 2	5' GGAGCGGGAGAAATGGATATG 3'	mouse

2.1.7.5 *Mouse recombination primers*

<i>Name</i>	<i>Sequence</i>
<i>Apc</i> FW1	5' CCTGTTCTGCAGTATGTTATCATTC 3'
<i>Apc</i> FW2	5' CTATCAGGACATAGCGTTGG 3'
<i>Apc</i> REV	5' AAGACACCAAGTCCAAAGCACAC 3'
<i>Dicer1</i> WT FW	5' CTCATTCTCTCAGCTCAGTGG 3'
<i>Dicer1</i> WT REV	5' GTCAGAATGAAAACGCGTC 3'
<i>Dicer1</i> Rec FW	5' CCTGGACGCGATAACTTCG 3'
<i>Dicer1</i> Rec REV	5' CCTCAGCACCGAGTTCACAG 3'

2.1.7.6 *siRNA Sequences*

<i>Name</i>	<i>Sequence</i>
<i>si Ctrl.</i>	AllStars Negative Control siRNA (Qiagen)
<i>si CTNNB1 1</i>	5' CAGGAUGAUCCUAGCUAUAUCGU 3' (Hs_ <i>CTNNB1</i> _9, Qiagen)
<i>si CTNNB1 2</i>	5' CUCGGAUGUUCACAACCGAA 3' (Hs_ <i>CTNNB1</i> _5, Qiagen)
<i>si Ctrl. 2 (si GFP)</i>	5' AAGCUACCUGUCCAUGGCCA 3'
<i>si CTNNB1 3</i>	5' AGCUGAUUAUGAUGGACAG 3'
<i>si CTNNB1 4</i>	5' AGUUGUGGUUAAGCUCUU 3'

2.1.8 *Antibodies*

2.1.8.1 *Primary antibodies*

<i>Name</i>	<i>Source</i>	<i>Clone</i>	<i>Dilution</i>	<i>Company</i>	<i>Use</i>
β -actin	mouse mAb	AC-15	1:2000	Sigma-Aldrich	WB
β -catenin	mouse mAb	14	1:300	BD Biosciences	IHC
			1:10000		WB

β -catenin	rabbit mAb	E247	1:10000	Epitomics	IF
CD26-PE	mouse mAb	FR10-11G9	1:11	Miltenyi Biotec	FACS
CD133/1-PE	mouse mAb	AC133	1:11	Miltenyi Biotec	FACS
cl. caspase 3	rabbit pAb		1:100	Cell Signaling	IHC
DICER1	rabbit pAb		1:80	Novus Biologicals	IHC
DICER1	rabbit pAb		1:1000	Sigma-Aldrich	WB
			1:75		IHC
E-cadherin	mouse mAb	4A2C7	1:1000	Invitrogen	WB
KI-67	mouse mAb	MIB-5	1:150	Dako	IHC
lysozyme	rabbit pAb		1:14000	Dako	IHC
V5	mouse mAb		1:3000	Novex	WB
vimentin	mouse mAb	V5	1:1000	Dako	WB

2.1.8.2 Secondary antibodies

<i>Name</i>	<i>Source</i>	<i>Dilution</i>	<i>Company</i>	<i>Use</i>
Alexa Fluor® 488-conjugate IgG (H+L)	rabbit pAb	1:500	Life-Technologies	IF
Biotinylated rabbit anti-rat, mouse adsorbed	rabbit pAb	1:100	Vector	IHC
Mouse anti-rabbit IgG (H+L), HRP conjugate	mouse pAb	1:1000	Pierce	WB
Rabbit anti-mouse IgG (H+L), HRP conjugate	rabbit pAb	1:10000 - 1:30000	Thermo Scientific	WB

2.1.9 Plasmids

<i>Plasmid</i>	<i>Source</i>
8xGTIIIC- <i>luciferase</i>	Addgene (Plasmid 34615)
pcDNA3- <i>CAT</i>	Invitrogen (Life Technologies)
pcl-neo- β - <i>catenin</i> - Δ 45	B. Vogelstein
pCMV- <i>Renilla</i>	Promega
pEGFP- <i>dnTCF-4</i>	A. Jung
pEF-ENTR A	Addgene (Plasmid 17427)
pGL3-basic	Promega
pGL3- <i>DICER1</i> -Prom	Addgene (Plasmid 25851)
pLenti X1 Puro DEST	Addgene (Plasmid 17297)
Super8x <i>FOPFlash</i>	R. T. Moon
Super8x <i>TOPFlash</i>	R. T. Moon

2.1.10 Bacteria

Bacteria	Company
Library Efficiency DH5 α Competent Cells	Thermo Fisher Scientific
One Shot Stb13 TM Chemically Competent <i>E.coli</i>	Thermo Fisher Scientific
Subcloning Efficiency DH5 α Competent Cells	Thermo Fisher Scientific

2.1.11 Cell lines

Cell line	Description/ Source
293T	human embryonic kidney cell line / DSMZ
Caco2	human colorectal adenocarcinoma cell line / DSMZ
coCSC-AS3	primary colorectal tumor cell line / A. Schäffauer
coCSC-AS4	primary colorectal tumor cell line / A. Schäffauer
Colo320	human colorectal adenocarcinoma cell line / DSMZ
DLD1	human colorectal adenocarcinoma cell line / DSMZ
HCT15	human colorectal adenocarcinoma cell line / DSMZ
HCT116	human colorectal carcinoma cell line / DSMZ
HCT116 +/+, <i>ex5</i>	human colorectal carcinoma cell line; w/o / with disruption of the helicase domain (<i>ex5</i>) of <i>DICER1</i> / B. Vogelstein (Cummins et al., 2006)
HT29	human colorectal adenocarcinoma cell line / DSMZ
LOVO	human colorectal adenocarcinoma cell line / DSMZ
LS174T	human colorectal adenocarcinoma cell line / DSMZ
RKO	human colon carcinoma cell line / ATCC
RKO +/+, <i>ex5</i>	human colon carcinoma cell line; w/o / with disruption of the helicase domain (<i>ex5</i>) of <i>DICER1</i> / B. Vogelstein (Cummins et al., 2006)
SW403	human colorectal adenocarcinoma cell line / DSMZ
SW480	human colorectal adenocarcinoma cell line / ATCC
SW620	human colorectal adenocarcinoma cell line / ATCC
SW1222	human colon carcinoma cell line / ATCC
T84	human colorectal carcinoma cell line / ATCC

2.1.12 Mouse strains

Mouse strain	Description/ Source
<i>Lgr5-EGFP-IRES-CreER^{T2}</i>	genetically modified C57BL/6 mouse line; contains a <i>Cre recombinase</i> under the <i>Lgr5</i> promoter which can only enter the nucleus after tamoxifen induction; in the following text also termed as <i>Lgr5-CreER^{T2}</i> / N. Barker, stock kindly supplied by H. Hermeking (Barker et al., 2007)

<i>Rosa26-LSL-LacZ</i>	genetically modified C57BL/6 mouse line; contains a <i>lacZ</i> gene (encodes β -galactosidase) that is expressed under the <i>Rosa26</i> -promoter; a STOP sequence, flanked by loxP sites, is located in front of the <i>lacZ</i> gene which were removed by Cre recombinase; in the following text also referred to as <i>Rosa26/</i> M. Schneider (Barker et al., 2007)
<i>Apc^{fl}</i>	genetically modified C57BL/6 mouse line; exon 14 of the <i>Apc</i> gene is flanked by loxP sites and can be removed by Cre recombinase/ H. Clevers (Shibata et al., 1997)
<i>Dicer1^{fl}</i>	genetically modified C57BL/6 mouse line; RNaseIII ₂ domain of the <i>Dicer1</i> gene is flanked by loxP sites and can be removed by Cre recombinase/ B. Harfe (Harfe et al., 2005)

Crossed mouse lines used in the experiments:

<i>Lgr5-CreER^{T2}</i>	<i>Rosa26-LacZ</i>	<i>Apc</i>	<i>Dicer1</i>	abbreviation	investigation	group size
+	<i>fl/fl</i>	<i>fl/fl</i>	+/+	<i>Lgr5(+)-Apc</i>	tumor formation	6
-	<i>fl/fl</i>	<i>fl/fl</i>	+/+	<i>Lgr5(-)-Apc</i>	control	3
+	<i>fl/fl</i>	<i>fl/fl</i>	<i>fl/+</i>	<i>Lgr5(+)-Apc-Dicer1^{het}</i>	tumor formation	6
-	<i>fl/fl</i>	<i>fl/fl</i>	<i>fl/+</i>	<i>Lgr5(-)-Apc-Dicer1^{het}</i>	control	3
+	<i>fl/fl</i>	<i>fl/fl</i>	<i>fl/fl</i>	<i>Lgr5(+)-Apc-Dicer1^{hom}</i>	tumor formation	6
-	<i>fl/fl</i>	<i>fl/fl</i>	<i>fl/fl</i>	<i>Lgr5(-)-Apc-Dicer1^{hom}</i>	control	3
+	<i>fl/fl</i>	+/+	<i>fl/+</i>	<i>Lgr5(+)-Dicer1^{het}</i>	tumor formation	6
-	<i>fl/fl</i>	+/+	<i>fl/+</i>	<i>Lgr5(-)-Dicer1^{het}</i>	control	3
+	<i>fl/fl</i>	+/+	<i>fl/fl</i>	<i>Lgr5(+)-Dicer1^{hom}</i>	tumor formation	6
-	<i>fl/fl</i>	+/+	<i>fl/fl</i>	<i>Lgr5(-)-Dicer1^{het}</i>	control	3

Table 1. Required mouse lines for the experiment.

The different mouse strains are described concerning genotype, abbreviation, reason for the respective mouse strain in the investigation and group size. + (*Lgr5-CreER^{T2}*): positive for *Lgr5-CreER^{T2}*, - (*Lgr5-CreER^{T2}*): negative for *Lgr5-CreER^{T2}*; *fl*: floxed; + (*Apc*, *Dicer1*): wildtype

In mice negative for *Lgr5-CreER^{T2}* (*Lgr5(-)*) recombination did not take place whereby they did not form tumors (control). The mice described above were kept in the Institute of Pathology, LMU, Munich, according to conditions of the German law for husbandry of laboratory animals. For *in vivo* experiments, the mice were introduced in the experimental procedures at the age of 8–12 weeks.

2.1.13 Software

<i>Software</i>	<i>Company</i>
C-Flow Plus Software	Becton & Dickinson
dChip software	Dana-Farber Institute
CorelDRAW Graphics Suite	Corel Corporation
Gene Construction Kit	Textco
Geneious	Biomatters Ltd.
ImageJ	NIH
NCBI	http://www.ncbi.nlm.nih.gov/
Office	Microsoft
Photoshop	Adobe Systems Incorporated
Universal ProbeLibrary Assay Design Center	http://lifescience.roche.com/webapp/wcs/stores/servlet/CategoryDisplay?catalogId=10001&tab=Assay+Design+Center&identifier=Universal+Probe+Library&langId=-1

2.1.14 Buffer

All buffers were prepared with dH₂O.

<i>Buffer</i>	<i>Composition</i>	
10x PBS (pH 7.4)	NaCl	80 g
	KCl	2 g
	Na ₂ HPO ₄ -7H ₂ O	26.8 g
	KH ₂ PO ₄	2.4 g
	H ₂ O	ad 1000 ml
	adjust to pH 7.4	
Lysis buffer	Tris-HCl 1M, pH 8.0	10 ml
	NaCl 5M	4 ml
	EDTA 0.5M	1 ml
	SDS 10%	2 ml
	H ₂ O nuclease free	83 ml
RIPA lysis buffer	Tris-HCl, pH 8.0	50 mM
	NaCl	250 mM
	NP40	1%
	sodium deoxycholate	0.5% (w/v)
	SDS	0.1 %
	Complete® protease inhibitor	

<i>4x Tris-HCl (pH 6.8)</i>	Tris base	6.05 g
	H ₂ O	40 ml
	adjust to pH 6.8	
	H ₂ O	ad 100 ml
	filter using 0.45 µm filter	
	SDS	0.4 g
<i>4x Tris-HCl (pH 8.8)</i>	Tris base	91 g
	H ₂ O	300 ml
	adjust to pH 8.8	
	H ₂ O	ad 500 ml
	filter using 0.45 µm filter	
	SDS	2.0 g
<i>5x Laemmli buffer</i>	Tris base	15.1 g
	glycine	72 g
	SDS	5 g
	H ₂ O	ad 1000 ml
<i>10x TBS</i>	Tris-HCl	15.76 g
	NaCl	7.57 g
	H ₂ O	ad 1000 ml
	adjust to pH 7.5	
<i>1x TBS/T (0.1%)</i>	1x TBS	1000 ml
	Tween 10%	10 ml
<i>10x Transfer buffer</i>	Tris base	30.2 g
	glycine	144.2 g
	H ₂ O	ad 900 ml
<i>1x Transfer buffer</i>	10x Transfer buffer	100 ml
	H ₂ O	800 ml
	methanol	100 ml
<i>Fixative</i>	glutaraldehyde 3%	6.7 ml
	formaldehyde 37%	2.7 ml
	NP40	20 µl
	1x PBS	90.5 ml
<i>Staining solution</i>	K ₃ Fe(CN) ₆ (500 mM)	0.5 ml
	K ₄ Fe(CN) ₆ ·3H ₂ O (500 mM)	0.5 ml
	MgCl ₂ (1 M)	0.1 ml

Materials and Methods

	X-Gal	100 mg
	dimethylformamide	2 ml
	PBS 1x	46.9 ml
	NP40	10 μ l
	sodium deoxycholate	50 mg
4% Paraformaldehyde	paraformaldehyde	1.6 g
	H ₂ O	20 ml
	NaOH 1N	40 μ l
	place in hot water until dissolved	
	10x PBS	4 ml
	H ₂ O	16 ml
5 % Blotting blocker	blotting grade blocker, non-fat dry milk	5 g
	1x TBS/T (0.1%)	100 ml

2.2 Methods

2.2.1 Methods used for working with DNA

2.2.1.1 Cloning techniques

2.2.1.1.1 Amplification of PCR products

To generate an *OLFM4* expressing plasmid, *OLFM4* encoding PCR (polymerase chain reaction) products (1561 bp) were amplified by PCR using LS174T cDNA (50 ng/μl) as a template. *CAT* (chloramphenicol acetyltransferase) encoding PCR products (810 bp) were amplified with pcDNA-*CAT* (10 ng/μl) as a template (for the cloning of the control vector). The PCR reaction proceeds in a cyclic order of denaturation of the DNA, annealing of the primers and elongation. For this amplification, KOD DNA polymerase (Novagen) was utilized because of its proof reading activity. The components and PCR conditions are listed below, primer sequences in 2.1.7.1.

<i>Component</i>	<i>Volume</i>	<i>Final conc.</i>
10x buffer	2 μl	1x
MgSO ₄ (25 mM)	1.2 μl	1.5 mM
dNTPs (2 mM each)	2 μl	0.2 mM each
primer mix (20 μM each)	0.3 μl	0.3 μM each
template	1 μl	
KOD Hot Start DNA polymerase (1 U/μl)	0.4 μl	0.02 U/μl
H ₂ O	13.1 μl	
	20 μl	

<i>PCR conditions: Temperature</i>	<i>Time</i>	
95 °C	2 min	
95 °C	20 sec	30 cycles
60 °C	30 sec	
70 °C	<i>CAT</i> : 30 sec, <i>OLFM4</i> : 40 sec	
70 °C	10 min	
4°C	hold	

2.2.1.1.2 Digest and ligation

After the PCR reaction, the PCR products were digested with FastDigest enzymes (*BamHI* and *NotI*, Thermo Scientific), following manufacturer’s instructions, and purified with the

QIAquick PCR Purification Kit (Qiagen), following manufacturer's instructions (QIAquick Spin Handbook - QIAquick PCR Purification Kit Protocol - using a microcentrifuge). 3 µg of the vector (pEF-ENTR A) were also digested with FastDigest enzymes (*Bam*HI and *Not*I) and subsequently, dephosphorylated with SAP according to manufacturer's instructions to prevent a religation of the vector without an insert. The plasmids were separated by agarose gel electrophoresis (see 2.2.1.5) to separate the digested plasmids from the plasmids where digestion did not work. The digested plasmids were cut out of the gel and purified using the QIAquick Gel Extraction Kit (Qiagen, QIAquick Spin Handbook - QIAquick Gel Extraction Kit Protocol - using a microcentrifuge). Subsequently, *OLFM4/CAT* was subcloned via *Bam*HI and *Not*I restriction sites into the pEF-ENTR A vector (Campeau et al., 2009) using T4 DNA ligase (Thermo Scientific) over night following manufacturer's instructions, transformed (see 2.2.1.1.3) and *OLFM4/CAT* encoding plasmids (pEF-ENTR A-*OLFM4/CAT*) were isolated (see 2.2.1.1.4). Then, pEF-ENTR A-*OLFM4/CAT* was cloned via the LR recombination reaction (GATEWAY®-technology, Life Technologies) into pLentiX1-DEST-PGK-*Puro*-vector which contains C-terminal His and V5 tags (Campeau et al., 2009), following the manufacturer's instructions. The LR reaction product was transformed into *E. coli* (Stb13) (see 2.2.1.1.3), plated on agar plates with the appropriate antibiotics and incubated over night at 37°C. Plasmids were isolated from colonies (see 2.2.1.1.4). Resulting DNA was digested (FastDigest enzymes, Thermo Scientific), separated by agarose gel electrophoresis (see 2.2.1.5) to control the band sizes and positives clones were sequenced by Sanger sequencing (see 2.2.1.6).

2.2.1.1.3 Transformation

For the amplification of plasmids, plasmids were transformed into DH5α (Library/Subcloning Efficiency DH5α Competent Cells, Thermo Fisher Scientific) or *E. coli* bacteria (One Shot Stb13™ Chemically Competent *E. coli*, Thermo Fisher Scientific; for unstable inserts such as lentiviral DNA), according to manufacturer's instructions, and plated out on agar plates with the appropriate antibiotics (kanamycin 50 µg/ml, ampicillin 100 µg/ml). The agar plates were incubated over night at 37°C. The next day, single colonies were inoculated in LB medium with the appropriate antibiotics (kanamycin 50 µg/ml, ampicillin 100 µg/ml).

2.2.1.1.4 DNA preparation

To isolate plasmids from bacteria, single colonies were picked from the agar plates (see 2.2.1.1.3), inoculated in LB medium as a liquid bacterial culture with appropriate antibiotics (kanamycin 50 µg/ml, ampicillin 100 µg/ml) and incubated over night at 37°C. Miniprep (4 ml LB medium) of plasmid DNA was done using QIAprep Spin Miniprep Kit (Qiagen) employing the QIAcube (QIAcube Standard Protocol: QIAprep Mini - Standard). For midiprep (200 ml LB medium), the PureYield™ Plasmid Midiprep System (Promega) was utilized, both following manufacturer's instructions.

2.2.1.2 Genomic DNA isolation and genotyping of cell lines

To verify the *DICER1* disruption (*DICER1ex5*) in cell lines, the cell lines RKO (+/+, *ex5*) and HCT116 (+/+, *ex5*) were harvested and genomic DNA was isolated from the cells by the QIAamp DNA Mini Kit (Qiagen) according to the manufacturer's instructions (QIAamp® DNA Mini and Blood Mini Handbook - Appendix B: Protocol for Cultured Cells). 5 µl of the isolated genomic DNA (diluted to 40 ng/µl in H₂O) was utilized as template in the following genotyping PCR reaction. PCR products were amplified with the Maxima Hot Start Taq DNA polymerase (Fermentas) because no proof reading activity was required. The PCR product size of wildtype (+/+) cell lines was 444 bp, of *ex5* cell lines 564 bp. The components and PCR conditions are listed below, primer sequences in 2.1.7.4.

<i>Component</i>	<i>Volume</i>	<i>Final conc.</i>
10x buffer	2.5 µl	1x
MgCl ₂ (25 mM)	1.5 µl	1.5 mM
dNTPs (10 mM each)	0.5 µl	0.2 mM each
primer mix (20 µM each)	0.5 µl	0.4 µM each
template (40 ng/µl)	5 µl	
Maxima Taq Hot Start DNA polymerase (5 U/µl)	0.2 µl	0.04 U/µl
H ₂ O	14.8 µl	
	25 µl	

<i>PCR conditions</i>	<i>Temperature</i>	<i>Time</i>
	95°C	4 min
	95°C	30 sec
	58°C	30 sec
	72°C	1 min
	72°C	10 min
	4°C	hold

40 cycles

2.2.1.3 *Genomic DNA isolation and genotyping of mouse tail biopsies*

For genotyping of the mouse lines, mouse tail tip biopsies were obtained from 4-12 weeks old mice. Subsequently, the biopsies were lysed in tissue lysis buffer with proteinase K (final concentration 0.1 µg/µl) over night at 56°C and 450 rpm. Then, the lysed tissue was centrifuged 10 min at maximum speed and the supernatant including the genomic DNA was transferred into a new tube. For genotyping of the mouse lines FIREPol DNA polymerase (Solis BioDyne) and 0.2 µl of the isolated genomic DNA was utilized. The PCR components and PCR conditions are listed below, primer sequences in 2.1.7.4.

<i>Component</i>	<i>Volume</i>	<i>Final conc.</i>
10x buffer B	2 µl	1x
MgCl ₂ (25 mM)	1.2 µl	1.5 mM
dNTPs (10 mM each)	0.4 µl	0.2 mM each
primer mix (20 µM each)	0.4 µl	0.4 µM each
template	0.2 µl	
FIREPol DNA polymerase (5 U/µl)	0.16 µl	0.04 U/µl
H ₂ O	15.64 µl	
	20 µl	

<i>PCR conditions</i>	<i>Temperature</i>	<i>Time</i>
	95°C	4 min
	95°C	30 sec
	anneal. temp. (see below)	30 sec
	72°C	elong. time (see below)
	72°C	10 min
	4°C	hold

40 cycles

<i>Primer</i>	<i>Anneal. temp.</i>	<i>Elong. time</i>	<i>PCR product size</i>
<i>Lgr5-CreER^{T2}</i>	66.0°C	30 sec	WT: 298 bp, Rec: 174 bp
<i>ROSA26LacZ</i>	61.6°C	1 min	WT: 650 bp, fl: 350 bp
<i>Apc</i>	60.2°C	40 sec	WT: 226 bp, fl: 314 bp
<i>Dicer1</i>	60.2°C	30 sec	WT: 351 bp, fl: 420 bp

2.2.1.4 Verification of the recombination after tamoxifen induction

For the verification whether the adenomas (2.2.5.1) showed recombination of the *Apc* and *Dicer1* genes, PCR was performed using genomic DNA as the template. For that purpose, the paraffin was removed from the slices by incubating 3 times for 10 min in xylene and 3 times for 10 min in absolute ethanol. Regions with and without adenomas were scratched out independently from each other with a scalpel blade and transferred directly into a tube containing ATL buffer and proteinase K, according to the manufacturer's instructions. Genomic DNA was isolated using the QIAamp[®] DNA FFPE Tissue Kit (Qiagen) employing the QIAcube according to the QIAcube Standard Protocol: QIAamp DNA FFPE Tissue - FFPE tissue sections - Standard. For the subsequent PCR reaction, Maxima Hot Start Taq DNA polymerase (Fermentas) was utilized because no proof reading activity was required. Information on primers and PCR conditions are listed below, primer sequences in 2.1.7.5. As template, 1 µl of the previously isolated DNA was utilized. To increase the amount of the PCR product, a nested PCR was done. Therefore, 1 µl of the previous PCR product was utilized as template, the other components and conditions were identical to the previous PCR; components and conditions are listed below. The PCR product size of *Apc* wildtype (WT) was 1300 bp, of *Apc* recombination (Rec) 350 bp, of *Dicer1* wildtype 84 bp and of *Dicer1* Rec 207 bp. *Apc* wildtype and recombination products were produced in one PCR reaction (primers: *Apc* FW1, *Apc* FW2, *Apc* FW3).

<i>Component</i>	<i>Volume</i>	<i>Final conc.</i>
10x buffer	2 μ l	1x
MgCl ₂ (25 mM)	1.2 μ l	1.5 mM
dNTPs (10 mM each)	0.4 μ l	0.2 mM each
primer mix (20 μ M each)	0.4 μ l	0.4 μ M each
template	1 μ l	
Maxima Taq Hot Start DNA polymerase (5 U/ μ l)	0.16 μ l	0.04 U/ μ l
H ₂ O	14.84 μ l	
	20 μ l	

<i>PCR conditions:</i>	<i>Temperature</i>	<i>Time</i>	
	95°C	4 min	
	95°C	30 sec	50 cycles
	58°C	30 sec	
	72°C	<i>Apc</i> : 1 min 30 sec	
		<i>Dicer1</i> WT: 20 sec	
		<i>Dicer1</i> Rec: 30 sec	
	72°C	10 min	
	4°C	hold	

2.2.1.5 Agarose gel electrophoresis

To determine the size of the PCR products, the amplified DNA fragments were separated by agarose gel electrophoresis. For the analysis of the size, 5 μ l of DNA size standard and 1% or 2% agarose gels were used. For that purpose, 1 g or 2 g of agarose were dissolved in 100 ml 0.5x TBE (Thermo Scientific) by heating. The evaporated liquid was filled up with H₂O and the liquid was cooled down to 50–60°C. Subsequently, 3 μ l ethidium bromide were added and the mixture was poured into the gel sledge.

2.2.1.6 Sanger sequencing

To verify that the amplified and cloned plasmids have the correct sequence, specific sequences were amplified by PCR and the PCR products were subsequently utilized for Sanger sequencing. The components and PCR conditions are listed below, primer sequences in 2.1.7.2.

<i>Component</i>	<i>Volume</i>	<i>Final conc.</i>
BigDye Terminator V3.1	1 μ l	
sequencing buffer (5x)	2 μ l	1x
primer (10 μ M)	0.5 μ l	0.5 μ M
template (DNA)	500 ng	
H ₂ O	ad 10 μ l	
10 μ l		

<i>PCR conditions:</i>	<i>Temperature</i>	<i>Time</i>	50 cycles
	96°C	10 sec	
	60°C	1 min 30 sec	

PCR products were purified (DyeEx 2.0 Spin Kit; Qiagen) and 4 μ l of the purified PCR products were finally mixed with 16 μ l HiDi formamide. The sequencing was performed by Sanger sequencing (ABI 3130; Life technologies) following the manufacturer's instructions.

2.2.2 *Methods used for working with RNA*

2.2.2.1 *Quantitative reverse transcriptase PCR (RT-qPCR)*

2.2.2.1.1 *RT-qPCR of miRNAs*

To detect and quantify the expression of miRNAs, cells were harvested and miRNAs were isolated using miRNeasy Mini Kit (Qiagen) which was performed in the QIAcube according to the QIAcube Standard Protocol: miRNeasy Mini - Animal tissues and cells - Aqueous phase - Part A+B. Isolated miRNAs were diluted to 5 ng/ μ l and reverse transcribed with the Universal cDNA Synthesis Kit II (Exiqon). The components and reverse transcription (RT) conditions are listed below.

<i>Component</i>	<i>Volume</i>	<i>Final conc.</i>
miRNA (5 ng/ μ l)	2 μ l	1 ng/ μ l
H ₂ O	5 μ l	
reaction buffer 5x	2 μ l	1x
enzyme mix	1 μ l	
10 μ l		

<i>RT conditions</i>	<i>Temperature</i>	<i>Time</i>
	42°C	60 min
	95°C	5 min
	4°C	hold

The cDNA was diluted 1:80 in H₂O and used for qPCR analysis. The qPCR components and conditions are listed below, primer sets in 2.1.7.3.1. The qPCR reaction was performed using a LightCycler 480 device (Roche).

<i>Component</i>	<i>Volume</i>
ExiLENT SYBR Green master mix 2x	5 µl
primer mix set	1 µl
diluted cDNA template	4 µl
	10 µl

<i>qPCR conditions</i>	<i>Temperature</i>	<i>Time</i>	
	95°C	10 sec	45 cycles
	95°C	10 sec	
	60°C	1 min	
	72°C	1 sec	
	melting curve		
	cooling		

2.2.2.1.2 RT-qPCR of mRNAs

To detect and quantify mRNA expression, cells were harvested and total RNA was isolated using RNeasy Mini Kit (Qiagen) which was performed in the QIAcube according to the QIAcube Standard Protocol: RNeasy Mini - Animal cells - QIAshredder DNase digest. Subsequently, cDNA was generated from 300-4000 ng mRNA using the RevertAid Reverse Transcriptase (Thermo Scientific). The components of the RT and RT conditions are listed below.

<i>Pre-Mix:</i>	<i>Component</i>	<i>Volume</i>
	RNA	300-4000 ng
	H ₂ O	ad 11.5 µl
	random hexamer primer mix	1 µl
		12.5 µl

<i>RT preincubation</i>	<i>Temperature</i>	<i>Time</i>
	65°C	5 min
	chill on ice	

Subsequently, the following components were added to the Pre-mix.

<i>Component</i>	<i>Volume</i>	<i>Final conc.</i>
Pre-mix	12.5 µl	
Thermo Scientific RiboLock RNase inhibitor	0.5 µl	
dNTP mix 10 mM each	2 µl	1 mM
RevertAid reverse transcriptase	1 µl	
	<hr/> 20 µl	

<i>RT conditions</i>	<i>Temperature</i>	<i>Time</i>
	25°C	10 min
	42°C	60 min
	70°C	10 min
	4°C	hold

The cDNA was diluted in H₂O to 10–50 ng/µl and used for qPCR analysis. qPCR was done using Light Cycler 480 Probes Master kits together with specific primer pairs and Universal Probe Library (UPL) Probes (Roche). The components of the qPCR and qPCR conditions are listed below, primer sequences and UPL probes in 2.1.7.3.2.

<i>Component</i>	<i>Volume</i>	<i>Final conc.</i>
Roche probe master 2x	5 µl	1x
primer FW (100 µM)	0.005-0.09 µl	50-900 nM (see 2.1.7.3.2)
primer REV (100 µM)	0.005-0.09 µl	50-900 nM (see 2.1.7.3.2)
probe UPL	0.1 µl	
H ₂ O	ad 8 µl	
cDNA template	2 µl	
	<hr/> 10 µl	

<i>qPCR conditions</i>	<i>Temperature</i>	<i>Time</i>
	95°C	10 sec
	95°C	10 sec
	60°C	15 sec
	72°C	1 sec
	40°C	10 sec
		45 cycles

For Cp (crossing point) values, the second derivative maximum method was chosen and determined using a LightCycler 480 device (Roche). Gene expression alterations were calculated as relative values on the basis of the expression levels of the reference genes *ACTB* (β -actin) and/or *HPRT1* (hypoxanthine phosphoribosyltransferase 1) (Pfaffl, 2001). All measurements were done in triplicates and repeated at least twice in independent experiments.

2.2.2.2 *Expression analysis*

For gene expression analysis, cDNA was measured employing a LightCycler 480 device (Roche) and gene expression alterations were calculated as relative values on the basis of *ACTB* (see 2.2.2.1.2). The normalized values of the different gene expressions were all calculated relative to the expression of the cell line HCT116-CAT-V5. For analysis of resulting values, the dChip software (Dana-Farber Institute) was used.

2.2.3 *Methods used for working with proteins*

2.2.3.1 *Immunofluorescence analysis*

The cellular localization of β -catenin was detected with a specific β -catenin antibody by immunofluorescence (IF). For that purpose, cells were seeded in 6 well plates on glass cover slides and cultivated for 48 h. After 48 h, cells were fixed on the cover slides in 4% paraformaldehyde in PBS for 10 min, washed 3 times in PBS, permeabilized with 0.2% Triton X100 in PBS for 20 min and washed 2 times in PBS. Subsequently, the cells were blocked with freshly filtered FBS (fetal bovine serum) (100%) for 1 h. Then, the fixed cells were stained with the β -catenin antibody (diluted in PBS/FBS 1:1) for 1 h, washed 3 times in 0.05% Tween 20 in PBS, stained with the secondary antibody (Alexa Fluor® 488) (diluted in 1:1 PBS/ FBS) for 1 h and washed 2 times in 0.05% Tween 20 in PBS. After that, the slides were covered with ProLong Gold antifade reagent with DAPI and cover slips and subsequently analyzed using an Axiovert 200M microscope (Zeiss). As negative control, a staining without primary antibody was done for all stainings. Antibodies are listed in 2.1.8.

2.2.3.2 *Western Blot*

For the detection and quantification of specific proteins, Western Blot analysis was performed. For that purpose, cells were washed with PBS, scraped off in RIPA lysis buffer and transferred into a reaction tube. After 20 min lysis on ice, lysates were sonicated and centrifuged at 16,000 × g for 15 min at 4°C. The supernatants were transferred in a new tube and the protein concentration of the lysates was determined using the DCTM Protein Assay (Bio-Rad) following the manufacturer's instructions. Rotiload loading buffer was added to 40 µg of each lysate in a ratio of 1:4, mixed, heated for 5 min at 95°C, loaded on 10% SDS-polyacrylamide gels and separated in Laemmli buffer (1x) for 1 h 30 min at 120 V. 5 µl PageRulerTM Plus Prestained Protein Ladder (Thermo Fisher Scientific) was loaded for the determination of the protein molecular weight.

10% SDS-polyacrylamide gel:

<i>Stacking gel:</i>	acrylamide rotiphorese gel 30%	5.00 ml
	4xTris-HCl, pH 8.8	3.75 ml
	H ₂ O	6.25 ml
	APS 10%	0.20 ml
	TEMED	0.04 ml
<i>Resolving gel:</i>	acrylamide rotiphorese gel 30%	0.65 ml
	4xTris-HCl, pH 6.8	1.25 ml
	H ₂ O	3.05 ml
	APS 10%	0.10 ml
	TEMED	0.02 ml

After their separation, proteins were transferred onto PVDF-membranes (0.2 µm, Bio-Rad) in Transfer buffer (1x) using the Mini Trans-Blot[®] Cell system (Bio-Rad) for 1 h at 100 V. After the transfer of the proteins on the membrane, the membrane was blocked with 5% Blotting blocker and stained with the primary antibody (diluted in 5% Blotting blocker) over night at 4°C. Subsequently, the membrane was washed 3 times with TBS/T (0.1%) and stained with the secondary antibody (diluted in 5% Blotting blocker) for 1 h at room temperature (RT). Then, the membrane was washed 3 times with TBS/T (0.1%) and detection was done with ImmobilonTM Western Chemiluminescent HRP Substrate (ECL) (Millipore). Resulting light signals were recorded employing a CF440 Imager (Kodak). Antibodies are listed in 2.1.8.

2.2.4 *Methods used for working with cells*

2.2.4.1 *Cell culture*

CRC cell lines were cultivated in DMEM with 10% FCS in the presence of 100 U/ml penicillin and 0.1 mg/ml streptomycin at 5% CO₂, only the cell line Colo320 was cultivated in RPMI with 10% FCS. Primary tumor cell lines were directly generated from fresh human colorectal carcinoma tissue, which was supplied by Klaus-Peter Janssen (Technische Universität, Munich), and performed as described in (Kreso and O'Brien, 2008) (Generating single-cell suspension from human colon cancer tissue). Established primary tumor cell lines were cultivated as described in (Kreso and O'Brien, 2008) (Culturing colon cancer cells as spheres) in Ultra-low attachment surface culture flasks with StemProR hESC SFM medium in the presence of 0.01 µg/ml FGFb.

2.2.4.2 *Virus production, conditional expression*

For the generation of cell pools with conditional expression of *OLFM4* as well as *CAT*, cells were lentivirally transduced. To produce lentiviral particles, 293T cells were seeded and transfected in 60 mm ø dishes with 3.68 µg transfer vector (for plasmid cloning see 2.2.1.1) together with 3.68 µg pCMV8.9 and 0.74 µg pVSV.G plasmids using Fugene 6 (Promega) according to manufacturer's instructions. 48 h after transfection, virus was harvested, the cell culture supernatant was filtered using sterile 0.45 µm filter and mixed with polybrene (8 µg/ml) and the CRC cell lines were infected with the filtered supernatant. For the subsequent selection of the infected cells, the cells were treated with different concentrations of puromycin (1–2.5 µg/ml; Sigma-Aldrich).

2.2.4.3 *Wnt3a production*

To activate the canonical Wnt signaling pathway, Wnt3a conditioned medium was added to the cells for 24 h. For the production of Wnt3a, L Wnt3a cells and L cells (for control conditioned medium) were split 1:20 from a T75 cell culture flask in 10 cm ø dishes with 6 ml medium (DMEM with 10% FCS) and cultivated for 4 days. After 4 days, the medium was harvested and filtered through sterile 0.2 µm filter. After this first batch, the medium was replenished (6 ml) and the cells were incubated for additional 3 days. After filtering the second batch, both batches were pooled and stored at 4°C before the conditioned medium was added to the cells.

2.2.4.4 *Knockdown of CTNNB1 using siRNAs*

To achieve the knockdown of *CTNNB1* in cultivated HCT116 cells, the cells were transfected with 30–50 nM siRNA specific for either *CTNNB1* siRNA or with a non-targeting siRNA (control) using Lipofectamine RNAiMAX (Invitrogen), following essentially the manufacturer's instructions. 24 h after transfection, the cell culture medium was changed. To measure the effects of the knockdown, cells were harvested 72 h after transfection and effects were measured on mRNA (see 2.2.2.1.2) and protein level (see 2.2.3.2).

2.2.4.5 *Luciferase reporter assay*

To analyze the activity of promoters *in vitro*, reporter gene constructs were utilized in a luciferase reporter assay. For the determination of the transcriptional activity of β -catenin/TCF4-responsive promoters, the *DICER1* promoter as well as the *TEAD* (TEA-domain-containing family) responsive promoter, the reporter plasmids were transiently transfected in the absence or presence of exogenous overexpressing plasmids. 2.5×10^4 cells were seeded in 24 cluster well plates. 24 h after seeding, cells were transfected with either 120–300 ng of firefly luciferase reporter plasmid or with 120–150 ng of firefly luciferase reporter plasmid together with 150–160 ng of overexpressing plasmids. In each case, 25–40 ng of the renilla luciferase reporter plasmid pCMV-*Renilla* (Promega) was additionally transfected for the normalization of results. The transfection was performed using Eugene 6 Transfection Reagent (Promega) according to the manufacturer's instructions. After 24–48 h, Dual luciferase reporter assays (Promega) were done according to the manufacturer's instructions. Fluorescence intensities were measured with an Orion II luminometer (Berthold) in a 96 well format and analyzed with the SIMPLICITY software package (DLR). All experiments were done in triplicates and at least two independent experiments were done.

2.2.4.6 *Chemoresistance assay*

To analyze changes of gene expression under 5-fluorouracil (5-FU) treatment, LS174T cells were incubated for 5 days in 6 well plates in the presence of 40 μ M or 50 μ M 5-FU (Sigma-Aldrich, dissolved in DMSO) or the corresponding concentration of DMSO. After 5 days, cells were harvested and mRNA isolated for RT-qPCR analysis (see 2.2.2.1.2). To

compare the proliferation under 5-FU treatment, HCT116 cells were incubated for 3 days with the LC50 concentration of 5-FU (12.12 μM ; information received from Arndt Stahler; dissolved in water (medac GmbH)) in 96 well plates and analyzed with the MTT assay (see 2.2.4.7). At least three independent experiments were done.

2.2.4.7 *MTT assay*

MTT assays (CellTiter 96® Non-Radioactive Cell Proliferation Assay; Promega) were performed to measure cell viability by mitochondrial activity which is a surrogate for proliferation. For that purpose, $1.5\text{--}3 \times 10^3$ cells were seeded in triplicates in 96 well plates. Proliferation was measured every 24 h over 5 days, following the manufacturer's instructions. For measuring chemoresistance, cells were seeded directly in medium containing 5-FU and proliferation was measured every 24 h over 3 days. To investigate the influence of *CTNNB1* knockdown (see 2.2.4.4) on proliferation and chemoresistance, cells were seeded 48 h after the knockdown and measured as previously described. Absorbances were measured at the wavelength of 570 nm using an ELISA reader (Varioskan, Thermo Scientific). At least two independent experiments were done.

2.2.4.8 *Wound healing assay*

To measure the migration of cells, wound healing experiments were carried out. Cells were seeded in chambers (ibidi) according to the manufacturer's instructions. 3 h before removing the chamber mitomycin C, that blocks proliferation, was added to a final concentration of 10 $\mu\text{g}/\text{ml}$. Thus, only the migration effect was detected in the subsequent assay. Then, the cells were washed twice with PBS and full culture medium or Wnt3a/Ctrl. conditioned medium was added. The defined gap between the cells was photographed at 0 h and 24 h/48 h. Resulting images were evaluated using ImageJ-Software (NIH) by measuring the free gap with the "freehand selection" and comparing the resulting values with each other. At least two independent experiments were done.

2.2.4.9 *Methyl cellulose assay*

To determine the transformation status of colorectal tumor cell lines, anchorage independent growth was analyzed by methyl cellulose assay. 500 µl of a cell suspension (included 250 cells) was mixed with 4.5 ml 0.01% methyl cellulose (Sigma-Aldrich). Per 35 mm ø petri dish, 1 ml of this mixture was seeded in quadruplicates. After 12–16 days, 200 µl Thiazolyl Blue Tetrazolium Bromide (MTT) solution (1 mg/ml; Sigma-Aldrich) was added on the petri dishes and incubated over night. The petri dishes with the colonies were photographed and analyzed by counting the blue colored colonies using ImageJ-Software (NIH). At least two independent experiments were done.

2.2.4.10 *Flow cytometric analysis of cells (FACS)*

2.2.4.10.1 *Aldefluor assay*

High levels of the enzyme ALDH1 are found in cells with CSC properties (Huang et al., 2009) and therefore, measuring of ALDH1 activity is a suitable marker to determine stemness of tumor cells. ALDH1 activity was measured using the ALDEFLUOR™ Kit (Stemcell Technologies) following the manufacturer's instructions. To determine changes of the gene expression in the cells with ALDH1 high and low activity, cells were separated in aldefluor positive (ALDH1+) and negative (ALDH1-) cells by isolating 5 % of the cells with the highest and the lowest ALDH1 activity respectively, using a FACS Aria® Cell Sorter (Becton & Dickinson). The cells were lysed, total RNA was isolated, reverse transcribed and RT-qPCR analysis were performed (see 2.2.2.1.2). Effects of ectopic *OLFM4* overexpression and thus, high *OLFM4* protein levels on ALDH1 activity were measured with the ALDEFLUOR™ Kit following the manufacturer's instructions by using a BD Accuri C6 flow cytometer (Becton & Dickinson) device with the corresponding C-Flow Plus Software. To exclude the dead cells from the measurement, 1 µg/ml propidium iodide (PI) solution (Sigma-Aldrich) was added to the cells 30 sec before running the measurement. To define the threshold of aldefluor positivity, a portion of the cells was incubated with the ALDH1 inhibitor DEAB (diethylaminobenzaldehyde) as a background control. At least two independent experiments were done.

2.2.4.10.2 *Antibody staining*

To determine the percentage of cells that express and synthesize a specific surface protein, cultured cells were trypsinized and centrifuged at $200 \times g$ for 5 min. Then, cells were counted, washed with PBS and diluted to 1×10^5 cells in 100 μ l PBS. Subsequently, cells were stained with an antibody directed against a specific protein following the manufacturer's instructions and analyzed using a BD Accuri C6 flow cytometer. For the analysis, a triplicate was utilized. At least three independent experiments were done.

2.2.4.10.3 *Cell cycle analysis with propidium iodide (PI)*

To analyze the distribution of the major phases of the cell cycle (G0/G1, S and G2/M-phase) in colorectal tumor cell lines, the DNA content was measured by PI staining. Cells were seeded in 6 well plates and cultivated for 2–3 days. Then, cells were trypsinized, centrifuged at $200 \times g$ for 5 min and fixed for > 2 h on ice. Subsequently, fixed cells were washed with PBS and incubated with PI/TritonX100/RNaseA solution for 15 min at 37°C (Darzynkiewicz and Huang, 2004). The measurement was done with the AccuriC6 flow cytometer and analyzed with the C-Flow Plus Software. The DNA histogram gave information about the amount (%) of apoptotic cells (subG1 peak) as well as the distribution of the different cell cycle phases. At least two independent experiments were done.

2.2.4.11 *Sphere formation assay*

The ability to form spheres under serum-free and non-adherent conditions is a feature of cells with CSC characteristics (Kreso and O'Brien, 2008). For measuring the CSC character of tumor cell lines after *OLFM4* overexpression, cells were trypsinized and 2×10^4 cells were seeded in 24 cluster well plates (Ultra-Low attachment surface) in 1 ml StemProR hESC SFM medium in the presence of 0.01 μ g/ml FGFb. After 7 days, the formed spheres were documented and counted using phase contrast microscopy.

2.2.5 *Methods used for working with mice*

2.2.5.1 *Experimental procedure*

For the induction of CreER^{T2} induced recombination of floxed genes in mice, tamoxifen (TAM; 100 mg for stock solution 10 mg/ml, 150 mg for stock solution 15 mg/ml) was dissolved in 1 ml 100% EtOH (10 min heated at 55°C), 9 ml sunflower oil was added and mixed. The mixture was stored in aliquots (2 ml) at -20°C. Mice were injected intraperitoneally with TAM at 4 consecutive days: day 0 - 3 mg TAM (200 µl of the 15 mg/ml stock solution); day 1, 2 and 3 - 2 mg TAM (200 µl of the 10 mg/ml stock solution). At day 21, mice were sacrificed and organs were harvested. The intestine was divided into four parts (small intestine into three equal parts, colon into one part) for a better handling and the cecum was removed. Then, all parts of the intestine were cleaned with PBS, put on Whatman paper, cut lengthwise and all organs were fixed over night in 4% formalin. Subsequently, the tissue was dehydrated and embedded in paraffin. The paraffin blocks were cut with the microtome in slices (2 µm thick) and put on slides.

2.2.5.2 *LacZ and eosin staining*

Mice were injected intraperitoneally with tamoxifen (3 mg in 200 µl) at day 0. At day 5, the mice were sacrificed and the intestine was harvested. Each of the four parts of the intestine (see 2.2.5.1) was cut into 0.5 cm long pieces and fixed in fixative in a 12 well plate for 2 h at 4°C while shaking. Then, the tissue was washed two times at RT with PBS and stained over night at RT in staining solution, protected from light, while shaking. Subsequently, the tissue was washed in PBS 2 times, put in embedding cassettes and fixed over night in 4% formalin. Then, the tissue was dehydrated and embedded in paraffin. Paraffin blocks were cut with the microtome in slices (2 µm thick), put on slides and stained with eosin. For that purpose, the paraffin was removed from the slices by incubating 3 times for 10 min in xylene and 3 times for 10 min in absolute ethanol. Then, the slices were stained in eosin Y (containing 90% ethanol) for 3 to 5 min. Afterwards, the slices were put in 80% ethanol, in absolute ethanol and subsequently in xylene, covered with VectaMount mounting medium and fixed with cover slips.

2.2.5.3 *Counting of adenomas by stereomicroscopy*

Number and size of adenomas of the four parts of the intestine (see 2.2.5.1) were counted macroscopically with the Stemi SV6 (Zeiss, objective S 1.6). The used magnification was 12.8-80 fold, depending on the size of the adenomas. The size of the adenomas was measured with the help of a ruler. Areas from each part of the intestine were photographed at 32 fold magnification.

2.2.6 *Methods used for working with tissue*

2.2.6.1 *Staining of mouse tissue*

2.2.6.1.1 *Immunohistochemistry*

The antibody staining of the mouse tissue was performed following the subsequently description.

<i>Step</i>	<i>Antigen</i>	<i>Treatment</i>
Dewaxing	all	xylene 3x 10 min, 100% EtOH 3x 10 min
Pretreatment	β -catenin	ProTaq _s IV Antigen Enhancer (Quartett); microwave 750 W 2x 15 min
	KI-67	Target retrieval Solution (Dako); microwave 750 W 2x 15 min
	cl. caspase 3	Citrate (Dako); microwave 750 W 2x 15 min
	DICER1	ERS6 (Novocastra); microwave 750 W 2x 15 min
	lysozyme	Proteinase Type XXIV (Sigma-Aldrich), 10 min
Blocking of endogenous peroxidase	all	hydrogen peroxide (7.5%); 10 min
Blocking of unspecific binding sites	β -catenin	DCS Crystal Mouse Block Solution A (DCS), 30 sec; DCS Crystal Mouse Block Solution B (DCS) for 5 min
	KI-67	Protein Block (Dako), 10 min
	cl. caspase 3, DICER1, lysozyme	blocking serum (ImmPRESS Reagent Kit; Vector), 20 min
	Antibody staining	β -catenin

	KI-67	primary antibody (anti-KI67/ TEC3; 1:150), 1 h at RT; biotinylated anti-rat IgG (Vector), 30 min at RT; Streptavidin HRP (Novocastra) and stained with chromogen AEC (Invitrogen)
	cl. caspase 3	anti-cleaved caspase 3 1:100, for 1 h at RT ImmPRESS Reagent Kit anti-rabbit Ig (Vector) 30 min; chromogen DAB+ (Dako) 3 min
	DICER1	anti-DICER1 1:80 1 h at RT; ImmPRESS Reagent Kit anti-rabbit Ig (Vector) 30 min; chromogen DAB+ (Dako) 3 min
	lysozyme	anti-lysozyme 1:14000 1h at RT; ImmPRESS Reagent Kit anti-rabbit Ig (Vector) 30 min; chromogen DAB+ (Dako) 3 min
Counterstaining	all	hematoxylin (Vector)
Fixation	all	Kaiser's glycerin gelatine (Merck)

The pictures of the sections stained by immunohistochemistry were taken with the Leica micro-photography system DMD108 with 200 and 400 fold magnification. The respective percent of positive stained cells in the adenomas were estimated per adenoma for at least 32 adenomas per genotype. For the evaluation of positive cells for cleaved caspase 3 (cl. caspase 3), positive cells were counted per adenoma. Additionally, the adenoma size was measured using ImageJ-Software (NIH) ("freehand selection") and the cell number was calculated relative to the adenoma area.

2.2.6.1.2 *H&E staining*

H&E stainings were done using the Tissue-Tek Prisma (Sakura), following the subsequent description.

<i>Step</i>	<i>Time</i>
drying station	12 min
xylene	2x 2 min
100%, 96%, 70% EtOH	each 1 min
wash station	30 sec
hematoxylin	6 min
wash station	4 min
70% EtOH	1 min
eosin Y (alcoholic)	2 min 30 sec
96%, 100% EtOH	each 1 min
xylene	2 min 30 sec

2.2.6.1.3 *PAS staining*

PAS stainings were done using the Tissue-Tek Prisma (Sakura), following the subsequent description.

<i>Step</i>	<i>Time</i>
drying station	12 min
xylene	2x 2 min
100 %, 96%, 70% EtOH	each 1 min
aqua dest.	30 sec
periodic acid	5 min
aqua dest.	1 min
Schiff reagent	5 min
wash station	5 min
hematoxylin	5 min
wash station	5 min
96%, 100% EtOH	each 1 min
xylene	2 min 30 sec

2.2.6.2 *Human tissue collection*

2.2.6.2.1 *Characteristics of the tissue collection*

The classification of the colorectal tumors follows the standards of the UICC (Union internationale contre le cancer). Here, the tumors are graded by the TNM-system (T: primary tumor, N: lymph node metastasis, M: distant metastasis) (Table 2). The primary tumor is graded in different T-stadiums according to the infiltration: T1 means that the

tumor infiltrates the submucosa, T2 the muscularis propria, T3 the subserosa or pericorectal tissue and T4 other organs or structures. Furthermore, the occurrence of lymph node metastases is classified as N0 (no regional lymph node metastases), N1 (1 to 3 regional lymph node metastases) or N2 (4 or more regional lymph node metastases) whereby at least 20 lymph nodes have to be investigated. Distant metastases are graduated in M0 (no distant metastases) and M1 (distant metastasis). Additionally, tumors can be graded concerning the differentiation of the tumor cells (grading, G). Here, G1 means that the tumor displays a well-, G2 moderately-, G3 poorly- and G4 undifferentiated epithelial differentiation of the tumor cells (Bosman et al., 2010; Bruns et al., 2013; Sobin et al., 2009).

<i>UICC stage</i>	<i>T</i>	<i>N</i>	<i>M</i>
I	T1, T2	N0	M0
II	T3, T4	N0	M0
III	every T	N1, N2	M0
IV	every T	every N	M1

Table 2. TNM-classification of the colorectal tumors, following the standards of the UICC (*Union internationale contre le cancer*).

T: primary tumor, N: lymph node metastasis, M: distant metastases (according to (Bosman et al., 2010; Bruns et al., 2013; Sobin et al., 2009).

In order to analyze the protein level of DICER1 during colorectal carcinogenesis and progression, formalin fixed and paraffin embedded (FFPE) samples of CRC specimens from 90 patients that underwent surgical tumour resection at the Hospital of the LMU München between 2003 and 2010 were obtained from the archives of the Institute for Pathology. The patients were selected randomly from the database of the Institute of Pathology according to their UICC stage (UICC stage I-IV) (Sobin et al., 2009). Furthermore, 27 endoscopically removed tubular colonic adenomas (15 with low grade and 12 with high grade intraepithelial neoplasia) were assembled. The clinico-pathological parameters according to WHO 2010 and TNM Classification of Malignant Tumors (Bosman et al., 2010) are summarized in Table 3. The study was carried out according to the recommendations of the local ethics committee of the Medical Faculty of the LMU München. For comparative analysis normal colonic tissue (123 patients) adjacent to the adenoma or carcinoma was analyzed.

<i>Parameter</i>	<i>Number of patients (%)</i>
Normal colonic mucosa	n=123
Adenoma	n=27
low grade IEN	15 (12.8)
high grade IEN	12 (10.3)
Carcinoma	n=90
UICC I	23 (19.7)
UICC II	19 (16.2)
UICC III	24 (20.5)
UICC IV	24 (20.5)
T1	6 (5.1)
T2	22 (18.8)
T3	45 (38.5)
T4	17 (14.5)
N0	52 (44.4)
N+	38 (21.5)
M0	66 (56.4)
M1	24 (20.5)
G1	3 (2.6)
G2	55 (47.0)
G3	31 (26.5)
G4	1 (0.9)

Table 3. Patient details of the human tissue collection.

This human tissue collection was used for the analysis of the DICER1 levels during cancer progression. IEN: intraepithelial neoplasia

2.2.6.2.2 *Immunohistochemistry*

5 µm sections from each paraffin block were stained with a DICER1 specific antibody (anti-DICER1, 1:75, Sigma–Aldrich). Staining was performed on a Ventana Benchmark XT autostainer with the XT ultraView DAB Kit (Ventana Medical Systems, Roche) following manufacturer’s instructions. Sections were evaluated by a pathologist. The staining of DICER1 was scored from 0 to 3, considering only the cytoplasmic reaction (Fig. 32).

2.2.7 *Statistical analysis*

The statistical analyses were performed using the two-tailed Student's t-test, except for the human tissue collection. For the human tissue collection, the χ^2 -test was used. Statistical significance was considered as follows: * $p < 0.05$, ** $p < 0.01$, *** $p < 0.001$.

3 Results

CSCs are crucial for the tumor initiation as well as tumor progression and can escape classical chemotherapy whereby they cause tumor recurrence with few or no therapeutic alternatives (Fanali et al., 2014; Marjanovic et al., 2013). Thus, alternatives have to be developed. A promising therapeutic concept might be specific CSC targeted therapies that kill the source of the tumor and lead to regression of the tumor (Fanali et al., 2014; Frank et al., 2010). A therapeutic target for CSCs might be SC sustaining molecules. Their expression and synthesis is often restricted to SCs such as CSCs. As *OLFM4* was described to be expressed in CBC cells of the human intestine, *OLFM4* was discussed to be a SC marker and to possess a comparable role as the SC marker *LGR5* (van der Flier et al., 2009). CBC cells can be transformed to CSCs by Wnt signaling pathway activation (Barker et al., 2009) and thus, the influence of *OLFM4* as a sustaining molecule for CSC features might be a promising target for CSC therapy. As the CSC feature stemness is associated with the other CSC features metastasis, EMT and chemoresistance, the interference of stemness should also influence the other features. The role of *OLFM4* as a CSC marker and its influence on CSC features and tumorigenesis are, however, not completely understood because of inconsistent studies (van der Flier et al., 2009; Ziskin et al., 2013). Therefore, the role of *OLFM4* regarding stemness and tumorigenesis was investigated. Subsequently, all cells with properties of CSCs are termed CSCs for the sake of simplification.

3.1 The role of *OLFM4* in colorectal cancer cell lines

Properties of *OLFM4* were already investigated in various cancer tissues, with inconclusive results; both, tumor promotion (Liu et al., 2012; Zhang et al., 2004) as well as limitation (Chen et al., 2011; Liu et al., 2008) have been described. On the one hand, enhanced *OLFM4* mRNA and *OLFM4* protein levels were found in tumors (Luo et al., 2011). Furthermore, *OLFM4* was described to act as an anti-apoptotic protein (Kim et al., 2010; Liu et al., 2012; Zhang et al., 2004) and to be necessary for proliferation and anchorage-independent growth (Kobayashi et al., 2007; Liu et al., 2012). On the other hand, *OLFM4* has been found to be reduced or undetectable in prostate cancer cell lines

and tissues (Chen et al., 2011) and to suppress proliferation, tumor growth, invasiveness and metastases formation (Chen et al., 2011; Park et al., 2012). In CRC, *OLFM4* was not expressed or downregulated at the invasion front as well as in poorly differentiated and metastatic tissues (Liu et al., 2008) which is not expected for a SC marker. Furthermore, the role of *OLFM4* was investigated in the CRC cell line HT29 concerning proliferation and migration (Liu et al., 2008), however, in the latter study, the morphology and the migration capacity of the cell line HT29 was different from that found in other publications (Banning et al., 2008; Tsukahara and Murakami-Murofushi, 2012) and thus, has to be viewed critically. Therefore, I performed in this study subsequent experiments to clarify the role of *OLFM4* concerning stemness and tumorigenesis in CRC.

3.1.1 Expression of *OLFM4* in CRC cell lines and in CSCs

To clarify the role of *OLFM4* concerning tumorigenesis, the expression pattern of *OLFM4* in 14 CRC cell lines was analyzed by RT-qPCR. Intriguingly, only two cell lines (SW1222 and LS174T) showed a measurable expression of *OLFM4* at the mRNA level (Fig. 15).

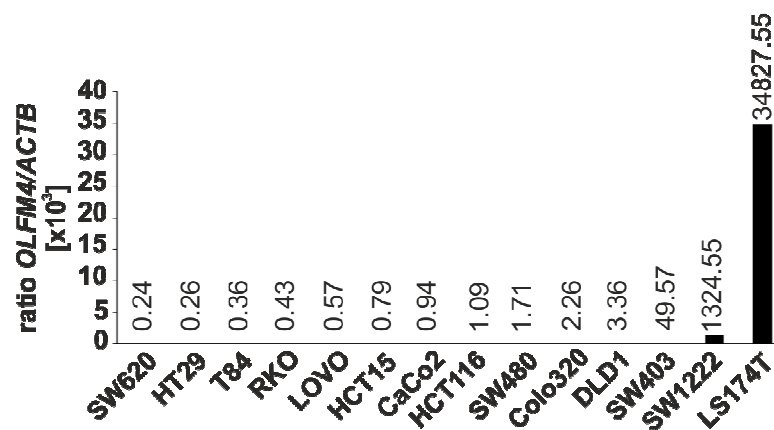


Fig. 15. *OLFM4* is endogenously expressed in the CRC cell lines SW1222 and LS174T.

To determine the endogenous *OLFM4* expression level in several CRC cell lines, different cell lines were harvested and mRNA isolated. Expression of the mRNAs was determined by RT-qPCR. The indicated values are the ratios of *OLFM4* and *ACTB* (β -actin), calculated from the Cp values. Surprisingly, only in two (SW1222 and LS174T) out of 14 cancer cell lines endogenous *OLFM4* expression was detectable.

Based on this result, *OLFM4* could possibly act as a tumor suppressor, as reported in prostate cancer (Li et al., 2013), and thus be inactivated or downregulated in CRC cell lines. Another explanation might be that *OLFM4* is only expressed in CSCs which are a

small subpopulation of the tumor cells and therefore, the *OLFM4* expression is not detectable in these cell lines. Thus, to clarify the latter possibility, I performed an aldefluor assay to separate CSCs. In this assay, the enzyme ALDH1 metabolizes the substrate ALDEFLUOR to a fluorescent product and, as a result, the fluorescent cells can be isolated. ALDH1 protein is present and enzymatically active in CSCs and responsible for the detoxification and thus oxidation of intracellular aldehydes (Huang et al., 2009). Thus, populations with high (ALDH1+) or low (ALDH1-) activity of ALDH1 were isolated from singularized spheroid tumor cells of the primary CRC cell lines coCSC-AS3 and -AS4 by aldefluor assay. As a proof of principle that the cell sorting (FACS) worked well, the expression of *ALDH1* was analyzed at the mRNA level by RT-qPCR (Fig. 16A). As expected, ALDH1+ cells showed a higher expression of *ALDH1* than ALDH1- cells. Moreover, RT-qPCR analysis revealed, as expected, a higher expression of the known stem cell markers *LGR5* and *PROM1* (Kemper et al., 2012; O'Brien et al., 2007) in the ALDH1+ cells since ALDH1+ cells are known to possess SC properties (Huang et al., 2009). Surprisingly, *OLFM4* expression decreased in these cells (Fig. 16A). Thus, no coexpression of *OLFM4* with known SC markers and rather decreased expression of *OLFM4* in the CSCs compared with the other tumor cells (non-CSCs) was detected.

To examine this observation further in a second independent approach, cells were selected for chemoresistance by chemotherapy whereby SC properties are induced and CSCs are enriched (Dallas et al., 2009). Hence, LS174T cells presenting a high expression of *OLFM4* (Fig. 15) were treated with the commonly used concentrations of 40 μ M or 50 μ M 5-FU for 5 days and analyzed by RT-qPCR. 5-FU treatment led to a higher expression of the stemness markers *PROM1* and *CD44* (Dalerba et al., 2007), whereas the *OLFM4* expression was decreased (Fig. 16B). Thus, this second approach revealed similar results as the aldefluor assay. Therefore, *OLFM4* is not increased expressed in CSCs and thus, not a CSC marker.

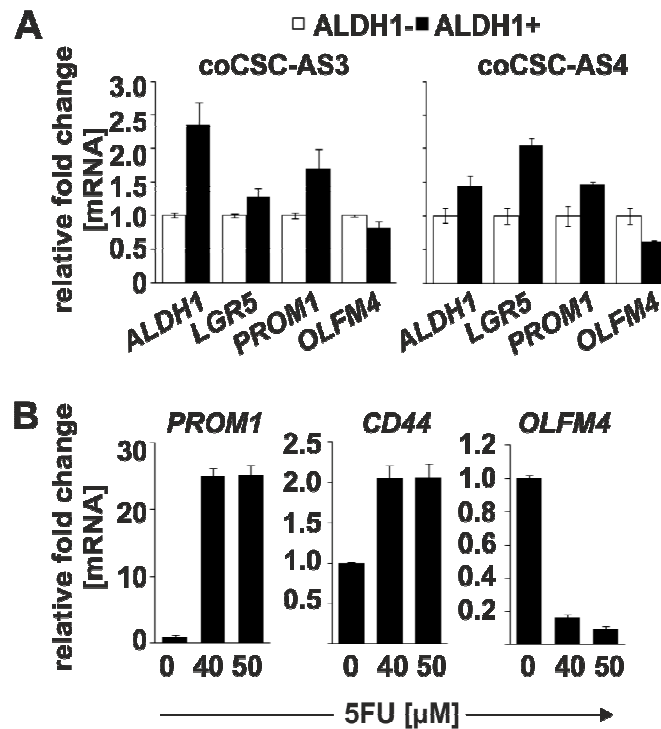


Fig. 16. *OLFM4* expression did not correlate with expression of characteristic CSC markers.

(A) Singularized spheroid tumor cells of the primary CRC cell lines coCSC-AS3 and -AS4 were separated by aldefluor assay in cells with high and low activity of ALDH1 (ALDH1+ and ALDH1-, respectively). Subsequently, mRNA was isolated and expression of the indicated mRNAs was determined by RT-qPCR and normalized to the reference genes *ACTB* and *HPRT1* (hypoxanthin phosphoribosyltransferase 1). ALDH1+ cells showed, compared to ALDH1- cells, increased expression of *ALDH1* and of the SC markers *LGR5* and *PROM1*, whereas *OLFM4* expression decreased in ALDH1+ cells compared to ALDH1- cells. (B) LS174T cells were treated with rising concentrations of 5-FU. Cells treated only with DMSO (0 μM 5-FU) were taken as control samples. 5 days after treatment, cells were harvested, mRNA isolated, analyzed by RT-qPCR and normalized to *ACTB*. Upon 5-FU treatment, *OLFM4* was downregulated, whereas the SC markers *PROM1* and *CD44* were upregulated. Data are represented as mean ± SD from two or three biological replicates.

3.1.2 *OLFM4* was ectopically overexpressed in CRC cell lines and had no influence on marker expression

Since *OLFM4* was not expressed in CSCs, in contrast to the known SC markers, the question arose what kind of role *OLFM4* has in CRC. Therefore, I ectopically expressed *OLFM4* in cancer cell lines which do not express *OLFM4* endogenously to investigate the functional influence of high *OLFM4* protein levels in CRC cell lines. To do so, *OLFM4* or chloramphenicol acetyltransferase (*CAT*) as control were overexpressed in the cell lines DLD1, HT29, HCT116, LOVO and SW480 because only two (LS174T, SW1222) of 14 investigated CRC cell lines endogenously expressed *OLFM4* (Fig. 15). I utilized a lentiviral vector system in which *OLFM4* and *CAT* were expressed with a C-terminal V5-tag to be able to easily detect the protein levels of *OLFM4*-V5 and *CAT*-V5. The

expression vectors were cloned, infectious lentivirus was made, the cell lines were lentivirally transduced and selected as bulk cultures by puromycin. The expression intensity of *OLFM4-V5* was verified by RT-qPCR and the *OLFM4-V5* protein amounts were measured by Western Blot. *OLFM4-V5* was overexpressed at the mRNA level and also high *OLFM4-V5* protein levels were present (Fig. 17A, B). With this a cellular system was generated that could be used in the following investigations if *OLFM4-V5* overexpression and thus, high *OLFM4-V5* protein levels have effects on CRC cell lines.

With the aforementioned generated cell lines, I explored in a first approach if the overexpression of *OLFM4-V5* and thus, high *OLFM4-V5* protein levels (*OLFM4* and *CAT* are subsequently synonyms for *OLFM4-V5* and *CAT-V5*) influenced marker expression/protein levels. In this analysis, different groups of markers were chosen known to influence or to be associated with several properties of tumor cells such as stemness, EMT and differentiation. Thus, to investigate marker expression concerning stemness, I chose the well known SC markers *PROM1*, *CD44*, *LGR5* and *ALDH1* (Barker et al., 2007; Dalerba et al., 2007; Huang et al., 2009) and analyzed the expression of these markers in the generated cell lines at the mRNA level by RT-qPCR. By forced expression of *OLFM4* and thus, high *OLFM4* protein levels, the expression of the SC markers compared to the control cells (*CAT*) was unaffected (Fig. 17C). Additionally, I chose a set of differentiation and EMT markers for analysis since during tumorigenesis and the metastasis process a change in the expression of these markers occurs. EMT comprises a change from an epithelial phenotype to a more mesenchymal phenotype. An overexpression of *OLFM4*, however, did not change the expression of the cell adhesion molecule gene *CDH1* (cadherin 1; E-cadherin) that is associated with the epithelial phenotype, measured at the mRNA level by RT-qPCR and at the protein level by Western Blot (Fig. 17C, B). Furthermore, the differentiation markers *KRT20* and *MUC2* that characterize the epithelial state and are connected with terminal differentiation in the crypt were determined at the mRNA level by RT-qPCR and were also unaffected (Fig. 17C). Markers indicative for the mesenchymal differentiation are the mesenchymal marker *VIM* (vimentin) or the master switches of EMT such as *SNAI1*, *SNAI2* or *ZEB1*. Consistent with the previous results, *VIM* expression was not influenced by a forced expression of *OLFM4* compared to control cells (*CAT*), determined at the mRNA level by RT-qPCR and at the protein level by Western Blot (Fig. 17C, B). Likewise, the expression of *SNAI1*, *SNAI2* or *ZEB1* was not influenced by an *OLFM4* overexpression, measured at the mRNA level by RT-qPCR (Fig.

17C). Thus, an overexpression of *OLFM4*/high levels of OLFM4 protein did not influence the expression of stemness, EMT and differentiation markers compared to control cells (CAT).

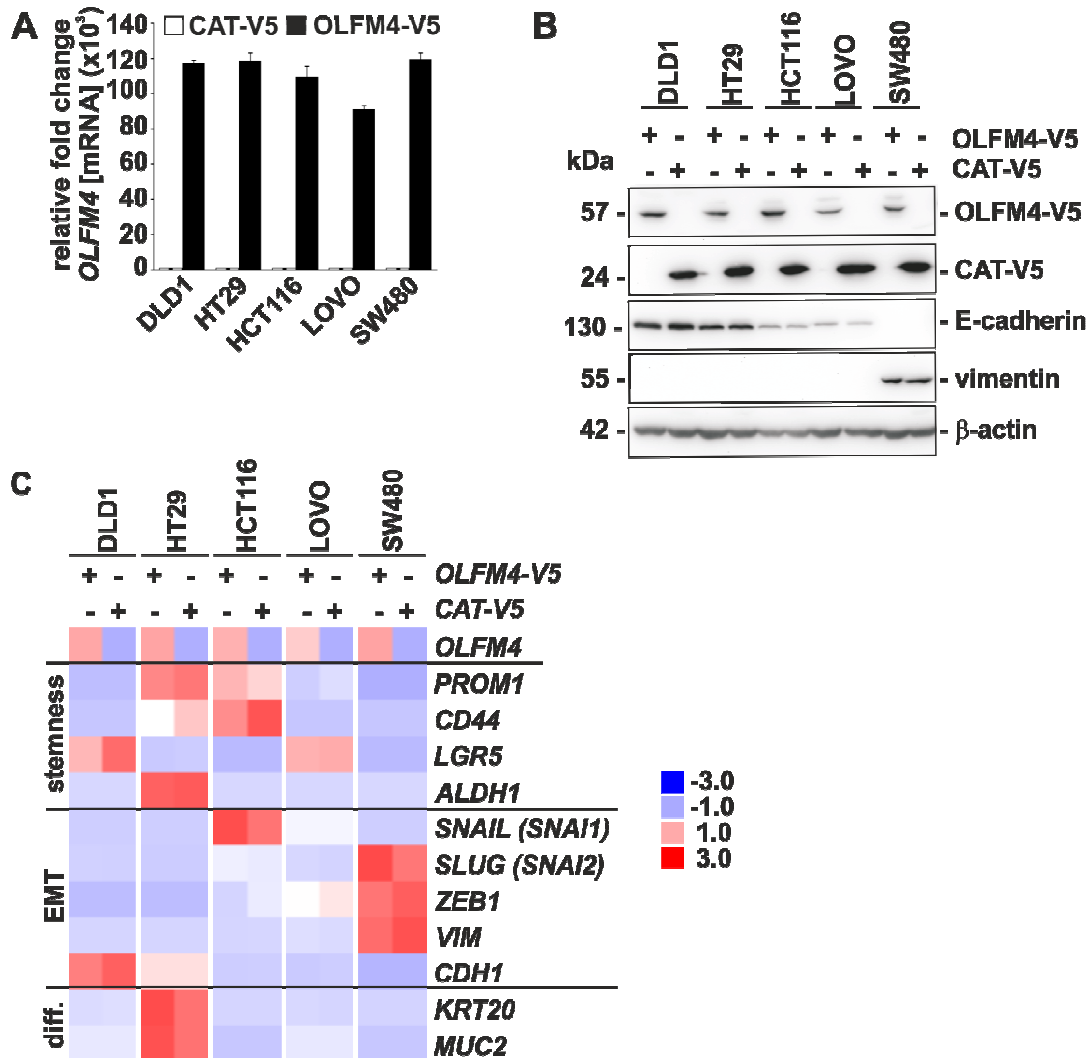


Fig. 17. Viral transduction of CRC cell lines with OLFM4-V5 resulted in high *OLFM4* mRNA and OLFM4 protein levels but did not alter marker expression/protein levels.

(A) Different OLFM4 negative cell lines were transduced with a C-terminal V5-tagged *OLFM4* or *CAT* (as a control) and selected via puromycin as bulk cultures. 48 h after seeding cells were harvested, mRNA was isolated, analyzed by RT-qPCR and normalized to *ACTB*. By a lentiviral vector system, high levels of *OLFM4-V5* mRNA were reached in various cancer cell lines. Data are represented as mean \pm SD from two biological replicates. (B) To determine the OLFM4-V5 and CAT-V5 amounts at the protein level, cells were harvested 48 h after seeding. Total cell lysates were analyzed by SDS-PAGE and immunoblotting. OLFM4-V5 and CAT-V5 protein levels were detected with a V5-specific antibody; additionally, E-cadherin and vimentin were detected with specific antibodies; β -actin served as a loading control. Upon viral transduction, OLFM4-V5 and CAT-V5 could be robustly detected in several CRC cell lines at the protein level. However, high ectopic OLFM4 protein levels did not lead to a change of the markers E-cadherin and vimentin, both associated with EMT. (C) 48 h after seeding, cells with stable ectopic expression of *OLFM4-V5* and *CAT-V5* (control) were harvested, mRNA was isolated and analyzed by RT-qPCR. Expression of the indicated

mRNAs was normalized to *ACTB*. The normalized values of the different genes were all calculated relative to the expression of the cell line HCT116-CAT-V5 and the resulting values were processed by the dChip software. *OLFM4* did not significantly affect stemness, EMT and differentiation markers compared to control cells (CAT). Data are represented as mean (n= 3).

3.1.3 *OLFM4* had no influence on proliferation

Because the investigation of the marker expression was only descriptive, in a next step functional assays were performed. In a first approach, the role of *OLFM4* in the regulation of proliferation, an important hallmark of cancer, was investigated. Therefore, proliferation of the ectopically *OLFM4* overexpressing CRC cell lines DLD1, HT29 and HCT116 was compared with *CAT* overexpressing cell lines employing the MTT assay. The MTT assay measures the cell vitality by mitochondrial activity. This is a surrogate for proliferation and therefore, MTT assay can be deployed to measure proliferation. High *OLFM4* protein levels did not affect proliferation of the analyzed CRC cell lines (Fig. 18). Thus, *OLFM4* is no driving force of proliferation.

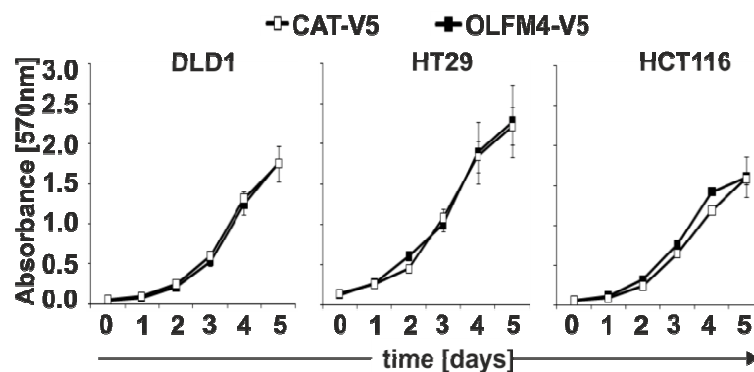


Fig. 18. High *OLFM4* protein levels had no effect on proliferation.

Proliferation was analyzed in *OLFM4* stably overexpressing cell lines (DLD1, HT29, HCT116) via MTT assay for 5 days. *CAT* stably overexpressing cells served as control. Measurement was conducted immediately after seeding and subsequently every 24 h at the wavelength of 570 nm by an ELISA reader. Data are represented as mean \pm SD from three biological replicates. High *OLFM4* protein levels had no functional relevance for the proliferation of CRC cell lines.

3.1.4 *Wnt* signaling pathway was not affected by *OLFM4*

Besides the proliferation, nuclear β -catenin localization is another important property of CRC and CSCs. Hence, I investigated whether *OLFM4* overexpression had an effect on the subcellular localization of β -catenin, a downstream transcription factor of the Wnt

signaling pathway. Nuclear localization of β -catenin implies transcriptional activity and is a known marker and inductor for stemness (Fodde and Brabletz, 2007; Vermeulen et al., 2010). The subcellular localization of β -catenin was examined by immunofluorescence analysis. Overexpression of *OLFM4* did not influence the subcellular localization of β -catenin compared to *CAT* overexpressing cell lines (Fig. 19A). The cell lines DLD1, HT29, HCT116 and LOVO showed a cytoplasmic and membranous localization of β -catenin, whereas in SW480 cells β -catenin was localized in the nucleus, both in *OLFM4* and *CAT* overexpressing cell lines. Thus, overexpression of *OLFM4*/high *OLFM4* protein levels did not influence the subcellular localization and therefore, transcriptional activity of β -catenin.

To verify whether *OLFM4* has an effect on the transcriptional activity of Wnt signaling pathway, I subsequently measured directly Wnt signaling pathway activity by luciferase reporter assay. Therefore, luciferase reporter plasmids with 7 TCF4 (transcription factor 4)-consensus binding sites (TOPflash) were transfected. However, *OLFM4* overexpression had no effect on the activity of Wnt signaling pathway (Fig. 19B).

To increase possible effects of *OLFM4* on Wnt signaling pathway activity and as some cell lines such as RKO have no strong endogenous Wnt signaling activity, I enhanced the Wnt signaling pathway activity by transfection of a constitutive active *CTNNB1* (β -catenin) expression clone which is resistant to degradation (β -catenin-D45; (Morin et al., 1997)). This expression clone was transfected together with TOPflash luciferase reporter plasmids in *OLFM4* and *CAT* overexpressing cell lines. The influence of high amounts of the *OLFM4* protein on the Wnt signaling pathway activity was analyzed by luciferase reporter assay and compared to the control cells (*CAT*) in the context of a strongly active Wnt signaling pathway. However, the presence of *OLFM4* had also no influence on the Wnt signaling pathway when Wnt signaling pathway was strongly activated (Fig. 19C). Thus, high amounts of the *OLFM4* protein do not influence the activity of Wnt signaling pathway even in the context of a strongly activated Wnt signaling pathway.

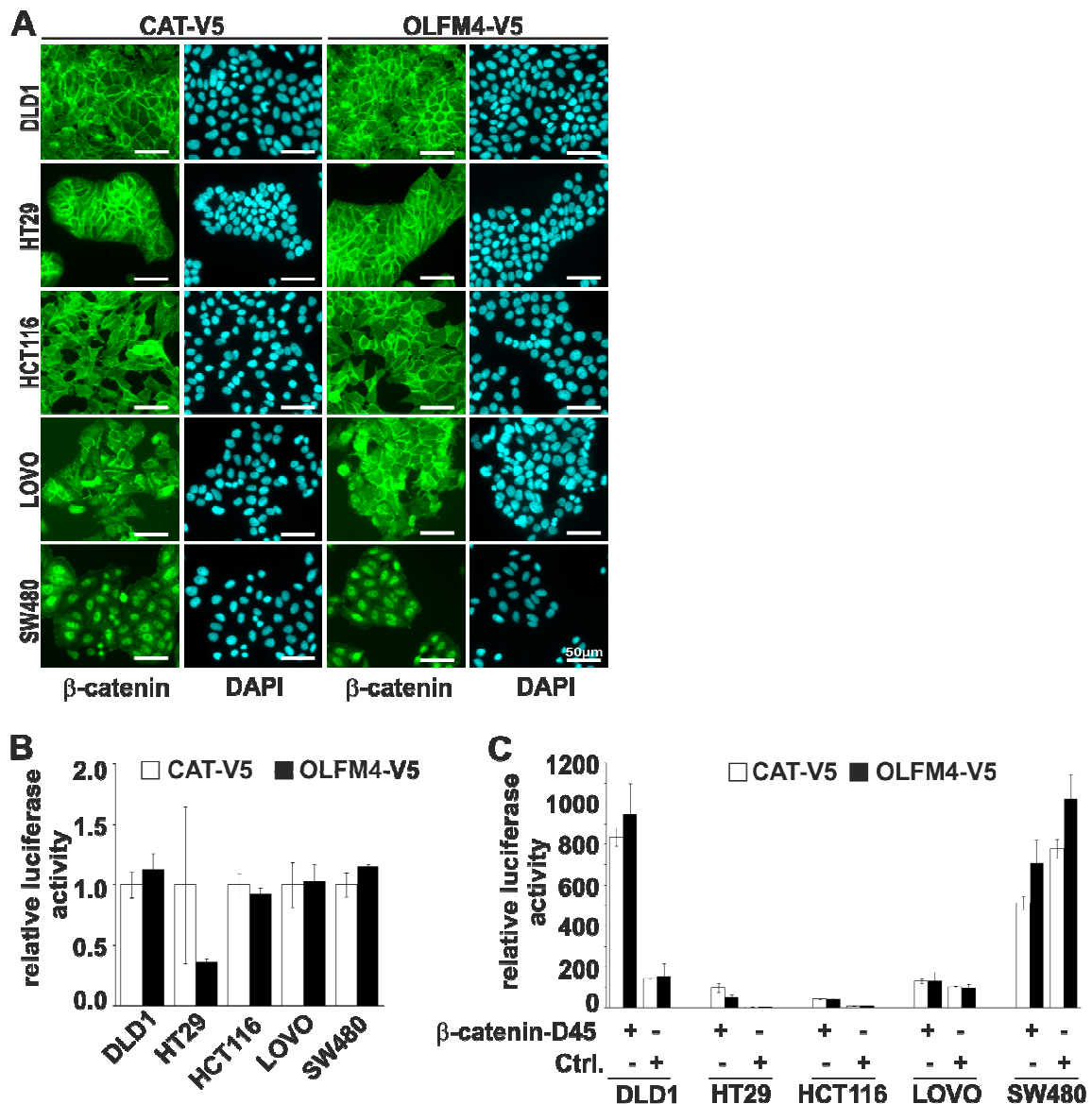


Fig. 19. Ectopic *OLFM4* expression had no influence on the cellular localization of β -catenin and the Wnt signaling pathway activity.

(A) *OLFM4* and *CAT* (control) stably overexpressing cells were fixed 72 h after seeding, stained with β -catenin specific and secondary antibody (green), covered with ProLong Gold antifade reagent with DAPI (blue; nuclear DNA) and analyzed by fluorescence microscopy. In SW480 cells β -catenin was localized in the nucleus, in the other analyzed cell lines β -catenin was localized in the cytosol and at the membrane. High *OLFM4* protein levels did not change the localization of β -catenin compared to the control cells (*CAT*). Scale bars represent 50 μ m, 200 \times magnification. (B) Luciferase reporter assay with the firefly TOPflash luciferase reporter (contains 7 TCF4 (transcription factor 4)-consensus binding sites) indicating activity of the Wnt signaling pathway. FOPflash reporter (contains mutated TCF4 binding sites) served as control. *OLFM4* and *CAT* stably overexpressing cells were transfected with either TOPflash or FOPflash reporter and additionally with a renilla luciferase vector for the normalization of the results. Luciferase activity was measured after 48 h, first normalized to renilla luciferase to exclude different transfection efficiencies and subsequently to the FOPflash reporter. The indicated values are TOP/FOP ratios. Wnt signaling pathway was not affected by high *OLFM4* protein levels. (C) To intensify the activity of the Wnt signaling pathway, a constitutive active *CTNNB1* (β -catenin) expression clone (β -catenin-D45) was transfected together with

TOP/FOPflash luciferase reporter and renilla luciferase vector and analyzed as described in (B). Wnt signaling pathway activity was enhanced by constitutive active β -catenin, however, the presence of OLFM4 had no influence on strongly activated Wnt signaling pathway. SW480 Ctrl. cells show a strong endogenous activity of the Wnt signaling pathway and thus, a high luciferase activity. Data are represented as mean \pm SD (two independent experiments taken together, per experiment n=3).

3.1.5 *OLFM4 did not influence stem cell characteristics*

Since Wnt signaling pathway activity is not the only factor that is related to stemness and to find more evidence for the unexpected result that an overexpression of *OLFM4* did not influence Wnt signaling pathway activity, a characteristic SC property, I employed the stemness indicating aldefluor assay. As mRNA expression of *OLFM4* was inversely correlated with the ALDH1 activity (ALDH1+ cells; Fig. 16A), an influence of OLFM4 on the ALDH1 activity is conceivable. The forced expression of *OLFM4* and thus, high OLFM4 protein levels in the cell lines, however, did not affect significantly the ALDH1 activity compared to *CAT* overexpression (Fig. 20A, B).

Another feature of CSCs is the ability to form spheres under serum-free, non-adherent conditions. Only CSC-like cells are capable to survive and proliferate under these conditions (Kreso and O'Brien, 2008). Therefore, by the sphere formation assay, the number of CSC-like cells in a population of tumor cells can be determined. *OLFM4* and *CAT* overexpressing cells were seeded in serum-free SC medium and after 7 days, the number of formed spheres was counted. Enforced *OLFM4* expression did not have a significant effect on the formation of spheres (Fig. 20C).

The sphere formation assay is considered to be a gold standard in the examination of the SC property *in vitro*. Another gold standard is the *in vivo* xenograft experiment. In this experiment, SW480 cells ectopically overexpressing *OLFM4* or *CAT*, respectively, were subcutaneously injected in different concentrations in NOD/SCID-mice to get a limited dilution. By the limited dilution, the frequency of CSCs in a population of tumor cells can be calculated (Kreso and O'Brien, 2008). After 7 weeks, tumors were harvested. However, SW480-*OLFM4* and SW480-*CAT* cells formed similar number of tumors. Thus, *OLFM4* or *CAT* cells possess a similar number of CSCs (Fig. 20D).

Taken together, enhanced OLFM4 protein levels did not have an effect on CSC properties such as ALDH1 activity, sphere formation assay and *in vivo* xenograft experiments.

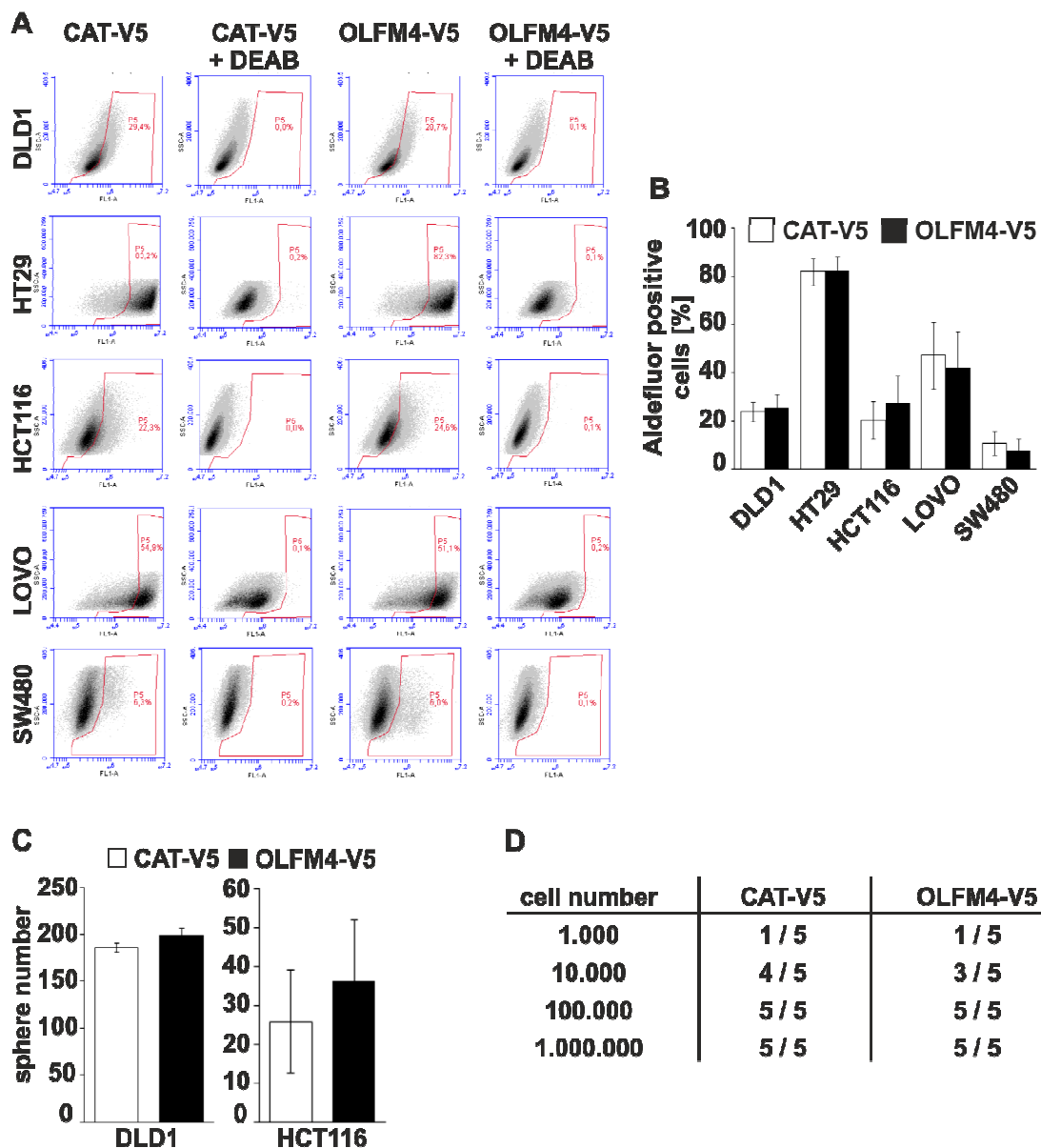


Fig. 20. OLFM4 did not change CSC features.

(A) Different *OLFM4-V5* and *CAT-V5* (control) stably overexpressing cell lines were analyzed by aldefluor assay. 48 h after seeding, cells were harvested and stained with ALDEFLUOR substrate. A portion of the cells was incubated with the ALDH1 inhibitor DEAB (diethylaminobenzaldehyde) as a background control to define the threshold of aldefluor positivity. Representative examples of the FACS analysis are shown. (B) Evaluation of the FACS analysis of ALDH1 positive cells (%). Data are represented as mean \pm SD (three independent experiments taken together, per experiment $n=3$). Stably ectopic overexpression of *OLFM4-V5* did not influence the ALDH1 activity that is associated with stemness features. (C) The capacity of *OLFM4-V5* expressing cells concerning sphere formation was analyzed compared to control cells (CAT). Cells were seeded in serum-free SC medium and after 7 days, sphere number was counted. The sphere number did not differ significantly between *OLFM4* and *CAT* overexpressing cells. Data are represented as mean \pm SD (two independent experiments, each experiment $n=2$). (D) SW480 cells, overexpressing *OLFM4-V5* and *CAT-V5* respectively, were subcutaneously injected in NOD/SCID-mice in different cell concentrations (*in vivo* xenograft). After 7 weeks, the tumors were harvested. The tumor number is described as number of mice which developed tumors/total number of mice used. No significant difference in the tumor number was detected between *OLFM4-V5* and *CAT-V5* cells (cooperation with Anne K uchler and David Horst).

3.1.6 *Metastatic characteristics were not affected by OLFM4*

Metastases formation is induced by tumor cells with CSC characteristics (Dieter et al., 2011). Aforementioned assays showed that an overexpression of *OLFM4* and thus, high amounts of *OLFM4* protein did not influence CSC characteristics in cell lines. Therefore, it is conceivable that enforced *OLFM4* expression also does not affect metastasis capacities. However, as *OLFM4* seemed to be associated with metastasis in a human tissue collection (Liu et al., 2008) and to be sure if there is an effect or not, I analyzed the influence of *OLFM4* on metastatic features in CRC cell lines. An influence of *OLFM4* concerning metastasis was measured by wound healing assay (ibidi chamber) whereby cell migration can be investigated. In accordance to the former findings, an overexpression of *OLFM4* did not affect the migration capacity of CRC cell lines because cells with high *OLFM4* protein levels migrated in 24 h (DLD1, HCT116) or 48 h (HT29) with the same rate as the control cells (CAT) (Fig. 21A, B).

During the metastatic process, cancer cells have to travel through the hemo- or lymphopoetic system and meanwhile, they have to tolerate the loss of stroma. Since tumorigenic cells develop the ability to grow autonomously, the tumor cells that are able to grow without anchorage are more tumorigenic and capable to metastasize. This state is imitated by anchorage-independent growth in methyl cellulose. The generated cell lines were seeded in methyl cellulose and allowed to grow for 12–16 days. However, the capacity to grow in methyl cellulose was not influenced by overexpression of *OLFM4* compared to control cells (CAT) (Fig. 21C, D).

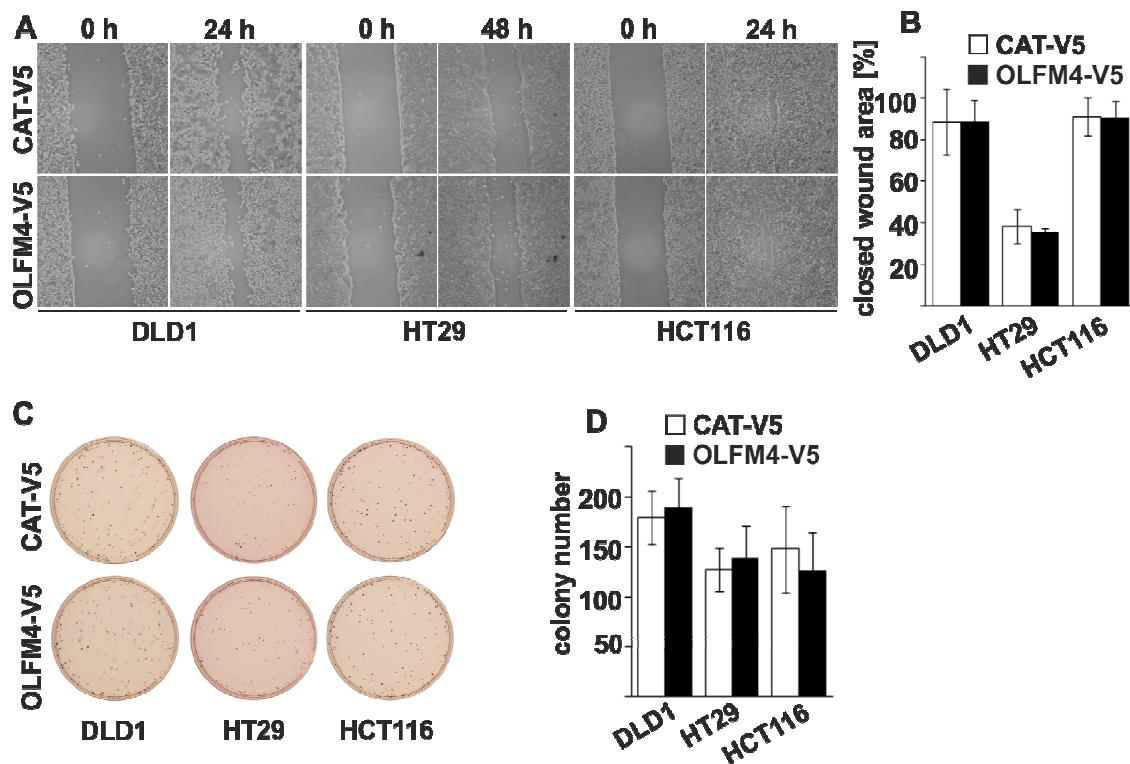


Fig. 21. OLFM4 had no influence on metastatic characteristics.

(A) To measure cell migration in wound healing assay, DLD1, HT29 and HCT116 cells which were either stably expressing *OLFM4-V5* or *CAT-V5* (control) were seeded in culture inserts (ibidi chambers). 24 h after seeding, mitomycin C was added to a final concentration of 10 $\mu\text{g}/\text{ml}$ for 3 h, the chamber was removed, culture medium was added and the defined gap between the cells was photographed at 0 h and 24 h (DLD1, HCT116)/48 h (HT29). Representative examples are shown. (B) Images were evaluated with ImageJ (NIH). Results represent the average (%) of wound closure \pm SD ($n = 3$). Cells with high *OLFM4-V5* protein levels migrated comparable to the control cells (*CAT-V5*). (C) Anchorage independent growth was analyzed in a colony formation assay. *OLFM4-V5* expressing cells were seeded in methyl cellulose. 12–16 days after seeding, cells were stained with MTT over night and photos were taken. *CAT-V5* expressing cells were analyzed as control cells. Representative examples are shown. (D) The colony number was analyzed with ImageJ (NIH). Data are represented as mean \pm SD (two independent experiments, each experiment $n=4$). The capacity to grow in methyl cellulose was not influenced by *OLFM4*.

Taken together, *OLFM4* overexpression and thus, high amounts of *OLFM4* protein did not have influence on proliferation, stemness or metastastatic features in CRC cells in cell culture. These results indicate that *OLFM4* is not a CSC marker in CRC cell lines.

3.2 The role of DICER1 and thus, the miRNAome in intestinal cancer

Besides CSC sustaining molecules, the miRNAome might also be a tool for CSC targeted therapies. Generally, miRNAs are downregulated in tumors (Lu et al., 2005). The downregulation of specific miRNAs leads e.g. to increased stemness caused by an activation of the Wnt signaling pathway (Bitarte et al., 2011; Vermeulen et al., 2010) and a less-differentiated state of tumor cells (Lujambio and Lowe, 2012). Mutations in or downregulation of molecules that are involved in the miRNA biogenesis (Lujambio and Lowe, 2012) can lead to a disruption of the miRNA biogenesis and thus, to a loss of the miRNAome. One molecule that has a central role in the miRNA biogenesis is DICER1. A downregulation or deletion of DICER1 was reported and mostly associated with advanced tumor stages, poorly differentiated tumors and reduced survival (Faggad et al., 2010; Karube et al., 2005; Kumar et al., 2009; Merritt et al., 2008). Furthermore, loss of DICER1 was investigated in various mouse models. In most cases, a conditional knockout of *Dicer1* and following downregulation of miRNAs promoted tumorigenesis (Kumar et al., 2009; Lambertz et al., 2010; Yoshikawa et al., 2013). These results indicate that DICER1 and thus, the miRNAome act as a tumor suppressor. However, loss of DICER1 in Wnt driven adenomas and its influence on intestinal tumorigenesis has not been investigated. As human CRCs and CSCs are mostly driven by the Wnt signaling pathway (Pino and Chung, 2010), investigations about the influence of the miRNAome on tumor promotion and CSC features in Wnt driven tumors might clarify the usefulness of the miRNAome as tool for CSC targeted therapy.

For that purpose, I chose a mouse model in which the knockout of *Apc* takes place specifically in the SC compartment (CBC cells) by an inducible Cre recombinase (*Lgr5-EGFP-IRES-creER^{T2}-Apc^{fl/fl}*) as deletion of the *Apc* gene in the TA cells of the crypts does not lead to adenoma formation (Barker et al., 2009). The *Apc* knockout leads to an activation of the Wnt signaling pathway in CBC cells and thus, to the generation of CSCs and efficient initiation of intestinal adenomas. In this mouse model, already after 8 days, the entire TA compartment is filled out with clusters of transformed cells which develop from microadenomas into macroscopic adenomas (Barker et al., 2009). This mouse model allows the analysis of the tumor initiation, a step in the early carcinogenesis. The crossing of this mouse model with a mouse strain with floxed *Dicer1* genes (*Dicer1^{fl/fl}*) (Harfe et al., 2005) allows the additional deletion of *Dicer1* in the CBC cells resulting in a reduction of miRNAs in these cells. The combination of the previously described mouse lines allows

the examination of the effect of the miRNAome loss on CSCs which were transformed by the activation of the Wnt signaling pathway.

3.2.1 *Design and system check of the Apc/Dicer1 mouse model*

For the generation of the aforementioned *Apc/Dicer1* mouse model, two mouse strains were crossed in the beginning: One mouse strain expresses a Cre recombinase (*CreER^{T2}*) under the *Lgr5* promoter which can enter the nucleus only after tamoxifen induction; in the other mouse strain, exon 14 of the *Apc* gene is flanked by loxP sites and can be removed by Cre recombinase (Barker et al., 2009). These mice were next crossed with mice expressing a *LacZ* (β -galactosidase) gene after recombination (Fig. 22A). Thus, cells which underwent a recombination after tamoxifen treatment can be traced via LacZ staining (Fig. 22B). Furthermore, mice in which the RNaseIII₂ domain of the *Dicer1* gene is flanked by loxP sites were additionally crossed in this mouse model, both hetero- and homozygous, to examine the influence of DICER1 on the intestinal carcinogenesis (Fig. 22A). The mouse lines which were required and used for this study are listed and described in Table 1. From now on, the abbreviations given in Table 1 are used for simplification. For a fair comparison between the mouse lines, only one factor was changed compared to another line. This ensures that the phenotype really occurs because of the presence or absence of a specific factor.

The genotypes of the mouse lines used in this study were verified via PCR of mouse tail DNA (Fig. 22B). To examine tumor formation *Lgr5(+)-Apc*, *Lgr5(+)-Apc-Dicer1^{het}* and *Lgr5(+)-Apc-Dicer1^{hom}* mice were utilized. Additionally, *Lgr5(+)-Dicer1^{het}* and *Lgr5(+)-Dicer1^{hom}* mice were employed to analyze if a sole *Dicer1* deletion in the stem cell compartment could also lead to adenoma formation. To control that adenoma formation is indeed due to the deletion of the floxed alleles, *Lgr5(-)* genotypes were used. To control after tamoxifen treatment the recombination at the crypt base where the LGR5 positive cells reside, *Lgr5(+)-Apc* mice were injected with one dose of 3 mg tamoxifen. Mice were sacrificed after 5 days and the intestine was stained via LacZ staining. After 5 days cells at the crypt base were stained (Fig. 22C). The recombined and stained cells migrated upwards the crypt indicating that the recombination worked in the LGR5 positive cells.

blocks were cut into slices. (E) Agarose gel of the PCR analysis deployed to verify the recombination of the *Apc* and *Dicer1* genes after TAM induction. For that reason, tissue of regions containing adenomas or not was scratched out independently of each other, genomic DNA was isolated and utilized for the PCR analysis. The recombination of the *Apc* and *Dicer1* genes was only detected in regions with adenomas indicating the specificity of the used mouse model. fl: floxed allele; +, WT: wildtype; rec: recombination. (F) The weight of the spleen (mg) was measured after organ removal. In *Lgr5(+)-Apc* and *Lgr5(+)-Apc-Dicer1^{het}* mice, the spleen was significantly enlarged compared to mice without adenoma formation. Data are represented as mean. Error bars indicate standard errors from six mice per genotype, except for the genotypes without adenomas (n=9). For significance, a Student's t-test was used. *p<0.05

To investigate the adenoma formation in the different genotypes, mice were injected with tamoxifen (TAM) for 4 consecutive days (day 0: 3 mg TAM; day 1, 2, 3: 2 mg TAM). After 21 days all mice were sacrificed (Fig. 22D). *Lgr5(+)* genotypes had a group size of n=6, *Lgr5(-)* had a group size of n=3 as they functioned only as control. Since the recombination of the *Dicer1* gene after tamoxifen treatment does not influence the stability of the DICER1 protein and DICER1 is still detected by the anti-DICER1 antibody (Harfe et al., 2005), a PCR was utilized to verify the recombination. Therefore, tissue of regions containing adenomas or not was scratched out independently of each other to ensure that adenoma formation was linked to recombination. Additionally, the recombination of *Apc* was controlled by PCR to link recombination in both sites to each other. Only in regions with adenomas, a recombination of *Apc* and *Dicer1* took place (Fig. 22E).

Adenoma formation in the intestine is often associated with anemia which comes along with an enlargement of the spleen. Since an enlargement of the spleen indicates that the mouse model is working well and is forming tumors, I compared the weight of the spleens of the genotypes 21 days after TAM induction. The spleens of *Lgr5(+)-Apc* as well as *Lgr5(+)-Apc-Dicer1^{het}* had significantly more weight than the spleens of mice without adenomas (Fig. 22F). This result indicated that the mouse model was working well.

Thus, with this mouse model the interaction of a conditional knockout of *Apc* and *Dicer1* in cells expressing the stem cell marker *Lgr5* could be investigated.

3.2.2 *An additional deletion of Dicer1 in an Apc knockout mouse model led to a higher adenoma number and a smaller adenoma size in the small intestine*

With this mouse model, it was now possible to investigate the tumor initiation which is a characteristic of CSCs. First, all genotypes (see Table 1) were injected with TAM for 4 subsequent days and sacrificed after 21 days because the mice started to become moribund. The organs were harvested and divided into four parts (duodenum, jejunum, ileum, colon) for a better handling. The different parts of the small and large intestine were examined macroscopically using a stereomicroscope. Sections of the intestine are shown from the duodenum to the colon (Fig. 23). Only mice positive for *Lgr5-CreER^{T2}* (*Lgr5(+)*) as well as *Apc* showed adenoma formation which was limited to the small intestine. In the colon no adenomas were observed. In *Apc* conditional knockout mice with an additional deletion of *Dicer1* in CBC cells, more adenomas than with a single deletion of *Apc* were observed. In contrast, *Dicer1* conditional knockout mice (*Lgr5(+)-Dicer1^{het}* and *Lgr5(+)-Dicer1^{hom}*) with an intact *Apc* gene presented no adenoma formation (data not shown; comparable to pictures in the left column Fig. 23). Furthermore, *Lgr5(-)* mice did not develop adenomas even if they were positive for *Apc* (Fig. 23). Therefore, only the three genotypes with adenoma formation were considered for further analysis (*Lgr5(+)-Apc*, *Lgr5(+)-Apc-Dicer1^{het}* and *Lgr5(+)-Apc-Dicer1^{hom}*) (Fig. 24).

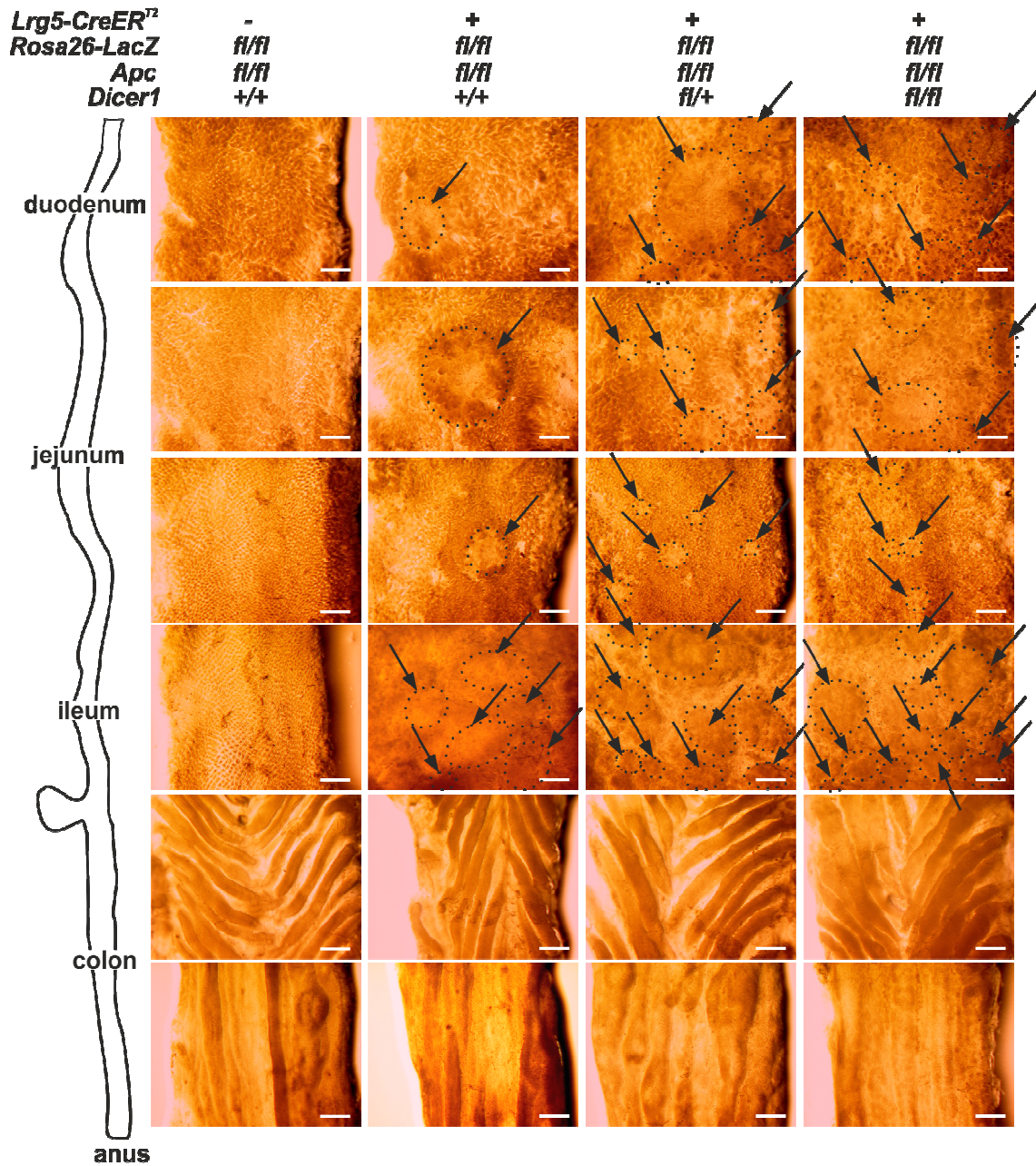


Fig. 23. *Dicer1* deletion resulted in a higher adenoma number in the small intestine of mice.

To examine the adenoma formation in the different genotypes, mice were injected with TAM for 4 consecutive days and sacrificed 21 days after the first TAM injection. Organs were harvested, the intestine was divided into 4 parts (duodenum, jejunum, ileum and colon), fixed and the adenoma formation was macroscopically analyzed by a stereomicroscope. The location of the pictures in the mouse intestine is reflected by the schematic drawing of the mouse intestine on the left side. Stereomicroscopical pictures of parts of the intestine of a mouse without adenomas (*Lgr5*⁻) and mice with adenomas (*Lgr5*⁺) are shown. Only mice in which *Apc* was conditionally knocked out (*Lgr5*⁺-*Apc*) developed adenomas in the small intestine, but not in the colon. Additional depletion of *Dicer1* (*Lgr5*⁺-*Apc*-*Dicer1*^{het}, *Lgr5*⁺-*Apc*-*Dicer1*^{hom}) resulted in an increased tumor load in the small intestine. Adenomas are indicated by black arrows and dotted lines. Scale bars represent 1 mm, 16 × magnification.

The adenoma number in the small intestine was counted using a stereomicroscope. Conditional *Apc* knockout mice with an additional deletion of *Dicer1* in CBC cells developed significantly more adenomas than conditional *Apc* knockout mice (Fig. 24A). This increase in the adenoma formation was dose-dependent of the DICER1 protein because mice with a homozygous deletion of *Dicer1* developed even more adenomas than mice with a heterozygous deletion. The number of adenomas in *Lgr5(+)-Apc* mice was comparable to the number observed by another group (O. Sansom, Beatson Institute, Glasgow; personal communication). Besides the tumor number, the general tumor burden (shown in mm²; surrogate of tumor volume) was determined. This was done by adding up the size of all adenomas per mouse. Between these three genotypes, no significant difference was visible in the general tumor burden (Fig. 24B). Nevertheless, the mean size of the adenomas (shown in mm²) significantly varied between the genotypes (Fig. 24C). A loss of DICER1 led to a smaller adenoma size which was again dose-dependent.

Taken together, an additional loss of DICER1 led in interaction with an activated Wnt signaling pathway in CBC cells to an increased tumor initiation but reduced growth of adenomas.

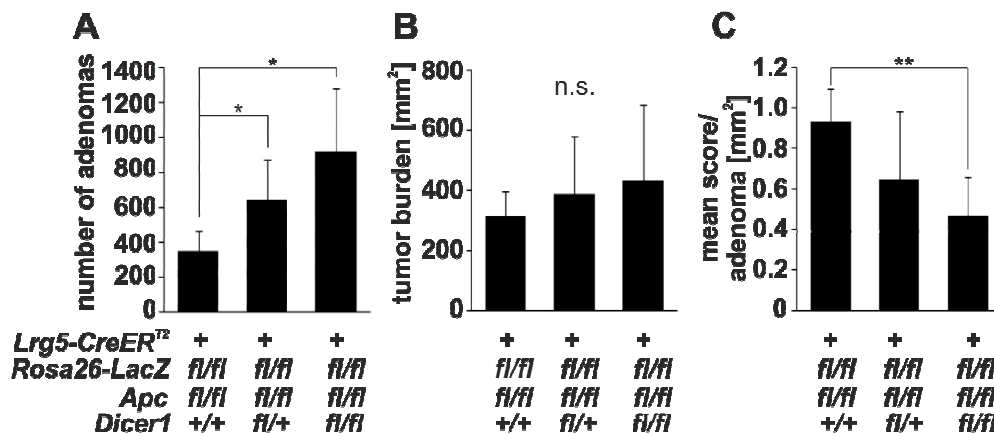


Fig. 24. *Dicer1* deletion led to an increased tumor initiation but slower tumor growth in the small intestine in the *Apc/Dicer1* mouse model.

(A) 21 days after TAM-induction the number of adenomas was macroscopically analyzed using a stereomicroscope in the indicated genotypes. Additional depletion of *Dicer1* resulted in the development of significantly more adenomas compared to *Lgr5(+)-Apc* mice. (B) The general tumor burden (mm²) was calculated from the size of all adenomas taken together per mouse. The general tumor burden did not differ significantly between the three genotypes. (C) The mean score of the adenoma size (mm²) was calculated from the number of adenomas divided by the general tumor burden per mouse. In mice with an additional homozygous deletion of *Dicer1* a significantly smaller mean score of the adenoma size than in *Lgr5(+)-Apc* mice was detected. Only genotypes that developed adenomas are listed. For significance, a Student's t-test was used. *p<0.05, **p<0.01, n.s. non significant

3.2.3 *Loss of DICER1 led to a reduced level of the proliferation marker KI-67 in adenomas*

Since a deletion of *Dicer1* resulted in a higher number and smaller size of the adenomas, the adenomas were further analyzed with respect to morphology and marker amounts by immunohistochemical staining. For that purpose, the four parts of the intestine were embedded in paraffin blocks, the blocks were cut and slices of the ileum were stained immunohistochemically. The staining of the different genotypes (*Lgr5(+)-Apc*, *Lgr5(+)-Apc-Dicer1^{het}*, *Lgr5(+)-Apc-Dicer1^{hom}*) were analyzed (200 x magnification) and the quantity of positive cells was counted for each staining (Fig. 25). Besides the three genotypes which developed adenomas, slices of a mouse without adenomas (*Lgr5(-)-Apc*) are shown as example. The latter presented an intestine without any transformations. The histology of the small intestine of mice with other genotypes that did not show any adenomas was comparable to the tissue histology of this mouse.

To analyze the morphology and differentiation of the adenomas, H&E staining was performed. The H&E staining demonstrated that the adenomas showed the morphology and differentiation that is known from tumors driven by Wnt signaling pathway referred by the WHO as adenomas NOS (not otherwise specified) (Bosman et al., 2010). The adenomas were characterized by severe dysplasia and tubular differentiation. Both, morphology and differentiation, did not differ between the analyzed genotypes (*Lgr5(+)-Apc*, *Lgr5(+)-Apc-Dicer1^{het}*, *Lgr5(+)-Apc-Dicer1^{hom}*) (Fig. 25). Thus, a deletion of *Dicer1* did not influence morphology and differentiation in Wnt signaling pathway driven adenomas.

Since the adenomas were driven by Wnt signaling pathway caused by loss of *Apc*, the number of cells with nuclear β -catenin indicating activity of Wnt signaling pathway was analyzed. As the knockout of *Apc* leads to a strong activation of Wnt signaling pathway in the adenomas, adenomas from *Lgr5(+)-Apc* mice showed, as expected, in almost 100% of the cells a nuclear staining of β -catenin (Fig. 25). Therefore, adenomas from the genotypes *Lgr5(+)-Apc-Dicer1^{het}* and *Lgr5(+)-Apc-Dicer1^{hom}* did not differ in the number of cells positive for nuclear β -catenin compared to *Lgr5(+)-Apc* mice. As β -catenin was nuclearly localized in almost 100% of the cells in the adenomas of the *Lgr5(+)-Apc* mice, no increase was possible by additional deletion of *Dicer1*. Besides the cells in the adenomas, also the cells at the crypt base of a normal crypt, the SCs, showed a nuclear localization of β -catenin. In cells with nuclear localization of β -catenin, no blue nucleus was visible. However, the vast majority of the cells in the normal, not transformed

crypts which did not undergo a recombination showed only a cytoplasmic localization of β -catenin and were characterized by a visible blue nucleus surrounded by a brown circle of β -catenin (Fig. 25; 200 and 400 x magnification). Thus, deletion of *Dicer1* did not change the nuclear localization of β -catenin in Wnt signaling pathway driven adenomas.

In adenomas, caused by an activation of Wnt signaling pathway, a deletion of *Dicer1* resulted in reduced adenoma size. The main factor influencing size is the hallmark proliferation. The proliferation can be measured immunohistochemically by the proliferation marker KI-67. In untransformed crypts, KI-67 levels were strong at the crypt base whereas towards the top of the crypt the levels declined and the villi were negative for KI-67. The adenomas generally showed a strong KI-67 staining (Fig. 25). Loss of *Dicer1* led to a significantly lower number of KI-67 positive cells, meaning less proliferation in the adenomas. Since apoptosis is another hallmark of cancer and can negatively influence proliferation, I investigated next whether the loss of DICER1 had an influence on apoptosis. Apoptosis can be measured by the number of cleaved caspase 3 positive cells. In the different genotypes (*Lgr5(+)-Apc*, *Lgr5(+)-Apc-Dicer1^{het}*, *Lgr5(+)-Apc-Dicer1^{hom}*), no difference was detectable in the number of cleaved caspase 3 positive cells per relative adenoma area. Additionally, the number of the differentiated intestinal cell types Paneth and goblet cells were investigated. However, there was also no difference visible examining lysozyme, characteristic for Paneth cells, as well as PAS staining, typical for goblet cells, with regard to the influence of DICER1 loss (Fig. 25).

Taken together, deletion of *Dicer1* in Wnt signaling pathway driven adenomas (*Lgr5(+)-Apc-Dicer1^{het}*, *Lgr5(+)-Apc-Dicer1^{hom}*) led to decreased proliferation but did not influence apoptosis or differentiation compared to adenomas from *Lgr5(+)-Apc* mice.

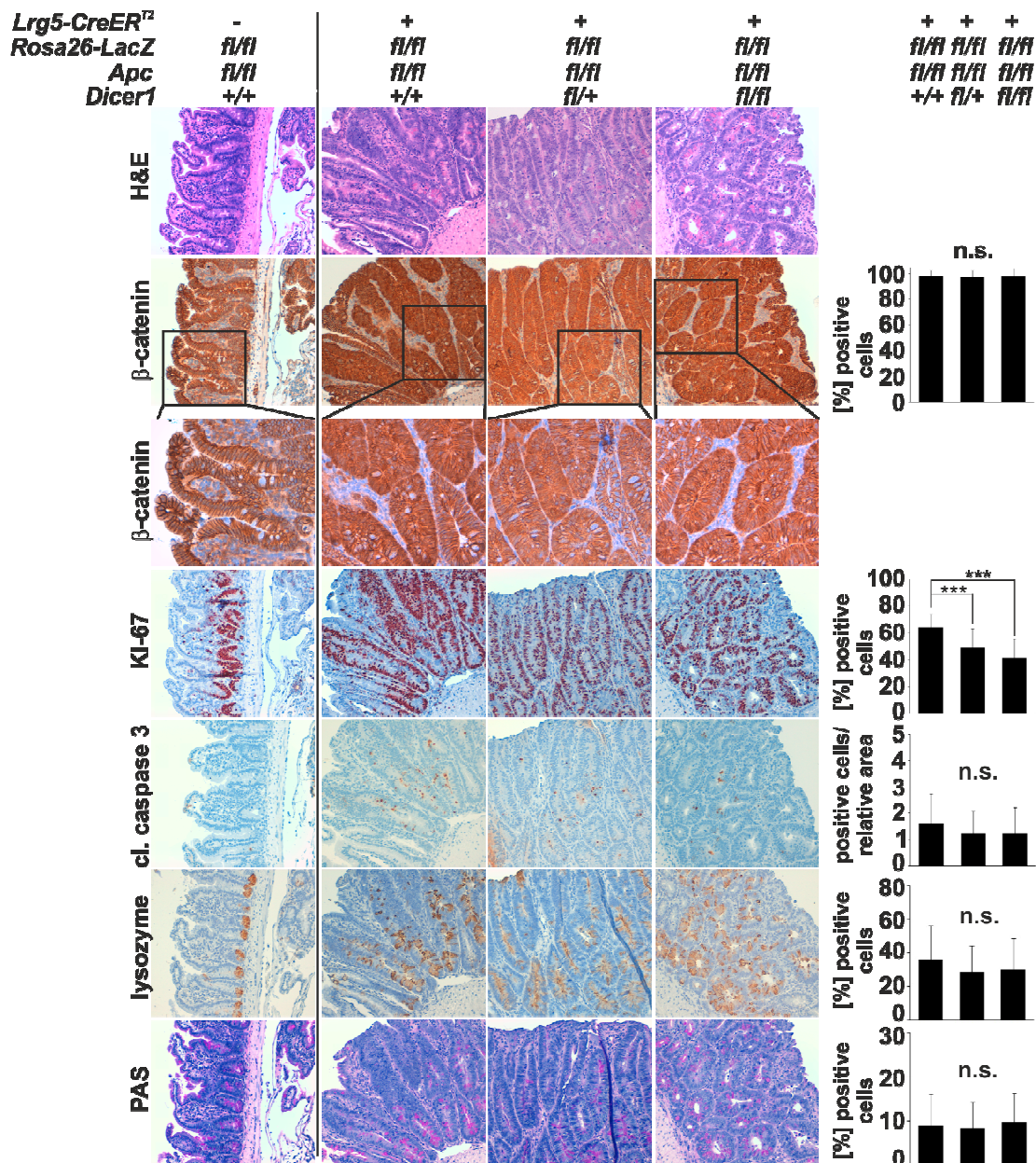


Fig. 25. *Dicer1* depletion resulted in less adenoma proliferation.

Paraffin blocks were cut into slices and stained with H&E, PAS and β -catenin-, KI-67-, cleaved caspase 3- and lysozyme-specific antibodies, respectively. As shown macroscopically (Fig. 24), also microscopically no adenomas were detected in the small intestines of *Lgr5(-)* mice (left panel). In mice which were positive for *Lgr5(+)-Apc*, *Lgr5(+)-Apc-Dicer1^{het}* and *Lgr5(+)-Apc-Dicer1^{fl/fl}* adenomas were detected. Adenomas showed a nuclear localization of β -catenin, whereas in the normal mucosa, β -catenin was predominantly localized in the cytoplasm except at the crypt base. Cytoplasmic staining of β -catenin is indicated by blue nuclei (DAPI) because of the missing of nuclear staining of β -catenin (brown), nuclear staining of β -catenin is indicated by brown nuclei (for the difference between cytoplasmic and nuclear staining of β -catenin see *Lgr5(+)-Apc-Dicer1^{het}* β -catenin). Quantifications of positive cells in adenomas are listed on the right side. Only the proliferation marker KI-67 showed a significant difference between the adenomas of the three genotypes. 200 \times magnification; black boxed regions 400 \times magnification. Error bars indicate standard error from more than 30 adenomas per genotype. For significance, a Student's t-test was used. *** $p < 0.001$, n.s. non significant.

3.2.4 Validation of CRC cell lines with a disruption of *DICER1*

The observation in the previously described mouse model that deletion of *Dicer1* had an influence on tumor initiation as well as adenoma size was only descriptive. Therefore, I chose a cell culture model to shed more light onto the role of *DICER1* and the underlying mechanism in the intestinal carcinogenesis. To do so, I utilized two human CRC cell lines (RKO, HCT116) with a homozygous disruption of the helicase domain (second RNaseIII domain; exon 5) of *DICER1* (Fig. 26A; (Cummins et al., 2006)). By Cre recombination, Cummins et al. cut out the *Neo* gene whereby one loxP site (yellow triangle; Fig. 26A) is still present. Because of the remaining part of the inserted DNA, the *DICER1* gene is disrupted. However, this disruption did not lead to a deletion of parts of the *DICER1* gene. In these cell lines the ability to process pre-miRNAs to mature miRNAs is impaired.

First, I verified the genotype of the cell lines via PCR analysis. Since all cell lines had the correct genotype (Fig. 26B), the functional effect on the miRNA biogenesis was checked via RT-qPCR. The two miRNAs *miR-21* and *miR-200a* were chosen for this assay based on data in (Cummins et al., 2006). Cells with a disruption of *DICER1* (hereafter referred to as *ex5*) showed reduced amounts of mature miRNAs compared to the parental cell lines (Fig. 26C). This revealed that the cell lines worked well.

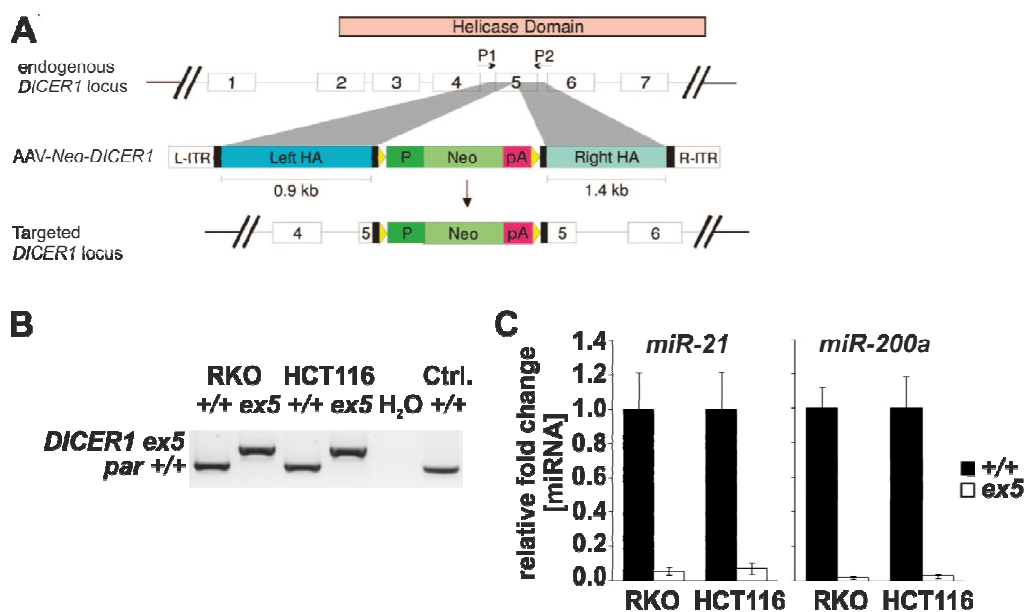


Fig. 26. Colorectal carcinoma cell lines with a homozygous disruption of the helicase domain (*ex5*) of *DICER1* showed impaired miRNA processing.

(A) Schematic diagram of the endogenous locus of the human *DICER1* helicase domain. Insertion of an AAV-Neo targeting construct into exon 5 of *DICER1* disrupted the *DICER1* locus (Cummins et al., 2006). (B) Agarose gel of the PCR analysis of the genomic DNA of parental (+/+) and homozygous clones (*ex5*) of

RKO and HCT116 cells. Cells were harvested, genomic DNA isolated and analyzed by PCR. The binding sites of the primer pair (P1 and P2) for the PCR analysis are depicted in (A). PCR analysis with parental (+/+) cells resulted in a PCR product of 444 bp size, with homozygous clones (*ex5*) of 564 bp size in both RKO and HCT116 cells. (C) RKO and HCT116 cells were harvested, miRNA isolated and analyzed by RT-qPCR. The relative expression of *miR-21* and *miR-200a* was normalized to that of *SNORD48* (small nucleolar RNA, reference). Depletion of *DICER1* in colorectal carcinoma cell lines led to decreased levels of mature *miR-21* and *miR-200a*, representative for the other miRNAs. Data are represented as mean \pm SD from three biological replicates.

3.2.5 *Disruption of DICER1 led to enhanced expression/protein levels of CSC, metastatic and EMT markers*

In the beginning, I explored in a first approach on a descriptive level if disruption of *DICER1* influenced marker expression/protein levels in HCT116 CRC cells. For that purpose, I chose CSC, metastatic and EMT markers. The CSC marker CD133 and the metastasis marker CD26 were analyzed by antibody staining via FACS analysis. The glycosylated epitope of CD133, AC133, was shown to be connected with SC properties (Kemper et al., 2010), the marker CD26 was associated with metastasis (Pang et al., 2010). Loss of *DICER1* resulted in increased levels of both markers, CD133 (Fig. 27A, B) and CD26 (Fig. 27C, D). As properties of SCs and metastasis are closely related to EMT (De Craene and Berx, 2013) the influence of *DICER1* on the expression of EMT factors was studied by RT-qPCR. Consistent with the previous results the expression of the master switches of EMT, *SLUG (SNAI2)* and *ZEB1*, were upregulated at the mRNA level after loss of *DICER1* (Fig. 27E). Taken together, disruption of *DICER1* led to increased levels of CSC, metastatic and EMT markers.

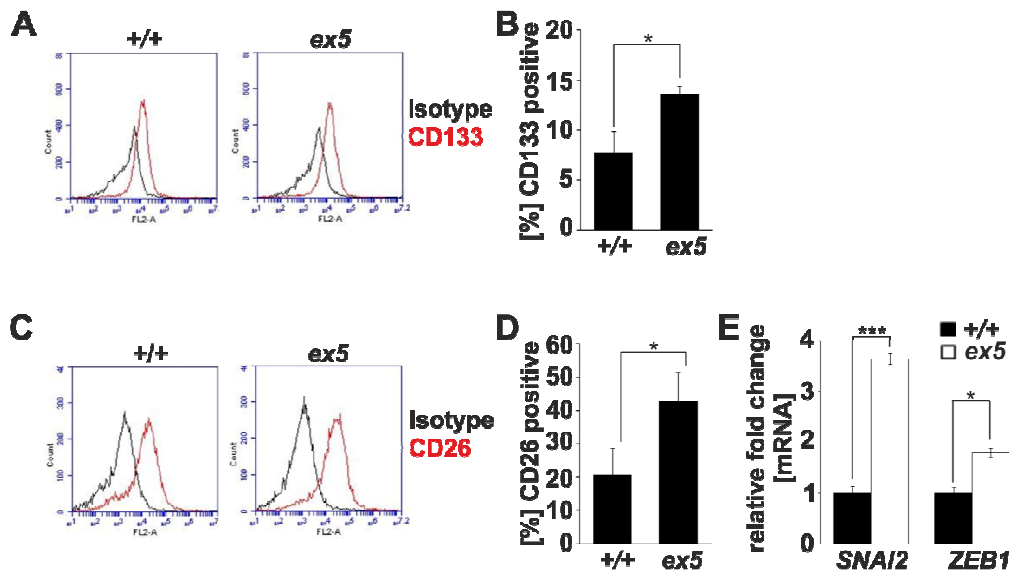


Fig. 27. Loss of DICER1 increased the levels of CSC, metastatic and EMT markers in HCT116 cells.

(A) HCT116 *ex5* and parental (+/+) cells were harvested, stained with the isotype control (black) or an antibody against a glycosylated epitope of CD133, AC133, (red) and analyzed by FACS. A representative example is shown. (B) Quantification of CD133 positivity. Disruption of *DICER1* increased the number of cells with the glycosylated epitope of CD133. (C) HCT116 *ex5* and parental (+/+) cells were harvested, stained with the Isotype control (black) or an antibody against the metastatic marker CD26 (red) and analyzed by FACS. A representative example is shown. (D) Quantification of CD26 positivity. Disruption of *DICER1* resulted in a higher positivity for CD26 in HCT116 cells. (E) 72 h after seeding, cells were harvested, mRNA was isolated and analyzed by RT-qPCR. The expression of the EMT markers snail family zinc finger 2 (*SNAI2*) and zinc finger E-box binding homeobox 1 (*ZEB1*) was normalized to the reference genes *ACTB* and *HPRT1*. In cells without *DICER1*, expression of the EMT markers *SNAI2* and *ZEB1* significantly increased. Data are represented as mean \pm SD from three biological replicates. A Student's t-test was used. * $p < 0.05$, ** $p < 0.01$, *** $p < 0.001$

3.2.6 A loss of *DICER1* resulted in a slower proliferation and enhanced G0/G1 arrest

After the descriptive investigation of marker expression and marker protein levels, functional experiments were performed. Since deletion of *DICER1* led to a smaller adenoma size in mice caused by less proliferation, the influence of *DICER1* on proliferation was also investigated in cell culture. For that purpose, HCT116 cells with and without functional *DICER1* were analyzed employing MTT assay for 5 days. Cells with loss of *DICER1* proliferated significantly slower than the parental cells (Fig. 28A). Thus, *DICER1* influenced proliferation not only in murine adenomas but also in human CRC cell lines.

Proliferation can be regulated by a multitude of factors among which the cell cycle is the most important. Therefore, a change in the cell cycle phases caused by a loss of *DICER1* was examined. The cell cycle analysis was performed by PI staining and FACS analysis. In the *ex5* cells, a significantly enhanced number of cells was in the G0/G1 phase compared to parental cells. As apoptosis is a counterbalance to proliferation, the apoptosis was investigated by the subG1 peak of the cell cycle analysis. However, apoptosis (subG1) was not influenced by loss of *DICER1* (Fig. 28B). Thus, disruption of *DICER1* in HCT116 cells resulted in an increased number of cells in the G0/G1 phase whereas the apoptosis was not influenced. Another possibility besides proliferation might be the regulation by size control. In the intestine, tissue size and proliferation is controlled by Hippo pathway (Zeng and Hong, 2008). Hence, the smaller adenoma size in mice could also be influenced by the activity of the Hippo pathway. The Hippo pathway activity was investigated in cell culture by luciferase reporter assay. For that purpose, a synthetic YAP/TAZ-responsive luciferase reporter (YAP/TAZ are the transcription factors of the Hippo pathway) was used. Cells with a loss of *DICER1* showed significant less activity of YAP/TAZ-responsive promoters compared to parental cells, measured by a reporter assay (Fig. 28C), and consequently less proliferation.

As in CRC cell lines proliferation is regulated by the Wnt signaling pathway via β -catenin target genes (Clevers, 2006), the role of Wnt signaling pathway activity in CRC cell lines with disrupted *DICER1* was investigated. The activity of the Wnt signaling pathway was impaired by knockdown of *CTNNB1* (β -catenin) via siRNAs. siRNA-mediated *CTNNB1* knockdown in HCT116 cells was verified at the mRNA level by RT-qPCR and at the protein level by Western Blot (Fig. 28D, E). Moreover, the expression of the β -catenin target gene *AXIN2* was measured by RT-qPCR (Yan et al., 2001). Strikingly, *CTNNB1* and *AXIN2* were both downregulated. By the knockdown of *CTNNB1*, the parental cells proliferated slower than the cells transfected with control siRNA, examined by MTT assay. Cells with a loss of *DICER1* (*ex5*) had a similar proliferation rate as the parental cells after β -catenin knockdown. When the *ex5* cells were transfected with siRNA against *CTNNB1*, the knockdown of *CTNNB1* led to an additional slowdown of the proliferation rate of the *ex5* cells (Fig. 28F).

Taken together, disruption of *DICER1* in CRC cell lines led to less proliferation by G0/G1 cell cycle arrest, associated with reduced Hippo pathway activity. Additionally, an impaired Wnt signaling pathway activity decelerated the proliferation in parental and *DICER1* disrupted CRC cell lines.

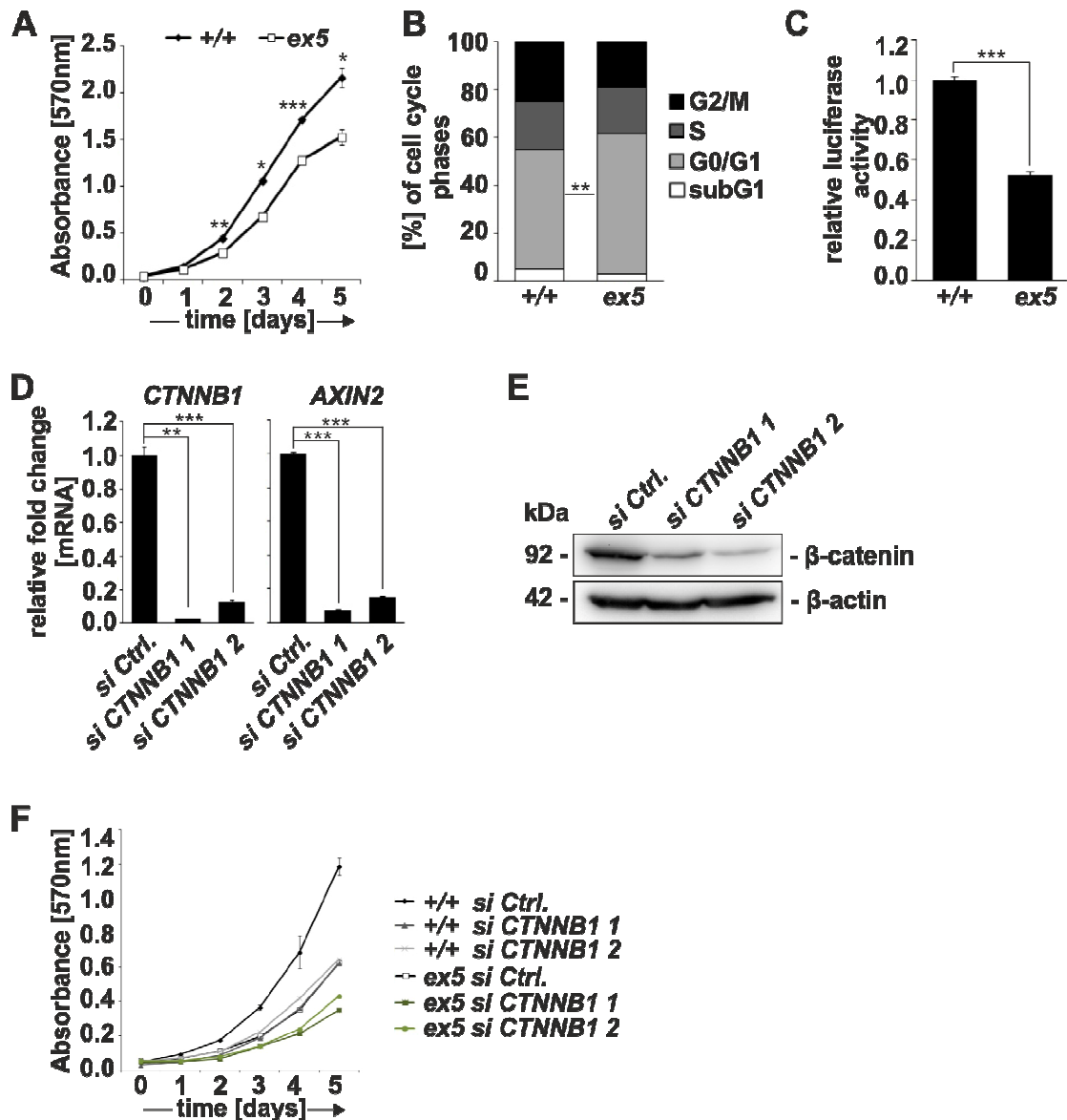


Fig. 28. Loss of DICER1 resulted in less proliferation and increased cell number in the G0/G1 phase, associated with reduced Hippo pathway activity in HCT116 cells.

(A) Proliferation was investigated by MTT assay for 5 days. Cells were measured directly after seeding and subsequently every 24 h at the wavelength of 570 nm by an ELISA reader. Cells with a *DICER1* disruption proliferated significantly slower compared to control cells. (B) For cell cycle analysis, cells were fixed, stained with propidiumiodide (PI) and analyzed by FACS. Loss of DICER1 led to a significantly enhanced number of cells in the G0/G1 phase compared to parental cells. (C) Hippo pathway activity was analyzed with an 8xGTIIC-luciferase reporter (firefly luciferase reporter with synthetic TEAD (TEA-domain-containing family) binding sites; binding sites for the transcription factors YAP/TAZ) via luciferase reporter assay. Cells were transfected with 8xGTIIC firefly luciferase reporter or a control firefly luciferase reporter (without TEAD binding sites) and additionally with a renilla luciferase vector for the normalization of the results. Luciferase activity was measured 48 h after transfection, first normalized to renilla luciferase to exclude different transfection efficiencies and subsequently to the control firefly luciferase reporter. The indicated values are 8xGTIIC/control vector ratios. In cells without DICER1, the activity of the Hippo pathway was significantly reduced, indicating less proliferation. (D) 72 h after transfection with *CTNNB1* (β -catenin) siRNA or control siRNA HCT116 (+/+) cells were harvested, mRNA isolated and analyzed by RT-

qPCR. The indicated genes were normalized to *ACTB*. Endogenous *CTNNB1* and its target gene *AXIN2* are efficiently silenced with *CTNNB1* siRNA. (E) In parallel, total cell lysates were analyzed by SDS-PAGE and immunoblotting with a specific β -catenin antibody; β -actin served as a loading control. Similar to RT-qPCR analysis, immunoblotting confirmed an efficient knockdown of β -catenin. (F) Proliferation was investigated in a MTT assay for 5 days. 48 h after transfection of *CTNNB1* siRNA or control siRNA, cells were again seeded and measured as in (A). Knockdown of *CTNNB1* led to a decreased proliferation rate compared to cells transfected with control siRNA. A knockdown of *CTNNB1* in the parental cells caused a similar proliferation rate as a disruption of *DICER1* (*ex5*). A combined disruption of *DICER1* and knockdown of *CTNNB1* led to an additional slowdown of the proliferation rate of the *ex5* cells. Data are represented as mean \pm SD from three biological replicates. A Student's t-test was used. * $p < 0.05$, ** $p < 0.01$, *** $p < 0.001$

3.2.7 Loss of *DICER1* increased chemoresistance

Since loss of *Dicer1*/miRNAome influenced tumor initiating capacity in a conditional *Apc* knockout mouse model and moreover, *DICER1* disruption in HCT116 cells led to increased levels of the SC marker CD133, I further analyzed the influence of *DICER1* on SC properties. As chemoresistance is associated with SC properties (Dallas et al., 2009), I investigated the influence of *DICER1* and thus, the miRNAome in this context. HCT116 cells (+/+ and *ex5*) were treated for 3 days with the chemotherapeutic 5-FU (LC50 concentration) and the vitality of the cells was measured by MTT assay. Impaired miRNA biogenesis (*ex5*) resulted in a higher number of viable cells and hence, more proliferation under 5-FU treatment. Thus, cells with loss of *DICER1* showed a higher resistance against 5-FU than parental cells (Fig. 29A).

Since cells without *DICER1* proliferated better under 5-FU treatment than parental cells, I analyzed if the higher resistance against 5-FU is reflected in the cell cycle phases. The cell cycle analysis was done by PI staining and FACS analysis. Consistent with the MTT assay, *ex5* cells showed a significant higher number of cells in the G2/M phase and a significant lower number in the G0/G1 phase, compared to parental cells (Fig. 29B). Thus, under 5-FU treatment, cells without *DICER1* proliferated better and fewer cells were in cell cycle arrest compared to control cells, indicating an increase in SC properties.

Moreover, since β -catenin target genes are involved in chemoresistance (Yamada et al., 2000), I investigated further the influence of Wnt signaling activity on the increased chemoresistance caused by loss of the miRNAome. For that purpose, *CTNNB1* was knocked down and chemoresistance was analyzed by MTT assay. Knockdown of *CTNNB1* (β -catenin) led to less chemoresistance in both cell lines (+/+ and *ex5*); but despite a loss of β -catenin the cells with an additional loss of *DICER1* were still more chemoresistant

then the parental cells after *CTNNB1* knockdown (Fig. 29C). Therefore, the increase of SC properties by loss of DICER1 is supported by an active Wnt signaling pathway.

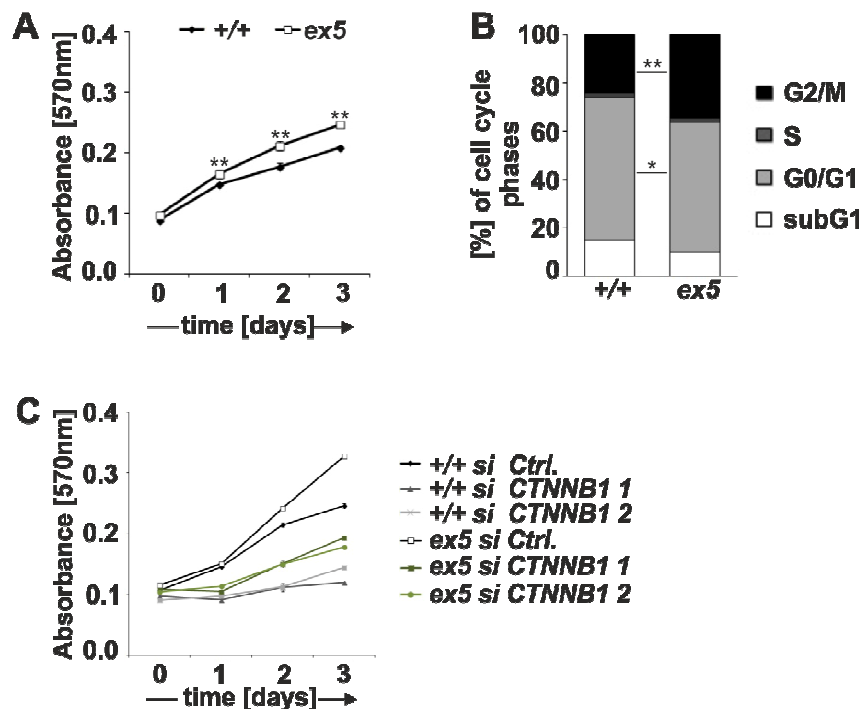


Fig. 29. Loss of DICER1 increased drug resistance in HCT116 cells.

(A) HCT116 cells (*ex5* and *+/+*, respectively) were seeded in medium containing 12.12 μ M 5-FU and chemoresistance was investigated for 3 days by MTT assay. Cells were measured directly after seeding and subsequently every 24 h at the wavelength of 570 nm using an ELISA reader. In cells depleted for *DICER1* (*ex5*) drug resistance significantly increased compared to parental cells. (B) HCT116 cells (*ex5* and *+/+*, respectively) were treated for 3 days with 12.12 μ M 5-FU, subsequently fixed, stained with PI for cell cycle analysis and investigated by FACS analysis. During 5-FU treatment, loss of *DICER1* led to a significantly increased number of cells in the G2/M phase and significantly less cells in the G0/G1 phase. (C) Proliferation was investigated under 5-FU conditions by MTT assay for 3 days. 48 h after transfection of *CTNNB1* siRNA or control siRNA, cells were seeded in medium containing 12.12 μ M 5-FU and measured as in (A). In both cell lines (*ex5* and *+/+*), a knockdown of *CTNNB1* led to less chemoresistance; *ex5* cells were, despite the loss of β -catenin (*ex5* si *CTNNB1* 1, *ex5* si *CTNNB1* 2), still more chemoresistant than parental cells (*+/+* si *CTNNB1* 1, *+/+* si *CTNNB1* 2). Data are represented as mean \pm SD from three biological replicates. A Student's t-test was used. * $p < 0.05$, ** $p < 0.01$

3.2.8 Migration capacity was higher without *DICER1*

As EMT and metastatic marker expression/protein levels (Fig. 27) indicate that cells without *DICER1* might also possess increased migration capacities (De Craene and Berx, 2013; Pang et al., 2010), the influence of *DICER1* in this context was analyzed by wound

healing assay (ibidi chamber) whereby cell migration can be investigated. RKO cells were treated for 24 h with Wnt3a conditioned medium which increased significantly Wnt signaling pathway activity (luciferase reporter assay; Fig. 30A). These cells showed a significantly enhanced migratory capacity after disruption of *DICER1* (*ex5*) compared to parental cells (Fig. 30B, C). This effect was also observed in RKO cells without an active Wnt signaling pathway. However, cells with a combination of an active Wnt signaling pathway as well as a loss of *DICER1* showed the highest migratory capacity after 24 h (Fig. 30B, C). Thus, disruption of *DICER1* and thus, the miRNAome increased cell migration capacity which is positively influenced by an active Wnt signaling pathway.

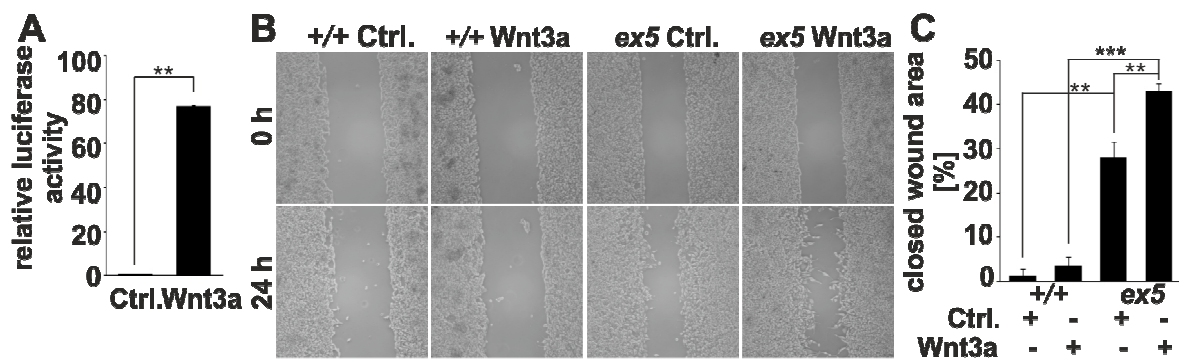


Fig. 30. Loss of *DICER1* resulted in enhanced migration capacity.

(A) RKO +/+ cells were transfected with the TOPflash or FOPflash reporter as control. Additionally, a renilla luciferase vector was transfected for the normalization of the results. Wnt3a conditioned medium or control medium was added 24 h after transfection. 48 h after transfection, luciferase activity was measured, normalized to renilla and subsequently to the luciferase control vector (FOPflash). The indicated values are TOP/FOP ratios. Addition of Wnt3a conditioned medium led to an enhanced signal in RKO parental cells compared to control (Ctrl.) medium. (B) To measure cell migration by wound healing assay, RKO cells were seeded in culture inserts (ibidi chambers). 24 h after seeding, mitomycin C was added to a final concentration of 10 $\mu\text{g/ml}$ for 3 h, the chamber was removed, Wnt3a conditioned medium or control medium was added and images of the defined gap between the cells were taken at 0 h and 24 h. (C) Images were analyzed with ImageJ (NIH). Results represent the average (%) of wound closure \pm SD ($n = 3$). Disruption of *DICER1* (*ex5*) led to a significantly enhanced migration capacity, and active Wnt signaling pathway had an additive effect on the enhanced migration capacity. Data are represented as mean \pm SD from three biological replicates. A Student's t-test was used. * $p < 0.05$, ** $p < 0.01$, *** $p < 0.001$

3.2.9 Wnt signaling pathway increased after loss of *DICER1*

Since β -catenin target genes are involved in CSC properties such as stemness (Du et al., 2008), proliferation (Clevers, 2006), chemoresistance (Yamada et al., 2000) and metastatic features (Vlad-Fiegen et al., 2012) and these features were all influenced by a loss of the

miRNAome, I tested whether the activity of the Wnt signaling pathway was consequently upregulated after loss of DICER1/miRNAome. For this experiment I used RKO and HCT116 cells, both parental (+/+) and *ex5*. As RKO does not have a mutation of the Wnt signaling pathway and hence, no active canonical Wnt signaling pathway, I activated this pathway by addition of Wnt3a conditioned medium. RKO +/+ and *ex5* cells showed an increased activity in the Wnt signaling pathway after addition of Wnt3a conditioned medium compared to control (unconditioned) medium, measured by luciferase reporter assay. Additionally, the activity of the Wnt signaling pathway was enhanced in the *ex5* cells compared to the parental cells. The same was observed in HCT116 cells (Fig. 31A). To verify the enhanced activity of the Wnt signaling pathway, the expression of the β -catenin target gene *AXIN2* (Yan et al., 2001) was analyzed at the mRNA level by RT-qPCR. *AXIN2* was higher expressed after disruption of *DICER1* in HCT116 cells (Fig. 31B).

Thus, loss of DICER1 resulted in increased activity of Wnt signaling pathway and enhanced expression of the β -catenin target gene *AXIN2*.

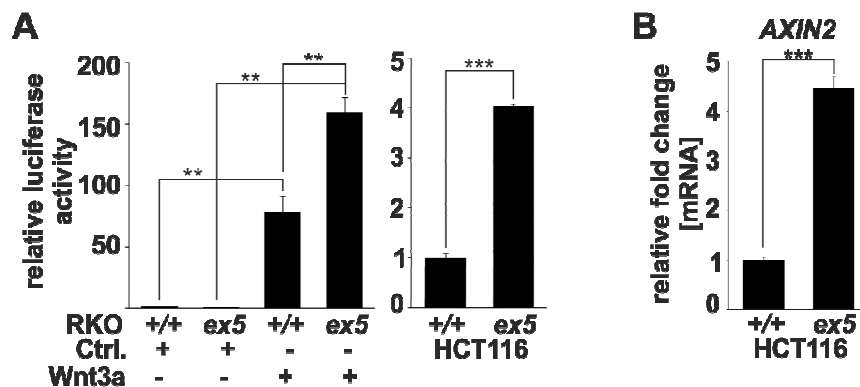


Fig. 31. Loss of DICER1 enhanced Wnt signaling pathway activity.

(A) RKO cells were transfected with the TOPflash or FOPflash reporter as control. Additionally, a renilla luciferase vector was transfected for the normalization of the results. 24 h after transfection, Wnt3a conditioned medium or control medium was added. Luciferase activity was measured 48 h after transfection. HCT116 cells were transfected with TOP/FOPflash and renilla luciferase vector and likewise, luciferase activity was measured 48 h after transfection. Luciferase values were normalized to renilla luciferase activity to exclude different transfection efficiencies and subsequently to the luciferase control vector activity (FOPflash). The indicated values are TOP/FOP ratios. Addition of Wnt3a conditioned medium led to an enhanced signal in RKO +/+ and *ex5* cells compared to control (Ctrl.) medium. Furthermore, loss of DICER1 caused an enhanced activity of the Wnt signaling pathway. The same effect was observed in HCT116 cells. (B) HCT116 cells were harvested 72 h after seeding, mRNA was isolated, analyzed by RT-qPCR and normalized to the reference genes *ACTB* and *HPRT1*. Deletion of *DICER1* led to a significantly increased expression of *AXIN2* compared to the parental cells. Data are represented as mean \pm SD from three biological replicates. A Student's t-test was used. ** $p < 0.01$, *** $p < 0.001$

Taken together, loss of DICER1 and thus, the miRNAome influenced expression/protein levels of CSC, metastatic and EMT markers, affected cell proliferation, enhanced drug resistance and migratory capacity and led to a more strongly activated Wnt signaling pathway. An activated Wnt signaling pathway enhanced these effects.

3.2.10 *DICER1 levels were higher in adenomas compared to normal colonic mucosa but decreased during progression from adenoma to carcinoma in human CRC*

Since a deletion of *Dicer1/DICER1* showed effects in a mouse model as well as in human CRC cells, I translated this result on human CRC tissue. Therefore, I next investigated if there was also a change of DICER1 levels during human colorectal carcinogenesis. For that purpose, I chose a human tissue collection of tissues including the different steps of colorectal carcinogenesis: normal colonic mucosa, adenoma and UICC stage I-IV (Table 2, 3). A staining score was developed based on intensity of cytoplasmic DICER1 staining (Fig. 32A). Score 0 was defined as no staining, score 1 as weak staining, score 2 as moderate staining and score 3 as strong staining. Next, all cases were evaluated applying the score. Score 0 and 1 were grouped as low DICER1 levels/staining intensities, score 2 and 3 as high DICER1 levels/staining intensities. In the human tissue collection, an increase of the DICER1 levels from normal mucosa to the adenoma was observed. Only 40% of the cases of the normal mucosa showed high levels of DICER1 whereas more than 86% of the adenomas with poor dysplasia showed high levels. However, during the progression from adenoma to carcinoma a decrease of the DICER1 levels was noted. The staining intensities of UICC stages III and IV were comparable to normal mucosa (Fig. 32B).

The loss of DICER1 during cancer progression complied with the results gained with the mouse model and cell culture thus indicating the value of the experimental results for describing the situation in humans.

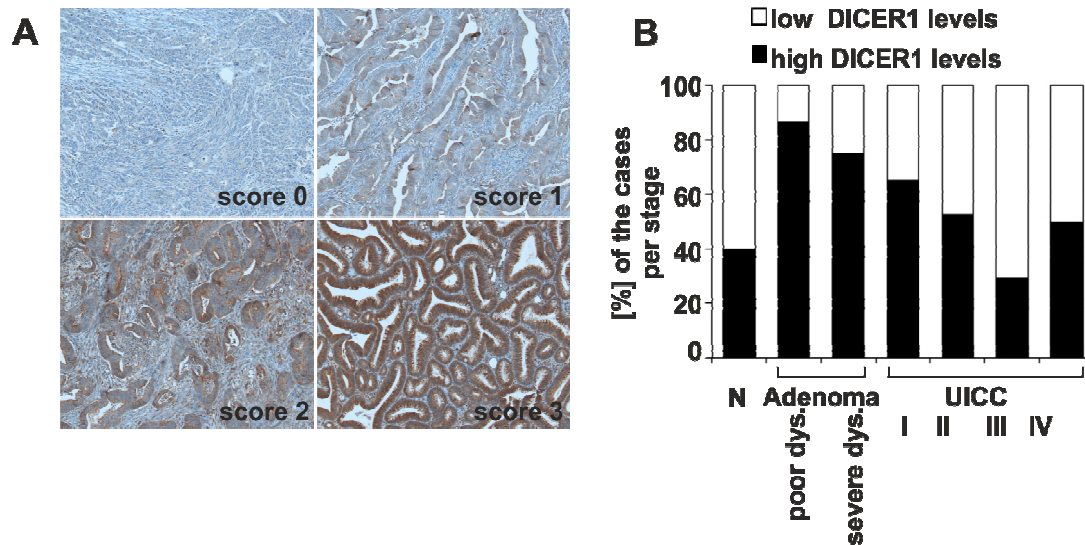


Fig. 32. DICER1 levels were higher in adenomas compared to normal colonic mucosa but decreased during progression from adenoma to carcinoma in human CRC.

(A) A human tissue collection was stained with a specific anti-DICER1 antibody. The score of the DICER1 staining was determined according to intensity of cytoplasmic staining; score 0: no staining, score 1: weak staining, score 2: moderate staining, score 3: strong staining. (B) A human tissue collection consisting of normal colonic mucosa, adenoma and UICC stage I-IV was analyzed. Cases were graded in low (score 0 and 1) and high (score 2 and 3) DICER1 levels/staining intensities. Compared to normal mucosa, adenomas presented an increase of DICER1 levels. However, during the progression from adenoma to carcinoma a decrease of the DICER1 levels was detected. The decreasing DICER1 levels from adenoma to carcinoma were statistically significant. A χ^2 -test was used; $p < 0.01$.

3.2.11 *Expression of DICER1 was influenced by the Wnt signaling pathway*

Because the staining intensity of DICER1 increased from normal mucosa to adenoma in a human tissue collection I determined whether the same could be observed in a mouse model. Therefore, I compared normal mucosa and adenomas in *Lgr5(+)-Apc* mice 21 days after TAM induction. For that purpose, the intestine was embedded in paraffin blocks, the blocks were cut and stained with antibodies specific for β -catenin and DICER1. Strikingly, the adenomas in the mouse model showed higher levels of DICER1 than the normal mucosa (Fig. 33A, B).

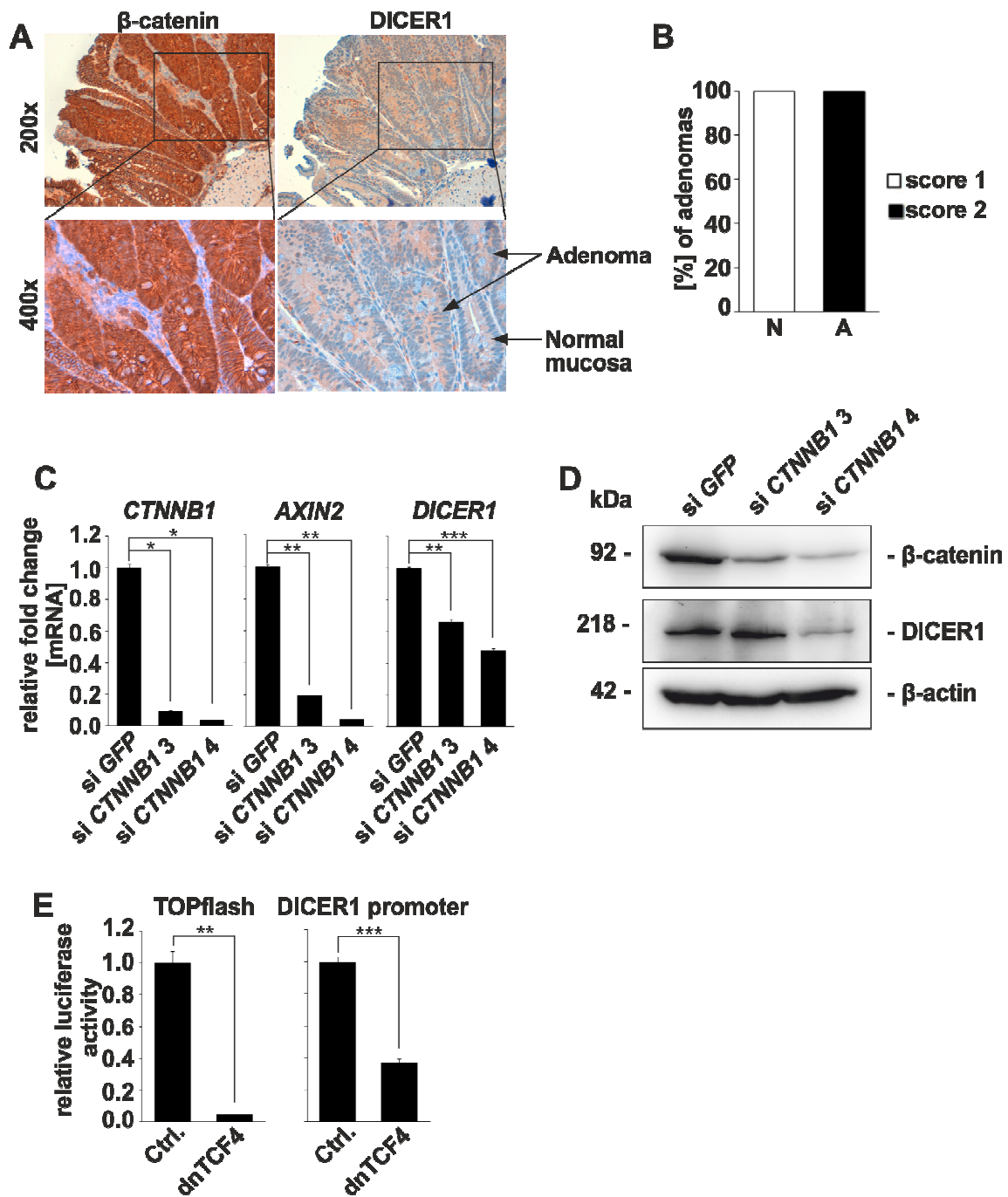


Fig. 33. *DICER1* expression was influenced by Wnt signaling pathway.

(A) Paraffin blocks of *Lgr5(+)-Apc* mice were cut and slices were immunohistochemically stained with β -catenin- and *DICER1*-specific antibodies. In adenomas, nuclear localization of β -catenin was observed. Additionally, the staining intensity of *DICER1* was increased in adenomas compared to normal mucosa. 200 \times magnification; black boxed regions 400 \times magnification. (B) Quantification of *DICER1* levels in normal mucosa (N) and adenomas (A) displayed higher *DICER1* levels in adenomas than in normal mucosa (n= 6 analyzed mice). (C) HCT116 (+/+) cells were transfected with si *CTNNB1* siRNA or control siRNA 24 h after seeding. 72 h after transfection cells were harvested, mRNA was isolated, analyzed by RT-qPCR and normalized to *ACTB*. RT-qPCR verified a significant reduction of *CTNNB1* mRNA and of the expression of the β -catenin target gene *AXIN2*. *DICER1* expression was also significantly decreased. (D) Total cell lysates were analyzed by SDS-PAGE and immunoblotting with β -catenin- and *DICER1*-specific antibodies; β -actin

served as loading control. Western blot analysis confirmed efficient knockdown of *CTNNB1*/β-catenin and a decrease of DICER1 protein levels. (E) HCT116 +/+ cells were transfected with dnTCF4 to impair the Wnt signaling pathway activity. CAT served as control. Additionally, the cells were transfected with the TOPflash reporter (FOPflash reporter as control) or the *DICER1* promoter reporter (an empty vector served as control). Furthermore, a renilla luciferase vector was transfected for the normalization of the results. Luciferase activity was measured 48 h after transfection. Luciferase signals were normalized to renilla luciferase and subsequently to the luciferase control vector. dnTCF4 led to a decreased activity of Wnt signaling (TOPflash) as well as of the *DICER1* promoter. Data are represented as mean ± SD from three biological replicates. A Student's t-test was used. **p<0.01, ***p<0.001

Since formation of the majority of human CRC cases and the adenomas in this mouse model were driven by an activation in the Wnt signaling pathway, I supposed that *Dicer1/DICER1* expression might be regulated by the Wnt signaling pathway. Thus, I confirmed this hypothesis in the human CRC cell line HCT116. Wnt signaling pathway activity was diminished by siRNA-mediated *CTNNB1* knockdown. The knockdown of *CTNNB1* was verified at the mRNA level by RT-qPCR and at the protein level by Western Blot (Fig. 33C, D). Additionally, the expression of the β-catenin target gene *AXIN2* was downregulated on mRNA level after *CTNNB1* knockdown (Fig. 32C). By the knockdown of *CTNNB1* and consequently loss of Wnt signaling pathway activity (measured by luciferase assay; data not shown), *DICER1* mRNA expression as well as DICER1 protein levels were diminished (Fig. 33C, D).

Finally, the influence of the Wnt signaling pathway on the activity of the *DICER1* promoter was measured employing a luciferase reporter assay. To impair the activity of the Wnt signaling pathway, dominant negative TCF4 (dnTCF4) was utilized. Transfection of dnTCF4 reduced Wnt signaling pathway activity measured by TOPflash activity. Furthermore, the activity of the *DICER1* promoter was also decreased (Fig. 33E).

Hence, these results convincingly demonstrated that *DICER1* mRNA expression as well as DICER1 protein levels were influenced by Wnt signaling pathway, observed in murine tissue as well as in human CRC cell lines in cell culture.

4 Discussion

4.1 The role of OLFM4 in colorectal cancer

Due to their progression driving activity in tumors, CSCs are crucial for the process of tumorigenesis. CSCs are characterized by the features cancer stemness, EMT, metastasis and chemoresistance. As the CSC features chemoresistance and metastasis are connected with cancer death, specific CSC targeted therapies might be an approach for future cancer therapies. By directly targeting and killing CSCs, the tumor should regress and cases of cancer death might be reduced. As the interference of SC sustaining molecules might be a tool for CSC targeted therapies, these molecules are one focus of the current research. One of these molecules is the adult SC marker OLFM4. OLFM4 was described to be a surrogate for the CSC marker LGR5 (van der Flier et al., 2009). However, conflicting results were published (van der Flier et al., 2009; Ziskin et al., 2013) whereby doubts arose concerning the role of OLFM4 as a CSC marker. Furthermore, conflicting result exist about the expression of *OLFM4* in cancer depending on the tissue. Whereas in some studies, *OLFM4* was higher expressed in breast, lung and colon cancer compared to normal tissue (Koshida et al., 2007; Zhang et al., 2004), other studies reported, that reduced or undetectable *OLFM4* expression was associated with prostate cancer (Chen et al., 2011), advanced prostate tumor stages (Li et al., 2013) and worse survival rate for CRC cancer (Seko et al., 2010). To clarify the role of OLFM4 as a SC marker and in CRC, I investigated in this study the expression pattern of *OLFM4* in CRC cell lines and CSCs and its functional role on CSC features.

4.1.1 OLFM4 was not a marker of cells with CSC properties

Since the expression of *OLFM4* in cancer might depend on the organ and has not yet been clarified for CRC, I examined first the expression pattern of *OLFM4* in CRC cell lines as a model system to clarify the expression intensity of *OLFM4* in CRC cell lines. The finding that only two out of 14 CRC cell lines expressed *OLFM4* (Fig. 15) indicated that *OLFM4* was downregulated as it acts as a tumor suppressor or as it is possibly difficult to detect in these cell lines since it is only expressed in stem cells as previously reported (van der Flier et al., 2009). Hence, the latter hypothesis was further investigated in this study, however, could not be confirmed by two independent experiments in which specifically CSCs were

enriched. Selection for CSCs (Fig. 16) showed that *OLFM4* expression was reduced in CSCs and therefore, not coexpressed with other SC markers such as *LGR5*, *PROM1* or *CD44*. These results demonstrated that *OLFM4* is not a surrogate of *LGR5* and not a marker of CSCs which agrees with another group that reported that *OLFM4* was not associated with CSCs in CRC (Ziskin et al., 2013). The reduced expression of *OLFM4* in CRC cell lines and the association of *OLFM4* with non-CSCs might indicate that *OLFM4* has a prognostic impact in CRC. This assumption was further supported by studies in which reduced or low levels of *OLFM4* were associated with poorly differentiated colonic tumors and metastasis (Besson et al., 2011; Liu et al., 2008) and reduced *OLFM4* levels were detected at the invasion front of colorectal tumors (Liu et al., 2008) where CSCs are located (Brabletz et al., 2009). However, this assumption was disproved as recent investigations showed that high *OLFM4* protein levels were not associated with survival and metastatic spread (unpublished data of Neumann et al.; manuscript in preparation which includes the results of this study). The staining of *OLFM4* at the protein level (IHC) was verified at the mRNA level by in situ hybridization. As both stainings showed perfect concordance, the immunohistochemical detection of *OLFM4* was reliable corroborating the validity of the findings. Furthermore, Neumann et al. found out that high *OLFM4* protein levels correlated with low grade (G2) and thus, epithelial differentiation. The findings of this study and from Neumann et al. demonstrate that *OLFM4* is neither a SC marker nor a prognostic marker for survival and metastatic spread. However, *OLFM4* expression in non-CSCs coincides with the finding that *OLFM4* correlates with differentiation. Thus, *OLFM4* expression/*OLFM4* protein levels are only associated with low grading of colorectal tumors (Fig. 34).

4.1.2 *OLFM4* possessed no functional role in CRC cells

Since *OLFM4* was absent or lowly expressed in the majority of CRC cell lines and CSCs, I investigated whether this was due to tumor suppressive and stemness reducing effects of *OLFM4*. To test this hypothesis, I ectopically overexpressed *OLFM4* in five CRC cell lines without endogenous *OLFM4* expression. The overexpression of *OLFM4* did not influence the expression/protein levels of CSC, EMT nor differentiation marker (Fig. 17). This descriptive approach was confirmed by functional assays. Proliferation which is an important hallmark of cancer cells (Hanahan and Weinberg, 2011) was not influenced by *OLFM4* overexpression (Fig. 18). Thus, *OLFM4* does not play a role in the proliferation of

CRC cells and thus, does not seem to be involved in the tumor growth. This finding is supported by another study showing that proliferation was not affected in mouse melanoma cells by overexpression of *OLFM4* (Park et al., 2012). However, the role of *OLFM4* concerning proliferation is tissue dependent as, in contrast to CRC cell lines, high *OLFM4* protein levels increased proliferation in gastric (Liu et al., 2012) and pancreatic (Kobayashi et al., 2007) cancer cell lines and suppressed proliferation in prostate cancer (Chen et al., 2011).

Since the Wnt signaling pathway is mechanistically the main driving force of CRC and influences CSC features by β -catenin target genes (Barker et al., 2007; Brabletz et al., 1999; Sanchez-Tillo et al., 2011; Yamada et al., 2000), the activity of the Wnt signaling pathway is a crucial feature of the tumor. Therefore, I investigated if the Wnt signaling pathway activity is correlated with *OLFM4* overexpression. It turned out that *OLFM4* did not influence the activity of the Wnt signaling pathway (Fig. 19). In contrast to *OLFM4*, two members of the olfactomedin family, *MYOC* and *OLFM1*, were described to be associated with the modulation of the Wnt signaling pathway (Kwon et al., 2009; Nakaya et al., 2008). The other way round, an active Wnt signaling pathway did also not affect *OLFM4* expression (unpublished data of D. Horst, manuscript in preparation). Thus, there is no correlation between *OLFM4* and the Wnt signaling pathway indicating that *OLFM4* did not interact with one of the most important pathways in CRC. The missing association between *OLFM4* and the Wnt signaling pathway and thus, with CSC features is further supported by the finding that high *OLFM4* protein levels were not associated with other stemness properties such as *ALDH1* activity and the gold standards of defining CSCs: sphere formation and subcutaneous growth of cells in mice (*in vivo* xenograft) (Fig. 20). Whereas *ALDH1* activity was associated with a reduced *OLFM4* expression (Fig. 16), this was not the case vice versa which confirms the solely association of *OLFM4* in CSCs and CRC cells. Besides the stemness features, I investigated finally the influence of *OLFM4* on the metastatic feature migration (Fig. 21). Like proliferation and stemness features, metastatic features were not influenced by an overexpression of *OLFM4* in CRC cell lines in contrast to prostate cancer (Chen et al., 2011) and melanomas (Park et al., 2012) in which *OLFM4* suppressed migration and invasion. In contrast to my data, another study described previously that migration was suppressed by *OLFM4* in the CRC cell line HT29 (Liu et al., 2008). However, the morphology of the HT29 cell was different and the migration capacity was much faster in Liu et al. compared to the HT29 cells used in this study and in other publications (Banning et al., 2008; Tsukahara and Murakami-Murofushi,

2012). Thus, it might be that Liu et al. have been used a subclone of HT29 or another cell line and therefore, the results from Liu et al. have to be viewed critically. In this study, five different CRC cell lines (all verified by DSMZ) were investigated and all attained the same results which underlines the validity of this study.

Taken together, these results demonstrate that *OLFM4* expression is reduced in CRC cell lines, ALDH1 positive CSCs and chemoresistant CSCs. The cause for the reduced expression of *OLFM4* in CRC cell lines and CSCs, however, is not yet resolved as the reduction of *OLFM4* does not take place due to a tumor suppressive role on cancer cells. Furthermore, *OLFM4* is correlated with differentiation and low grading of CRC (unpublished data of J. Neumann). Thus, *OLFM4* is only associated with differentiation and non-CSCs, does not have a prognostic impact concerning survival and metastatic spread and is not a stem cell marker in CRC. The missing prognostic relevance of *OLFM4* in CRC is reflected by the missing functional relevance of high *OLFM4* protein levels on CSC features such as proliferation, cancer stemness and metastatic features. Therefore, *OLFM4* does neither exert tumor promoting nor tumor suppressing influences on CRC cells and CSCs and does not contribute to tumor initiation, growth or the process of tumor progression. These data demonstrate that *OLFM4* is not a stemness sustaining molecule and thus, is not a suitable tool for CSC targeted therapy. Thus, this study contributes to reveal the lack of a role of *OLFM4* as a CSC marker and in the process of carcinogenesis of CRC (Fig. 34).

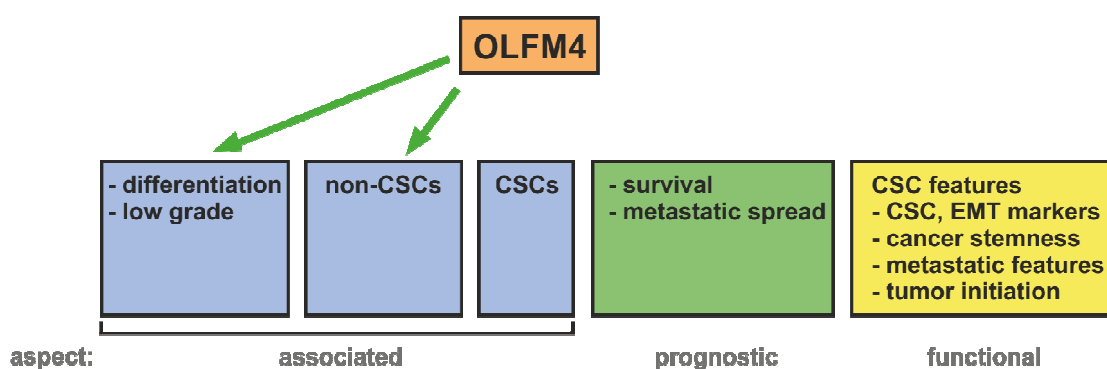


Fig. 34. The impact of OLFM4 in CRC.

OLFM4 is associated with differentiation, low grade and non-CSCs. However, *OLFM4* is not associated with CSCs, has no prognostic impact in CRC and no functional impact on CSC features in CRC cell lines.

4.2 The role of DICER1 in intestinal cancer

Besides stemness sustaining molecules, the miRNAome might be also a target for CSC targeted therapy since the downregulation of miRNAs resulted in a less-differentiated state of tumor cells (Lujambio and Lowe, 2012). The less-differentiated state leads to increased stemness features and chemoresistance (Singh and Settleman, 2010) whereby the cells become more tumorigenic. Recent studies revealed that knockout of *Dicer1* and subsequently downregulation of miRNAs in mouse models promoted tumor initiation (Kumar et al., 2009; Lambertz et al., 2010; Yoshikawa et al., 2013). As the majority of the human CRCs is driven by the Wnt signaling pathway (Pino and Chung, 2010), the knowledge about the role of the miRNAome on tumor promotion and CSC features in Wnt driven tumors might be a crucial tool for the development of CSC targeted therapy.

4.2.1 *Loss of DICER1 led to increased adenoma formation but reduced adenoma size in a murine intestinal cancer model*

As most of the CRC cases are thought to be driven by an *APC* mutation in the SC compartment, I used a mouse model (*Lgr5(+)-Apc*) in which the knockout of *Apc* in CBC cells led to the generation of CSCs and subsequently, very efficiently to the formation of adenomas (Barker et al., 2009). For the investigation of the loss of the miRNAome, the *Apc* mouse model was combined with another mouse model in which a conditional knockout of the miRNA generator *Dicer1* leads to miRNA loss. The validity of the *Apc* mouse model was examined in this study by three different approaches: (1) tracing of the cell recombination at the crypt base (LGR5 positive SCs) and characteristic migration of these cells from the crypt base crypt upwards by X-Gal staining (Fig. 22C), (2) verification of the *Apc* recombination in adenomas by PCR analysis (Fig. 22E) and (3) determination of the weight of the spleens that is typically increased after adenoma formation (Fig. 22F). All approaches confirmed that the *Apc* mouse model reproducibly presents adenoma formation similar to what was described in other studies (Barker et al., 2009; Qian et al., 2005) indicating the validity of the *Apc* mouse model in this study. Additional knockout of *Dicer1* in this mouse model led to downregulation of the miRNAome and thus, to a loss of tumor suppressive and oncogenic miRNAs. The loss of the miRNAome resulted in a significant higher number of adenomas which agreed with the aforementioned studies (Kumar et al., 2009; Lambertz et al., 2010; Yoshikawa et al., 2013). Thus, loss of the

miRNAome enables cells, which were transformed by *Apc* knockout, to achieve a higher rate of tumor initiation. In this study, I detected a higher adenoma number after both, hetero- and homozygous deletion of *Dicer1* (Fig. 24 A). This observation agrees with another study in which enhanced tumor numbers after homozygous deletion of *Dicer1* (Kumar et al., 2007) were described and additionally, sarcoma cell lines were more tumorigenic after both, hetero- and homozygous deletion of *Dicer1* (Ravi et al., 2012). However, other studies reported that only heterozygous but not homozygous deletion of *Dicer1* resulted in a higher tumor number (Kumar et al., 2009; Lambertz et al., 2010; Yoshikawa et al., 2013). Furthermore, in human tumors only heterozygous mutations of *DICER1* are reported (Hill et al., 2009). Thus, it is controversially discussed if a homozygous and/or only heterozygous deletion of *Dicer1 in vivo* leads to tumor formation. One reason that only heterozygous deletion of *Dicer1* can lead to tumor formation might be that homozygous deletion of *Dicer1* and therefore, complete ablation of miRNA biogenesis is disadvantageous for tumor formation (Kumar et al., 2009). However, this hypothesis is contrary to other tumor suppressor genes in which only a homozygous mutation or loss of the gene/protein advances tumorigenesis. Thus, my data showed novel evidence that both, hetero- and homozygous deletion of *Dicer1*, leads in combination with a deletion of *Apc* to increased adenoma numbers indicating that the less miRNAs are processed the higher the tumor promoting impact is. Reduction of the protein level of DICER1 could not be demonstrated because the recombination and therefore, the deletion of the RNaseIII₂ domain of *Dicer1* does not disturb the stability of the DICER1 protein with the result that this protein can still be detected by the anti-DICER1-antibody (Harfe et al., 2005). Thus, an antibody specific against the RNaseIII₂ domain would be necessary for the verification of the loss of the DICER1 protein by recombination. Therefore, I chose PCR analysis by which I verified that the recombination of *Apc* and *Dicer1* took place only in adenomas but not in normal mucosa (Fig. 22E). However, the proof that a complete recombination of both alleles of *Dicer1* took place in the adenomas of the homozygous *Dicer1* knockout mice, meaning that there is no floxed allele left in the adenomas, is missing. Therefore, it might be possible that the recombination of *Dicer1* took place only in one instead of both alleles of *Dicer1*. Additionally, even if only a heterozygous recombination of *Dicer1* took place in the adenomas, a second hit in *Dicer1* might take place leading to a homozygous deletion of *Dicer1*. To clarify this thought, the tumors have to be deeper investigated concerning spontaneous mutations by e.g. next generation

sequencing. Furthermore, measurement of the miRNAome in the adenomas would show whether there are still mature miRNAs generated by a remaining *Dicer1* allele or not.

Loss of DICER1 in CBC cells without an activated Wnt signaling pathway did not lead to adenoma formation suggesting that loss of DICER1 leads to tumor formation only in a background with an activated oncogenic pathway. This is supported by the findings of several recent studies of mouse models in which *Dicer1* deletion resulted only in tumor formation in combination with an activated oncogenic pathway. This was the case for retinoblastoma formation in a retinoblastoma-sensitized background (Lambertz et al., 2010), lung tumor formation in combination with a mutated *KRAS* (Kumar et al., 2009) and intestinal tumor formation in an intestinal inflammation background (Yoshikawa et al., 2013). Thus, the miRNAome as a whole exerts a tumor suppressive influence on intestinal cells in mice that are transformed by an oncogene. This tumor suppressive effect is absent after loss of the miRNAome resulting in increased tumor formation.

Loss of the miRNAome resulted, besides the increased tumor initiation, also in smaller adenoma size (Fig. 24 C) caused by less proliferation (Fig. 25). Apoptosis, however, did not influence the smaller adenoma size as indicated by cleaved caspase 3 staining. The lower proliferation rate complied with observations in breast (Bu et al., 2009) and sarcoma (Ravi et al., 2012) cell lines. Therefore, the regulation of the miRNAome affects proliferation and thus, the growth of the tumor. Furthermore, as Wnt signaling drives adenoma formation and loss of DICER1 led to increased adenoma numbers, a higher activity of the Wnt signaling pathway would be expected after loss of DICER1 which was here not the case. The cause for this result is that the knockout of *Apc* in the stem cells led to a maximal activation of the Wnt signaling pathway and thus, to a nuclear localization of β -catenin in almost 100% of the cells in the adenomas which cannot be further increased. Further characterization of the adenomas did not reveal any morphological difference between the genotypes *Lgr5(+)-Apc*, *Lgr5(+)-Apc-Dicer1^{het}* and *Lgr5(+)-Apc-Dicer1^{hom}* (Fig. 25). All adenomas exhibited tubular differentiation (H&E staining) and showed the same differentiation status indicated by the frequency of Paneth (lysozyme staining) and goblet cells (PAS staining). Therefore, *Dicer1* deletion did not lead to a transition towards another subgroup of tumor differentiation such as villous, tubulovillous or mucinous (Lanza et al., 2011). However, future studies might possibly show whether loss of DICER1 is favoring the transition to another, more malignant subtype of differentiation which would occur by additional mutations. Then, deletion of *Dicer1* would not be causal for the

development of the adenomas to carcinomas but would contribute to the process of carcinogenesis. Loss of miRNAs might therefore facilitate the process of carcinogenesis as an additive element in a context of additional mutations. A future project might clarify this question by investigating this mouse model to a later time point in which loss of DICER1 might possibly contribute to the development of carcinomas by the accumulation of additional mutations.

Taken together, this study shows that deletion of *Dicer1*/loss of the miRNAome in CSCs in combination with the activated Wnt signaling pathway leads to increased adenoma formation. Furthermore, loss of the miRNAome decelerates proliferation and thus, tumor growth. However, the tumor morphology is not influenced by the loss of the miRNAome after 21 days. These observations are the case for hetero- and homozygous deletion of *Dicer1* whereby a dose-dependent effect of DICER1 is visible. In this study, deletion of *Dicer1* results in the loss of the whole miRNAome which includes tumor suppressive miRNAs and oncogenic miRNAs. As deletion of *Dicer1*/loss of the whole miRNAome leads to increased tumor initiation, the loss of the tumor suppressor miRNAs has in this context more effect than loss of the oncogenic miRNAs. Although for the tumor formation, both, the suppression of tumor suppressive miRNAs as well as the activation of oncogenic miRNAs are important, the suppression of tumor suppressive miRNAs seems to be more relevant for the tumor. Furthermore, the decreased proliferation after loss of the miRNAome indicated that the loss of miRNAs that lead to increased proliferation by targeting mRNAs has a high influence on the tumor growth (Fig. 35).

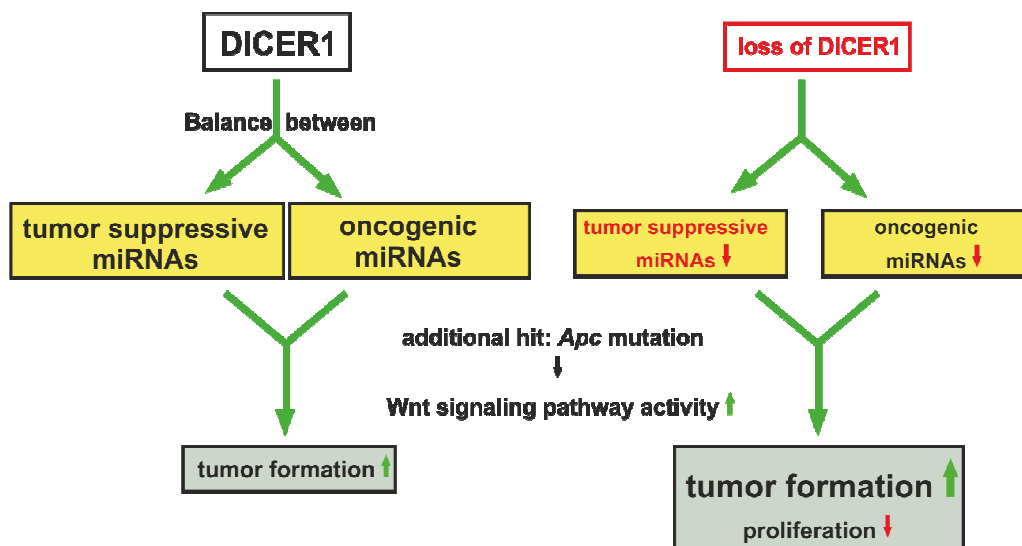


Fig. 35. Model of the impact of DICER1 on adenoma formation.

DICER1 is involved in the biogenesis of miRNAs whereby a balance between tumor suppressive and oncogenic miRNAs exists. An *Apc* mutation in CBC cells and thus, activation of the Wnt signaling pathway and generation of CSCs leads to adenoma formation. Loss of DICER1 leads to a downregulation of tumor suppressive and oncogenic miRNAs. In combination with an *Apc* mutation, the downregulation of miRNAs in CSCs leads to an increased tumor formation and decreased proliferation. Despite downregulation of both, tumor suppressive and oncogenic miRNAs, the loss of tumor suppressive miRNAs has a higher impact as tumor formation is increased. Letter and arrow size reflect the amount of activity or loss.

4.2.2 *Loss of DICER1 resulted in slower proliferation but increased stemness and metastatic capacities in CRC cell lines*

The previous findings of the mouse model showed that loss of the miRNAome in CSCs, which originated by *APC* mutation in CBC cells, promotes tumor initiation. However, knowledge of the mechanistical background is crucial to develop CSC targeted therapies. Furthermore, in the mouse model, the influence of the miRNAome loss was investigated concerning adenoma formation. To translate this investigation to a carcinoma model, CRC cell lines are an appropriate tool for these examinations. Moreover, the influence on CSC features is easier to examine in cell culture than in a mouse model. The further investigation of the mechanistical background might help to understand the influence of the miRNAome on CSC features and on the process of carcinogenesis. I chose the CRC cell lines RKO and HCT116 with a homozygous disruption of *DICER1* (Cummins et al., 2006) which are impaired in miRNA maturation leading to a reduction of mature miRNAs (Fig. 26). However, it is remarkable that mature miRNAs are strongly reduced but still

present despite complete loss of DICER1. Possibly, there are other DICER1 independent miRNA-biogenesis mechanisms as described in (Dueck and Meister, 2010).

Since deletion of *Dicer1* in a mouse model resulted in a reduced size of the adenomas by less proliferation, I investigated also the influence of DICER1 on proliferation of CRC cell lines. As in the mouse model, loss of DICER1 led to a slower proliferation in HCT116 cells (Fig. 28A). Consistent with my data, another group (Iliou et al., 2014) reported the same result during preparation of this thesis. This finding was further verified in this study by cell cycle analysis in which *DICER1* disruption led to a higher number of cells in the G0/G1 phase (Fig. 28B) indicating cell cycle arrest and by Hippo pathway analysis which showed a decreased transcriptional activity of YAP/TAZ (Fig. 28C). Thereby it is crucial to know that Hippo pathway regulates the size of organs. Since both, cell cycle (Calabrese et al., 2007; Wang et al., 2008) and Hippo pathway (Lee et al., 2009) are regulated by specific miRNAs, the loss of these miRNAs might contribute to these changes. In total, the reduction of both, tumor suppressive and oncogenic miRNAs influences these changes. As previously observed in adenomas of the mouse model, apoptosis, measured by the subG1 phase, was not influenced by loss of DICER1 in CRC cell lines (Fig. 28B). As in the mouse model, the loss of the whole miRNAome in CRC cell lines has a suppressive function on the proliferation. Among the plethora of lost miRNAs, the loss of the growth promoting miRNAs dominates whereby proliferation is decreased, cell cycle arrest enhanced and YAP/TAZ-activity reduced. These cellular changes lead to slower cell and thus, tumor growth. The decreased proliferation and increased cell cycle arrest in the cellular system and in the mouse model might further be associated with the increased expression of the cell cycle inhibitor *CDKN2A* which is a β -catenin target gene (Wassermann et al., 2009) and thus, might be expressed in both, the *Apc* mouse model and HCT116 cells. The expression of *CDKN2A* can repress the proliferation promoting effect of the β -catenin target genes *MYC* and *CCND1*. Thus, the enforced expression of *CDKN2A* which is associated with the CSC features EMT and metastasis (Brabletz et al., 2005) might decrease the proliferation rate after loss of the miRNAome however also increase CSC features such as stemness, EMT, metastasis and chemoresistance. This hypothesis would explain the increased tumor initiation (increased stemness) and the decreased proliferation after loss of the miRNAome in the *Apc* mouse model. However, this has to be proved by further investigations.

Moreover, as loss of DICER1 increased tumor initiation I investigated the impact of the miRNAome loss on CSC features to understand the influence of the miRNAome on the

process of carcinogenesis. In a first descriptive approach, I determined that CSC and EMT markers were upregulated in HCT116 cells after *DICER1* disruption (Fig. 27) thus indicating more pronounced stemness and EMT properties of the cells after loss of *DICER1* as the expression of CSC and EMT markers is associated with SC properties (Mani et al., 2008). This is supported by results from another group (Iliou et al., 2014). This finding is corroborated by chemoresistance that is known to be connected with stemness (Dallas et al., 2009). CRC cells were more chemoresistant against 5-FU after loss of the miRNAome (Fig. 29A, B) and thus, the miRNAome as a whole suppresses mechanisms that lead to chemoresistance. Hence, loss of the miRNAome might contribute to the chemoresistance and consequently, to a worse response on chemotherapy in patients. This supposition is supported by the finding that low *DICER1* protein levels led to a worse response to 5-FU in oral squamous cell carcinoma (Kawahara et al., 2014). Chemoresistance is one of the major reasons for the nonresponse of patients and is associated with increased expression of EMT markers (Dean et al., 2005; Frank et al., 2010; Singh and Settleman, 2010) or ABC transporters (Dean et al., 2005; Zinzi et al., 2014). As both, EMT factors (Gregory et al., 2008; Siemens et al., 2011) and ABC transporters (Bitarte et al., 2011) are downregulated by miRNAs, loss of the miRNAome might lead to the upregulation of EMT factors and ABC transporters and consequently, to increased chemoresistance. Metastatic features which characterize CSC besides the CSC features stemness, EMT and chemoresistance were also increased after loss of *DICER1* and thus, of the whole miRNAome. The levels of the metastatic marker CD26 (Pang et al., 2010) (Fig. 27C, D) and migration were enhanced after loss of the miRNAome (Fig. 30B, C). The loss of *DICER1* and thus, of the whole miRNAome leads to the downregulation of migration inhibiting miRNAs (Korpál et al., 2008) whereby the cells are enabled to migrate. Consistent with this, increased *DICER1* expression by the tumor suppressor tumor protein p63 suppressed metastasis (Su et al., 2010). As β -catenin target genes are involved in the crucial features of CSCs such as cancer stemness, metastasis, EMT and chemoresistance and these features are all influenced by disruption of *DICER1*, I investigated whether *DICER1* disruption influenced also the activity of the Wnt signaling pathway. Indeed, the loss of the miRNAome increased the activity of the Wnt signaling pathway (Fig. 31), possibly by downregulation of *miR-451* (Bitarte et al., 2011).

Taken together, the loss of most of the miRNAome leads to increased expression/protein levels of CSC, EMT and metastatic markers, enhanced chemoresistance, migration and

Wnt signaling pathway activity. Thus, the downregulation of the whole miRNAome promotes features that are characteristic for CSCs. These results agree with the finding that loss of the miRNAome in mice leads to increased tumor initiation and thus, increased stemness. As both, tumor suppressive and oncogenic miRNAs are downregulated, the influence of the tumor suppressive miRNAs dominates in intestinal cancer and hence, the loss of the miRNAome is advantageous for the tumor formation and the process of carcinogenesis. Based on the results in this study I conclude that DICER1 and thus, the miRNAome acts as a tumor suppressor.

4.2.3 *Loss of DICER1 led to tumor formation and provides cancer properties in combination with an active oncogenic pathway*

Since target genes of the Wnt signaling pathway are involved in CSC properties such as tumor initiation (Du et al., 2008), proliferation (Clevers, 2006), chemoresistance (Yamada et al., 2000) and metastasis (Vlad-Fiegen et al., 2012), I investigated the impact of the Wnt signaling pathway on these features which were influenced by loss of the miRNAome. The effects of the loss of the miRNAome on CSC features were enhanced by an active Wnt signaling pathway (Fig. 28F; 29C; 30B, C). In the CRC cell lines, the combination of an active Wnt signaling pathway and a loss of the miRNAome showed the largest effects on the cancer cell properties. However, the effects, which caused by a loss of the miRNAome, on proliferation, chemoresistance and migration, were also visible with a reduced Wnt signaling pathway activity and thus, an active Wnt signaling pathway was dispensable for these effects. In the mouse model, the combination of an active Wnt signaling pathway and deletion of *Dicer1* resulted also in the highest number of adenomas (Fig. 24A). However, in contrast to the cell lines, an activation of the Wnt signaling pathway was indispensable for the adenoma formation in the mouse model. This might be the case because the stem cells, in which the activation of the Wnt signaling pathway by *Apc* deletion took place, contained no further mutation or activation of another oncogenic pathway. These cells were only transformed by the activation of the Wnt signaling pathway. Therefore, the cells that possessed only a deletion of *Dicer1* did not develop adenomas. In contrast to the mouse model, the cancer cell lines RKO and HCT116 possess also mutations in other oncogenic pathways. Both cell lines show mutations in *PIK3* (Ahmed et al., 2013) and additionally, *BRAF* (RKO) or *KRAS* mutations (HCT116) (Ahmed et al., 2013) which increase cell proliferation, survival and chemoresistance (Fruman and Rommel, 2014;

Hirschi et al., 2014; Maurer et al., 2011; Sunaga et al., 2011). Consequently, these cell lines possess activated oncogenic PI3K/AKT and RAS/RAF/MAPK pathways and thus, tumor promoting features. An additional activation of the Wnt signaling pathway increased the effects in the cell lines after disruption of *DICER1*. However, the cell lines were not completely dependent on the Wnt signaling pathway. Thus, I suggest that *DICER1* and thus, the miRNAome acts as a tumor suppressor in CRC cell lines as well in the mouse model and loss of *DICER1* leads in combination with an activated oncogenic pathway such as the Wnt/ β -catenin, PI3K/AKT or RAS/RAF/MAPK to tumor formation and increased CSC properties.

The aforementioned hypothesis (see 4.2.1) that loss of *DICER1* and therefore, loss of miRNAs in the mouse model might lead to carcinomas at later time points is supported by the cell culture results. The investigations in the mouse model take place at an early time point of the tumorigenesis where the cells did not accumulate additional mutations because of the short time span. In contrast, the further experiments in cell culture were performed in carcinoma cell lines which already accumulated additional mutations directing the cells into a more malignant route and further in cancer progression. A loss of *DICER1* in the carcinoma cells can therefore enhance the malignancy of the carcinogenesis as the cells did already pursue this route, in contrast to the mouse model. Thus, deletion of *DICER1* and thus, of the miRNAome in the carcinoma cells led to enhanced stemness and malignancy whereas in the mouse model, a higher tumor initiation was indeed detectable, however, no shift towards increased malignancy.

4.2.4 *DICER1 mRNA expression and protein levels increased in adenomas mediated by Wnt signaling pathway but decreased during progression from adenoma to carcinoma in human CRC*

Since the finding that *DICER1* and the miRNAome function as a tumor suppressor was gained in a mouse model and in cell culture, I next translated this result to human CRC tissue. The animal and cell culture systems are very useful to investigate gene deletions or activations and the mechanistical background. However, the translation of the findings to human tissue is the next step as the final aim of the investigations is the investigation of the relevance for human tumors. As in humans, tumor suppressors are often inactivated during cancer development and progression (Fearon and Vogelstein, 1990) I investigated in this

study the levels of DICER1 during CRC progression. As expected from the previous results in this study, DICER1 decreased continually from adenoma during carcinoma progression in a collection of normal and tumorous colonic tissues (Fig. 32B). Consistent with my data, another group reported also a decrease of DICER1 during human colorectal carcinogenesis (Faggad et al., 2012). This result supports the previous findings since loss of DICER1 increased stemness features in cancer cells which are involved in progression and advanced tumor stages (Frank et al., 2010). The result that DICER1 levels decreased during carcinoma progression demonstrated that loss of DICER1 contributed to this progression. The mechanism for the downregulation of DICER1, however, is not yet clarified. In previous studies, no methylation of the *DICER1* promoter was found (Karube et al., 2005; Melo et al., 2009) that could lead to silencing (Issa, 2004) of the *DICER1* gene. However, mutations in the *DICER1* gene were detected (Hill et al., 2009) and in advanced CRC, loss of heterozygosity occurs frequently on the long arm (q) of chromosome 14 (Young et al., 1993) on which *DICER1* is located. Additionally, mutations in *TARBP2* (Melo et al., 2009) or loss of *TARBP2* (Chendrimada et al., 2005), the interaction partner of DICER1, led to a destabilization of the DICER1 protein. Thus, further studies are required to unveil the mechanism for the downregulation of DICER1 during CRC progression.

Furthermore, it turned out unexpectedly in the human tissue collection used here that adenomas showed an increase of DICER1 levels compared to normal mucosa (Fig. 32B) which was confirmed in murine adenomas (Fig. 33A). Since the murine adenomas in this study and likewise, the majority of the human CRCs (Pino and Chung, 2010) are driven by the Wnt signaling pathway, both show a higher Wnt signaling pathway activity compared to normal mucosa. Therefore, the influence of Wnt signaling on *DICER1* expression was further investigated namely in cell culture as cells are more suited for this investigation than tissue. I determined in CRC cells that a reduction of the Wnt signaling pathway activity by knockdown of *CTNNB1* or transfection of dnTCF4 reduced the expression of *DICER1* and also the activity of the *DICER1* promoter (Fig. 33). From this result I conclude that the Wnt/ β -catenin signaling pathway is involved in the regulation of the *DICER1* expression. This finding is supported by a recent study that *DICER1* is a target gene of β -catenin in the brain (Dias et al., 2014). The result that *DICER1* is a β -catenin target gene connects the Wnt signaling pathway with the miRNA biogenesis and shows an additional function of β -catenin and its target genes besides the other differential functions. β -catenin target genes regulate many different features in the cancer cells such

as **proliferation** (*MYC* (He et al., 1998), *CCND1* (Shtutman et al., 1999) but also *CDKN2A* (Wassermann et al., 2009)), **stemness** (*CD44* (Wielenga et al., 1999), *LGR5* (Barker et al., 2007)), **chemoresistance** (*ABCB1* (Yamada et al., 2000), **EMT** (*VIM* (Gilles et al., 2003), *ZEB1* (Sanchez-Tillo et al., 2011)) and **invasion** (*MMP7* (Brabletz et al., 1999), *PLAU* (Hiendlmeyer et al., 2004) and *TNC* (Beiter et al., 2005)). Additionally, I identified *TERT* as a β -catenin target gene (Hoffmeyer et al., 2012; Jaitner et al., 2012) that mediates the hallmark replicative immortality to cancer cells (see also 1.2.3.2). Thus, Wnt signaling pathway regulates, besides other important cancer properties, also the **miRNA biogenesis** (Fig. 36).

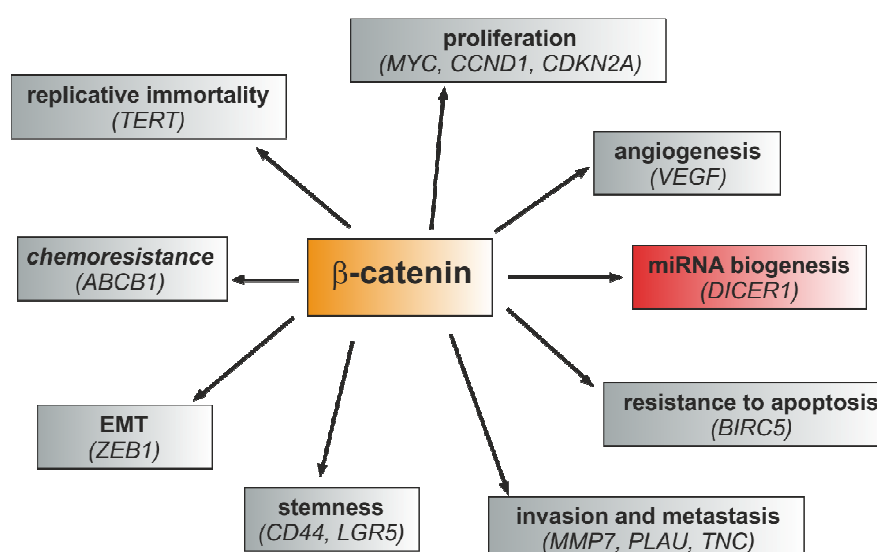


Fig. 36. The influence of β -catenin on hallmarks of cancer and its target genes.

Besides the already known target genes (grey), I demonstrated in this study that β -catenin regulates additionally the expression of *DICER1* (red) and thus, the miRNA biogenesis.

The result that *DICER1* is downregulated during carcinogenesis (Fig. 32B) was also observed for other genes such as *DKK-1* (Gonzalez-Sancho et al., 2005) or *ITF-2* (Herbst et al., 2009) which are both also β -catenin target genes but downregulated in colorectal tumors. This finding demonstrates that the role of *DICER1* and thus, the miRNAome is very complex in CRC. Notably, the upregulation of *DICER1* in adenomas leads to an increase of oncogenic miRNAs whereas the downregulation of *DICER1* and consequently, of tumor suppressive miRNAs was more favorable for advanced tumor stages. Another explanation might be that *DICER1* is induced by β -catenin at the beginning of the tumorigenesis, in the adenomas, as *DICER1* has a tumor protective function and is

upregulated by β -catenin as an endogenous protective mechanism. However, at later time points, *DICER1* and miRNAs are not further relevant but rather unfavorable whereby *DICER1* and thus, miRNAs are downregulated during the process of colorectal carcinogenesis.

Taken together, the findings gained from cell culture experiments and results from the human CRC tissue collection demonstrate that the regulation of *DICER1* and thus, the miRNAome is complex during the process of colorectal carcinogenesis. The initial hit in this process of cancer formation is a mutation in the *APC* gene and thus, an activation of the Wnt signaling pathway leading to adenoma formation. The β -catenin target gene *DICER1* and thus, the miRNAome increases and supports adenoma formation. However, during the process of carcinogenesis, *DICER1* is downregulated/inactivated and leads to a downregulation of the miRNAome which supports the process of carcinogenesis. As an activated Wnt signaling pathway and loss of the miRNAome increase CSC features, both promote the process of carcinogenesis (Fig. 37).

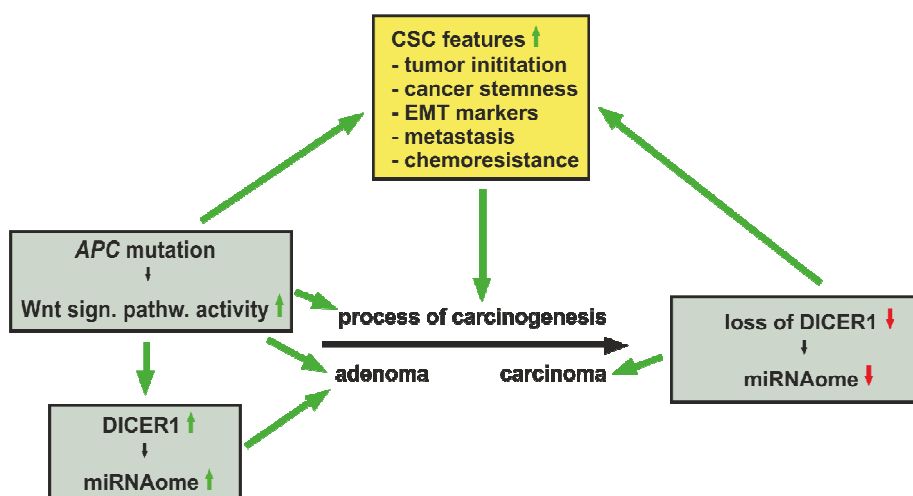


Fig. 37. Model of *DICER1* protein levels during the process of colorectal carcinogenesis.

The initial hit, the *APC* mutation and thus, activation of the Wnt signaling pathway, leads to adenoma formation. Furthermore, the Wnt signaling pathway increases *DICER1* expression/*DICER1* protein levels and thus, the miRNAome which supports adenoma formation. During the process of carcinogenesis, *DICER1* is downregulated/inactivated leading to a downregulation of the miRNAome and thus, to a promotion of carcinogenesis. Both, Wnt signaling pathway activity and loss of the miRNAome increase CSC features which again support the process of carcinogenesis.

4.2.5 *Future investigations*

The human situation in which *DICER1* is upregulated in adenomas and subsequently, downregulated during the process of carcinogenesis in CRC, is difficult to translate into a mouse model for further investigations. To answer the questions whether the complex regulation of *DICER1*, which was observed in a human CRC tissue collection (Fig. 32, 37), supports the process of carcinogenesis and drives adenomas to carcinomas at a later time point, a suitable mouse model has to be generated. The generation of a multistep carcinogenesis mouse model (Schonhuber et al., 2014) might better reflect the human situation. Therefore, a mouse model should be generated in which *Apc* and *Dicer1* can be knocked out inducible at different timepoints. To do so, two different recombinase systems have to be used (Fig. 38) (Collins et al., 2012; Schonhuber et al., 2014). In this multistep carcinogenesis mouse model, two systems (*rtTA* (recombinant tetracycline controlled transcription factor) and *CreER^{T2}*) are expressed under the *Lgr5* promoter in CBC cells. Thus, the *FLP* (flippase) recombinase which is controlled by *TetO* (tet operator) can be induced by the administration of doxycycline (dox), e.g. administration in drinking water. By the expression of *FLP*, *Apc* could be knocked out at timepoint 1 (day 0) via the FRT (flippase recognition target) sites to activate the Wnt signaling pathway in CBC cells. After the formation of adenomas, *Dicer1* could be knocked out by TAM injection at a second timepoint (day x) whereby *CreER^{T2}* could translocate to the nucleus and *Dicer1* could be knocked out by the flox sites. In the *Apc* mouse model, the knockout of *Apc* leads very fast to adenomas. At day 8 after the *Apc* knockout, microadenomas become evident, at day 14 after the *Apc* knockout, large adenomas are visible and at day 36 after the *Apc* knockout, the mice have to be killed because of the high tumor burden (Barker et al., 2009). Thus, the additional knockout of *Dicer1* should take place between day 8 and day 14 after the *Apc* knockout to make sure that the mice live long enough for further investigations. This mouse model would allow the investigation of the effects of *DICER1* on the process of carcinogenesis at later time points. This might reflect the human situation in which *DICER1* was upregulated in adenomas by β -catenin but later in tumorigenesis, *DICER1* was downregulated.

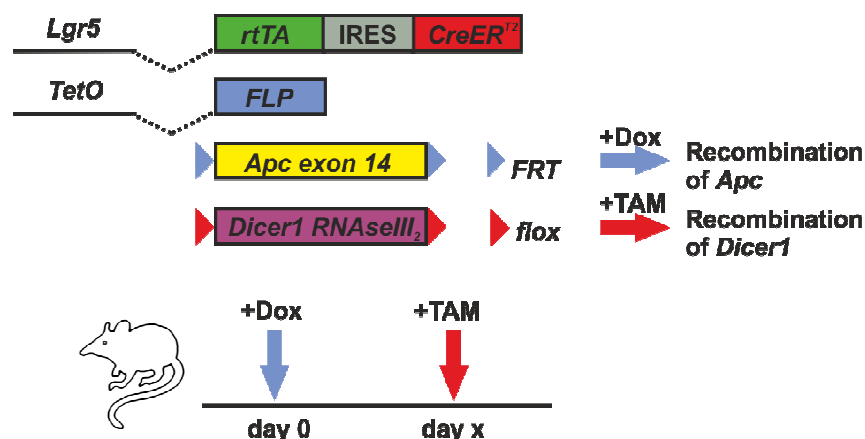


Fig. 38. Multistep carcinogenesis mouse model.

In this mouse model *rtTA* (recombinant tetracycline controlled transcription factor) and *CreER^{T2}* are expressed under the control of the *Lgr5* promoter. Thus, both, *rtTA* and *CreER^{T2}* can be induced in *Lgr5* expressing cells (CBC cells). Administration of doxycycline (dox) at timepoint 1 (day 0) leads to binding of *rtTA* to TetO (tet operator) and thus, to expression of the *FLP* (flippase) recombinase. By the expression of the *FLP* recombinase, recombination of *Apc* can take place. Injection of TAM to a second timepoint (day x) leads to recombination of *Dicer1* in CBC cells.

The adenomas and possibly carcinomas from this mouse model might be further isolated and used to investigate the changes of the targeted mRNAs by transcriptome analysis. These investigations might shed light on the altered expression of mRNAs after loss of the miRNAome. The investigations of the changes in the transcriptome might be used to identify the corresponding miRNAs whose loss is responsible for the process of carcinogenesis. Furthermore, transcriptome analysis of the cell lines (HCT116/RKO +/+/*ex5*) might be a promising tool to identify responsible miRNAs whose loss promotes the process of carcinogenesis by targeting specific mRNAs. These identified miRNAs might further be tested as possible targets for therapies. The identified miRNAs might be delivered to the mouse model (Fig. 38) at a specific timepoint 3 to examine whether the administration of specific tumor suppressive miRNAs can inhibit the process of carcinogenesis in this Wnt driven mouse model. In previous studies the restoration of some tumor suppressive miRNAs that were downregulated in the tumor were tested for the treatment of tumors in mouse models (Melo and Kalluri, 2012). Promising effects had e.g. the delivery of the miRNA *let-7b* which targeted enhanced proliferation, invasion and metastasis formation in a mouse model which were caused by overexpressed oncogenes (Trang et al., 2010; Trang et al., 2011). Furthermore, the application of *miR-34a* (Liu et al.,

2011; Trang et al., 2011) and *miR-143/145* inhibited tumor growth (Pramanik et al., 2011). Besides the single miRNA based therapy, also the promotion of the miRNA biogenesis and thus, upregulation of multiple miRNAs by application of small molecules is possible (Melo and Kalluri, 2012). These increased level of miRNAs, among them also tumor suppressive miRNAs, inhibited tumor growth (Melo et al., 2011; Shan et al., 2008) which could be more effective for therapeutic success than the application of a single miRNA (Melo and Kalluri, 2012). However, since miRNA biogenesis is promoted by this application, no mutation or inactivation of the miRNA biogenesis components such as DICER1 may exist in the latter approach. Furthermore, the application of miRNAs might lead to sensitization of tumors for chemotherapy and therefore, to growth inhibition and shrinkage of the tumor (Melo and Kalluri, 2012). This decrease of chemoresistance might be mediated e.g. by delivery of miRNAs which reduce the expression of ABC transporters (Jeon et al., 2011) or increase the sensitivity for tamoxifen (Cittelly et al., 2010). Besides the application of tumor suppressive miRNAs, miRNA based tumor therapy is also possible by inhibition of oncogenic miRNAs. Of course, nonspecific side effects might appear since one miRNA can target a high number of mRNAs. Methods that deliver the miRNAs or small molecules to the appropriate cell types or tissues might help to reduce side effects (Melo and Kalluri, 2012). Delivery methods were already improved whereby the therapeutic miRNAs can be delivered intranasally, intratumorally or systemically. The improvement of the delivery methods to get safer delivery vehicles such as lipid-based nanoparticles was a good step towards clinical application. However, it has to be validated in clinical trials whether the success of miRNA application can also be recapitulated in human patients (Kasinski and Slack, 2011). Nevertheless, the application of tumor suppressive miRNAs or inhibition of oncogenic miRNAs is a promising tool for the therapy of tumors. Therefore, further studies are required to clarify the success of these therapies, to enhance efficacy, to reduce side effects (Melo and Kalluri, 2012) and finally, to translate these findings to human tumors.

References

Ahmed, D., Eide, P.W., Eilertsen, I.A., Danielsen, S.A., Eknaes, M., Hektoen, M., Lind, G.E., and Lothe, R.A. (2013). Epigenetic and genetic features of 24 colon cancer cell lines. *Oncogenesis* 2, e71.

Al-Hajj, M., Wicha, M.S., Benito-Hernandez, A., Morrison, S.J., and Clarke, M.F. (2003). Prospective identification of tumorigenic breast cancer cells. *Proceedings of the National Academy of Sciences of the United States of America* 100, 3983-3988.

Arrate, M.P., Vincent, T., Odvody, J., Kar, R., Jones, S.N., and Eischen, C.M. (2010). MicroRNA biogenesis is required for Myc-induced B-cell lymphoma development and survival. *Cancer Research* 70, 6083-6092.

Banning, A., Kipp, A., Schmitmeier, S., Lowinger, M., Florian, S., Krehl, S., Thalmann, S., Thierbach, R., Steinberg, P., and Brigelius-Flohe, R. (2008). Glutathione Peroxidase 2 Inhibits Cyclooxygenase-2-Mediated Migration and Invasion of HT-29 Adenocarcinoma Cells but Supports Their Growth as Tumors in Nude Mice. *Cancer Research* 68, 9746-9753.

Barca-Mayo, O., and Lu, Q.R. (2012). Fine-Tuning Oligodendrocyte Development by microRNAs. *Frontiers in Neuroscience* 6, 13.

Barker, N., Ridgway, R.A., van Es, J.H., van de Wetering, M., Begthel, H., van den Born, M., Danenberg, E., Clarke, A.R., Sansom, O.J., and Clevers, H. (2009). Crypt stem cells as the cells-of-origin of intestinal cancer. *Nature* 457, 608-611.

Barker, N., van de Wetering, M., and Clevers, H. (2008). The intestinal stem cell. *Genes & Development* 22, 1856-1864.

Barker, N., van Es, J.H., Kuipers, J., Kujala, P., van den Born, M., Cozijnsen, M., Haegbarth, A., Korving, J., Begthel, H., Peters, P.J., *et al.* (2007). Identification of stem cells in small intestine and colon by marker gene *Lgr5*. *Nature* 449, 1003-1007.

Battle, E., Henderson, J.T., Begthel, H., van den Born, M.M., Sancho, E., Huls, G., Meeldijk, J., Robertson, J., van de Wetering, M., Pawson, T., *et al.* (2002). Beta-catenin and TCF mediate cell positioning in the intestinal epithelium by controlling the expression of EphB/ephrinB. *Cell* 111, 251-263.

Beiter, K., Hiendlmeyer, E., Brabletz, T., Hlubek, F., Haynl, A., Knoll, C., Kirchner, T., and Jung, A. (2005). beta-Catenin regulates the expression of tenascin-C in human colorectal tumors. *Oncogene* 24, 8200-8204.

Bernstein, E., Kim, S.Y., Carmell, M.A., Murchison, E.P., Alcorn, H., Li, M.Z., Mills, A.A., Elledge, S.J., Anderson, K.V., and Hannon, G.J. (2003). Dicer is essential for mouse development. *Nature Genetics* 35, 215-217.

Besson, D., Pavageau, A.H., Valo, I., Bourreau, A., Belanger, A., Eymerit-Morin, C., Mouliere, A., Chassevent, A., Boisdron-Celle, M., Morel, A., *et al.* (2011). A quantitative

proteomic approach of the different stages of colorectal cancer establishes OLFM4 as a new nonmetastatic tumor marker. *Molecular & Cellular Proteomics* : MCP 10, M111 009712.

Bitarte, N., Bandres, E., Boni, V., Zarate, R., Rodriguez, J., Gonzalez-Huarriz, M., Lopez, I., Javier Sola, J., Alonso, M.M., Fortes, P., *et al.* (2011). MicroRNA-451 is involved in the self-renewal, tumorigenicity, and chemoresistance of colorectal cancer stem cells. *Stem Cells* 29, 1661-1671.

Bonnet, D., and Dick, J.E. (1997). Human acute myeloid leukemia is organized as a hierarchy that originates from a primitive hematopoietic cell. *Nature Medicine* 3, 730-737.

Bosman, F.T., Carneiro, F., Hruban, R.H., and Theise, N.D. (2010). WHO Classification of Tumours of the Digestive System, Vol 3, 4 edn (International Agency for Research on Cancer (IARC): Lyon).

Brabletz, S., Schmalhofer, O., and Brabletz, T. (2009). Gastrointestinal stem cells in development and cancer. *The Journal of Pathology* 217, 307-317.

Brabletz, T., Jung, A., Dag, S., Hlubek, F., and Kirchner, T. (1999). beta-catenin regulates the expression of the matrix metalloproteinase-7 in human colorectal cancer. *The American Journal of Pathology* 155, 1033-1038.

Brabletz, T., Jung, A., Reu, S., Porzner, M., Hlubek, F., Kunz-Schughart, L.A., Knuechel, R., and Kirchner, T. (2001). Variable beta-catenin expression in colorectal cancers indicates tumor progression driven by the tumor environment. *Proceedings of the National Academy of Sciences of the United States of America* 98, 10356-10361.

Brabletz, T., Jung, A., Spaderna, S., Hlubek, F., and Kirchner, T. (2005). Opinion: migrating cancer stem cells - an integrated concept of malignant tumour progression. *Nature Reviews Cancer* 5, 744-749.

Bruns, C.J., Angele, M.K., Auernhammer, C.J., Beraldi, A., Gertler, R., Heinemann, V., Jung, A., Kalusche, E.-M., Keller, G., Kleespies, A., *et al.* (2013). *Gastrointestinale Tumoren* (W. Zuckerschwerdt Verlag, München).

Bu, Y., Lu, C., Bian, C., Wang, J., Li, J., Zhang, B., Li, Z., Brewer, G., and Zhao, R.C. (2009). Knockdown of Dicer in MCF-7 human breast carcinoma cells results in G1 arrest and increased sensitivity to cisplatin. *Oncology Reports* 21, 13-17.

Cai, W.Y., Wei, T.Z., Luo, Q.C., Wu, Q.W., Liu, Q.F., Yang, M., Ye, G.D., Wu, J.F., Chen, Y.Y., Sun, G.B., *et al.* (2013). The Wnt-beta-catenin pathway represses let-7 microRNA expression through transactivation of Lin28 to augment breast cancer stem cell expansion. *Journal of Cell Science* 126, 2877-2889.

Calabrese, J.M., Seila, A.C., Yeo, G.W., and Sharp, P.A. (2007). RNA sequence analysis defines Dicer's role in mouse embryonic stem cells. *Proceedings of the National Academy of Sciences of the United States of America* 104, 18097-18102.

- Campeau, E., Ruhl, V.E., Rodier, F., Smith, C.L., Rahmberg, B.L., Fuss, J.O., Campisi, J., Yaswen, P., Cooper, P.K., and Kaufman, P.D. (2009). A versatile viral system for expression and depletion of proteins in mammalian cells. *PloS One* 4, e6529.
- Carragher, L.A., Snell, K.R., Giblett, S.M., Aldridge, V.S., Patel, B., Cook, S.J., Winton, D.J., Marais, R., and Pritchard, C.A. (2010). V600EBraf induces gastrointestinal crypt senescence and promotes tumour progression through enhanced CpG methylation of p16INK4a. *EMBO Molecular Medicine* 2, 458-471.
- Chen, L., Li, H., Liu, W., Zhu, J., Zhao, X., Wright, E., Cao, L., Ding, I., and Rodgers, G.P. (2011). Olfactomedin 4 suppresses prostate cancer cell growth and metastasis via negative interaction with cathepsin D and SDF-1. *Carcinogenesis* 32, 986-994.
- Chendrimada, T.P., Gregory, R.I., Kumaraswamy, E., Norman, J., Cooch, N., Nishikura, K., and Shiekhattar, R. (2005). TRBP recruits the Dicer complex to Ago2 for microRNA processing and gene silencing. *Nature* 436, 740-744.
- Cheng, G.Z., Chan, J., Wang, Q., Zhang, W., Sun, C.D., and Wang, L.H. (2007). Twist transcriptionally up-regulates AKT2 in breast cancer cells leading to increased migration, invasion, and resistance to paclitaxel. *Cancer Research* 67, 1979-1987.
- Christofori, G. (2006). New signals from the invasive front. *Nature* 441, 444-450.
- Cittelly, D.M., Das, P.M., Salvo, V.A., Fonseca, J.P., Burow, M.E., and Jones, F.E. (2010). Oncogenic HER2{Delta}16 suppresses miR-15a/16 and deregulates BCL-2 to promote endocrine resistance of breast tumors. *Carcinogenesis* 31, 2049-2057.
- Clevers, H. (2006). Wnt/beta-catenin signaling in development and disease. *Cell* 127, 469-480.
- Clevers, H. (2013). The intestinal crypt, a prototype stem cell compartment. *Cell* 154, 274-284.
- Clevers, H., and Nusse, R. (2012). Wnt/beta-catenin signaling and disease. *Cell* 149, 1192-1205.
- Clevers, H.C., and Bevins, C.L. (2013). Paneth cells: maestros of the small intestinal crypts. *Annual Review of Physiology* 75, 289-311.
- Collins, M.A., Bednar, F., Zhang, Y., Brisset, J.C., Galban, S., Galban, C.J., Rakshit, S., Flannagan, K.S., Adsay, N.V., and Pasca di Magliano, M. (2012). Oncogenic Kras is required for both the initiation and maintenance of pancreatic cancer in mice. *The Journal of Clinical Investigation* 122, 639-653.
- Conacci-Sorrell, M., Simcha, I., Ben-Yedidia, T., Blechman, J., Savagner, P., and Ben-Ze'ev, A. (2003). Autoregulation of E-cadherin expression by cadherin-cadherin interactions: the roles of beta-catenin signaling, Slug, and MAPK. *The Journal of Cell Biology* 163, 847-857.

- Conacci-Sorrell, M., Zhurinsky, J., and Ben-Ze'ev, A. (2002). The cadherin-catenin adhesion system in signaling and cancer. *The Journal of Clinical Investigation* *109*, 987-991.
- Crabtree, M., Sieber, O.M., Lipton, L., Hodgson, S.V., Lamlum, H., Thomas, H.J., Neale, K., Phillips, R.K., Heinimann, K., and Tomlinson, I.P. (2003). Refining the relation between 'first hits' and 'second hits' at the APC locus: the 'loose fit' model and evidence for differences in somatic mutation spectra among patients. *Oncogene* *22*, 4257-4265.
- Creighton, C.J., Li, X., Landis, M., Dixon, J.M., Neumeister, V.M., Sjolund, A., Rimm, D.L., Wong, H., Rodriguez, A., Herschkowitz, J.I., *et al.* (2009). Residual breast cancers after conventional therapy display mesenchymal as well as tumor-initiating features. *Proceedings of the National Academy of Sciences of the United States of America* *106*, 13820-13825.
- Crosnier, C., Stamataki, D., and Lewis, J. (2006). Organizing cell renewal in the intestine: stem cells, signals and combinatorial control. *Nature Reviews Genetics* *7*, 349-359.
- Cummins, J.M., He, Y., Leary, R.J., Pagliarini, R., Diaz, L.A., Jr., Sjoblom, T., Barad, O., Bentwich, Z., Szafranska, A.E., Labourier, E., *et al.* (2006). The colorectal microRNAome. *Proceedings of the National Academy of Sciences of the United States of America* *103*, 3687-3692.
- Dalerba, P., Dylla, S.J., Park, I.K., Liu, R., Wang, X., Cho, R.W., Hoey, T., Gurney, A., Huang, E.H., Simeone, D.M., *et al.* (2007). Phenotypic characterization of human colorectal cancer stem cells. *Proceedings of the National Academy of Sciences of the United States of America* *104*, 10158-10163.
- Dallas, N.A., Xia, L., Fan, F., Gray, M.J., Gaur, P., van Buren, G., 2nd, Samuel, S., Kim, M.P., Lim, S.J., and Ellis, L.M. (2009). Chemoresistant colorectal cancer cells, the cancer stem cell phenotype, and increased sensitivity to insulin-like growth factor-I receptor inhibition. *Cancer Research* *69*, 1951-1957.
- Darzynkiewicz, Z., and Huang, X. (2004). Analysis of cellular DNA content by flow cytometry. *Current Protocols in Immunology* / edited by John E Coligan [et al] *Chapter 5*, Unit 5 7.
- De Craene, B., and Berx, G. (2013). Regulatory networks defining EMT during cancer initiation and progression. *Nature Reviews Cancer* *13*, 97-110.
- de la Chapelle, A. (2004). Genetic predisposition to colorectal cancer. *Nature Reviews Cancer* *4*, 769-780.
- Dean, M., Fojo, T., and Bates, S. (2005). Tumour stem cells and drug resistance. *Nature Reviews Cancer* *5*, 275-284.
- Dias, C., Feng, J., Sun, H., Shao, N.Y., Mazei-Robison, M.S., Damez-Werno, D., Scobie, K., Bagot, R., LaBonte, B., Ribeiro, E., *et al.* (2014). beta-catenin mediates stress resilience through Dicer1/microRNA regulation. *Nature* *516*, 51-55.

- Dieter, S.M., Ball, C.R., Hoffmann, C.M., Nowrouzi, A., Herbst, F., Zavidij, O., Abel, U., Arens, A., Weichert, W., Brand, K., *et al.* (2011). Distinct types of tumor-initiating cells form human colon cancer tumors and metastases. *Cell Stem Cell* 9, 357-365.
- Du, L., Wang, H., He, L., Zhang, J., Ni, B., Wang, X., Jin, H., Cahuzac, N., Mehrpour, M., Lu, Y., *et al.* (2008). CD44 is of functional importance for colorectal cancer stem cells. *Clinical cancer research : an official journal of the American Association for Cancer Research* 14, 6751-6760.
- Dueck, A., and Meister, G. (2010). MicroRNA processing without Dicer. *Genome Biology* 11, 123.
- Dylla, S.J., Beviglia, L., Park, I.K., Chartier, C., Raval, J., Ngan, L., Pickell, K., Aguilar, J., Lazetic, S., Smith-Berdan, S., *et al.* (2008). Colorectal cancer stem cells are enriched in xenogeneic tumors following chemotherapy. *PloS One* 3, e2428.
- Esquela-Kerscher, A., and Slack, F.J. (2006). Oncomirs - microRNAs with a role in cancer. *Nature Reviews Cancer* 6, 259-269.
- Esteller, M. (2011). Non-coding RNAs in human disease. *Nature Reviews Genetics* 12, 861-874.
- Faggad, A., Budczies, J., Tchernitsa, O., Darb-Esfahani, S., Sehouli, J., Muller, B.M., Wirtz, R., Chekerov, R., Weichert, W., Sinn, B., *et al.* (2010). Prognostic significance of Dicer expression in ovarian cancer-link to global microRNA changes and oestrogen receptor expression. *The Journal of Pathology* 220, 382-391.
- Faggad, A., Kasajima, A., Weichert, W., Stenzinger, A., Elwali, N.E., Dietel, M., and Denkert, C. (2012). Down-regulation of the microRNA processing enzyme Dicer is a prognostic factor in human colorectal cancer. *Histopathology* 61, 552-561.
- Fagotto, F., Gluck, U., and Gumbiner, B.M. (1998). Nuclear localization signal-independent and importin/karyopherin-independent nuclear import of beta-catenin. *Current Biology : CB* 8, 181-190.
- Fanali, C., Lucchetti, D., Farina, M., Corbi, M., Cufino, V., Cittadini, A., and Sgambato, A. (2014). Cancer stem cells in colorectal cancer from pathogenesis to therapy: controversies and perspectives. *World Journal of Gastroenterology : WJG* 20, 923-942.
- Fearon, E.R., and Vogelstein, B. (1990). A genetic model for colorectal tumorigenesis. *Cell* 61, 759-767.
- Fevr, T., Robine, S., Louvard, D., and Huelsken, J. (2007). Wnt/beta-catenin is essential for intestinal homeostasis and maintenance of intestinal stem cells. *Molecular and Cellular Biology* 27, 7551-7559.
- Filipowicz, W., Bhattacharyya, S.N., and Sonenberg, N. (2008). Mechanisms of post-transcriptional regulation by microRNAs: are the answers in sight? *Nature Reviews Genetics* 9, 102-114.

- Fodde, R., and Brabletz, T. (2007). Wnt/beta-catenin signaling in cancer stemness and malignant behavior. *Current Opinion in Cell Biology* *19*, 150-158.
- Foulkes, W.D., Priest, J.R., and Duchaine, T.F. (2014). DICER1: mutations, microRNAs and mechanisms. *Nature Reviews Cancer* *14*, 662-672.
- Frank, N.Y., Margaryan, A., Huang, Y., Schatton, T., Waaga-Gasser, A.M., Gasser, M., Sayegh, M.H., Sadee, W., and Frank, M.H. (2005). ABCB5-mediated doxorubicin transport and chemoresistance in human malignant melanoma. *Cancer Research* *65*, 4320-4333.
- Frank, N.Y., Schatton, T., and Frank, M.H. (2010). The therapeutic promise of the cancer stem cell concept. *The Journal of Clinical Investigation* *120*, 41-50.
- Fruman, D.A., and Rommel, C. (2014). PI3K and cancer: lessons, challenges and opportunities. *Nature Reviews Drug Discovery* *13*, 140-156.
- Gilles, C., Polette, M., Mestdagt, M., Nawrocki-Raby, B., Ruggeri, P., Birembaut, P., and Foidart, J.M. (2003). Transactivation of vimentin by beta-catenin in human breast cancer cells. *Cancer Research* *63*, 2658-2664.
- Global_Cancer_Facts_and_Figures (2nd edition).
<http://www.cancer.org/acs/groups/content/@epidemiologysurveillance/documents/document/acspc-027766.pdf>.
- Gonzalez-Sancho, J.M., Aguilera, O., Garcia, J.M., Pendas-Franco, N., Pena, C., Cal, S., Garcia de Herreros, A., Bonilla, F., and Munoz, A. (2005). The Wnt antagonist DICKKOPF-1 gene is a downstream target of beta-catenin/TCF and is downregulated in human colon cancer. *Oncogene* *24*, 1098-1103.
- Grabl, D., Kuhl, M., and Wedlich, D. (1999). The Wnt/Wg signal transducer beta-catenin controls fibronectin expression. *Molecular and Cellular Biology* *19*, 5576-5587.
- Gregorieff, A., and Clevers, H. (2005). Wnt signaling in the intestinal epithelium: from endoderm to cancer. *Genes & Development* *19*, 877-890.
- Gregory, P.A., Bert, A.G., Paterson, E.L., Barry, S.C., Tsykin, A., Farshid, G., Vadas, M.A., Khew-Goodall, Y., and Goodall, G.J. (2008). The miR-200 family and miR-205 regulate epithelial to mesenchymal transition by targeting ZEB1 and SIP1. *Nature Cell Biology* *10*, 593-601.
- Grover, P.K., Hardingham, J.E., and Cummins, A.G. (2010). Stem cell marker olfactomedin 4: critical appraisal of its characteristics and role in tumorigenesis. *Cancer Metastasis Reviews* *29*, 761-775.
- Gupta, P.B., Onder, T.T., Jiang, G., Tao, K., Kuperwasser, C., Weinberg, R.A., and Lander, E.S. (2009). Identification of selective inhibitors of cancer stem cells by high-throughput screening. *Cell* *138*, 645-659.

- Hanahan, D., and Weinberg, R.A. (2011). Hallmarks of cancer: the next generation. *Cell* 144, 646-674.
- Harfe, B.D., McManus, M.T., Mansfield, J.H., Hornstein, E., and Tabin, C.J. (2005). The RNaseIII enzyme Dicer is required for morphogenesis but not patterning of the vertebrate limb. *Proceedings of the National Academy of Sciences of the United States of America* 102, 10898-10903.
- He, T.C., Sparks, A.B., Rago, C., Hermeking, H., Zawel, L., da Costa, L.T., Morin, P.J., Vogelstein, B., and Kinzler, K.W. (1998). Identification of c-MYC as a target of the APC pathway. *Science* 281, 1509-1512.
- Hecht, A., Vleminckx, K., Stemmler, M.P., van Roy, F., and Kemler, R. (2000). The p300/CBP acetyltransferases function as transcriptional coactivators of beta-catenin in vertebrates. *The EMBO Journal* 19, 1839-1850.
- Henderson, B.R., and Fagotto, F. (2002). The ins and outs of APC and beta-catenin nuclear transport. *EMBO Reports* 3, 834-839.
- Herbst, A., Bommer, G.T., Kriegl, L., Jung, A., Behrens, A., Csanadi, E., Gerhard, M., Bolz, C., Riesenberger, R., Zimmermann, W., *et al.* (2009). ITF-2 is disrupted via allelic loss of chromosome 18q21, and ITF-2B expression is lost at the adenoma-carcinoma transition. *Gastroenterology* 137, 639-648, 648 e631-639.
- Hiendlmeyer, E., Regus, S., Wassermann, S., Hlubek, F., Haynl, A., Dimmler, A., Koch, C., Knoll, C., van Beest, M., Reuning, U., *et al.* (2004). Beta-catenin up-regulates the expression of the urokinase plasminogen activator in human colorectal tumors. *Cancer Research* 64, 1209-1214.
- Hill, D.A., Ivanovich, J., Priest, J.R., Gurnett, C.A., Dehner, L.P., Desruisseau, D., Jarzembowski, J.A., Wikenheiser-Brokamp, K.A., Suarez, B.K., Whelan, A.J., *et al.* (2009). DICER1 mutations in familial pleuropulmonary blastoma. *Science* 325, 965.
- Hinkal, G.W., Grelier, G., Puisieux, A., and Moyret-Lalle, C. (2011). Complexity in the regulation of Dicer expression: Dicer variant proteins are differentially expressed in epithelial and mesenchymal breast cancer cells and decreased during EMT. *British Journal of Cancer* 104, 387-388.
- Hirschi, B., Gallmeier, E., Ziesch, A., Marschall, M., and Kolligs, F.T. (2014). Genetic targeting of B-RafV600E affects survival and proliferation and identifies selective agents against BRAF-mutant colorectal cancer cells. *Molecular Cancer* 13, 122.
- Hoffmeyer, K., Raggioli, A., Rudloff, S., Anton, R., Hierholzer, A., Del Valle, I., Hein, K., Vogt, R., and Kemler, R. (2012). Wnt/beta-catenin signaling regulates telomerase in stem cells and cancer cells. *Science* 336, 1549-1554.
- Horst, D., Chen, J., Morikawa, T., Ogino, S., Kirchner, T., and Shivdasani, R.A. (2012). Differential WNT activity in colorectal cancer confers limited tumorigenic potential and is regulated by MAPK signaling. *Cancer Research* 72, 1547-1556.

- http://web.stanford.edu/group/nusselab/cgi-bin/wnt/target_genes. The Wnt homepage (2015/01/15).
- <http://www.nature.com/tcga/>. Nature TCGA pan-cancer analysis (2015/01/15).
- <http://www.niddk.nih.gov/Pages/default.aspx>. National Digestive Diseases Information Clearinghouse (2014/12/21).
- Huang, E.H., Hynes, M.J., Zhang, T., Ginestier, C., Dontu, G., Appelman, H., Fields, J.Z., Wicha, M.S., and Boman, B.M. (2009). Aldehyde dehydrogenase 1 is a marker for normal and malignant human colonic stem cells (SC) and tracks SC overpopulation during colon tumorigenesis. *Cancer Research* *69*, 3382-3389.
- Huber, M.A., Kraut, N., and Beug, H. (2005). Molecular requirements for epithelial-mesenchymal transition during tumor progression. *Current Opinion in Cell Biology* *17*, 548-558.
- Iliou, M.S., da Silva-Diz, V., Carmona, F.J., Ramalho-Carvalho, J., Heyn, H., Villanueva, A., Munoz, P., and Esteller, M. (2014). Impaired DICER1 function promotes stemness and metastasis in colon cancer. *Oncogene* *33*, 4003-4015.
- Issa, J.P. (2004). CpG island methylator phenotype in cancer. *Nature Reviews Cancer* *4*, 988-993.
- Jaitner, S., Reiche, J.A., Schaffauer, A.J., Hiendlmeyer, E., Herbst, H., Brabletz, T., Kirchner, T., and Jung, A. (2012). Human telomerase reverse transcriptase (hTERT) is a target gene of beta-catenin in human colorectal tumors. *Cell Cycle* *11*, 3331-3338.
- Jeon, H.M., Sohn, Y.W., Oh, S.Y., Kim, S.H., Beck, S., Kim, S., and Kim, H. (2011). ID4 imparts chemoresistance and cancer stemness to glioma cells by derepressing miR-9*-mediated suppression of SOX2. *Cancer Research* *71*, 3410-3421.
- Jung, A., Schrauder, M., Oswald, U., Knoll, C., Sellberg, P., Palmqvist, R., Niedobitek, G., Brabletz, T., and Kirchner, T. (2001). The invasion front of human colorectal adenocarcinomas shows co-localization of nuclear beta-catenin, cyclin D1, and p16INK4A and is a region of low proliferation. *The American Journal of Pathology* *159*, 1613-1617.
- Kaplan, K.B., Burds, A.A., Swedlow, J.R., Bekir, S.S., Sorger, P.K., and Nathke, I.S. (2001). A role for the Adenomatous Polyposis Coli protein in chromosome segregation. *Nature Cell Biology* *3*, 429-432.
- Karube, Y., Tanaka, H., Osada, H., Tomida, S., Tatematsu, Y., Yanagisawa, K., Yatabe, Y., Takamizawa, J., Miyoshi, S., Mitsudomi, T., *et al.* (2005). Reduced expression of Dicer associated with poor prognosis in lung cancer patients. *Cancer Science* *96*, 111-115.
- Kasinski, A.L., and Slack, F.J. (2011). Epigenetics and genetics. MicroRNAs en route to the clinic: progress in validating and targeting microRNAs for cancer therapy. *Nature Reviews Cancer* *11*, 849-864.

- Kawahara, K., Nakayama, H., Nagata, M., Yoshida, R., Hirose, A., Tanaka, T., Nakagawa, Y., Matsuoka, Y., Kojima, T., Takamune, Y., *et al.* (2014). A low Dicer expression is associated with resistance to 5-FU-based chemoradiotherapy and a shorter overall survival in patients with oral squamous cell carcinoma. *Journal of oral pathology & medicine : official publication of the International Association of Oral Pathologists and the American Academy of Oral Pathology* *43*, 350-356.
- Kemper, K., Prasetyanti, P.R., De Lau, W., Rodermond, H., Clevers, H., and Medema, J.P. (2012). Monoclonal antibodies against Lgr5 identify human colorectal cancer stem cells. *Stem Cells* *30*, 2378-2386.
- Kemper, K., Sprick, M.R., de Bree, M., Scopelliti, A., Vermeulen, L., Hoek, M., Zeilstra, J., Pals, S.T., Mehmet, H., Stassi, G., *et al.* (2010). The AC133 epitope, but not the CD133 protein, is lost upon cancer stem cell differentiation. *Cancer Research* *70*, 719-729.
- Kim, K.K., Park, K.S., Song, S.B., and Kim, K.E. (2010). Up regulation of GW112 Gene by NF kappaB promotes an antiapoptotic property in gastric cancer cells. *Molecular Carcinogenesis* *49*, 259-270.
- Kinzler, K.W., Nilbert, M.C., Su, L.K., Vogelstein, B., Bryan, T.M., Levy, D.B., Smith, K.J., Preisinger, A.C., Hedge, P., McKechnie, D., *et al.* (1991). Identification of FAP locus genes from chromosome 5q21. *Science* *253*, 661-665.
- Kinzler, K.W., and Vogelstein, B. (1996). Lessons from hereditary colorectal cancer. *Cell* *87*, 159-170.
- Kobayashi, D., Koshida, S., Moriai, R., Tsuji, N., and Watanabe, N. (2007). Olfactomedin 4 promotes S-phase transition in proliferation of pancreatic cancer cells. *Cancer Science* *98*, 334-340.
- Korinek, V., Barker, N., Moerer, P., van Donselaar, E., Huls, G., Peters, P.J., and Clevers, H. (1998). Depletion of epithelial stem-cell compartments in the small intestine of mice lacking Tcf-4. *Nature Genetics* *19*, 379-383.
- Korpai, M., Lee, E.S., Hu, G., and Kang, Y. (2008). The miR-200 family inhibits epithelial-mesenchymal transition and cancer cell migration by direct targeting of E-cadherin transcriptional repressors ZEB1 and ZEB2. *The Journal of Biological Chemistry* *283*, 14910-14914.
- Koshida, S., Kobayashi, D., Moriai, R., Tsuji, N., and Watanabe, N. (2007). Specific overexpression of OLFM4(GW112/HGC-1) mRNA in colon, breast and lung cancer tissues detected using quantitative analysis. *Cancer Science* *98*, 315-320.
- Kreso, A., and O'Brien, C.A. (2008). Colon cancer stem cells. *Current Protocols in Stem Cell Biology* *Chapter 3*, Unit 3 1.
- Kuhnert, F., Davis, C.R., Wang, H.T., Chu, P., Lee, M., Yuan, J., Nusse, R., and Kuo, C.J. (2004). Essential requirement for Wnt signaling in proliferation of adult small intestine and colon revealed by adenoviral expression of Dickkopf-1. *Proceedings of the National Academy of Sciences of the United States of America* *101*, 266-271.

- Kumar, M.S., Lu, J., Mercer, K.L., Golub, T.R., and Jacks, T. (2007). Impaired microRNA processing enhances cellular transformation and tumorigenesis. *Nature Genetics* 39, 673-677.
- Kumar, M.S., Pester, R.E., Chen, C.Y., Lane, K., Chin, C., Lu, J., Kirsch, D.G., Golub, T.R., and Jacks, T. (2009). Dicer1 functions as a haploinsufficient tumor suppressor. *Genes & Development* 23, 2700-2704.
- Kwon, H.S., Lee, H.S., Ji, Y., Rubin, J.S., and Tomarev, S.I. (2009). Myocilin is a modulator of Wnt signaling. *Molecular and Cellular Biology* 29, 2139-2154.
- Lambertz, I., Nittner, D., Mestdagh, P., Denecker, G., Vandesompele, J., Dyer, M.A., and Marine, J.C. (2010). Monoallelic but not biallelic loss of Dicer1 promotes tumorigenesis in vivo. *Cell Death and Differentiation* 17, 633-641.
- Lanza, G., Messerini, L., Gafa, R., Risio, M., Gruppo Italiano Patologi Apparato, D., and Societa Italiana di Anatomia Patologica e Citopatologia Diagnostica/International Academy of Pathology, I.d. (2011). Colorectal tumors: the histology report. *Digestive and liver disease : official journal of the Italian Society of Gastroenterology and the Italian Association for the Study of the Liver* 43 Suppl 4, S344-355.
- Lee, K.H., Goan, Y.G., Hsiao, M., Lee, C.H., Jian, S.H., Lin, J.T., Chen, Y.L., and Lu, P.J. (2009). MicroRNA-373 (miR-373) post-transcriptionally regulates large tumor suppressor, homolog 2 (LATS2) and stimulates proliferation in human esophageal cancer. *Experimental Cell Research* 315, 2529-2538.
- Li, H., Rodriguez-Canales, J., Liu, W., Zhu, J., Hanson, J.C., Pack, S., Zhuang, Z., Emmert-Buck, M.R., and Rodgers, G.P. (2013). Deletion of the olfactomedin 4 gene is associated with progression of human prostate cancer. *The American Journal of Pathology* 183, 1329-1338.
- Li, L., and Clevers, H. (2010). Coexistence of quiescent and active adult stem cells in mammals. *Science* 327, 542-545.
- Liu, C., Kelnar, K., Liu, B., Chen, X., Calhoun-Davis, T., Li, H., Patrawala, L., Yan, H., Jeter, C., Honorio, S., *et al.* (2011). The microRNA miR-34a inhibits prostate cancer stem cells and metastasis by directly repressing CD44. *Nature Medicine* 17, 211-215.
- Liu, R.H., Yang, M.H., Xiang, H., Bao, L.M., Yang, H.A., Yue, L.W., Jiang, X., Ang, N., Wu, L.Y., and Huang, Y. (2012). Depletion of OLFM4 gene inhibits cell growth and increases sensitization to hydrogen peroxide and tumor necrosis factor-alpha induced-apoptosis in gastric cancer cells. *Journal of Biomedical Science* 19, 38.
- Liu, W., Chen, L., Zhu, J., and Rodgers, G.P. (2006). The glycoprotein hGC-1 binds to cadherin and lectins. *Experimental Cell Research* 312, 1785-1797.
- Liu, W., Liu, Y., Zhu, J., Wright, E., Ding, I., and Rodgers, G.P. (2008). Reduced hGC-1 protein expression is associated with malignant progression of colon carcinoma. *Clinical*

Cancer Research : an official journal of the American Association for Cancer Research *14*, 1041-1049.

Liu, W., Zhu, J., Cao, L., and Rodgers, G.P. (2007). Expression of hGC-1 is correlated with differentiation of gastric carcinoma. *Histopathology* *51*, 157-165.

Longley, D.B., Harkin, D.P., and Johnston, P.G. (2003). 5-fluorouracil: mechanisms of action and clinical strategies. *Nature Reviews Cancer* *3*, 330-338.

Lu, J., Getz, G., Miska, E.A., Alvarez-Saavedra, E., Lamb, J., Peck, D., Sweet-Cordero, A., Ebert, B.L., Mak, R.H., Ferrando, A.A., *et al.* (2005). MicroRNA expression profiles classify human cancers. *Nature* *435*, 834-838.

Lujambio, A., and Lowe, S.W. (2012). The microcosmos of cancer. *Nature* *482*, 347-355.

Luo, Z., Zhang, Q., Zhao, Z., Li, B., Chen, J., and Wang, Y. (2011). OLFM4 is associated with lymph node metastasis and poor prognosis in patients with gastric cancer. *Journal of Cancer Research and Clinical Oncology* *137*, 1713-1720.

Mani, S.A., Guo, W., Liao, M.J., Eaton, E.N., Ayyanan, A., Zhou, A.Y., Brooks, M., Reinhard, F., Zhang, C.C., Shipitsin, M., *et al.* (2008). The epithelial-mesenchymal transition generates cells with properties of stem cells. *Cell* *133*, 704-715.

Marjanovic, N.D., Weinberg, R.A., and Chaffer, C.L. (2013). Cell plasticity and heterogeneity in cancer. *Clinical Chemistry* *59*, 168-179.

Marshman, E., Booth, C., and Potten, C.S. (2002). The intestinal epithelial stem cell. *BioEssays : news and reviews in molecular, cellular and developmental biology* *24*, 91-98.

Martello, G., Rosato, A., Ferrari, F., Manfrin, A., Cordenonsi, M., Dupont, S., Enzo, E., Guzzardo, V., Rondina, M., Spruce, T., *et al.* (2010). A MicroRNA targeting dicer for metastasis control. *Cell* *141*, 1195-1207.

Mattick, J.S., and Makunin, I.V. (2006). Non-coding RNA. *Human Molecular Genetics* *15 Spec No 1*, R17-29.

Maurer, G., Tarkowski, B., and Baccarini, M. (2011). Raf kinases in cancer-roles and therapeutic opportunities. *Oncogene* *30*, 3477-3488.

Melo, S., Villanueva, A., Moutinho, C., Davalos, V., Spizzo, R., Ivan, C., Rossi, S., Setien, F., Casanovas, O., Simo-Riudalbas, L., *et al.* (2011). Small molecule enoxacin is a cancer-specific growth inhibitor that acts by enhancing TAR RNA-binding protein 2-mediated microRNA processing. *Proceedings of the National Academy of Sciences of the United States of America* *108*, 4394-4399.

Melo, S.A., and Kalluri, R. (2012). Molecular pathways: microRNAs as cancer therapeutics. *Clinical cancer research : an official journal of the American Association for Cancer Research* *18*, 4234-4239.

Melo, S.A., Ropero, S., Moutinho, C., Aaltonen, L.A., Yamamoto, H., Calin, G.A., Rossi, S., Fernandez, A.F., Carneiro, F., Oliveira, C., *et al.* (2009). A TARBP2 mutation in

- human cancer impairs microRNA processing and DICER1 function. *Nature Genetics* 41, 365-370.
- Merritt, W.M., Lin, Y.G., Han, L.Y., Kamat, A.A., Spannuth, W.A., Schmandt, R., Urbauer, D., Pennacchio, L.A., Cheng, J.F., Nick, A.M., *et al.* (2008). Dicer, Drosha, and outcomes in patients with ovarian cancer. *The New England Journal of Medicine* 359, 2641-2650.
- Moon, R.T., Kohn, A.D., De Ferrari, G.V., and Kaykas, A. (2004). WNT and beta-catenin signalling: diseases and therapies. *Nature Reviews Genetics* 5, 691-701.
- Morin, P.J., Sparks, A.B., Korinek, V., Barker, N., Clevers, H., Vogelstein, B., and Kinzler, K.W. (1997). Activation of beta-catenin-Tcf signaling in colon cancer by mutations in beta-catenin or APC. *Science* 275, 1787-1790.
- Morita, H., Mazerbourg, S., Bouley, D.M., Luo, C.W., Kawamura, K., Kuwabara, Y., Baribault, H., Tian, H., and Hsueh, A.J. (2004). Neonatal lethality of LGR5 null mice is associated with ankyloglossia and gastrointestinal distension. *Molecular and Cellular Biology* 24, 9736-9743.
- Nakaya, N., Lee, H.S., Takada, Y., Tzchori, I., and Tomarev, S.I. (2008). Zebrafish olfactomedin 1 regulates retinal axon elongation in vivo and is a modulator of Wnt signaling pathway. *The Journal of Neuroscience : the Official Journal of the Society for Neuroscience* 28, 7900-7910.
- O'Brien, C.A., Pollett, A., Gallinger, S., and Dick, J.E. (2007). A human colon cancer cell capable of initiating tumour growth in immunodeficient mice. *Nature* 445, 106-110.
- Oue, N., Sentani, K., Noguchi, T., Ohara, S., Sakamoto, N., Hayashi, T., Anami, K., Motoshita, J., Ito, M., Tanaka, S., *et al.* (2009). Serum olfactomedin 4 (GW112, hGC-1) in combination with Reg IV is a highly sensitive biomarker for gastric cancer patients. *International Journal of Cancer Journal International du Cancer* 125, 2383-2392.
- Pang, R., Law, W.L., Chu, A.C., Poon, J.T., Lam, C.S., Chow, A.K., Ng, L., Cheung, L.W., Lan, X.R., Lan, H.Y., *et al.* (2010). A subpopulation of CD26+ cancer stem cells with metastatic capacity in human colorectal cancer. *Cell Stem Cell* 6, 603-615.
- Park, K.S., Kim, K.K., Piao, Z.H., Kim, M.K., Lee, H.J., Kim, Y.C., Lee, K.S., Lee, J.H., and Kim, K.E. (2012). Olfactomedin 4 suppresses tumor growth and metastasis of mouse melanoma cells through downregulation of integrin and MMP genes. *Molecules and Cells* 34, 555-561.
- Pfaffl, M.W. (2001). A new mathematical model for relative quantification in real-time RT-PCR. *Nucleic Acids Research* 29, e45.
- Pino, M.S., and Chung, D.C. (2010). The chromosomal instability pathway in colon cancer. *Gastroenterology* 138, 2059-2072.
- Pinto, D., and Clevers, H. (2005). Wnt, stem cells and cancer in the intestine. *Biology of the cell / under the auspices of the European Cell Biology Organization* 97, 185-196.

- Potten, C.S., Gandara, R., Mahida, Y.R., Loeffler, M., and Wright, N.A. (2009). The stem cells of small intestinal crypts: where are they? *Cell Proliferation* *42*, 731-750.
- Pramanik, D., Campbell, N.R., Karikari, C., Chivukula, R., Kent, O.A., Mendell, J.T., and Maitra, A. (2011). Restitution of tumor suppressor microRNAs using a systemic nanovector inhibits pancreatic cancer growth in mice. *Molecular Cancer Therapeutics* *10*, 1470-1480.
- Qian, C.N., Knol, J., Igarashi, P., Lin, F., Zylstra, U., Teh, B.T., and Williams, B.O. (2005). Cystic renal neoplasia following conditional inactivation of *apc* in mouse renal tubular epithelium. *The Journal of Biological Chemistry* *280*, 3938-3945.
- Ravi, A., Gurtan, A.M., Kumar, M.S., Bhutkar, A., Chin, C., Lu, V., Lees, J.A., Jacks, T., and Sharp, P.A. (2012). Proliferation and tumorigenesis of a murine sarcoma cell line in the absence of DICER1. *Cancer Cell* *21*, 848-855.
- Ricci-Vitiani, L., Lombardi, D.G., Pilozzi, E., Biffoni, M., Todaro, M., Peschle, C., and De Maria, R. (2007). Identification and expansion of human colon-cancer-initiating cells. *Nature* *445*, 111-115.
- Romanov, S.R., Kozakiewicz, B.K., Holst, C.R., Stampfer, M.R., Haupt, L.M., and Tlsty, T.D. (2001). Normal human mammary epithelial cells spontaneously escape senescence and acquire genomic changes. *Nature* *409*, 633-637.
- Royer, C., and Lu, X. (2011). Epithelial cell polarity: a major gatekeeper against cancer? *Cell Death and Differentiation* *18*, 1470-1477.
- Rustgi, A.K. (2007). The genetics of hereditary colon cancer. *Genes & Development* *21*, 2525-2538.
- Sanchez-Tillo, E., de Barrios, O., Siles, L., Cuatrecasas, M., Castells, A., and Postigo, A. (2011). beta-catenin/TCF4 complex induces the epithelial-to-mesenchymal transition (EMT)-activator ZEB1 to regulate tumor invasiveness. *Proceedings of the National Academy of Sciences of the United States of America* *108*, 19204-19209.
- Sato, T., van Es, J.H., Snippert, H.J., Stange, D.E., Vries, R.G., van den Born, M., Barker, N., Shroyer, N.F., van de Wetering, M., and Clevers, H. (2011). Paneth cells constitute the niche for Lgr5 stem cells in intestinal crypts. *Nature* *469*, 415-418.
- Schonhuber, N., Seidler, B., Schuck, K., Veltkamp, C., Schachtler, C., Zukowska, M., Eser, S., Feyerabend, T.B., Paul, M.C., Eser, P., *et al.* (2014). A next-generation dual-recombinase system for time- and host-specific targeting of pancreatic cancer. *Nature Medicine* *20*, 1340-1347.
- Schuijers, J., and Clevers, H. (2012). Adult mammalian stem cells: the role of Wnt, Lgr5 and R-spondins. *The EMBO Journal* *31*, 2685-2696.

- Schuijers, J., van der Flier, L.G., van Es, J., and Clevers, H. (2014). Robust cre-mediated recombination in small intestinal stem cells utilizing the *olm4* locus. *Stem Cell Reports* 3, 234-241.
- Schwitalla, S., Fingerle, A.A., Cammareri, P., Nebelsiek, T., Goktuna, S.I., Ziegler, P.K., Canli, O., Heijmans, J., Huels, D.J., Moreaux, G., *et al.* (2013). Intestinal tumorigenesis initiated by dedifferentiation and acquisition of stem-cell-like properties. *Cell* 152, 25-38.
- Seko, N., Oue, N., Noguchi, T., Sentani, K., Sakamoto, N., Hinoi, T., Okajima, M., and Yasui, W. (2010). Olfactomedin 4 (GW112, hGC-1) is an independent prognostic marker for survival in patients with colorectal cancer. *Experimental and Therapeutic Medicine* 1, 73-78.
- Shan, G., Li, Y., Zhang, J., Li, W., Szulwach, K.E., Duan, R., Faghihi, M.A., Khalil, A.M., Lu, L., Paroo, Z., *et al.* (2008). A small molecule enhances RNA interference and promotes microRNA processing. *Nature Biotechnology* 26, 933-940.
- Shibata, H., Toyama, K., Shioya, H., Ito, M., Hirota, M., Hasegawa, S., Matsumoto, H., Takano, H., Akiyama, T., Toyoshima, K., *et al.* (1997). Rapid colorectal adenoma formation initiated by conditional targeting of the *Apc* gene. *Science* 278, 120-123.
- Shtutman, M., Zhurinsky, J., Simcha, I., Albanese, C., D'Amico, M., Pestell, R., and Ben-Ze'ev, A. (1999). The cyclin D1 gene is a target of the beta-catenin/LEF-1 pathway. *Proceedings of the National Academy of Sciences of the United States of America* 96, 5522-5527.
- Siemens, H., Jackstadt, R., Hunten, S., Kaller, M., Menssen, A., Gotz, U., and Hermeking, H. (2011). miR-34 and SNAIL form a double-negative feedback loop to regulate epithelial-mesenchymal transitions. *Cell Cycle* 10, 4256-4271.
- Singh, A., and Settleman, J. (2010). EMT, cancer stem cells and drug resistance: an emerging axis of evil in the war on cancer. *Oncogene* 29, 4741-4751.
- Singh, S.K., Hawkins, C., Clarke, I.D., Squire, J.A., Bayani, J., Hide, T., Henkelman, R.M., Cusimano, M.D., and Dirks, P.B. (2004). Identification of human brain tumour initiating cells. *Nature* 432, 396-401.
- Sobin, L., Gospodarowicz, M., and Wittekind, C. (2009). *TNM Classification of Malignant Tumours*, 7 edn (Wiley).
- Spaderna, S., Schmalhofer, O., Wahlbuhl, M., Dimmler, A., Bauer, K., Sultan, A., Hlubek, F., Jung, A., Strand, D., Eger, A., *et al.* (2008). The transcriptional repressor ZEB1 promotes metastasis and loss of cell polarity in cancer. *Cancer Research* 68, 537-544.
- Su, X., Chakravarti, D., Cho, M.S., Liu, L., Gi, Y.J., Lin, Y.L., Leung, M.L., El-Naggar, A., Creighton, C.J., Suraokar, M.B., *et al.* (2010). TAp63 suppresses metastasis through coordinate regulation of Dicer and miRNAs. *Nature* 467, 986-990.
- Sunaga, N., Shames, D.S., Girard, L., Peyton, M., Larsen, J.E., Imai, H., Soh, J., Sato, M., Yanagitani, N., Kaira, K., *et al.* (2011). Knockdown of oncogenic KRAS in non-small cell

lung cancers suppresses tumor growth and sensitizes tumor cells to targeted therapy. *Molecular Cancer Therapeutics* *10*, 336-346.

Talmadge, J.E., and Fidler, I.J. (2010). AACR centennial series: the biology of cancer metastasis: historical perspective. *Cancer Research* *70*, 5649-5669.

Thiery, J.P. (2002). Epithelial-mesenchymal transitions in tumour progression. *Nature Reviews Cancer* *2*, 442-454.

Thiery, J.P. (2003). Epithelial-mesenchymal transitions in development and pathologies. *Current Opinion in Cell Biology* *15*, 740-746.

Thiery, J.P., Acloque, H., Huang, R.Y., and Nieto, M.A. (2009). Epithelial-mesenchymal transitions in development and disease. *Cell* *139*, 871-890.

Todaro, M., Francipane, M.G., Medema, J.P., and Stassi, G. (2010). Colon cancer stem cells: promise of targeted therapy. *Gastroenterology* *138*, 2151-2162.

Tomarev, S.I., and Nakaya, N. (2009). Olfactomedin domain-containing proteins: possible mechanisms of action and functions in normal development and pathology. *Molecular Neurobiology* *40*, 122-138.

Townsley, F.M., Cliffe, A., and Bienz, M. (2004). Pygopus and Legless target Armadillo/beta-catenin to the nucleus to enable its transcriptional co-activator function. *Nature Cell Biology* *6*, 626-633.

Trang, P., Medina, P.P., Wiggins, J.F., Ruffino, L., Kelnar, K., Omotola, M., Homer, R., Brown, D., Bader, A.G., Weidhaas, J.B., *et al.* (2010). Regression of murine lung tumors by the let-7 microRNA. *Oncogene* *29*, 1580-1587.

Trang, P., Wiggins, J.F., Daige, C.L., Cho, C., Omotola, M., Brown, D., Weidhaas, J.B., Bader, A.G., and Slack, F.J. (2011). Systemic delivery of tumor suppressor microRNA mimics using a neutral lipid emulsion inhibits lung tumors in mice. *Molecular therapy : the journal of the American Society of Gene Therapy* *19*, 1116-1122.

Tsukahara, T., and Murakami-Murofushi, K. (2012). Release of cyclic phosphatidic acid from gelatin-based hydrogels inhibit colon cancer cell growth and migration. *Scientific Reports* *2*, 687.

Ueno, H., Murphy, J., Jass, J.R., Mochizuki, H., and Talbot, I.C. (2002). Tumour 'budding' as an index to estimate the potential of aggressiveness in rectal cancer. *Histopathology* *40*, 127-132.

van de Wetering, M., Sancho, E., Verweij, C., de Lau, W., Oving, I., Hurlstone, A., van der Horn, K., Batlle, E., Coudreuse, D., Haramis, A.P., *et al.* (2002). The beta-catenin/TCF-4 complex imposes a crypt progenitor phenotype on colorectal cancer cells. *Cell* *111*, 241-250.

van den Brink, G.R., and Hardwick, J.C. (2006). Hedgehog Wnteraction in colorectal cancer. *Gut* *55*, 912-914.

- van der Flier, L.G., Haegbarth, A., Stange, D.E., van de Wetering, M., and Clevers, H. (2009). OLFM4 is a robust marker for stem cells in human intestine and marks a subset of colorectal cancer cells. *Gastroenterology* 137, 15-17.
- van Es, J.H., Haegbarth, A., Kujala, P., Itzkovitz, S., Koo, B.K., Boj, S.F., Korving, J., van den Born, M., van Oudenaarden, A., Robine, S., *et al.* (2012). A critical role for the Wnt effector Tcf4 in adult intestinal homeostatic self-renewal. *Molecular and Cellular Biology* 32, 1918-1927.
- van Es, J.H., Jay, P., Gregorieff, A., van Gijn, M.E., Jonkheer, S., Hatzis, P., Thiele, A., van den Born, M., Begthel, H., Brabletz, T., *et al.* (2005a). Wnt signalling induces maturation of Paneth cells in intestinal crypts. *Nature Cell Biology* 7, 381-386.
- van Es, J.H., van Gijn, M.E., Riccio, O., van den Born, M., Vooijs, M., Begthel, H., Cozijnsen, M., Robine, S., Winton, D.J., Radtke, F., *et al.* (2005b). Notch/gamma-secretase inhibition turns proliferative cells in intestinal crypts and adenomas into goblet cells. *Nature* 435, 959-963.
- Vanuytsel, T., Senger, S., Fasano, A., and Shea-Donohue, T. (2013). Major signaling pathways in intestinal stem cells. *Biochimica et Biophysica Acta* 1830, 2410-2426.
- Vasudevan, S., Tong, Y., and Steitz, J.A. (2007). Switching from repression to activation: microRNAs can up-regulate translation. *Science* 318, 1931-1934.
- Vermeulen, L., De Sousa, E.M.F., van der Heijden, M., Cameron, K., de Jong, J.H., Borovski, T., Tuynman, J.B., Todaro, M., Merz, C., Rodermond, H., *et al.* (2010). Wnt activity defines colon cancer stem cells and is regulated by the microenvironment. *Nature Cell Biology* 12, 468-476.
- Vlad-Fiegen, A., Langerak, A., Eberth, S., and Muller, O. (2012). The Wnt pathway destabilizes adherens junctions and promotes cell migration via beta-catenin and its target gene cyclin D1. *FEBS Open Bio* 2, 26-31.
- Wang, Y., Baskerville, S., Shenoy, A., Babiarz, J.E., Baehner, L., and Belloch, R. (2008). Embryonic stem cell-specific microRNAs regulate the G1-S transition and promote rapid proliferation. *Nature Genetics* 40, 1478-1483.
- Wassermann, S., Scheel, S.K., Hiendlmeyer, E., Palmqvist, R., Horst, D., Hlubek, F., Haynl, A., Kriegel, L., Reu, S., Merkel, S., *et al.* (2009). p16INK4a is a beta-catenin target gene and indicates low survival in human colorectal tumors. *Gastroenterology* 136, 196-205 e192.
- Weinberg, R.A. (2007). *The biology of cancer* (Garland Science, Taylor & Francis Group).
- Weisenberger, D.J., Siegmund, K.D., Campan, M., Young, J., Long, T.I., Faasse, M.A., Kang, G.H., Widschwendter, M., Weener, D., Buchanan, D., *et al.* (2006). CpG island methylator phenotype underlies sporadic microsatellite instability and is tightly associated with BRAF mutation in colorectal cancer. *Nature Genetics* 38, 787-793.

Wentzensen, N., Wilz, B., Findeisen, P., Wagner, R., Dippold, W., von Knebel Doeberitz, M., and Gebert, J. (2004). Identification of differentially expressed genes in colorectal adenoma compared to normal tissue by suppression subtractive hybridization. *International Journal of Oncology* 24, 987-994.

Wielenga, V.J., Smits, R., Korinek, V., Smit, L., Kielman, M., Fodde, R., Clevers, H., and Pals, S.T. (1999). Expression of CD44 in Apc and Tcf mutant mice implies regulation by the WNT pathway. *The American Journal of Pathology* 154, 515-523.

World_Cancer_Factsheet (2008). <http://gicr.iarc.fr/public/docs/20120906-WorldCancerFactSheet.pdf>.

World_Cancer_Factsheet (2012). http://publications.cancerresearchuk.org/downloads/product/CS_REPORT_WORLD.pdf.

Yamada, T., Takaoka, A.S., Naishiro, Y., Hayashi, R., Maruyama, K., Maesawa, C., Ochiai, A., and Hirohashi, S. (2000). Transactivation of the multidrug resistance 1 gene by T-cell factor 4/beta-catenin complex in early colorectal carcinogenesis. *Cancer Research* 60, 4761-4766.

Yan, D., Wiesmann, M., Rohan, M., Chan, V., Jefferson, A.B., Guo, L., Sakamoto, D., Caothien, R.H., Fuller, J.H., Reinhard, C., *et al.* (2001). Elevated expression of axin2 and hnk4 mRNA provides evidence that Wnt/beta-catenin signaling is activated in human colon tumors. *Proceedings of the National Academy of Sciences of the United States of America* 98, 14973-14978.

Yan, K.S., Chia, L.A., Li, X., Ootani, A., Su, J., Lee, J.Y., Su, N., Luo, Y., Heilshorn, S.C., Amieva, M.R., *et al.* (2012). The intestinal stem cell markers Bmi1 and Lgr5 identify two functionally distinct populations. *Proceedings of the National Academy of Sciences of the United States of America* 109, 466-471.

Yang, Z.F., Ho, D.W., Ng, M.N., Lau, C.K., Yu, W.C., Ngai, P., Chu, P.W., Lam, C.T., Poon, R.T., and Fan, S.T. (2008). Significance of CD90+ cancer stem cells in human liver cancer. *Cancer Cell* 13, 153-166.

Yoshikawa, T., Otsuka, M., Kishikawa, T., Takata, A., Ohno, M., Shibata, C., Kang, Y.J., Yoshida, H., and Koike, K. (2013). Unique haploinsufficient role of the microRNA-processing molecule Dicer1 in a murine colitis-associated tumorigenesis model. *PloS One* 8, e71969.

Young, J., Leggett, B., Ward, M., Thomas, L., Buttenshaw, R., Searle, J., and Chenevix-Trench, G. (1993). Frequent loss of heterozygosity on chromosome 14 occurs in advanced colorectal carcinomas. *Oncogene* 8, 671-675.

Yu, F., Yao, H., Zhu, P., Zhang, X., Pan, Q., Gong, C., Huang, Y., Hu, X., Su, F., Lieberman, J., *et al.* (2007). let-7 regulates self renewal and tumorigenicity of breast cancer cells. *Cell* 131, 1109-1123.

Zeng, L.C., Han, Z.G., and Ma, W.J. (2005). Elucidation of subfamily segregation and intramolecular coevolution of the olfactomedin-like proteins by comprehensive

phylogenetic analysis and gene expression pattern assessment. *FEBS Letters* 579, 5443-5453.

Zeng, Q., and Hong, W. (2008). The emerging role of the hippo pathway in cell contact inhibition, organ size control, and cancer development in mammals. *Cancer Cell* 13, 188-192.

Zhang, J., Liu, W.L., Tang, D.C., Chen, L., Wang, M., Pack, S.D., Zhuang, Z., and Rodgers, G.P. (2002). Identification and characterization of a novel member of olfactomedin-related protein family, hGC-1, expressed during myeloid lineage development. *Gene* 283, 83-93.

Zhang, T., Otevrel, T., Gao, Z., Gao, Z., Ehrlich, S.M., Fields, J.Z., and Boman, B.M. (2001a). Evidence that APC regulates survivin expression: a possible mechanism contributing to the stem cell origin of colon cancer. *Cancer Research* 61, 8664-8667.

Zhang, X., Gaspard, J.P., and Chung, D.C. (2001b). Regulation of vascular endothelial growth factor by the Wnt and K-ras pathways in colonic neoplasia. *Cancer Research* 61, 6050-6054.

Zhang, X., Huang, Q., Yang, Z., Li, Y., and Li, C.Y. (2004). GW112, a novel antiapoptotic protein that promotes tumor growth. *Cancer Research* 64, 2474-2481.

Zinzi, L., Contino, M., Cantore, M., Capparelli, E., Leopoldo, M., and Colabufo, N.A. (2014). ABC transporters in CSCs membranes as a novel target for treating tumor relapse. *Frontiers in Pharmacology* 5, 163.

Ziskin, J.L., Dunlap, D., Yaylaoglu, M., Fodor, I.K., Forrest, W.F., Patel, R., Ge, N., Hutchins, G.G., Pine, J.K., Quirke, P., *et al.* (2013). In situ validation of an intestinal stem cell signature in colorectal cancer. *Gut* 62, 1012-1023.

List of Figures

Fig. 1. The structure of the intestinal epithelium and an intestinal crypt.	6
Fig. 2. Schematic representation of the major signaling pathways of the crypt/villus homeostasis and its interaction.	10
Fig. 3. The canonical Wnt signaling pathway.	11
Fig. 4 World cancer burden.	13
Fig. 5. Familial adenomatous polyposis (FAP).	15
Fig. 6. The influence of β -catenin on hallmarks of cancer and its target genes.	17
Fig. 7. The multistep carcinogenesis model of colorectal cancer.	18
Fig. 8. The plastic CSC model.	20
Fig. 9. Concept of stationary and migrating cancer stem cells (SCS and MCS cells).	21
Fig. 10. Model of the CSC features.	24
Fig. 11. CSC-specific therapy as a new therapeutic approach.	25
Fig. 12. Gene and protein structure of OLFM4.	27
Fig. 13. The canonical biogenesis of miRNAs.	31
Fig. 14. Structure and domains of DICER1.	32
Fig. 15. <i>OLFM4</i> is endogenously expressed in the CRC cell lines SW1222 and LS174T.	73
Fig. 16. <i>OLFM4</i> expression did not correlate with expression of characteristic CSC markers.	75
Fig. 17. Viral transduction of CRC cell lines with OLFM4-V5 resulted in high <i>OLFM4</i> mRNA and OLFM4 protein levels but did not alter marker expression/protein levels.	77
Fig. 18. High OLFM4 protein levels had no effect on proliferation.	78
Fig. 19. Ectopic <i>OLFM4</i> expression had no influence on the cellular localization of β -catenin and the Wnt signaling pathway activity.	80
Fig. 20. OLFM4 did not change CSC features.	82
Fig. 21. OLFM4 had no influence on metastatic characteristics.	84
Fig. 22. <i>Apc</i> and <i>Dicer1</i> gene can be conditionally deleted in mice.	87
Fig. 23. <i>Dicer1</i> deletion resulted in a higher adenoma number in the small intestine of mice.	90
Fig. 24. <i>Dicer1</i> deletion led to an increased tumor initiation but slower tumor growth in the small intestine in the <i>Apc/Dicer1</i> mouse model.	91
Fig. 25. <i>Dicer1</i> depletion resulted in less adenoma proliferation.	94
Fig. 26. Colorectal carcinoma cell lines with a homozygous disruption of the helicase domain (<i>ex5</i>) of <i>DICER1</i> showed impaired miRNA processing.	95
Fig. 27. Loss of DICER1 increased the levels of CSC, metastatic and EMT markers in HCT116 cells.	97
Fig. 28. Loss of DICER1 resulted in less proliferation and increased cell number in the G0/G1 phase, associated with reduced Hippo pathway activity in HCT116 cells.	99
Fig. 29. Loss of DICER1 increased drug resistance in HCT116 cells.	101
Fig. 30. Loss of DICER1 resulted in enhanced migration capacity.	102
Fig. 31. Loss of DICER1 enhanced Wnt signaling pathway activity.	103
Fig. 32. DICER1 levels were higher in adenomas compared to normal colonic mucosa but decreased during progression from adenoma to carcinoma in human CRC.	105
Fig. 33. <i>DICER1</i> expression was influenced by Wnt signaling pathway.	106
Fig. 34. The impact of OLFM4 in CRC.	111
Fig. 35. Model of the impact of DICER1 on adenoma formation.	116
Fig. 36. The influence of β -catenin on hallmarks of cancer and its target genes.	122

Fig. 37. Model of DICER1 protein levels during the process of colorectal carcinogenesis.
..... 123

Fig. 38. Multistep carcinogenesis mouse model..... 125

List of Tables

Table 1. Required mouse lines for the experiment..... 45
Table 2. TNM-classification of the colorectal tumors, following the standards of the UICC
(*Union internationale contre le cancer*)..... 69
Table 3. Patient details of the human tissue collection..... 70

Abbreviations

+	wildtype
3'UTR	3' untranslated regions
5-FU	5-fluoruracil
A	adenine
aa	amino acids
ABC	ATP binding cassette
ABCB1	ATP-binding cassette, sub-family B (MDR/TAP)
ACTB	β -actin
AEC	3-amino-9-ethylcarbazol
AGO	argonaute
AJ	adherens junctions
AKT	v-akt murine thymoma viral oncogene homolog
ALDH1/ALDH1A1	aldehyde dehydrogenase 1
anneal.	annealing
APC	adenomatous polyposis coli
APS	Ammoniumpersulfate
ATCC	American Type Culture Collection
BIRC5	baculoviral inhibitor of apoptosis repeat-containing 5
BMI1	B lymphoma Mo-MLV insertion region 1
BMP	bone morphogenetic protein
bp	base pair
C	cytosine
CAT	chloramphenicol acetyltransferase
CBC cell	crypt base columnar cell
CBP	CREB (cAMP response element-binding protein)-binding protein
CCND1	cyclin D1
CD26	cluster of differentiation 26
CD44	cluster of differentiation 44
CD133	prominin 1
CDH1	cadherin 1, E-cadherin
CDH2	N-cadherin
CDKN2A	cyclin-dependent kinase inhibitor 2A
cDNA	complementary DNA
CIN	chromosomal instability
CK1	casein kinase 1
Conc.	concentration
Cp	crossing point
CBP	CREB binding protein
CRB	crumbs
CRC	colorectal cancer
Cre recombinase	(causes recombination) recombinase

CreER ^{T2}	tamoxifen-inducible variant of Cre recombinase
CSC	cancer stem cell
C-terminus	carboxy terminus
CTNNB1	β-catenin
Ctrl.	control
DAB+	3,3'-diaminobenzidine
DAPI	4',6'-diamidino-2-phenylindole
DEAB	diethylaminobenzaldehyde
DEST	destination (sequence)
DGCR8	DiGeorge syndrome critical region gene 8
dH ₂ O	distilled water
DICER1	dicer 1, ribonuclease type III
DKK-1	DICKKOPF-1
DMEM	Dulbecco's Modified Eagle's medium
DMSO	Dimethyl sulfoxide
DNA	deoxyribonucleic acid
dNTP	deoxynucleotide
dox	doxycycline
DROSHA	drosha, ribonuclease type III
DSH	dishevelled
DSMZ	Deutsche Sammlung von Mikroorganismen und Zellkulturen GmbH
dsRNA	double-stranded RNA
e.g.	for example
ECL	enhanced chemiluminescence
EDTA	ethylenediaminetetraacetic acid solution
EGFP	enhanced green fluorescent protein
ELISA	enzyme-linked immunosorbent assay
Elong.	elongation
EMT	epithelial-mesenchymal transition
EPHB2	ephrin type-B receptor 2
EPHB3	ephrin type-B receptor 3
ERS6	Epitope Retrieval Solution
EtOH	ethanol
ex5	exon 5
FACS	fluorescence-activated cell sorting
FAP	familial adenomatous polyposis
FBS	fetal bovine serum
FCS	fetal calf serum
FFPE	formalin-fixed, paraffin-embedded
FGFb	fibroblast growth factor basic
Fig.	Figure
fl, flox	flanked by loxP
FLP	flippase

FOPflash	luciferase reporter construct which contains mutated TCF4 consensus binding sites
FW	forward
FZ	frizzled
G	guanine
GBP	GSK3 binding protein
GRO	groucho
GSK3	glycogen synthase kinase 3
h	hour
H&E	hematoxylin and eosin
HCl	hydrochloric acid solution
het	heterozygous
HGF	hepatocyte growth factor
HH	Hedgehog
HiDi	highly deionized
HMG	high mobility group factor
HNPCC	hereditary nonpolyposis colorectal cancer
hom	homozygous
HPRT1	hypoxanthine phosphoribosyltransferase 1
HRP	horseradish peroxidase
hsa	<i>homo sapiens</i>
IF	immunofluorescence
IgG (H+L)	immunoglobulin G (heavy and light chain)
IHC	immunohistochemistry
IHH	indian hedgehog
IRES	internal ribosomal entry site
ISEMFs	intestinal subepithelial myofibroblasts
ITF-2	immunoglobulin transcription factor 2
K ₃ Fe(CN) ₆	potassium hexacyanoferrate(III)
kb	kilo bases
KCl	potassium chloride
kDa	kilo Dalton
KH ₂ PO ₄	potassium dihydrogen phosphate
KI-67	marker of proliferation Ki-67
KOD	<i>thermococcus kodakaraensis</i>
KRAS	Kirsten rat sarcoma viral oncogene homolog
KRT20	keratin 20
LacZ	β-galactosidase
LB medium	Lysogeny broth medium
LC50	lethal concentration 50; concentration that kills 50% of cells
LEF1	lymphoid enhancer-binding factor 1
LGR5	leucine-rich-repeat-containing G-protein coupled receptor 5
lincRNAs	large intergenic non-coding RNAs

LoxP	locus of X(cross)-over in P1
LRP5	LDL (low density lipoprotein) receptor-related proteins 5
LRP6	LDL (low density lipoprotein) receptor-related proteins 6
LSL	Lox Stop Lox
mAb	monoclonal antibody
MAPK	mitogen-activated protein kinases
MCS cells	migratory CSCs
MET	mesenchymal-epithelial transition
mg	milligram
MgCl ₂	magnesium chlorid
min	minute
miRISC	miRNA-associated multiprotein RNA-induced silencing complex
miRNA	microRNA
miRNAome	microRNAome
ml	millilitre
MLH1	mutL homolog
mM	millimolar
MMR	DNA mismatch repair
MMP7	matrix metalloproteinase-7
mRNA	messenger RNA
MSH2	mutS homolog 2
MSH6	mutS homolog 6
MSI	microsatellite instability
MTT	Thiazolyl Blue Tetrazolium Bromide
MUC2	mucin 2
MUT	mutated
MYC	v-myc avian myelocytomatosis viral oncogene homolog
Na ₂ HPO ₄ -7H ₂ O	sodium phosphate dibasic heptahydrate
NaCl	sodium chloride
NaOH	sodium hydroxide
ncRNAs	non-coding RNAs
NF-κB	nuclear factor 'kappa-light-chain-enhancer' of activated B-cells
ng	nanogram
NOG	noggin
NOS	not otherwise specified
N-terminus	Amino terminus
OLFM4	olfactomedin-4
ORF	open reading frame
p300	E1A binding protein p300
pAb	polyclonal antibody
PARD3	par-3 family cell polarity regulator
PAS	Periodic acid–Schiff
PAZ	piwi, argonaute, zwillie

PBS	phosphate buffered saline
PCR	polymerase chain reaction
PI	propidium iodide
PI3K/PIK3	phosphatidylinositol-4,5-bisphosphate 3-kinase
piRNAs	PIWI-interacting RNAs
PLAU	urokinase-type plasminogen activator
PMS2	postmeiotic segregation increased 2 (<i>S. cerevisiae</i>)
pre-miRNA	precursor miRNA
pri-miRNA	primary miRNAs
PROM1	prominin 1
PTEN	phosphatase and tensin homolog
PVDF	polyvinylidene difluoride
qPCR	quantitative PCR
RAF	rapidly accelerated fibrosarcoma
RAS	rat sarcoma
rec	recombination
REV	reverse
RISC	RNA-induced silencing complex
RNA	ribonucleic acid
RNase	ribonuclease
RPMI	Roswell Park Memorial Institute medium
RT	room temperature
RT	reverse transcription
RT-qPCR	reverse transcribed- quantitative PCR
rtTA	recombinant tetracycline controlled transcription factor
SAP	shrimps alkaline phosphatase
SC	stem cell
SCRIB	scribbled planar cell polarity protein
SDS	sodium dodecyl sulfate
sec	second
Seq	sequencing
siRNA	small interfering RNA
SLUG/SNAI2	snail family zinc finger 2
SMAD4	mothers against decapentaplegic homolog 4
SNAI2	snail family zinc finger 2
SNAIL/ SNAI1	snail family zinc finger 1
snoRNAs	small nucleolar RNAs
T	thymidine
TA cells	transit amplifying cells
TAM	tamoxifen
Taq	<i>thermus aquaticus</i>
TARBP2	TAR (HIV-1) RNA binding protein 2
TAZ	transcriptional coactivator with PDZ-binding motif
TBE	tris/borate/EDTA

TCF	T-cell specific transcription factor
TEAD	TEA-domain-containing family
TEMED	tetramethylethylenediamin
TERT	telomerase reverse transcriptase
TetO	tet operator
TGFβ	transforming growth factor β
TNC	tenascin C
TNM-system	(T: primary tumor, N: lymph node metastasis, M: distant metastasis)-system
TOPflash	luciferase reporter construct which contains 7 TCF4 consensus binding sites
TP53	tumor protein p53
TRBP	TAR RNA-binding protein
TWIST/TWIST1	twist family bHLH transcription factor 1
U	Unit
UICC	Union internationale contre le cancer
UPL	Universal ProbeLibrary
V	Volt
V5	V5-Tag
VEGF	vascular endothelial growth factor
VIM	vimentin
w/o	without
WB	Western Blot
WHO	World Health Organisation
Wnt	wingless-type MMTV integration site family
Wnt3a	wingless-type MMTV integration site family, member 3A
WT	wildtype
X-Gal	5-bromo-4-chloro-3-indolyl-β-D-galactopyranoside
XPO5	exportin 5
YAP	YES-associated protein
YES	transcriptional coactivator with PDZ-binding motif
ZEB1	zinc finger E-box binding homeobox 1
ZEB2	zinc finger E-box binding homeobox 2
μg	microgram
μl	microlitre
μm	micrometer

Acknowledgements

„So eine Arbeit wird eigentlich nie fertig; man muss sie für fertig erklären, wenn man nach Zeit und Umständen das Mögliche getan hat.“ - Johann Wolfgang von Goethe

Vielen Dank...

... **Prof. Dr. Andreas Jung** für die gute wissenschaftliche Betreuung meiner Doktorarbeit und die große Unterstützung in den letzten Jahren. Du hast mir immer sehr viel Geduld entgegengebracht und mir bei vielen Fragen geholfen. Ich habe durch Dich während der letzten Jahre sehr viel gelernt und konnte mich weiterentwickeln.

... **Prof. Dr. Thomas Kirchner** für die anhaltende Unterstützung während meiner Doktorarbeit und die Bereitstellung der guten Arbeitsbedingungen.

... **der gesamten Prüfungskommission** für die Übernahme der Beurteilung meiner Doktorarbeit. Besonders danken möchte ich **Prof. Dr. Wolfgang Zimmermann** für die Übernahme des Zweitgutachtens sowie **Prof. Dr. Olivier Gires, PD Dr. Andreas Herbst** und **Prof. Dr. Roland Kappler** für die Übernahme der mündlichen Promotionsprüfung.

... **allen aktuellen und ehemaligen Mitgliedern der AG Jung** sowie **Kooperationen, die bei uns im Labor saßen**, für ihre Hilfsbereitschaft, die Unterstützung in allen Laborfragen und die angenehme und freundschaftliche Laboratmosphäre, die die schwierigen Zeiten durch ihre Hilfe erträglicher gemacht und mich wieder aufgebaut haben. Besonderer Dank geht an **Alexandra Schindler** für die Hilfe bei den Maus-Genotypisierungen und auch sonstige tolle Unterstützung im Labor, **Jana Reiche** und **Dr. Achim Schäffauer** für wertvolle Ratschläge, Projektbesprechungen und Ideen und **Sabine Sagebiel-Kohler** für die vielen Bestellungen, Zellkultur-Hilfe und auch sonstige tolle Unterstützung im Labor, ganz besonders am Ende der Doktorarbeit. **Alexandra Schindler** und **Jana Reiche** danke ich außerdem für die schönen und unterhaltsamen gemeinsamen Mittagspausen und **allen**, die bei den lustigen Ausflügen und Abenden dabei waren.

... **Steffen Ormanns** für Zelllinien, Reagenzien und viele gute Ratschläge.

... **Beate Luthardt** für das Zuhören und die vielen Ratschläge das Labor aber auch viele andere Dinge betreffend.

... **PD Dr. David Horst** für seine Unterstützung, Ideen und Ratschläge bei allen Anliegen, mit denen ich zu ihm kam, die Kooperation bezüglich der subkutanen Injektion sowie für zur Verfügung gestellte Reagenzien. **Allen ehemaligen und aktuellen Mitgliedern der AG Horst** danke ich für die schönen gemeinsamen Mittagspausen, auf die ich mich immer sehr gefreut habe und die eine tolle Unterbrechung vom stressigen Laboralltag waren. Außerdem danke ich besonders **Anne Küchler, Cristina Blaj** und **Marina Schmidt** für die Unterstützung im Labor, die tolle Hilfsbereitschaft und das Zuhören. **Sebastian Lamprecht** danke ich besonders auch für die lustigen Tage in Berlin.

... **Dr. Dr. Jens Neumann** für die tolle Kooperation, die Auswertung der DICER1-IHC und die gute Unterstützung und geduldige Beantwortung aller meiner "pathologischen" Fragen.

... **Prof. Dr. Heiko Hermeking** für die Bereitstellung der Mauslinie Lgr5-CreER^{T2}. **Allen ehemaligen und aktuellen Mitgliedern der AG Hermeking** möchte ich für die kollegiale Unterstützung danken bei allen Fragen, mit denen ich zu ihnen kam, sowie für viele lustige Gespräche. Ganz besonders möchte ich mich bei **Dr. René Jackstadt, Dr. Stefanie Hahn, Uschi Götz** und **Stephanie Jäckel** bedanken, die mir bei vielen wichtigen Fragen geholfen haben.

... **Andrea Sendelhofert** und **Anja Heier** für die Färbungen des Mausegewebes und viele wertvolle Ratschläge zum Schneiden am Rotationsmikrotom.

... **allen Mitarbeitern des Tierstalles** für die tolle Versorgung der Mäuse. Besonderer Dank geht an **Monika Kociol**, die mich immer sehr unterstützt hat bei Fragen rund um die Mäuse, beim Genotypisieren und allem anderen.

... **den Mädels aus der Molekularen Diagnostik** für ihre Hilfsbereitschaft und die immer lustigen Gespräche zwischendurch.

... **allen Mitarbeitern des Pathologischen Institutes**, die immer sehr hilfsbereit waren. Besonderer Dank geht an die **Mitarbeiterinnen des Eingangslabors in der Innenstadt** für das Entwässern des Mausegewebes und die H&E und PAS Färbungen und die **Immunhistochemie in Großhadern** für die DICER1-Färbungen des humanen Kollektivs bedanken.

... **Prof. Dr. Eckhard Wolf** für die Benutzung des Stereomikroskopes. Besonderer Dank geht an **Dr. Maik Dahlhoff** für die tolle Unterstützung bei meinem Mausprojekt und bei sämtlichen Fragen zur Zucht, zu Versuchen, zum Mikroskopieren und zu vielem anderen.

... **PD Dr. Marlon Schneider** für die Bereitstellung der Mauslinie Rosa26-LSL-LacZ, **Dr. Brian Harfe** für die Dicer^{fl}-Mäuse und **Prof. Dr. Hans Clevers** für die APC^{fl}-Mäuse

... **meinen Würzburg-Mädels** für die unvergessliche Studienzeit und die tolle Unterstützung währenddessen und bis heute. Vielen Dank, dass Ihr mir immer zugehört und mich immer wieder aufgebaut habt. Besonders bedanken möchte ich mich bei **Eva** für ihre tolle Unterstützung während der Doktorarbeit und vor allem für das Korrekturlesen dieser Arbeit. Bei meinen **Kissinger-Mädels** möchte ich mich auch für das Zuhören und viele liebe, unterstützenden Worte bedanken sowie die schönen Treffen, bei denen ich mal an etwas ganz anderes denken konnte.

... **meinen Eltern**, die mich immer bedingungslos bei allem unterstützen und ohne die ich das alles nicht geschafft hätte. Ganz lieben Dank auch an **meine Schwester**, die auch immer für mich da ist. Ich bin sehr froh, Euch als meine Familie zu haben!

... **Ben** für die Unterstützung in jeder Lebenslage, auch in den schwierigen Zeiten. Vielen Dank, dass Du mich immer wieder aufbaust, immer für mich da bist und ich mich voll und ganz auf Dich verlassen kann!

Curriculum vitae

Die privaten Informationen aus dem Lebenslauf sind aus Gründen des Datenschutzes in dieser Version nicht enthalten.

Die privaten Informationen aus dem Lebenslauf sind aus Gründen des Datenschutzes in dieser Version nicht enthalten.

Publication

Peer-review article

Jaitner S, Reiche JA, Schäffauer AJ, Hiendlmeyer E, Herbst H, Brabletz T, Kirchner T, Jung A.

Human telomerase reverse transcriptase (hTERT) is a target gene of β -catenin in human colorectal tumors

Cell Cycle, 2012 Sep 1;11(17):3331-8. doi: 10.4161/cc.21790. Epub 2012 Aug 16.